



JOHANNES KEPLER
UNIVERSITÄT LINZ
Netzwerk für Forschung, Lehre und Praxis



High Order Finite Element Methods for Electromagnetic Field Computation

DISSERTATION

zur Erlangung des akademischen Grades

DOKTORIN DER TECHNISCHEN WISSENSCHAFTEN

Angefertigt am *Institut für Numerische Mathematik*

Begutachter:

Prof. Dr. Joachim Schöberl

Prof. Dr. Leszek Demkowicz, University of Texas at Austin

Eingereicht von:

Dipl.-Ing. Sabine Zaglmayr

Linz, Juli, 2006

Abstract

This thesis deals with the higher-order Finite Element Method (FEM) for computational electromagnetics. The hp -version of FEM combines local mesh refinement (h) and local increase of the polynomial order of the approximation space (p). A key tool in the design and the analysis of numerical methods for electromagnetic problems is the de Rham Complex relating the function spaces $H^1(\Omega)$, $H(\text{curl}, \Omega)$, $H(\text{div}, \Omega)$, and $L_2(\Omega)$ and their natural differential operators. For instance, the range of the gradient operator on $H^1(\Omega)$ is spanned by the space of irrotational vector fields in $H(\text{curl})$, and the range of the curl-operator on $H(\text{curl}, \Omega)$ is spanned by the solenoidal vector fields in $H(\text{div}, \Omega)$.

The main contribution of this work is a general, unified construction principle for $H(\text{curl})$ - and $H(\text{div})$ -conforming finite elements of variable and arbitrary order for various element topologies suitable for unstructured hybrid meshes. The key point is to respect the de Rham Complex already in the construction of the finite element basis functions and not, as usual, only for the definition of the local FE-space. A short outline of the construction is as follows. The gradient fields of higher-order H^1 -conforming shape functions are $H(\text{curl})$ -conforming and can be chosen explicitly as shape functions for $H(\text{curl})$. In the next step we extend the gradient functions to a hierarchical and conforming basis of the desired polynomial space. An analogous principle is used for the construction of $H(\text{div})$ -conforming basis functions. By our separate treatment of edge-based, face-based, and cell-based functions, and by including the corresponding gradient functions, we can establish the local exact sequence property: the subspaces corresponding to a single edge, a single face or a single cell already form an exact sequence. A main advantage is that we can choose an arbitrary polynomial order on each edge, face, and cell without destroying the global exact sequence. Further practical advantages will be discussed by means of the following two issues.

The main difficulty in the construction of efficient and parameter-robust preconditioners for electromagnetic problems is indicated by the different scaling of solenoidal and irrotational fields in the curl-curl problem. Robust Schwarz-type methods for Maxwell's equations rely on a FE-space splitting, which also has to provide a correct splitting of the kernel of the curl operator. Due to the local exact sequence property this is already satisfied for simple splitting strategies. Numerical examples illustrate the robustness and performance of the method.

A challenging topic in computational electromagnetics is the Maxwell eigenvalue problem. For its solution we use the subspace version of the locally optimal preconditioned gradient method. Since the desired eigenfunctions belong to the orthogonal complement of the gradient functions, we have to perform an orthogonal projection in each iteration step. This requires the solution of a potential problem, which can be done approximately by a couple

of PCG-iterations. Considering benchmark problems involving highly singular eigensolutions, we demonstrate the performance of the constructed preconditioners and the eigenvalue solver in combination with hp -discretization on geometrically refined, anisotropic meshes.

Zusammenfassung

Die vorliegende Arbeit beschäftigt sich mit der Methode der Finiten Elemente (FEM) höherer Ordnung zur Simulation elektromagnetischer Feldprobleme. Die hp -Version der FEM kombiniert lokale Netzverfeinerung (h) und lokale Erhöhung des Polynomgrades des Approximationsraumes (p). In der analytischen wie auch numerischen Behandlung elektromagnetischer Probleme spielt die exakte de Rham Folge der Funktionenräume $H^1(\Omega)$, $H(\text{curl}, \Omega)$, $H(\text{div}, \Omega)$, $L_2(\Omega)$ eine wesentliche Rolle: So ist zum Beispiel das Bild des Gradienten-Operators von $H^1(\Omega)$ der Raum der rotationsfreien Funktionen in $H(\text{curl}, \Omega)$ und das Bild des Rotations-Operators von $H(\text{curl}, \Omega)$ der Raum der divergenzfreien Funktionen in $H(\text{div}, \Omega)$.

Der wesentliche Beitrag dieser Arbeit ist eine einheitliche Konstruktionsmethode für $H(\text{curl})$ -konforme und $H(\text{div})$ -konforme Finite Elemente beliebiger und variabler Ordnung für unterschiedlichen Elementgeometrien auf unstrukturierten hybriden Vernetzungen. Ein wichtiger Punkt dabei, ist die exakte de Rham Folge bereits in der Konstruktion der Basisfunktionen höherer Ordnung zu berücksichtigen und nicht, wie üblich, nur in der Definition der globalen diskreten Räume. Kurz zur Konstruktion: Gradientenfelder von H^1 -konformen hierarchischen Basisfunktionen höherer Ordnung sind $H(\text{curl})$ -konform und können daher explizit als $H(\text{curl})$ -Basisfunktionen gewählt werden. Im nächsten Schritt werden die Gradientenfunktionen zu einer hierarchischen und konformen Basis für den gewünschten Polynomraum vervollständigt. Das analoge Prinzip wird auch zur Konstruktion $H(\text{div})$ -konformer Finiten Elemente angewendet. Die hierarchische Konstruktion der Basisfunktionen impliziert ein natürliches Raumsplitting in den globalen Raum der Ansatzfunktionen niedrigster Ordnung und in lokale Kanten-, Flächen- und Zellen-basierte Räume der Ansatzfunktionen höherer Ordnung. Durch die spezielle Wahl der Ansatzfunktionen gilt eine exakte de Rham Folge auch auf den lokalen Teilräumen - man spricht von lokalen exakten Folgen. Ein wesentlicher Vorteil ist, dass der Polynomgrad auf jeder einzelnen Kante, Fläche und Zelle des FE-Netzes beliebig variieren kann, ohne die globale exakte Sequenz zu zerstören. Weitere praktische Vorteile werden anhand der folgenden Beispiele genauer diskutiert.

Die Herausforderung in der Konstruktion von effizienten und Parameter-robusten Vorkonditionierern für curl-curl-Probleme liegt in der richtigen Behandlung des nicht-trivialen Kerns des curl-Operators. Die lokale Zerlegung (lokale exakte Sequenz) des FE-Raumes höherer Ordnung garantiert auch eine korrekte Zerlegung des Kerns. Dadurch wird bereits für einfache Schwarz Vorkonditionierer die notwendige Robustheit im Parameter erzielt. Numerische Beispiele demonstrieren Robustheit und Performance der Methode.

Die Lösung von Maxwell Eigenwertproblemen erfolgt mittels simultaner inexakter inverser

Iteration und deren Beschleunigung durch die vorkonditionierte konjugierte Gradientenmethode (Locally Optimal Block PCG-Methoden). Da die Eigenfunktionen auf dem orthogonalen Komplement der Gradientenfunktionen gesucht werden, ist in jedem Iterationsschritt eine orthogonale Projektion erforderlich. Das entspricht der Lösung eines Potentialproblems und kann durch einige PCG-Iterationen näherungsweise durchgeführt werden. Anhand eines Benchmark-Problems mit singulären Eigenfunktionen werden Vorkonditionierer und Eigenwertlöser in Verbindung mit hp -Diskretisierung auf geometrisch verfeinerten, anisotropen Netzen getestet.

Acknowledgements

My special thanks go to my advisor J. Schöberl for supervising and inspiring my work and for countless time-intensive discussions during the last years. At the same time, I am greatly indebted to L. Demkowicz for co-refereeing this work and for his constructive remarks.

Special thanks go to H. Egger, C. Pechstein, V. Pillwein, and D. Copeland for numerous discussions and for proof-reading this work, their comments significantly improved the presentation. Furthermore, I want to thank all my colleagues, especially those from the START-Project, from the Institute of Computational Mathematics, and from RICAM for scientific and social support.

I want to acknowledge the scientific environment and the hostage of the Insitute of Numerical Mathematics, chaired by U. Langer, and the Radon Institute for Computational Mathematics, leaded by H.W. Engl.

Financial support by the Austrian Science Fund "Fonds zur Förderung der wissenschaftlichen Forschung in Österreich" (FWF) through the START Project Y-192 is acknowleged.

Contents

1	Introduction	1
2	Fundamentals of Electromagnetics	5
2.1	Maxwell's equations	5
2.1.1	The fundamental equations	5
2.1.2	Material properties	7
2.1.3	Initial, boundary and interface conditions	8
2.2	Vector and scalar potentials	10
2.3	Special electromagnetic regimes	12
2.3.1	Time-harmonic Maxwell equations	12
2.3.2	Magneto-Quasistatic Fields: The Eddy-Current Problem	13
2.3.3	Static field equations	13
2.4	The general curl-curl problem	14
3	A Variational Framework	17
3.1	Function Spaces, Trace Operators and Green's formulas	17
3.2	Mapping Properties of Differential Operators	23
3.2.1	The de Rham Complex and Exact Sequences	25
3.3	Abstract Variational Problems: Existence and Uniqueness	26
3.3.1	Coercive variational problems	26
3.3.2	Mixed formulations	26
3.4	Variational formulation of electromagnetic problems	27
3.4.1	The electrostatic problem: A Poisson problem	27
3.4.2	The magnetostatic problem	28
3.4.3	The time-harmonic electromagnetic and magneto-quasi-static problems	32
4	The Finite Element Method	35
4.1	Basic Concepts	35
4.1.1	Galerkin Approximation	35
4.1.2	The Triangulation	36
4.1.3	The Finite Element	36
4.1.4	The reference element and its transformation to physical elements	37
4.1.5	Simplicial elements and barycentric coordinates	38
4.2	Approximation properties of conforming FEM	39
4.3	An exact sequence of conforming finite element spaces	40
4.3.1	The classical H^1 -conforming Finite Element Method	40
4.3.2	Low-order $H(\text{curl})$ -conforming Finite Element Methods	42

4.3.3	Low-order $H(\text{div})$ -conforming Finite Elements Methods	46
4.3.4	The lowest-order L_2 -conforming Finite Element Method	49
4.3.5	Discrete exact sequences	50
4.3.6	Element matrices and assembling of FE-matrices	53
4.4	Commuting Diagram and Interpolation Error Estimates	55
5	High Order Finite Elements	59
5.1	High-order FE-spaces of variable order	60
5.2	Construction of conforming shape functions	63
5.2.1	Preliminaries	63
5.2.2	The quadrilateral element	68
5.2.3	The triangular element	73
5.2.4	The hexahedral element	82
5.2.5	The prismatic element	89
5.2.6	The tetrahedral element	97
5.2.7	Nédélec elements of the first kind and other incomplete FE-spaces . . .	107
5.2.8	Elements with anisotropic polynomial order distribution	108
5.3	Global Finite Element Spaces	109
5.3.1	The H^1 -conforming global finite element space	109
5.3.2	The $H(\text{curl})$ -conforming global finite element space	110
5.3.3	The $H(\text{div})$ -conforming global finite element space	111
5.3.4	The L_2 -conforming global finite element space	112
5.4	The Local Exact Sequence Property	113
6	Iterative Solvers	115
6.1	Basic Concepts	115
6.1.1	Additive Schwarz Methods (ASM)	116
6.1.2	A two-level concept	118
6.1.3	Static Condensation	118
6.2	Parameter-Robust Preconditioning for $H(\text{curl})$	119
6.2.1	Two Motivating Examples	120
6.2.2	The smoothers of Arnold-Falk-Winther and Hiptmair	124
6.2.3	Schwarz methods for parameter-dependent problems	125
6.2.4	Parameter-robust ASM methods and the local exact sequence property	127
6.3	Reduced Nédélec Basis and Special Gauging Strategies	128
6.4	Numerical Results	129
6.4.1	The magnetostatic problem	130
6.4.2	The magneto quasi-static problem: A practical application	133
7	The Maxwell Eigenvalue Problem	135
7.1	Formulation of the Maxwell Eigenvalue Problem	135
7.2	Preconditioned Eigensolvers	138
7.2.1	Preconditioned gradient type methods	139
7.2.2	Block version of the locally optimal preconditioned gradient method . .	140
7.3	Preconditioned Eigensolvers for the Maxwell Problem	141
7.3.1	Exact and inexact projection onto the complement of the kernel function	142
7.3.2	A preconditioned eigensolver for the Maxwell problem with inexact pro- jection	143

7.3.3	Exploiting the local exact sequence property	144
7.4	Numerical Results	144
7.4.1	An h - p -refinement strategy	145
7.4.2	The Maxwell EVP on the thick L-Shape	145
7.4.3	The Maxwell EVP on the Fichera corner	149
A	APPENDIX	151
A.1	Notations	151
A.2	Basic Vector Calculus	151
A.3	Some more orthogonal polynomials	151
A.3.1	Some Calculus for Scaled Legendre Polynomials	153
A.3.2	Some technical things	153
	Bibliography	154
	Eidesstattliche Erklärung	A1
	Curriculum Vitae	A3

Chapter 1

Introduction

State of the Art

Electromagnetic processes are present everywhere in our daily life. Classical applications are generators, transformers and motors, converting mechanical to electric energy and vice versa. Wireless communication is based on electromagnetic waves in free space. Here, the design of antennas is a sophisticated task. A fastly growing application field is optics. Optical fibers allow the transport of light pulses over much longer distances than achieved by electric signals through cables. Short light pulses are generated by laser resonators. Optical multiplexers realized by photonic crystals have obtained much attraction over recent years. All these applications are rather complex, hence for further technical developments and optimization a deeper insight into electromagnetic processes is necessary.

Similar to many other physical and technical effects (such as solid and fluid mechanics, heat transfer, quantum mechanics, geoscience, astrophysics, etc.) electromagnetic phenomena are modelled by partial differential equations (PDEs). This is the basis for the mathematical analysis and numerical treatment.

Only for very special problems can the solution of partial differential equations be done analytically. This calls for numerical discretization techniques. The analysis of partial differential equations is commonly done within a variational framework. In the last fifty years, the Finite Element Method (FEM) has been established as certainly the most powerful tool in numerical simulation. This discretization technique is based on the variational formulation of partial differential equations. The main advantages are its general applicability to linear and nonlinear PDEs, coupled multi-physics systems, complex geometries, varying material coefficients and boundary conditions. Furthermore, the method is based on a profound functional analysis (cf. e.g. CIARLET [35], BRENNER-SCOTT [31], BRAESS [27]). In classical (h -version) finite element methods we obtain convergence by global or local refinement of the underlying mesh (h -refinement). The polynomial order of approximation on each element is fixed to a low degree, typically $p = 1$ or $p = 2$. The error in the numerical solution decays algebraically in the number of unknowns.

The p -version of the finite element method (see BABUSKA-SZABO [87]) allows an increase of the polynomial order, while keeping the mesh fixed. In case of analytic solutions one obtains exponential convergence, but in case of lower regularity the convergence rate reduces again to an algebraic one. Hence, in the presence of singularities, which occur very frequently in

practical problem settings, not much is gained compared with the h -version FEM. However, by a proper combination of (geometric) h -refinement and local increase of the polynomial degree p – the hp -method – exponential convergence can be regained for piecewise analytic solutions involving singularities, e.g. due to re-entrant corners and edges. This is the typical situation in practical applications. For pioneering works on hp -version FEM see BABUSKA-GUO [10] and BABUSKA-SURI [11]. We refer also to the books by SCHWAB [83], MELENK [68], and KARNIADAKIS [60]. The recent textbook DEMKOWICZ [42] copes also with the aspects of practical implementation and automatic generation of hp -meshes. For the successful application to mechanics see e.g. SZABO ET AL. [86].

In linear as well as nonlinear time-dependent, time-harmonic, and magneto-static regimes of Maxwell's equations the general *curl-curl problem*

$$\text{Find } \mathbf{u} \in V \text{ such that } \int_{\Omega} \mu^{-1} \operatorname{curl} \mathbf{u} \cdot \operatorname{curl} \mathbf{v} \, d\mathbf{x} + \int_{\Omega} \kappa \mathbf{u} \cdot \mathbf{v} \, d\mathbf{x} = \int_{\Omega} \mathbf{j} \cdot \mathbf{v} \, d\mathbf{x} \quad \forall \mathbf{v} \in V$$

appears, where \mathbf{u} is the magnetic vector potential.

Using standard continuous finite elements in the discretization of electromagnetic problems fails. In the presence of re-entrant corners and edges, the method may even converge to a wrong solution (cf. COSTABEL-DAUGE [38]). Moreover, in eigenvalue computation, using standard elements is one source of spurious (non-physical) eigenvalues, which pollute the computed spectrum (see BOSSAVIT [26], BOFFI ET AL. [21]).

The natural function space for the solution of the curl-curl problem is the vector-valued space $H(\operatorname{curl})$, which has less smoothness than H^1 , namely only tangential continuity over material interfaces. This property goes along with the physical nature of electric and magnetic fields. The classical $H(\operatorname{curl})$ -conforming finite element spaces have been introduced in NÉDÉLEC [72], [73].

The adaption of hp -methods to electromagnetic problems is not straightforward. Investigations in this direction started only in the last decade, and the numerical analysis is not complete, especially in 3D. A key tool in the design of numerical methods for Maxwell's equations and their numerical analysis is the *de Rham Complex* (cf. BOSSAVIT [22], [25] and more recently ARNOLD ET AL. [8],[9]), which relates function spaces and their natural differential operators, and reads in 3D:

$$\mathbb{R} \xrightarrow{\operatorname{id}} H^1(\Omega) \xrightarrow{\nabla} H(\operatorname{curl}, \Omega) \xrightarrow{\operatorname{curl}} H(\operatorname{div}, \Omega) \xrightarrow{\operatorname{div}} L_2(\Omega) \xrightarrow{0} \{0\}.$$

The sequence is exact in the following sense: the range of an operator in the sequence coincides with the kernel of the next operator.

The de Rham Complex perfectly fits to electromagnetics: in a variational setting $H^1(\Omega)$ is the natural function space for the electrostatic potential, the magnetic and the electric fields lie in $H(\operatorname{curl}, \Omega)$ and their fluxes belong to $H(\operatorname{div}, \Omega)$. For a proper conforming hp -finite element method, the discrete spaces have to form an analogous exact sequence.

High-order p -version elements for $H(\operatorname{curl})$ are analyzed for constant order p in MONK [69]. Variable order elements are proposed for the first time in DEMKOWICZ-VARDAPETYAN [45]. The consideration of hp -finite elements, allowing variable order approximation, on the basis of the de Rham Complex is presented in DEMKOWICZ ET AL. [44] and DEMKOWICZ [41].

A first general construction strategy for tetrahedral shape functions on unstructured grids was recently introduced by AINSWORTH-COYLE [2] for the whole sequence of H^1 -, $H(\operatorname{curl})$ -

$H(\text{div})$ - and L_2 -conforming spaces (for arbitrary but uniform p). For the formulation of finite elements in the context of differential forms we refer to BOSSAVIT [24],[25] and HIPTMAIR [54]. The construction of $H(\text{curl})$ -conforming finite elements is also an active research area in the engineering community, cf. LEE [66], WEBB-FORGHANI [96], WEBB [95], and SUN ET AL. [85].

Due to the non-trivial, large kernel of the curl-operator - the gradient fields of $H^1(\Omega)$ - not only the convergence analysis but also the iterative solution of discretized Maxwell problems becomes very challenging. The main difficulty stems from the different scaling of solenoidal and irrotational fields in the curl-curl problem. This leads to very ill-conditioned system matrices and standard Schwarz-type preconditioners like multigrid/multilevel techniques yield only bad convergence behavior. In this context, we want to mention the pioneering works on robust preconditioning in $H(\text{curl})$ and $H(\text{div})$ by ARNOLD ET AL. [7] and HIPTMAIR [55], revisited and unified in SCHÖBERL [78]. The difficulties can be resolved by a careful choice of the Schwarz smoothers, in particular the space splitting has to respect the kernel of the curl-operator. Further works on this topic are TOSELLI [89], HIPTMAIR-TOSELLI [58], BECK ET AL. [16], and PASCIAK-ZHAO [75].

A rather complete overview on finite element methods for Maxwell's equations can be found in MONK [70]; for another comprehensive survey we refer to HIPTMAIR [56]. The topic of hp -methods for Maxwell's equations, including implementational aspects, is covered by DEMKOWICZ [42].

On this work

In this work we present a general, unified construction principle for $H(\text{curl})$ - and $H(\text{div})$ -conforming finite elements of variable and arbitrary order. In order to allow for geometric h -refinement, we have to consider hybrid meshes, involving hexahedral, tetrahedral, and prismatic elements. The innovation of our framework is to respect the exact de Rham sequence already in the construction of the FE basis functions. We shortly outline the main points of the construction for $H(\text{curl})$:

- We start with the classical lowest-order Nédélec shape functions. Note that the lowest-order space always has to be treated separately by applying h -version methods, e.g. also in linear solvers.
- We take the gradients of edge-based, face-based and cell-based shape functions of the higher-order H^1 -conforming FE-space.
- Finally, we extend these sets of functions to a conforming basis of the desired polynomial space.

By our separate treatment of the edge-based, face-based, and cell-based functions, and by including the corresponding gradient functions, we can establish the following *local exact sequence property*: the subspaces corresponding to a single edge, a single face or a single cell already form an exact sequence.

This construction has several practical advantages:

- We can choose an arbitrary polynomial order on each edge, face, and cell independently, without destroying the global exact sequence property, see Section 5.4.

- A correct Schwarz splitting can be constructed by simple strategies, and only the lowest-order space has to be treated globally or by standard h -methods. The parameter-robustness is implied automatically by the local sequence property, see Section 6.2.4.
- Since gradients are explicitly available, we can implement gauging strategies by simply skipping the corresponding degrees of freedom (*Reduced Basis Gauging*). We will illustrate in numerical tests that this approach tremendously improves the condition numbers and solving times, see Section 6.4.1.
- Discrete differential operators, for instance used within the projection for preconditioned eigenvalue solvers, can be implemented very easily, see Section 7.3.3.

The full family of finite element shape functions for all sorts of element topologies, covering also anisotropic polynomial degrees and regular geometric h -refinement towards pre-defined corners, edges and faces, has been implemented in the open-source software package Netgen/NgSolve

<http://www.hpfem.jku.at/>.

Other resources for higher-order Maxwell FE-packages are e.g. EMSolve (CASC, Lawrence Livermore National Lab.), 3Dhp90 by L. Demkowicz (ICES University of Texas Austin, RACHOWICZ-DEMKOWICZ [76]), Concepts by P. Frauenfelder (ETH Zürich).

The thesis is organized as follows.

In *Chapter 2*, we present the Maxwell equations. We pay special attention to scalar and vector potential formulations, and consider time-harmonic, quasi-static, and magneto-static regimes in more detail. All these problems involve the abstract parameter-dependent curl-curl-problem, mentioned before.

The first part of *Chapter 3* recalls the natural function spaces and their properties. We formally introduce the de Rham Complex, which is a guiding principle through the whole work. We conclude this chapter with presenting variational formulations of the electromagnetic problems introduced in Chapter 2.

Chapter 4 briefly overviews the basic concepts of conforming low-order finite element methods, including the non-standard function spaces $H(\text{curl}, \Omega)$ and $H(\text{div}, \Omega)$.

Chapter 5 contains the main contribution of this thesis: We present in detail our construction of high-order FE-shape functions for the space $H^1(\Omega)$, $H(\text{curl}, \Omega)$, $H(\text{div}, \Omega)$ and $L_2(\Omega)$ and show that the local exact sequence property, mentioned above, holds.

Chapter 6 deals with parameter-robust Schwarz-type preconditioners for $H(\text{curl})$. We prove that parameter-robust solvers are obtained also even by simple Schwarz-type smoothers, if the presented conforming high-order FE-basis is used. In the second part the concept of reduced basis gauging is introduced. Finally, we present numerical tests for magneto-static and magneto-quasi-static problems, illustrating the benefits of our methods.

Chapter 7 is concerned with the numerical solution of Maxwell eigenvalue problems. We investigate preconditioned eigensolvers and their combination with (in)exact projection methods. The performance of the eigensolver in combination with reduced-basis preconditioners is demonstrated by the solution of benchmark problems.

Chapter 2

Electromagnetics: Fundamental equations and formulations

2.1 Maxwell's equations

Classical electromagnetics treats electric and magnetic macroscopic phenomena including their interaction. Electric fields which vary in time cause magnetic fields and vice versa. James Clark Maxwell described these phenomena in his "Treatise on Electricity and Magnetism" in 1862.

The classic theory mainly involves the following four time- and space-dependent vector fields:

- the electric field intensity denoted by \mathbf{E} [V/m],
- the magnetic field intensity \mathbf{H} [A/m],
- the electric displacement field (electric flux) \mathbf{D} [As/m^2],
- the magnetic induction field (magnetic flux) \mathbf{B} [Vs/m^2].

The sources of electromagnetic fields are electric charges and currents described by

- the charge density ρ [As/m^3] and
- the current density function \mathbf{j} [A/m^2],

where the SI units denotes meter (m), seconds (s), Ampère (A), Volt (V).

2.1.1 The fundamental equations

The basic relations of electromagnetics are based on experiments and laws by Faraday, Ampère, and Gauß. We start here with integral formulation of the main governing equations, which facilitates a physical interpretation. In the following we refer by A to a surface and by V to a volume in \mathbb{R}^3 . The corresponding boundaries are denoted by ∂V with outer unit normal vector \mathbf{n} , and ∂A with unit tangential vector $\boldsymbol{\tau}$.

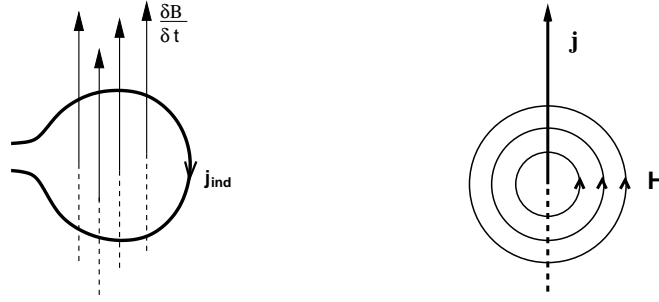


Figure 2.1: Faraday's and Ampère's law

Faraday's induction law describes how the change (in time) of the magnetic flux through a surface A induces a voltage in the loop (∂A) and hence gives rise to an electric field E :

$$\int_A \frac{\partial \mathbf{B}}{\partial t} \cdot \mathbf{n} dA + \int_{\partial A} \mathbf{E} \cdot \boldsymbol{\tau} ds = 0. \quad (2.1)$$

Since there exist no magnetic charges (monopoles), the magnetic field is *solenoidal* (source-free). Moreover, magnetic field lines are closed. The magnetic flux \mathbf{B} through the surface of a bounded volume V is conservative, i.e.

$$\int_{\partial V} \mathbf{B} \cdot \mathbf{n} dA = 0. \quad (2.2)$$

Ampère's law states how electric currents through a surface A induce a magnetic field as illustrated in Figure 2.1. The integral of the magnetic field along a closed path (∂A) is proportional to the current through the enclosed surface, i.e.,

$$\int_{\partial A} \mathbf{H} \cdot \boldsymbol{\tau} ds = \int_A \mathbf{j} \cdot \mathbf{n} dA.$$

Maxwell generalized this law by adding the displacement current density $\frac{\partial \mathbf{D}}{\partial t}$, which yields

$$\int_{\partial A} \mathbf{H} \cdot \boldsymbol{\tau} ds = \int_A \frac{\partial \mathbf{D}}{\partial t} \cdot \mathbf{n} dA + \int_A \mathbf{j} \cdot \mathbf{n} dA. \quad (2.3)$$

Gauß' law describes how electric charges give rise to an electric field. It has the form

$$\int_{\partial V} \mathbf{D} \cdot \mathbf{n} dA = \int_V \rho d\mathbf{x}. \quad (2.4)$$

The electric flux \mathbf{D} through the boundary of a volume V is proportional to the enclosed volume charges.

Applying Gauß' and Stokes' theorems

$$\int_V \operatorname{div} \mathbf{B} d\mathbf{x} = \int_{\partial V} \mathbf{B} \cdot \mathbf{n} dA \quad \text{and} \quad \int_A \operatorname{curl} \mathbf{H} \cdot \mathbf{n} dA = \int_{\partial A} \mathbf{H} \cdot \boldsymbol{\tau} ds$$

to the integral equations (2.1)-(2.4) yields the *Maxwell equations* in the following (classical) differential form:

$$\frac{\partial \mathbf{B}}{\partial t} + \text{curl } \mathbf{E} = 0, \quad (2.5a)$$

$$\text{div } \mathbf{B} = 0, \quad (2.5b)$$

$$\frac{\partial \mathbf{D}}{\partial t} - \text{curl } \mathbf{H} = -\mathbf{j}, \quad (2.5c)$$

$$\text{div } \mathbf{D} = \rho. \quad (2.5d)$$

The conservation of charges

An important physical property can be derived by taking the divergence of equation (2.5c) in combination with equation (2.5d), which yields the *continuity equation*

$$\text{div } \mathbf{j} + \frac{\partial \rho}{\partial t} = 0. \quad (2.6)$$

By integration over a volume V and application of Gauß' theorem we see that this equation describes the conservation of charges. This can be seen from the Integral formulation, namely

$$\int_{\partial V} \mathbf{j} \cdot \mathbf{n} dA + \frac{\partial}{\partial t} \int_V \rho d\mathbf{x} = 0, \quad (2.7)$$

which states that the total charge in a volume V changes according to the net flow of electric charges across its surface ∂V .

2.1.2 Material properties

The system (2.5) is still undertetermined, i.e., it provides only 8 equations for 12 unknowns. The gap is closed by including appropriate constitutive laws. First, the magnetic and electric field intensities are related with the corresponding fluxes by

$$\mathbf{D} = \epsilon \mathbf{E}, \quad (2.8a)$$

$$\mathbf{B} = \mu \mathbf{H}. \quad (2.8b)$$

Furthermore, in conducting materials the electric field induces a *conduction current* with density \mathbf{j}_c , which is given by *Ohm's law*

$$\mathbf{j} = \mathbf{j}_c + \mathbf{j}_i \quad \text{with} \quad \mathbf{j}_c = \sigma \mathbf{E}, \quad (2.9)$$

where \mathbf{j} and \mathbf{j}_i denote the *total* and the *impressed* current densities, respectively. As a special class of conduction currents we want to mention *eddy currents*, which arise in metallic bodies if excited by varying magnetic fields.

Hence, the electric and magnetic properties of a medium are characterized by

- the electric permittivity ϵ [As/Vm],
- the magnetic permeability μ [Vs/Am],
- the electric conductivity σ [As].

In general, the three parameters are tensors depending on space and time, and on the electromagnetic fields themselves. However, in isotropic media they simplify to scalars, and in so-called *linear materials*, they are independent of the field intensities. We will consider only isotropic, linear materials in this thesis, and moreover assume the material parameters to be time independent.

The values of the parameters in vacuum are

$$\epsilon_0 \approx 8.854 \cdot 10^{-12} \text{ Fm}^{-1}, \quad \mu_0 = 4\pi \cdot 10^{-7} \text{ Hm}^{-1}, \quad \sigma_0 = 0.$$

ϵ_0 and μ_0 are further connected by $\frac{1}{\sqrt{\epsilon_0\mu_0}} = c$, where c denotes the speed of light.

2.1.3 Initial, boundary and interface conditions

Although the number of equations now coincides with the number of unknowns, the system of differential equations (2.5) is not yet complete. We have to impose initial and boundary conditions as well as interface conditions between different materials where the material parameters jump. Below we will mainly focus on time-harmonic or static settings, and we therefore skip the treatment of initial conditions at this point. We only remark that applying the divergence to Faraday's and Ampère's law yields

$$\frac{\partial}{\partial t} \operatorname{div} \mathbf{B}(\mathbf{x}, t) = 0 \quad \text{and} \quad \frac{\partial}{\partial t} \operatorname{div} \mathbf{D}(\mathbf{x}, t) = -\operatorname{div} \mathbf{j}(\mathbf{x}, t).$$

Hence, if the magnetic field is solenoidal ($\operatorname{div} \mathbf{B} = 0$) at the initial time, then it is solenoidal for any time. The second relation together with Gauß' law (2.5d) yields that the change of the charge density is given by the electric current density \mathbf{j} , see also the continuity equation (2.6).

Interface conditions

Assume a partition of the domain $V \subset \mathbb{R}^3$ into two disjoint domains V_1, V_2 such that $\bar{V} = \bar{V}_1 \cup \bar{V}_2$. By $\Gamma := \bar{V}_1 \cap \bar{V}_2$ we denote the common interface, and by \mathbf{n}_Γ we refer to the unit normal vector pointing from V_2 to V_1 . In the following we derive the continuity requirements at interfaces by Gauß' theorem and Stokes' theorem assuming that the involved functions, domains and surfaces are sufficiently smooth.

From equation (2.2) we obtain

$$\begin{aligned} 0 &= -\int_{\partial V} \mathbf{B} \cdot \mathbf{n} \, d\mathbf{x} + \int_{\partial V_1} \mathbf{B}_1 \cdot \mathbf{n} \, d\mathbf{x} + \int_{\partial V_2} \mathbf{B}_2 \cdot \mathbf{n} \, d\mathbf{x} \\ &= -\int_{\partial V_1 \cap \Gamma} \mathbf{B}_1 \cdot \mathbf{n}_\Gamma \, dA + \int_{\partial V_2 \cap \Gamma} \mathbf{B}_2 \cdot \mathbf{n}_\Gamma \, dA \\ &= \int_{\Gamma} [\mathbf{B} \cdot \mathbf{n}_\Gamma] \, dA, \end{aligned}$$

where $\mathbf{B}_1 := \mathbf{B}|_{V_1}$, $\mathbf{B}_2 := \mathbf{B}|_{V_2}$, and $[\mathbf{B} \cdot \mathbf{n}_\Gamma] = (\mathbf{B}_2 - \mathbf{B}_1) \cdot \mathbf{n}_\Gamma$ denotes the jump over the interface Γ . Since the above formula is valid for arbitrary subsets of V , we obtain that the normal component of the induction field has to be continuous over the interface, which reads as

$$[\mathbf{B} \cdot \mathbf{n}]_\Gamma = 0, \tag{2.10}$$

where now \mathbf{n} denotes a normal vector to the surface (interface) Γ .

A similar argument works for the electric flux density \mathbf{D} , but here we also take surface charges ρ_S on the interface into account. Hence, the total electric charge in \bar{V} is given by $\int_V \rho \, d\mathbf{x} = \int_{V_1} \rho \, d\mathbf{x} + \int_{V_2} \rho \, d\mathbf{x} + \int_{\Gamma} \rho_S \, dA$, and via (2.5d) we obtain

$$[\mathbf{D} \cdot \mathbf{n}_{\Gamma}] = \rho_S. \quad (2.11)$$

Next we derive interface conditions for the electric field \mathbf{E} . Let the interface Γ be as above and A denote an arbitrary plane surface intersecting the interface Γ along a line $L := A \cap \Gamma$. Let $A_1 := A \cap V_1$, $A_2 := A \cap V_2$ be the two disjoint parts of A such that $\bar{A}_1 \cup \bar{A}_2 = \bar{A}$ and $\bar{A}_1 \cap \bar{A}_2 = L$. Considering Faraday's law (2.1) in integral form for A, A_1, A_2 , we see that

$$\begin{aligned} 0 &= - \int_{\partial A} \mathbf{E} \cdot \boldsymbol{\tau} \, ds + \int_{\partial A_1} \mathbf{E}_1 \cdot \boldsymbol{\tau}_1 \, ds + \int_{\partial A_2} \mathbf{E}_2 \cdot \boldsymbol{\tau}_2 \, ds \\ &= \int_{\partial A_1 \cap \Gamma} \mathbf{E}_1 \cdot \boldsymbol{\tau}_1 \, ds + \int_{\partial A_2 \cap \Gamma} \mathbf{E}_2 \cdot \boldsymbol{\tau}_2 \, ds \\ &= \int_L [\mathbf{E} \cdot \boldsymbol{\tau}_L] \, ds \end{aligned}$$

with $\mathbf{E}_1 := E|_{A_1}$ and $\mathbf{E}_2 := E|_{A_2}$ and $\boldsymbol{\tau}_L = \boldsymbol{\tau}_1 = -\boldsymbol{\tau}_2$. Since A was arbitrary, we conclude that the tangential components of the electric field have to be continuous over the interface Γ , which is equivalent to

$$[\mathbf{E} \times \mathbf{n}_{\Gamma}] = 0, \quad (2.12)$$

where as before \mathbf{n} denotes a normal to the surface Γ .

Similar arguments can be applied for the magnetic field \mathbf{H} . Taking into account also the possibility of impressed surface currents $\mathbf{j}_{\Gamma,i}$ on the interface, we obtain

$$[\mathbf{H} \times \mathbf{n}_{\Gamma}] = -\mathbf{j}_{\Gamma,i}. \quad (2.13)$$

We conclude this section on interface conditions with some remarks on those components of the electromagnetic fields that were not considered above: It can be shown easily that the normal components of fluxes and the tangential components of the field intensities may be discontinuous when the material parameters jump across the interface. To see this, we assume for simplicity $\rho_S = 0$ and $j_{S,i} = 0$ on the interface Γ . Then substituting the constitutive laws (2.8a), (2.8b) and (2.9) into the above (2.10)-(2.13) yields

$$[\mathbf{E} \cdot \mathbf{n}_{\Gamma}] \neq 0, [\mathbf{H} \cdot \mathbf{n}_{\Gamma}] \neq 0, [\mathbf{D} \times \mathbf{n}_{\Gamma}] \neq 0, \text{ and } [\mathbf{B} \times \mathbf{n}_{\Gamma}] \neq 0$$

in general, namely if $[\mu] \neq 0$ and $[\epsilon] \neq 0$ across the interface Γ .

Boundary conditions

In the sequel we present several frequently used boundary conditions for the normal or the tangential components of the electromagnetic fields. We focus here on standard boundary conditions of Dirichlet-, Neumann- or Robin-type. For a detailed review of classical boundary conditions, we refer to BÍRÓ [18].

Perfect electric conductors (PEC) Let Ω_{PEC} denote a perfectly conducting region with $\sigma \sim \infty$. Then Ohm's law $\mathbf{j} = \sigma \mathbf{E}$ implies $E|_{\Omega_{\text{PEC}}} \sim 0$ as long as the currents \mathbf{j} are bounded. Hence, the interface condition (2.12) justifies to substitute perfectly conducting regions by the PEC-boundary condition for the electric field, i.e., we assume

$$\mathbf{E} \times \mathbf{n} = 0 \quad \text{on } \Gamma_{\text{PEC}}. \quad (2.14)$$

The PEC-wall is in particular suitable for modeling adjacent metallic domains, e.g., metallic electrodes.

Perfect magnetic conductors (PMC) model materials with very high permeability, where one can assume a vanishing magnetic field $\mathbf{H}_{\Omega_1} = 0$. The interface condition (2.13) then implies that an adjacent PMC-region can be substituted by the boundary condition

$$\mathbf{H} \times \mathbf{n} = 0 \quad \text{on } \Gamma_{\text{PMC}} \quad (2.15)$$

Prescribed surface charges ρ_S on the boundary Γ are introduced by a condition

$$\mathbf{D} \cdot \mathbf{n} = -\rho_S \quad \text{on } \Gamma \quad (2.16)$$

on the normal electric flux, cf. the interface condition (2.11).

Impressed surface currents $\mathbf{j}_{\Gamma,i}$ yield a condition on the normal component of the magnetic field at the boundary Γ in analogy to the interface condition (2.13), i.e.

$$\mathbf{H} \times \mathbf{n} = \mathbf{j}_{\Gamma,i} \quad \text{on } \Gamma. \quad (2.17)$$

Impedance boundary conditions It is well-known that in highly conducting materials, eddy currents are concentrated near the surface. If one is interested in the field intensities in regions adjacent to highly (but still finitely) conducting materials, the reflection at the interface can be modeled by *impedance boundary conditions*. These are Robin-type boundary conditions relating the magnetic and electric fields in the following form:

$$\mathbf{H} \times \mathbf{n} - \kappa(\mathbf{E} \times \mathbf{n}) \times \mathbf{n} = 0 \quad \text{on } \Gamma, \quad (2.18)$$

where κ is called the impedance parameter.

2.2 Vector and scalar potentials

Let Ω be a bounded, simply connected domain in \mathbb{R}^3 . Then due to $\text{div } \mathbf{B} = 0$, and by $\text{curl } \nabla \varphi = 0$ and $\text{div } \text{curl } \mathbf{v} = 0$, we know that \mathbf{B} can be expressed by a *vector potential* $\mathbf{A}(\mathbf{x}, t)$, i.e.,

$$\mathbf{B} = \text{curl } \mathbf{A}.$$

Substituting into Faraday's law (2.5a) yields

$$\text{curl} \left(\mathbf{E} + \frac{\partial \mathbf{A}}{\partial t} \right) = 0,$$

which in turn implies the existence of a *scalar potential* $\varphi(\mathbf{x}, t)$ such that

$$\mathbf{E} = -\nabla\varphi - \frac{\partial\mathbf{A}}{\partial t}.$$

Hence, Ampère's law (2.3) can be expressed by

$$\text{curl } \mu^{-1} \text{curl } \mathbf{A} + \sigma \frac{\partial\mathbf{A}}{\partial t} + \epsilon \frac{\partial^2\mathbf{A}}{\partial t^2} = \mathbf{j}_i - \sigma \nabla\varphi - \epsilon \frac{\partial}{\partial t} \nabla\varphi. \quad (2.19)$$

Note, that for any arbitrary scalar function ψ the potentials

$$\begin{aligned} \tilde{\mathbf{A}} &= \mathbf{A} + \nabla\psi \\ \tilde{\varphi} &= \varphi - \frac{\partial\psi}{\partial t} \end{aligned}$$

provide the same magnetic and electric fields, since $\mathbf{B}(\mathbf{A}, \varphi) = \mathbf{B}(\tilde{\mathbf{A}}, \tilde{\varphi})$ and $\mathbf{E}(\mathbf{A}, \varphi) = \mathbf{E}(\tilde{\mathbf{A}}, \tilde{\varphi})$. By choosing a vector potential \mathbf{A}^* such that

$$\mathbf{A}^* = \mathbf{A} + \int_{t_0}^t \nabla\varphi dt,$$

we obtain $\mathbf{E} = -\frac{\partial\mathbf{A}^*}{\partial t}$ and $\text{curl } \mathbf{A} = \text{curl } \mathbf{A}^*$, and the following *vector potential formulation* of Maxwell's equations

$$\text{curl } \mu^{-1} \text{curl } \mathbf{A}^* + \sigma \frac{\partial\mathbf{A}^*}{\partial t} + \epsilon \frac{\partial^2\mathbf{A}^*}{\partial t^2} = \mathbf{j}_i, \quad (2.20)$$

which is the type of equation whose numerical solution we will investigate in detail in this theses. Once \mathbf{A}^* is determined, the electric and the magnetic fields can be calculated by $\mathbf{B} = \text{curl } \mathbf{A}^*$ and $\mathbf{E} = -\frac{\partial\mathbf{A}^*}{\partial t}$.

In analogy to (2.12), the continuity requirements of vector potentials across an interface Γ between are given by

$$[\mathbf{A}^* \times \mathbf{n}]_{\Gamma} = 0.$$

A perfect electric conducting (PEC) wall is modeled by homogenous essential boundary condition for the vector potential \mathbf{A}^* , cf. (2.14), i.e.,

$$\mathbf{A}^* \times \mathbf{n} = 0 \quad \text{on } \Gamma_{\text{PEC}}. \quad (2.21)$$

A PMC wall is described by natural boundary conditions

$$\mu^{-1} \text{curl } \mathbf{A}^* \times \mathbf{n} = 0 \quad \text{on } \Gamma_{\text{PMC}}. \quad (2.22)$$

Compare to (2.15), respectively by

$$\mu^{-1} \text{curl } \mathbf{A}^* \times \mathbf{n} = -\mathbf{j}_{\Gamma,i} \quad \text{on } \Gamma \quad (2.23)$$

if impressed surface currents $\mathbf{j}_{\Gamma,i}$ are included.

As already mentioned above, the introduced potentials \mathbf{A}^* and ϕ are not unique. Uniqueness can be enforced by imposing additional conditions, which is called *gauging*. In case of constant coefficients the so-called *Coulomb-gauge* is commonly used, where

$$\text{div } \mathbf{A}^* = 0$$

is required together with the additional boundary condition $\mathbf{A}^* \cdot \mathbf{n} = 0$. Furthermore, the impressed currents are assumed to be divergence free, i.e. $\text{div } \mathbf{j}_i = 0$.

2.3 Special electromagnetic regimes

In many practical applications one does not have to deal with the full system of Maxwell's equations (2.5a)-(2.5d). Taking into account the physics of the considered problem, the system (2.5) can often be simplified. We will distinguish between the time-harmonic case, slowly and fast varying electromagnetic fields, and the static regime. For a detailed overview of the most commonly investigated problem classes, we refer to VAN RIENEN [92], BÍRÓ [18], and in the special case of high-frequency scattering problems to MONK [70].

2.3.1 Time-harmonic Maxwell equations

The investigation of a time harmonic setting is interesting for two reasons: First, the Fourier transformation in time can be applied to the nonstationary equations, and a general solution can be obtained afterwards by superposition of the solutions at the several frequencies. Secondly, if a system is excited with a signal of a single frequency, then a single-frequency analysis is appropriate. We assume the electromagnetic fields \mathbf{E} , \mathbf{D} , \mathbf{H} and \mathbf{B} to be time-harmonic, i.e. of the form

$$\mathbf{u}(\mathbf{x}, t) = \operatorname{Re}(\hat{\mathbf{u}}(\mathbf{x})e^{i\omega t}), \quad (2.24)$$

where the hat accounts for complex-valued functions and Re denotes the real part of complex numbers. To stay consistent we assume also the charge density ρ , as well as the current density \mathbf{j} to be of the form (2.24). For ease of notation, we will omit the hat marker in the sequel, e.g., we denote $\hat{\mathbf{E}}$ by \mathbf{E} and so on. The transformation into the frequency domain implies complex-valued fields, but has the advantage that the derivative with respect to time is replaced by a simple multiplication operator, i.e.,

$$\frac{\partial u}{\partial t}(\mathbf{x}, t) \rightarrow i\omega u(\mathbf{x}, t).$$

By this transformation, the time-harmonic Maxwell equations can be stated as

$$\operatorname{curl} \mathbf{E}(\mathbf{x}) + i\omega\mu\mathbf{H}(\mathbf{x}) = 0, \quad (2.25a)$$

$$\operatorname{div} \mu\mathbf{H}(\mathbf{x}) = 0, \quad (2.25b)$$

$$\operatorname{curl} \mathbf{H}(\mathbf{x}) - (i\omega\epsilon + \sigma)\mathbf{E}(\mathbf{x}) = \mathbf{j}_i(\mathbf{x}), \quad (2.25c)$$

$$\operatorname{div} \epsilon\mathbf{E}(\mathbf{x}) = \rho(\mathbf{x}). \quad (2.25d)$$

The continuity equation (2.6) transforms to

$$i\omega\rho(\mathbf{x}) + \operatorname{div} \mathbf{j}(\mathbf{x}) = 0. \quad (2.26)$$

Thus we can easily eliminate the charge density in a time-harmonic setting. The *vector potential formulation* (2.20) then reads

$$\operatorname{curl} \mu^{-1} \operatorname{curl} \mathbf{A} + i\omega\sigma\mathbf{A} - \omega^2\epsilon\mathbf{A} = \mathbf{j}_i \quad (2.27)$$

where we used $\mathbf{E} = -i\omega\mathbf{A}$ and $\mathbf{B} = \operatorname{curl} \mathbf{A}$. Furthermore, the mixed impedance boundary condition (2.18) on $\Gamma_R \subset \partial\Omega$ is transformed into a Robin-type condition of the form

$$\mu^{-1} \operatorname{curl} \mathbf{A} \times \mathbf{n} + \kappa i\omega\mathbf{A} \times \mathbf{n} = 0 \quad \text{on } \Gamma_R.$$

2.3.2 Magneto-Quasistatic Fields: The Eddy-Current Problem

A special class of time-dependent electromagnetic problems arises, when at least one of the electromagnetic fields varies only slowly in time. In so-called *quasistatic models* the time-derivative of the magnetic flux or the electric flux is therefore neglected. We focus here on *magneto-quasistatic* problems, which are suitable for low-frequency applications like, e.g., electric motors, relays and transformers. In this case, the magnetic induction is the dominant factor, and the contribution of the displacement currents is negligible in comparison to the currents, i.e. $|\frac{\partial \mathbf{D}}{\partial t}| \ll |\mathbf{j}|$. We can therefore neglect the contribution of the displacement currents and use Ampère's law in its original form to obtain

$$\begin{aligned}\frac{\partial \mathbf{B}}{\partial t} + \operatorname{curl} \mathbf{E} &= 0, \\ \operatorname{div} \mathbf{B} &= 0, \\ \operatorname{curl} \mathbf{H} &= \mathbf{j}, \\ \operatorname{div} \mathbf{D} &= \rho.\end{aligned}$$

Note that a coupling between magnetic and electric fields occurs only in conducting materials. The quasi-static electromagnetic equations in vector potential formulation are given by

$$\sigma \frac{\partial \mathbf{A}}{\partial t} + \operatorname{curl} \mu^{-1} \operatorname{curl} \mathbf{A} = \mathbf{j}_i \quad (2.28)$$

with $\mathbf{B} = \operatorname{curl} \mathbf{A}$ and $\mathbf{E} = -\frac{\partial \mathbf{A}}{\partial t}$; the conduction current is given by $\mathbf{j}_c = -\sigma \frac{\partial \mathbf{A}}{\partial t}$. The time harmonic magneto-quasistatic vector potential formulation reads

$$\operatorname{curl} \mu^{-1} \operatorname{curl} \mathbf{A} + i\omega\sigma \mathbf{A} = \mathbf{j}_i. \quad (2.29)$$

2.3.3 Static field equations

If the electromagnetic field is generated only by static or uniformly moving charges, we can assume all fields to be time-independent. We can skip the terms involving time-derivatives in Faraday's and Ampère's law, namely (2.5a) and (2.5c).

Electrostatic fields can only occur in non-conducting regions ($\sigma = 0$). Hence the magnetic and the electric fields are decoupled and we can deduce two independent systems.

The electrostatic problem is described by the system

$$\begin{aligned}\operatorname{curl} \mathbf{E} &= 0, \\ \operatorname{div} \mathbf{D} &= \rho, \\ \mathbf{D} &= \epsilon \mathbf{E}.\end{aligned}$$

By introducing the scalar potential ϕ such that $\mathbf{E} = -\nabla\phi$, the electrostatic problem simplifies to the Poisson-equation

$$-\operatorname{div}(\epsilon \nabla \phi) = \rho \quad \text{in } \Omega. \quad (2.30)$$

Note that the potential ϕ is defined only up to constants. Suitable boundary conditions can be derived from the boundary conditions for the electric field and its flux. Given surface charges $D \cdot \mathbf{n} = -\rho_S$ are introduced as a natural boundary condition

$$\epsilon \frac{\partial \phi}{\partial \mathbf{n}} = -\rho_S \quad \text{on } \Gamma_N. \quad (2.31)$$

In case of an adjacent perfect electric conductor (PEC) we require $\nabla\phi \times \mathbf{n} = 0$, which is satisfied if the potential is constant on each connected part $\Gamma_{\text{PEC},i}$ of the PEC boundary, i.e.,

$$\phi = U_i \quad \text{on } \Gamma_{\text{PEC},i}. \quad (2.32)$$

Here, the constants $U_i = \int_{\Gamma_i} \mathbf{E} \cdot \mathbf{n} dA$ are the applied voltages at the boundary $\Gamma_{\text{PEC},i}$.

The magnetostatic problem simplifies to

$$\begin{aligned} \text{curl } \mathbf{H} &= \mathbf{j}_i, \\ \text{div } \mathbf{B} &= 0, \\ \mathbf{B} &= \mu \mathbf{H}. \end{aligned}$$

Applying the divergence on the first equation shows that impressed currents have to be divergence free, i.e.

$$\text{div } \mathbf{j}_i = 0, \quad (2.33)$$

in order to provide consistency. We again introduce a vector potential \mathbf{A} satisfying $\mathbf{B} = \text{curl } \mathbf{A}$. Then the magnetostatic vector potential problem reads

$$\text{curl } \mu^{-1} \text{curl } \mathbf{A} = \mathbf{j}_i. \quad (2.34)$$

As outlined above, the vector potential \mathbf{A} of the magnetostatic problem is only defined up to gradient functions. Uniqueness can be enforced, e.g., by *Coulomb Gauge*, where we additionally require

$$\text{div } \mathbf{A} = 0 \quad \text{in } \Omega. \quad (2.35)$$

Essential boundary conditions

$$\mathbf{A} \times \mathbf{n} = 0 \quad \text{on } \Gamma_B, \quad (2.36)$$

imply that the magnetic flux through the boundary is zero, i.e. $\mathbf{B} \cdot \mathbf{n} = 0$. Impressed surface currents ($\mathbf{H} \times \mathbf{n} = -\mathbf{j}_S$) are introduced by *natural boundary conditions*

$$\mu^{-1} \text{curl } \mathbf{A} \times \mathbf{n} = -\mathbf{j}_S \quad \text{on } \Gamma_H \quad (2.37)$$

The homogeneous condition $\mu^{-1} \text{curl } \mathbf{A} \times \mathbf{n} = 0$ models magnetic symmetry planes or adjacent perfectly magnetic conduction regions. We note that in the case of multiple non-connected parts of Γ_H , one has to pose some further integral conditions for the magnetic flux over each several part of Γ_H or the magnetic voltage between these parts. For details we refer to BÍRÓ [18].

2.4 The general curl-curl problem

The time-harmonic and magneto-static problems discussed in the previous section have a common structure, which suggest to treat them - analytically and numerically - in a common framework. Note that similar problems also arise in the solution of Maxwell eigenvalue problems (see Chapter 7), in the solution of time dependent problems in each time step of a numerical integration scheme, but also in the solution of nonlinear problems via Newton's method. The general structure is that of the the following curl-curl problem:

Problem 2.1. Let $\Omega \subset \mathbb{R}^3$ a bounded domain with boundary $\partial\Omega = \Gamma_D \cup \Gamma_N$. Find \mathbf{u} such that

$$\begin{aligned} \operatorname{curl} \mu^{-1} \operatorname{curl} \mathbf{u} + \kappa \mathbf{u} &= \mathbf{f} && \text{in } \Omega \subset \mathbb{R}^3, \\ (\mathbf{u} \times \mathbf{n}) \times \mathbf{n} &= g_D && \text{on } \Gamma_D, \\ \mu^{-1} \operatorname{curl} \mathbf{u} \times \mathbf{n} &= g_N && \text{on } \Gamma_N. \end{aligned}$$

The parameter κ is defined problem-depending as

- $\kappa = 0$ for the magnetostatic problem (2.34),
- $\kappa = i\omega\sigma - \epsilon\omega^2 \in \mathbb{C}$ for the time-harmonic Maxwell equations in the vector potential formulation (2.27),
- $\kappa = i\omega\sigma$ for quasi-static problems (2.29) in case of low-frequency applications,
- $\kappa = -\epsilon\omega^2 \in \mathbb{R}^-$ for high-frequency applications (electromagnetic waves in cavities).

For the sake of simplicity we assume below that the parameters μ, ϵ, σ are scalars, i.e. the underlying material is isotropic.

In order to be able to treat the various problems in this common framework, we have to focus on numerical methods that are robust with respect to the parameter κ . This will be one of the key aspects in our analysis.

In order to show applicability in all regimes of κ values, we will investigate magneto-static, time-harmonic quasistatic (low-frequency), and eigenvalue problems in more detail.

Chapter 3

Function Spaces and Variational Formulations

In the previous chapter we discussed several problems governed by Maxwell's equations. The electrostatic problem resulted in a Poisson-type problem

$$-\operatorname{div}(\kappa\nabla\varphi) = f \quad + b.c. \quad (3.1)$$

for the scalar potential φ . In time-harmonic formulations as well as in time-stepping schemes we obtained curl-curl problems of the form

$$\operatorname{curl} \mu^{-1} \operatorname{curl} \mathbf{u} + \kappa \mathbf{u} = \mathbf{j} \quad + b.c., \quad (3.2)$$

with a vector field \mathbf{u} , a given current density \mathbf{j} , permeability μ and a problem depending parameter $\kappa \in \mathbb{C}$.

In this chapter we introduce the natural function spaces for a variational formulation of the partial differential equations under consideration, i.e., $H^1(\Omega)$, $H(\operatorname{curl}, \Omega)$, and $H(\operatorname{div}, \Omega)$, and provide a short overview of definitions and basic results on weak derivatives and trace operators. We then discuss in some detail properties of the involved differential operators, namely the gradient, the divergence and the curl operator, and show that the function spaces are naturally connected via the differential operators. This leads to the formalism of the *de Rham Complex*, which is an important property of the function spaces on the continuous level that should also be conserved for finite dimensional approximations. Hence de Rham complexes will play an important role in our construction of finite element spaces as well as design and analysis of preconditioners and error estimators presented below. Finally, we recall the basic existence and uniqueness results for variational problems and derive the existence and uniqueness of solutions to the electromagnetic problems under consideration.

3.1 Vector-valued Function Spaces, Trace Operators and Green's formulas

We start with the definition and basic properties of the operators involved in the various formulations of Maxwell's equations presented so far: Let $\Omega \subset \mathbb{R}^d$, $d = 2, 3$ be a domain. The *gradient* operator of a scalar function φ is defined as

$$\nabla\varphi := \left(\frac{\partial\varphi}{\partial x_1}, \dots, \frac{\partial\varphi}{\partial x_d} \right) \quad (3.3)$$

and the *divergence* of a vector $\mathbf{v} = (v_1, \dots, v_d)$ is defined as

$$\operatorname{div} \mathbf{v} = \nabla \cdot \mathbf{v} := \sum_{i=1}^d \frac{\partial v_i}{\partial x_i}. \quad (3.4)$$

In two dimensions, there are two definitions of the curl-operator. For $\Omega \subset \mathbb{R}^2$, the *vector curl* operator of a scalar function q is defined as

$$\operatorname{Curl} q := \left(\frac{\partial q}{\partial x_2}, -\frac{\partial q}{\partial x_1} \right)^T, \quad (3.5)$$

and the *scalar curl* operator acting on a vector function $\mathbf{v} = (v_1, v_2)$ as

$$\operatorname{curl} \mathbf{v} = \nabla \times \mathbf{v} := \frac{\partial v_2}{\partial x_1} - \frac{\partial v_1}{\partial x_2}. \quad (3.6)$$

For $\Omega \subset \mathbb{R}^3$ the *curl* operator of a vector function $\mathbf{v} = (v_1, v_2, v_3)$ is defined as

$$\operatorname{curl} \mathbf{v} = \nabla \times \mathbf{v} := \left(\frac{\partial v_2}{\partial x_3} - \frac{\partial v_3}{\partial x_2}, \frac{\partial v_1}{\partial x_3} - \frac{\partial v_3}{\partial x_1}, \frac{\partial v_1}{\partial x_2} - \frac{\partial v_2}{\partial x_1} \right)^T. \quad (3.7)$$

We next recall the definition of derivatives in the weak sense:

Definition 3.1 (Generalized differential operators).

1. For $w \in L_2(\Omega)$ we call $\mathbf{g} = \nabla w$ the (generalized) gradient of w , if there holds

$$\int_{\Omega} \mathbf{g} \cdot \mathbf{v} \, d\mathbf{x} = - \int_{\Omega} w \operatorname{div} \mathbf{v} \, d\mathbf{x} \quad \forall \mathbf{v} \in (C_0^\infty(\overline{\Omega}))^3.$$

2. For $\mathbf{u} \in (L_2(\Omega))^3$ we call $\mathbf{c} = \operatorname{curl} \mathbf{u} \in (L_2(\Omega))^3$ the (generalized) curl of \mathbf{u} , if there holds

$$\int_{\Omega} \mathbf{c} \cdot \mathbf{v} \, d\mathbf{x} = \int_{\Omega} \mathbf{u} \cdot \operatorname{curl} \mathbf{v} \, d\mathbf{x} \quad \forall \mathbf{v} \in [C_0^\infty(\overline{\Omega})]^3.$$

3. For $\mathbf{q} \in (L_2(\Omega))^3$ we call $d = \operatorname{div} \mathbf{q} \in L_2(\Omega)$ the (generalized) divergence of \mathbf{q} , if there holds

$$\int_{\Omega} d \, v \, d\mathbf{x} = - \int_{\Omega} \mathbf{q} \cdot \nabla v \, d\mathbf{x} \quad \forall v \in C_0^\infty(\overline{\Omega}).$$

The following function spaces will turn out to provide a natural setting for the investigation of the PDEs discussed above.

Definition 3.2 (Function Spaces). *Let us define the spaces*

$$\begin{aligned} L_2(\Omega) &:= \{u \mid \int_{\Omega} u^2 \, d\mathbf{x} < \infty\} \\ H^1(\Omega) &:= \{\varphi \in L_2(\Omega) \mid \nabla \varphi \in [L_2(\Omega)]^3\} \\ H(\operatorname{curl}, \Omega) &:= \{\mathbf{v} \in [L_2(\Omega)]^3 \mid \operatorname{curl} \mathbf{v} \in [L_2(\Omega)]^3\} \\ H(\operatorname{div}, \Omega) &:= \{\mathbf{q} \in [L_2(\Omega)]^3 \mid \operatorname{div} \mathbf{q} \in L_2(\Omega)\} \end{aligned}$$

and the corresponding scalar products by

$$\begin{aligned} (u, v)_0 &= \int_{\Omega} uv \, d\mathbf{x} \\ (\varphi, \psi)_1 &= \int_{\Omega} \nabla \varphi \cdot \nabla \psi \, d\mathbf{x} + (\varphi, \psi)_0 \\ (\mathbf{u}, \mathbf{v})_{\text{curl}} &= \int_{\Omega} \text{curl } \mathbf{u} \cdot \text{curl } \mathbf{v} \, d\mathbf{x} + (\mathbf{u}, \mathbf{v})_0 \\ (\mathbf{p}, \mathbf{q})_{\text{div}} &= \int_{\Omega} \text{div } \mathbf{p} \, \text{div } \mathbf{q} \, d\mathbf{x} + (\mathbf{p}, \mathbf{q})_0 \end{aligned}$$

The induced norms are denoted by $\|\cdot\|_0$, $\|\cdot\|_1$, $\|\cdot\|_{\text{curl}}$, and $\|\cdot\|_{\text{div}}$.

We only mention that elements in the above spaces have to be understood as equivalence classes, i.e., two functions are considered to be equal (belong to the same equivalence class) if they coincide up to a set of zero measure. All the above spaces are Hilbert spaces when equipped with the corresponding scalar products, in particular they are complete.

For the results of this section we need some conditions on the underlying domain Ω and its boundary $\Gamma := \partial\Omega$.

Definition 3.3 (Lipschitz-domain). *The boundary of a domain $\Omega \subset \mathbb{R}^3$ is called Lipschitz-continuous, if there exist a finite number of domains ω_i , local coordinate systems (ξ_i, η_i, ζ_i) , and Lipschitz-continuous functions $b(\xi_i, \eta_i)$ such that*

- $\partial\Omega \subset \bigcup \omega_i$ with $\partial\Omega \cap \omega_i = \{(\xi_i, \eta_i, \zeta_i) | \zeta_i = b(\xi_i, \eta_i)\}$,
- $\Omega \cap \omega_i = \{(\xi_i, \eta_i, \zeta_i) | \zeta_i > b(\xi_i, \eta_i)\}$.

Ω is then called a Lipschitz-domain.

The boundary $\partial\Omega$ of a Lipschitz-domain can be represented locally by the graph of b_i and Ω lies locally on one side of this graph. We want to mention that this definition allows domains with corners, but cuts are excluded. We refer to MCLEAN [67] for other examples of non-Lipschitz domains. Also note that a Lipschitz-boundary enables the definition of an outer unit vector \mathbf{n} almost everywhere on $\partial\Omega$.

For Lipschitz-domains with $\partial\Omega$ bounded the following density results hold (see GIRAULT-RAVIART [49]):

$$H^1(\Omega) = \overline{C^\infty(\overline{\Omega})}^{\|\cdot\|_1}, \quad H(\text{curl}, \Omega) = \overline{C^\infty(\overline{\Omega})}^{\|\cdot\|_{\text{curl}}}, \quad \text{and} \quad H(\text{div}, \Omega) = \overline{C^\infty(\overline{\Omega})}^{\|\cdot\|_{\text{div}}}, \quad (3.8)$$

which allows to easily extend classical properties of C^∞ functions also to the above function spaces.

In the sequel, we recall important trace and extension theorems, and different versions of Green's formula. Those results will be needed to state the differential equations in a variational setting and to consider boundary and interface conditions.

Trace theorems for the space $H^1(\Omega)$

The trace of a smooth function $\varphi \in C(\overline{\Omega})$ is defined pointwise as

$$(tr_{\partial\Omega} u)(x) = u(x) \quad \forall x \in \partial\Omega, \quad \text{briefly } tr_{\partial\Omega}(u) = u|_{\partial\Omega}.$$

Using the density result (3.8) we can extend the classical trace concept to more general function spaces:

Theorem 3.4 (Trace theorem and Greens formula for $H^1(\Omega)$). *Let $\Omega \subset \mathbb{R}^d$, $d = 2, 3$ be a bounded Lipschitz-domain.*

1. *The classical trace mapping $tr_{\partial\Omega}$ defined on $C^\infty(\Omega)$ can be uniquely extended to a continuous, linear operator*

$$tr_{\partial\Omega} : H^1(\Omega) \rightarrow H^{1/2}(\partial\Omega) \quad \text{with} \quad \|tr_{\partial\Omega}(v)\|_{1/2} \preceq \|v\|_1 \quad \forall v \in H^1(\Omega),$$

where $H^{1/2}(\partial\Omega) := \overline{C^\infty(\partial\Omega)}^{\|\cdot\|_{1/2}}$ and $\|u\|_{1/2}^2 = \|u\|_0^2 + \int_{\partial\Omega} \int_{\partial\Omega} \frac{|u(\mathbf{x}) - u(\mathbf{y})|^2}{|\mathbf{x} - \mathbf{y}|^d} d\mathbf{x} d\mathbf{y}$, where \preceq refers to \leq up to a constant.

2. *There holds the integration by parts formula*

$$\int_{\Omega} \nabla u \cdot \mathbf{v} d\mathbf{x} = - \int_{\Omega} u \operatorname{div} \mathbf{v} d\mathbf{x} + \int_{\partial\Omega} tr_{\partial\Omega}(u) \mathbf{v} \cdot \mathbf{n} d\mathbf{x} \quad \forall u \in H^1(\Omega) \quad \forall \mathbf{v} \in H(\operatorname{div}, \Omega). \quad (3.9)$$

3. *Let $g \in H^{1/2}(\partial\Omega)$. Then there holds*

$$\exists v \in H^1(\Omega) : tr_{\partial\Omega}(v) = g \quad \text{with} \quad \|v\|_1 \preceq \|g\|_{1/2}.$$

The third statement is an *extension theorem*, which is important for incorporation of Dirichlet boundary conditions. Here and below, we use Sobolev spaces of fractional order on manifolds, which can be defined similarly as in the theorem above, or as traces of certain classes of functions on Ω ; for their definition we refer in particular to MCLEAN [67].

The following corollary discusses the interface conditions of H^1 -functions.

Corollary 3.5. *Let $\Omega_1, \dots, \Omega_m$ be bounded Lipschitz domains and a non-overlapping domain decomposition of Ω , i.e. $\Omega_i \cap \Omega_j = \emptyset$ for $i \neq j$ and $\bigcup \overline{\Omega}_i = \overline{\Omega}$ with interfaces $\Gamma_{ij} := \partial\Omega_i \cap \partial\Omega_j$. Suppose $u_i := u|_{\Omega_i} \in H^1(\Omega_i)$ and $tr_{\Gamma_{ij}} u_i = tr_{\Gamma_{ij}} u_j$. Then*

$$u \in H^1(\Omega) \quad \text{and} \quad (\nabla u)|_{\Omega_i} = \nabla u_i.$$

This result is fundamental for the construction of conforming finite element methods, where the discrete space is chosen as a subspace of $H^1(\Omega)$. If the finite element functions, which are defined elementwise, are continuous over the element interfaces, then the global FE-function is in $H^1(\Omega)$. Note also that the space $H_0^1(\Omega) := \overline{C_0^\infty(\Omega)}^{\|\cdot\|_1}$ is equal to the space of H^1 functions with homogenous Dirichlet boundary conditions, i.e.,

$$H_0^1(\Omega) = \{u \in H^1(\Omega) \mid tr_{\partial\Omega} u = 0\}.$$

For Poisson problems with pure Neumann boundary conditions, we will utilize the quotient space,

$$H^1(\Omega)/\mathbb{R} = \{u \in H^1(\Omega) \mid \int_{\partial\Omega} u d\mathbf{x} = 0\}.$$

Some results concerning the space $H(\text{curl})$

Let us consider the following tangential traces for vector functions $\mathbf{v} \in [C^\infty(\bar{\Omega})]^d$, $d = 2, 3$:

- $tr_\tau(\mathbf{v})(\mathbf{x}) := \mathbf{v}(\mathbf{x}) \cdot \boldsymbol{\tau}(\mathbf{x})$ for $\mathbf{x} \in \Gamma$ and $\Omega \subset \mathbb{R}^2$,
- $tr_\tau(\mathbf{v})(\mathbf{x}) := \mathbf{v}(\mathbf{x}) \times \mathbf{n}(\mathbf{x})$ for $\mathbf{x} \in \Gamma$ and $\Omega \subset \mathbb{R}^3$,
- $tr_T(\mathbf{v})(\mathbf{x}) := (\mathbf{v}(\mathbf{x}) \times \mathbf{n}(\mathbf{x})) \times \mathbf{n}(\mathbf{x})$ for $\mathbf{x} \in \Gamma$ and $\Omega \subset \mathbb{R}^3$,

with $\boldsymbol{\tau}$ denoting the tangential vector and \mathbf{n} the outer unit normal vector on $\Gamma := \partial\Omega$. Due to the density result (3.8) we can extend the trace mapping to a wider class of functions:

Theorem 3.6 (Trace theorem and integration by parts in $H(\text{curl})$). *Let Ω be a bounded Lipschitz-domain.*

1. *The classical trace map tr_τ can be extended from $[C^\infty(\bar{\Omega})]^d$ to a continuous and linear map (still denoted by tr_τ)*

$$tr_\tau : H(\text{curl}, \Omega) \rightarrow [H^{-1/2}(\partial\Omega)]^m, \quad \text{and} \quad \|tr_\tau(\mathbf{v})\|_{-1/2} \preceq \|\mathbf{v}\|_{\text{curl}} \quad \forall \mathbf{v} \in H(\text{curl}),$$

where $m = 3$ if $\Omega \subset \mathbb{R}^3$ or $m = 1$ if $\Omega \subset \mathbb{R}^2$.

2. *There holds the integration by parts formula*

$$\int_{\Omega} \text{curl } \mathbf{u} \cdot \boldsymbol{\varphi} \, d\mathbf{x} = \int_{\Omega} \mathbf{u} \cdot \text{Curl } \boldsymbol{\varphi} \, d\mathbf{x} - s \int_{\Gamma} tr_\tau(\mathbf{u}) \cdot \boldsymbol{\varphi} \, d\mathbf{x} \quad \forall \mathbf{u} \in H(\text{curl}, \Omega) \forall \boldsymbol{\varphi} \in (H^1(\Omega))^d. \quad (3.10)$$

For $m = 3$ Curl and curl are defined to be the same.

In 3D, the generalized tangential trace operator tr_τ is not surjective onto $H^{-1/2}(\partial\Omega)$, its range coincides with

$$H^{-1/2}(\text{div}, \partial\Omega) := \{ \mathbf{v} \in (H^{-1/2}(\partial\Omega))^3 \mid \mathbf{v} \cdot \mathbf{n} = 0 \text{ a.e. on } \partial\Omega, \text{div}_{\partial\Omega} \mathbf{v} \in H^{-1/2}(\partial\Omega) \}.$$

This results in the following

Theorem 3.7 (Extension theorem for $H(\text{curl})$). *For $\mathbf{g} \in H^{-1/2}(\text{div}, \partial\Omega)$ there exists a $\mathbf{v} \in H(\text{curl}, \Omega)$ with*

$$tr_\tau(\mathbf{v}) = \mathbf{g} \quad \text{and} \quad \|\mathbf{v}\|_{\text{curl}}^2 \preceq \|\mathbf{g}\|_{-1/2}^2 + \|\text{div}_{\partial\Omega} \mathbf{g}\|_{-1/2}^2.$$

The closure, with respect to the $H(\text{curl})$ -norm, of the space of infinitely differentiable functions with compact support in Ω is denoted by

$$H_0(\text{curl}) := \overline{[C_0^\infty(\Omega)]^3}^{\|\cdot\|_{\text{curl}}}.$$

This space is equal to the space of $H(\text{curl})$ functions with homogenous tangential boundary conditions, i.e.,

$$H_0(\text{curl}, \Omega) = \{ \mathbf{u} \in H(\text{curl}, \Omega) \mid (\mathbf{u} \times \mathbf{n}) \times \mathbf{n} = 0 \}.$$

The following corollary treats the interface conditions for $H(\text{curl})$ -functions.

Corollary 3.8. *Let $\Omega_1, \dots, \Omega_m$ be a non-overlapping domain decomposition of Ω , i.e. $\Omega_i \cap \Omega_j = \emptyset$ and $\bigcup \bar{\Omega}_i = \bar{\Omega}$ with interfaces $\Gamma_{ij} = \partial\Omega_i \cap \partial\Omega_j$. Suppose $\mathbf{u}_i := \mathbf{u}|_{\Omega_i} \in H(\text{curl}, \Omega_i)$ and $\text{tr}_{T_i, \Gamma_{ij}} \mathbf{u}_i = \text{tr}_{T_i, \Gamma_{ij}} \mathbf{u}_j$. Then*

$$\mathbf{u} \in H(\text{curl}, \Omega) \quad \text{and} \quad (\text{curl } \mathbf{u})|_{\Omega_i} = \text{curl } \mathbf{u}_i.$$

Thus conforming finite element spaces for discretization of $H(\text{curl})$ can be constructed by requiring the tangential components to be continuous over the element interfaces. This ensures that the resulting global finite element functions are in $H(\text{curl}, \Omega)$. Note that the normal components of $H(\text{curl})$ functions need not to be continuous.

Basic results on the $H(\text{div})$ space

For $\mathbf{v} \in (C_0^\infty(\bar{\Omega}))^d$, $d = 2, 3$ the normal trace is defined by

$$(\text{tr}_{\mathbf{n}}(\mathbf{v}))(\mathbf{x}) := \mathbf{v}(\mathbf{x}) \cdot \mathbf{n}(\mathbf{x}) \quad \forall \mathbf{x} \text{ on } \Gamma := \partial\Omega,$$

where \mathbf{n} denotes the outward unit normal vector on Γ . Utilizing that $[C^\infty(\bar{\Omega})]^d$ is dense in $H(\text{div}, \Omega)$, the trace operator can be extended to the whole $H(\text{div})$ space.

Theorem 3.9 (Trace theorems and integration by parts for $H(\text{div}, \Omega)$). *Let Ω be a bounded Lipschitz-domain.*

1. *The trace map $\text{tr}_{\mathbf{n}}$ can be extended as a bounded, linear mapping (still denoted by $\text{tr}_{\mathbf{n}}$)*

$$\text{tr}_{\mathbf{n}} : H(\text{div}, \Omega) \rightarrow [H^{-1/2}(\partial\Omega)]^3, \quad \text{and} \quad \|\text{tr}_{\mathbf{n}}(\mathbf{v})\|_{-1/2} \preceq \|\mathbf{v}\|_{\text{div}} \quad \forall \mathbf{v} \in H(\text{div}, \Omega).$$

2. *There holds the following version of Green's theorem:*

$$\int_{\Omega} \text{div } \mathbf{u} \varphi \, d\mathbf{x} = - \int_{\Omega} \mathbf{u} \cdot \nabla \varphi \, d\mathbf{x} + \langle \text{tr}_{\mathbf{n}}(\mathbf{u}), \varphi \rangle \quad \forall \mathbf{u} \in H(\text{div}, \Omega), \quad \forall \varphi \in (H^1(\Omega))^3, \quad (3.11)$$

where $\langle \cdot, \cdot \rangle$ denotes the duality product $\langle \cdot, \cdot \rangle_{H^{-\frac{1}{2}} \times H^{\frac{1}{2}}}$.

3. *Suppose $g \in H^{-1/2}(\Gamma)$. Then there holds the extension theorem:*

$$\exists \mathbf{v} \in H(\text{div}, \Omega) : \quad \text{tr}_{\mathbf{n}} \mathbf{v} = g \quad \text{and} \quad \|\mathbf{v}\|_{\text{div}} \preceq \|g\|_{-1/2}.$$

The closure of arbitrary differentiable functions with compact support in Ω in the $H(\text{div})$ -norm is denoted by

$$H_0(\text{div}) := \overline{[C_0^\infty(\Omega)]^3}^{\|\cdot\|_{\text{curl}}}$$

and equals the space of $H(\text{div})$ functions with homogeneous normal boundary condition, i.e.,

$$H_0(\text{div}, \Omega) = \{\mathbf{v} \in H(\text{div}, \Omega) \mid \text{tr}_{\mathbf{n}, \partial\Omega}(\mathbf{v}) = 0\}.$$

The following corollary deals with appropriate interface conditions for $H(\text{div})$ -functions.

Corollary 3.10. *Let $\Omega_1, \dots, \Omega_m$ be a non-overlapping domain decomposition of Ω , i.e. $\Omega_i \cap \Omega_j = \emptyset$ and $\bigcup \bar{\Omega}_i = \bar{\Omega}$ with interfaces $\Gamma_{ij} = \partial\Omega_i \cap \partial\Omega_j$. Suppose $\mathbf{u}_i := \mathbf{u}|_{\Omega_i} \in H(\text{div}, \Omega_i)$ and $\mathbf{u}_i|_{\Gamma_{ij}} \cdot \mathbf{n}_i = \mathbf{u}_j|_{\Gamma_{ij}} \cdot \mathbf{n}_i$. Then*

$$\mathbf{u} \in H(\text{div}, \Omega) \quad \text{and} \quad (\text{div } \mathbf{u})|_{\Omega_i} = \text{div } \mathbf{u}_i.$$

Due to this corollary conformity of finite element functions in $H(\text{div})$ can be guaranteed by requiring continuity of the normal components across element interfaces.

3.2 Mapping Properties of Differential Operators

In the previous chapter we introduced vector and scalar potential formulations for Maxwell's equations in their classical, strong form. Now, we want to extend this concept also to the generalized differentiability setting presented in this chapter. The question on the existence of potential fields is strongly connected to the characterization of the kernel and the range of the involved differential operators.

The following notation for the kernel of the differential operators will be used:

$$\begin{aligned}\ker(\nabla) &:= \{\mathbf{v} \in H^1(\Omega) \mid \nabla \mathbf{v} = 0\}, \\ \ker(\operatorname{curl}) &:= \{\mathbf{v} \in H(\operatorname{curl}, \Omega) \mid \operatorname{curl} \mathbf{v} = 0\}, \\ \ker(\operatorname{div}) &:= \{\mathbf{v} \in H(\operatorname{div}, \Omega) \mid \operatorname{div} \mathbf{v} = 0\},\end{aligned}$$

The corresponding range spaces are denoted by $\nabla H^1(\Omega)$, $\operatorname{curl} H(\operatorname{curl}, \Omega)$, $\operatorname{div} H(\operatorname{div}, \Omega)$.

The well-known identities

$$\operatorname{curl}(\nabla \phi) = 0, \quad (3.12a)$$

$$\operatorname{div}(\operatorname{curl} \mathbf{u}) = 0, \quad (3.12b)$$

which are trivially satisfied for twice continuously differentiable functions, can be generalized to the Hilbert spaces under consideration in the following way:

$$\nabla H^1(\Omega) \subset \ker(\operatorname{curl}), \quad (3.13a)$$

$$\operatorname{curl} H(\operatorname{curl}, \Omega) \subset \ker(\operatorname{div}), \quad (3.13b)$$

$$\operatorname{div} H(\operatorname{div}, \Omega) \subset L_2(\Omega). \quad (3.13c)$$

Identities instead of inclusions hold in general only under additional assumptions on the domain Ω . For the following statements, we assume Ω to be a bounded, simply-connected Lipschitz-domain (the case of multiply-connected domains is treated in GIRAULT-RAVIART [49] and DAUTRAY-LIONS [40]. For more general domains, namely pseudo-Lipschitz domains where also cuts are allowed, we refer to AMROUCHE ET AL. [4]).

Assumption 3.11. *Let Ω be a bounded, simply-connected Lipschitz-domain.*

The nullspace (in $H^1(\Omega)$) of the gradient operator is the set of constant functions. Consequently, the nullspace can be made trivial by restriction to $H_0^1(\Omega)$ or $H^1(\Omega)/\mathbb{R}$:

$$\ker(\nabla, H^1(\Omega)) = \mathbb{R} \quad \text{and} \quad \ker(\nabla, H_0^1(\Omega)) = \ker(\nabla, H^1(\Omega)/\mathbb{R}) = \{0\}.$$

The classical Stokes theorem on the existence of a scalar potential of curl-free functions can be extended in the following way, cf. [49, Theorem 2.9].

Theorem 3.12 (Existence of scalar potentials). *Let $\mathbf{u} \in L_2(\Omega)^d$ denote a vector field. Then $\operatorname{curl} \mathbf{u} = 0$ in Ω*

- *if and only if there exists a scalar-potential $\phi \in H^1(\Omega)$ such that $\mathbf{u} = \nabla \phi$, where ϕ is unique up to an additive constant.*
- *if and only if there exists a unique scalar-potential $\phi \in H^1(\Omega)/\mathbb{R}$ such that $\mathbf{u} = \nabla \phi$.*

In other words, $\nabla(H^1(\Omega)) = \ker(\text{curl})$.

Theorem 3.13 (Existence of vector potentials, cf. [49, Theorem 3.4, 3.5, and 3.6]). *Let $\mathbf{u} \in [L_2(\Omega)]^3$ denote a vector field.*

1. \mathbf{u} is divergence-free

$$\text{div } \mathbf{u} = 0$$

if and only if there exists a vector potential $\boldsymbol{\psi} \in [H^1(\Omega)]^3$ such that

$$\mathbf{u} = \text{curl } \boldsymbol{\psi}.$$

Furthermore, $\boldsymbol{\psi}$ can be chosen such that $\text{div } \boldsymbol{\psi} = 0$.

2. Let $\mathbf{u} \in \ker(\text{div})$. Then there exists a unique vector potential $\boldsymbol{\psi} \in H(\text{curl}, \Omega)$ such that

$$\text{curl } \boldsymbol{\psi} = \mathbf{u}, \quad \text{div } \boldsymbol{\psi} = 0, \quad \text{and } \boldsymbol{\psi} \cdot \mathbf{n} = 0.$$

3. Let $\mathbf{u} \in \ker(\text{div})$ and $\text{tr}_{\mathbf{n}, \partial\Omega}(\mathbf{u}) = 0$. Then there exists a unique vector potential $\boldsymbol{\psi} \in H(\text{curl}, \Omega)$ such that

$$\text{curl } \boldsymbol{\psi} = \mathbf{u}, \quad \text{div } \boldsymbol{\psi} = 0, \quad \text{and } \text{tr}_{\boldsymbol{\tau}, \partial\Omega} \boldsymbol{\psi} = \boldsymbol{\psi} \times \mathbf{n}|_{\partial\Omega} = 0.$$

We only mention that in both cases (2. and 3.) the vector potential can be derived as the solution of a boundary value problem for the Laplace operator. Note that Theorem 3.13 implies

$$\ker(\text{div}) = \text{curl}(H(\text{curl}, \Omega)).$$

A substantial tool within the analysis of the Maxwell equations is the *Helmholtz-decomposition*: Every vector field in $L_2(\Omega)^3$ can be decomposed into a divergence- and a curl-free function, which can be specified by means of vector and scalar potentials.

Theorem 3.14 (Helmholtz decomposition). *Every vector field $\mathbf{u} \in L_2(\Omega)^3$ has an orthogonal decomposition*

$$\mathbf{u} = \nabla\phi + \text{curl } \boldsymbol{\psi}, \quad \text{with } \phi \in H^1(\Omega) \text{ and } \boldsymbol{\psi} \in H(\text{curl}, \Omega).$$

Here, ϕ in $H^1(\Omega)/\mathbb{R}$ being the solution of the Laplace-problem $-\Delta\phi = -\text{div } \mathbf{u}$; the vector potential $\boldsymbol{\psi} \in H(\text{curl}, \Omega)$ is as in Theorem 3.13. For other choices of the vector and scalar potential in the Helmholtz decomposition we refer to AMROUCHE ET AL. [4], GIRAULT-RAVIART [49] or DAUTRAY-LIONS [40].

For stating the De Rham Complex we need one last result on the image of the divergence operator.

Lemma 3.15. *The divergence operator is surjective from $H(\text{div}, \Omega)$ onto $L_2(\Omega)$ as well as from $H_0(\text{div}, \Omega)$ onto $L_{2,0}(\Omega) := \{q \in L_2(\Omega) \mid \int_{\Omega} q \, d\mathbf{x} = 0\}$.*

Proof. For $f \in L_2(\Omega)$ we choose $\mathbf{u} = \nabla\psi \in L_2(\Omega)$ with $\psi \in H_0^1(\Omega)$ solution of the Dirichlet problem

$$(\text{div}(\nabla\psi), \phi) = -(\nabla\psi, \nabla\phi) = (f, \phi) \quad \forall \phi \in H_0^1(\Omega).$$

Since $\text{div } \mathbf{u} = f$, there holds $\mathbf{u} \in H(\text{div})$. For $f \in L_{2,0}(\Omega)$ we choose $\mathbf{u} = \nabla\psi \in L_2(\Omega)$ with $\psi \in H^1(\Omega)$ being the solution of the Neumann problem

$$(\text{div}(\nabla\psi), \phi) = -(\nabla\psi, \nabla\phi) = (f, \phi) \quad \forall \phi \in H^1(\Omega).$$

Since $\mathbf{u} \cdot \mathbf{n}|_{\partial\Omega} = \nabla\psi \cdot \mathbf{n}|_{\partial\Omega} = 0$ and $\text{div } \mathbf{u} = f$, there holds $\mathbf{u} \in H_0(\text{div})$. □

3.2.1 The de Rham Complex and Exact Sequences

The relation between the functional spaces through their differential operators can be summarized in the *de Rham Complex*, which reads as

$$\mathbb{R} \xrightarrow{\text{id}} H^1(\Omega) \xrightarrow{\nabla} H(\text{curl}, \Omega) \xrightarrow{\text{curl}} H(\text{div}, \Omega) \xrightarrow{\text{div}} L_2(\Omega) \xrightarrow{0} \{0\}. \quad (3.14)$$

For domains $\Omega \subset \mathbb{R}^2$ the De Rham Sequence shortens to

$$\mathbb{R} \xrightarrow{\text{id}} H^1(\Omega) \xrightarrow{\nabla} H(\text{curl}, \Omega) \xrightarrow{\text{curl}} L_2(\Omega) \xrightarrow{0} \{0\}, \quad (3.15)$$

respectively

$$\mathbb{R} \xrightarrow{\text{id}} H^1(\Omega) \xrightarrow{\text{Curl}} H(\text{div}, \Omega) \xrightarrow{\text{div}} L_2(\Omega) \xrightarrow{0} \{0\}. \quad (3.16)$$

The main property of the de Rham Complex is the coincidence of ranges and kernels of consecutive operators.

Corollary 3.16. *The de Rham Complexes (3.14)-(3.16) form exact sequences, also known as complete sequences. This means that the range of each operator coincides with the kernel of the following operator.*

In fact the exactness of the sequence summarizes the results of Theorem 3.12, Theorem 3.13, and Lemma 3.15, namely the coincidence of the following range and kernel spaces:

$$\ker(\nabla) = \mathbb{R}, \quad (3.17a)$$

$$\ker(\text{Curl}) = \nabla H^1(\Omega), \quad (3.17b)$$

$$\ker(\text{div}) = \text{curl}(H(\text{curl}, \Omega)), \quad (3.17c)$$

$$L_2(\Omega) = \text{div}(H(\text{div}, \Omega)), \quad (3.17d)$$

for 3 dimensional spaces, whereas in 2 dimensional spaces there holds

$$\ker(\nabla) = \mathbb{R}, \quad (3.18a)$$

$$\ker(\text{Curl}) = \mathbb{R}, \quad (3.18b)$$

$$\ker(\text{curl}) = \nabla H^1(\Omega), \quad (3.18c)$$

$$\ker(\text{div}) = \text{Curl } H^1(\Omega), \quad (3.18d)$$

$$L_2(\Omega) = \text{curl}(H(\text{curl}, \Omega)), \quad (3.18e)$$

$$L_2(\Omega) = \text{div}(H(\text{div}, \Omega)). \quad (3.18f)$$

Remark 3.17 (De Rham Complex with essential boundary conditions). *In case of essential boundary conditions on $\partial\Omega$, the restricted sequence*

$$\mathbb{R} \xrightarrow{\text{id}} H_0^1(\Omega) \xrightarrow{\nabla} H_0(\text{curl}, \Omega) \xrightarrow{\text{curl}} H_0(\text{div}, \Omega) \xrightarrow{\text{div}} L_{2,0}(\Omega) \xrightarrow{0} \{0\}, \quad (3.19)$$

where $L_{2,0}(\Omega) := \{q \in L_2(\Omega) \mid \int_{\Omega} q \, d\mathbf{x} = 0\}$, is still exact.

In the two-dimensional setting the exactness of the shortened de Rham Complexes (3.15) and (3.16) still holds in the case of essential boundary conditions.

In case that the domain Ω is more complex, i.e. involves holes or if mixed boundary conditions are imposed, the de Rham Complex need not be exact: the range of an operator is a subset of the kernel of the following map, but the kernel and the range spaces need not coincide. There is a low dimensional subspace of kernel functions which cannot be represented as gradient fields of a scalar potential. The dimension of this space depends on the topological properties of Ω . The issue of so-called cohomology spaces is treated in AMROUCHE ET. AL. [4], BOSSAVIT [25] and HIPTMAIR [56].

3.3 Abstract Variational Problems: Existence and Uniqueness

In this section, we briefly recall the main existence and uniqueness results for variational problems. We will then apply these theorems to our classes of problems for Maxwell's equations.

Let V and W denote Hilbert-spaces provided with the scalar products $(\cdot, \cdot)_V$, $(\cdot, \cdot)_W$. The induced norms are denoted by $\|\cdot\|_V$, $\|\cdot\|_W$. By V^* we refer to the dual space, and the duality pairing is denoted by $\langle \cdot, \cdot \rangle$. A mapping $a(\cdot, \cdot) : V \times W \rightarrow \mathbb{C}$ is called a *sesquilinear form* if

$$\begin{aligned} a(c_1 u_1 + c_2 u_2, v) &= c_1 a(u_1, v) + c_2 a(u_2, v) & \forall c_1, c_2 \in \mathbb{C}, \forall u_1, u_2 \in V, v \in W, \\ a(u, c_1 v_1 + c_2 v_2) &= \overline{c_1} a(u, v_1) + \overline{c_2} a(u, v_2) & \forall c_1, c_2 \in \mathbb{C}, \forall u \in V, v_1, v_2 \in W, \end{aligned}$$

where $\overline{c_1}$ denotes the complex conjugate of c_1 .

The following properties are at the core of the basic results below:

Definition 3.18. *A sesquilinear form is called*

1. bounded if

$$|a(u, w)| \leq \alpha \|u\|_V \|w\|_W \quad \forall u \in V, \forall w \in W.$$

2. coercive if $V = W$ and,

$$\exists \beta > 0 : |a(u, u)| \geq \beta \|u\|_V^2 \quad \forall u \in V.$$

3.3.1 Coercive variational problems

We investigate *variational problems* of the form

Problem 3.19. *For given $f \in V^*$, find $u \in V$ such that*

$$a(u, v) = f(v) \quad \forall v \in V. \quad (3.20)$$

Existence and uniqueness of a solution is guaranteed by

Theorem 3.20 (Lax-Milgram). *Let $a : V \times V \rightarrow \mathbb{C}$ denote a bounded and coercive sesquilinear form. Then, for any continuous linear form $f \in V^*$, there exists a unique solution $u \in V$ satisfying*

$$a(u, v) = f(v) \quad \forall v \in V, \quad \text{and} \quad \|u\|_V \leq \frac{\alpha}{\beta} \|f\|_{V^*},$$

where α and β are as in Definition 3.18.

3.3.2 Mixed formulations

In the context of magnetostatic problems we utilize a mixed formulation of the variational problem. We consider *mixed problems* – also called saddle-point problems – of the following type:

$$\begin{aligned} a(u, v) + b(v, p) &= f(v) & \forall v \in V, \\ b(u, q) &= g(q) & \forall q \in W. \end{aligned} \quad (3.21)$$

The equivalent to the results of the Lax-Milgram Theorem is given by the following result.

Theorem 3.21 (Brezzi). *Let V and W be Hilbert-spaces, and the sesquilinear forms $a : V \times V \rightarrow \mathbb{C}$ and $b : V \times W \rightarrow \mathbb{C}$ fulfill the following properties:*

1. *The sesquilinear forms are bounded, i.e.*

$$\begin{aligned} \exists \alpha_1 \geq 0 : \quad & |a(v, w)| \leq \alpha_1 \|v\|_V \|w\|_V \quad \forall v, w \in V, \\ \exists \alpha_2 \geq 0 : \quad & |b(v, q)| \leq \alpha_2 \|v\|_V \|q\|_W \quad \forall v \in V \forall q \in W. \end{aligned}$$

2. *$b(\cdot, \cdot)$ satisfies the Babuska-Brezzi condition, i.e.*

$$\exists \beta_2 > 0 : \quad \sup_{v \in V} \frac{b(v, q)}{\|v\|_V} \geq \beta_2 \|q\|_W \quad \forall q \in W. \quad (3.22)$$

3. *$a(\cdot, \cdot)$ is $\ker b$ -coercive, i.e.*

$$\exists \beta_1 > 0 \quad |a(v, v)| \geq \beta_1 \|v\|_V^2 \quad \forall v \in \ker b, \quad (3.23)$$

where $\ker b := \{u \in V \mid b(u, q) = 0 \forall q \in W\}$.

Then there exists a unique solution $(u, p) \in V \times W$ of (3.21) satisfying the a-priori estimates

$$\begin{aligned} \|u\|_V &\leq \frac{1}{\beta_1} \|f\|_{V^*} + \frac{1}{\beta_2} \left(1 + \frac{\alpha_1}{\beta_1}\right) \|g\|_{W^*}, \\ \|p\|_W &\leq \frac{1}{\beta_2} \left(1 + \frac{\alpha_1}{\beta_1}\right) \|f\|_{V^*} + \frac{\alpha_1}{\beta_2^2} \left(1 + \frac{\alpha_1}{\beta_1}\right) \|g\|_{W^*}. \end{aligned}$$

3.4 Variational formulation of electromagnetic problems

We will now utilize the definitions and results of the previous sections to state the electromagnetic problems discussed in Chapter 2 in a variational form, and to prove existence and uniqueness of solutions. Throughout we assume Ω to be a bounded Lipschitz domain. The general structure of the derivation of variational formulations is to multiply the partial differential equations by a suitable test function, integrate over Ω , and apply integration by parts (Green's formula).

3.4.1 The electrostatic problem: A Poisson problem

In the electrostatic regime, the four Maxwell equations can be reduced to a single Poisson equation for the scalar potential ϕ of the electric field intensity \mathbf{E} , i.e.,

$$\begin{aligned} -\operatorname{div}(\epsilon \nabla \phi) &= \rho \quad \text{in } \Omega, \\ \phi &= g_D \quad \text{on } \Gamma_D, \\ \frac{\partial \phi}{\partial n} &= g_N \quad \text{on } \Gamma_N, \quad \partial \Omega = \bar{\Gamma}_D \cup \bar{\Gamma}_N, \end{aligned}$$

It is well-known that subspaces of $H^1(\Omega)$ are appropriate for the variational formulation in this case. By including the Dirichlet boundary conditions in the ansatz space, we arrive at

Problem 3.22. *Find $\phi \in H_{g_D, D}^1 = \{\phi \in H^1(\Omega) \mid \operatorname{tr} \phi|_{\Gamma_D} = g_D\}$ such that*

$$\int_{\Omega} \epsilon(x) \nabla \phi(x) \cdot \nabla \psi(x) \, dx = \int_{\Omega} \rho(x) \psi(x) \, dx + \int_{\Gamma_N} \epsilon(x) g_N(x) \psi(x) \, ds \quad \forall \psi \in H_{0, D}^1(\Omega).$$

For bounded permittivity, i.e. $0 < \epsilon_0 \leq \epsilon \leq \epsilon_1$ almost everywhere, the bilinear form $a(\phi, \psi) := \int_{\Omega} \epsilon \nabla \phi \cdot \nabla \psi \, dx$ is

- *bounded* with $|a(\phi, \psi)| \leq \epsilon_1 \|\phi\|_V \|\psi\|_V$.
- *coercive*, since $a(\phi, \phi) \geq c_F^{-1} \epsilon_0 \|\phi\|_1^2$ owing to Poincaré's-Friedrichs' inequality

$$\|\phi\|_0 \leq c_F \|\nabla \phi\|_1 \quad \forall \phi \in H_{0,D}^1(\Omega)$$

where we assumed $\text{meas}_{\mathbb{R}^{d-1}}(\Gamma_D) > 0$.

Corollary 3.23. *Suppose that the permittivity is bounded by $0 < \epsilon_0 \leq \epsilon(x) \leq \epsilon_1$, the boundary data satisfy $g_D \in H^{\frac{1}{2}}(\Gamma_D)$ with $\text{meas}_{\mathbb{R}^{d-1}}(\Gamma_D) > 0$ and $g_N \in H^{-\frac{1}{2}}(\Gamma_N)$, and $\rho \in H^{-1}(\Omega)$. Then Theorem 3.20 (Lax-Milgram) guarantees the existence of a unique solution $\phi \in H_{g_D,D}^1(\Omega)$ for the variational electrostatic potential problem 3.22.*

For pure Neumann problems, i.e. $\Gamma_N = \partial\Omega$, the solution of the electrostatic problem is unique only up to constants. Uniqueness can be restored by imposing a gauging condition, e.g. $\int_{\Omega} \phi \, dx = 0$. The electric field \mathbf{E} can be recovered by $\mathbf{E} = -\nabla \phi$. Note that by Theorem 3.12 we have $\mathbf{E} \in H(\text{curl})$ and $\text{curl } \mathbf{E} = 0$.

3.4.2 The magnetostatic problem

Next we consider the curl-curl problem (2.34): As it becomes clear from the variational formulation below, the appropriate spaces (incorporating the boundary conditions (2.36), (2.37)) are subspaces of $H(\text{curl}, \Omega)$.

Problem 3.24. *Find $\mathbf{u} \in H_{g_D,D}(\text{curl}, \Omega) := \{\mathbf{v} \in H(\text{curl}, \Omega) : \mathbf{v} \times \mathbf{n} = \mathbf{g}_D \text{ on } \Gamma_D\}$ such that*

$$\int_{\Omega} \mu^{-1} \text{curl } \mathbf{u} \text{ curl } \mathbf{v} \, dx = \int_{\Omega} \mathbf{j} \cdot \mathbf{v} \, dx \quad \forall \mathbf{v} \in H_{0,D}(\text{curl}, \Omega). \quad (3.25)$$

Note that we assume the impressed currents \mathbf{j} to be consistent here, i.e. to satisfy the continuity equation

$$\text{div } \mathbf{j} = 0 \text{ in } \Omega \text{ and } \mathbf{j} \cdot \mathbf{n} = 0 \text{ on } \partial\Omega. \quad (3.26)$$

The bilinear form $a(\mathbf{u}, \mathbf{v}) = \int_{\Omega} \text{curl } \mathbf{u} \text{ curl } \mathbf{v} \, dx$ is *not coercive*, since for all $\phi \in H_{0,D}^1(\Omega)$ there holds $a(\mathbf{u}, \nabla \phi) = 0$, while $\|\nabla \phi\|_{\text{curl}} = \|\nabla \phi\|_0$. Therefore, we cannot apply the Lax-Milgram Theorem directly. As in the potential problem with pure Neumann boundary conditions above, uniqueness and coercivity can be restored by appropriate gauging. For simplicity, we assume for the moment homogeneous boundary conditions (e.g., the boundary conditions are incorporated in the right hand side by homogenization). The Coulomb gauging condition $\text{div } \mathbf{u} = 0$ with $\mathbf{u} \cdot \mathbf{n} = 0$ then reads

$$(\mathbf{u}, \nabla \phi) = 0, \quad \forall \phi \in W = H^1(\Omega).$$

Hence we look for a solution \mathbf{u} which is orthogonal to gradients. In case of Dirichlet data, we alternatively set $W = H_0^1(\Omega)$.

Mixed formulation of the magnetostatic problem

We incorporate the gauging condition $\mathbf{u} \in (\nabla H^1(\Omega))^\perp$ by reformulating the magnetostatic problem as a mixed variational problem.

Problem 3.25. Find (\mathbf{u}, ϕ) in $V \times W := H_0(\text{curl}, \Omega) \times H_0^1(\Omega)$ such that

$$\int_{\Omega} \mu^{-1} \text{curl } \mathbf{u} \cdot \text{curl } \mathbf{v} \, d\mathbf{x} + \int_{\Omega} \mathbf{v} \cdot \nabla \phi \, d\mathbf{x} = \int_{\Omega} \mathbf{j} \cdot \mathbf{v} \, d\mathbf{x} \quad \forall \mathbf{v} \in H_{0,D}(\text{curl}, \Omega), \quad (3.27a)$$

$$\int_{\Omega} \mathbf{u} \cdot \nabla \psi \, d\mathbf{x} = 0 \quad \forall \psi \in H_0^1(\Omega). \quad (3.27b)$$

We further assume that the permeability is bounded by $0 < \mu_0 \leq \mu(x) \leq \mu_1$, and denote the involved bilinear forms by $a(\mathbf{u}, \mathbf{v}) := \int_{\Omega} \mu^{-1} \text{curl } \mathbf{u} \cdot \text{curl } \mathbf{v} \, d\mathbf{x}$ and $b(\mathbf{v}, \psi) := \int_{\Omega} \mathbf{v} \cdot \nabla \psi \, d\mathbf{x}$.

In order to be able to apply Brezzi's Theorem we have to prove the ker b -coercivity of $a(\cdot, \cdot)$. For this purpose we require the following theorem.

Theorem 3.26 (Friedrichs' inequality for $H(\text{curl})$). *Let Ω be a simply-connected Lipschitz domain.*

1. Suppose $\mathbf{v} \in H(\text{curl}, \Omega)$ is orthogonal to gradient functions, i.e. $(\mathbf{v}, \nabla \psi) = 0$ for all $\psi \in H^1(\Omega)$. Then

$$\|\mathbf{v}\|_0 \preceq \|\text{curl } \mathbf{v}\|_0.$$

2. Suppose $\mathbf{v} \in H_0(\text{curl}, \Omega)$ is orthogonal to gradient functions, i.e. $(\mathbf{v}, \nabla \psi) = 0$ for all $\psi \in H_0^1(\Omega)$. Then the same estimate holds.

For a proof we refer to Lemma 3.4 and Lemma 3.6 in GIRAULT-RAVIART [49].

Applying the $H(\text{curl})$ Friedrichs' inequalities, the bilinear forms of the magnetostatic problem can be shown to satisfy the following properties.:

- The bilinear forms $a(\cdot, \cdot)$ and $b(\cdot, \cdot)$ are *bounded*, i.e., $|a(\mathbf{u}, \mathbf{v})| \leq \mu_0 \|\mathbf{u}\|_V \|\mathbf{v}\|_V$ and by $|b(\mathbf{v}, \psi)| \leq \|\mathbf{u}\|_V \|\psi\|_W$.
- $b(\cdot, \cdot)$ satisfies the *Babuska-Brezzi condition*, as there is

$$\sup_{v \in V} \frac{\int_{\Omega} \mathbf{v} \cdot \nabla \psi \, d\mathbf{x}}{\|\mathbf{v}\|_{\text{curl}}} \stackrel{(*)}{\geq} \frac{\int_{\Omega} \nabla \psi \cdot \nabla \psi \, d\mathbf{x}}{\|\nabla \psi\|_{\text{curl}}} \stackrel{(**)}{\geq} \|\nabla \psi\|_0 \stackrel{(***)}{\geq} \|\psi\|_1$$

by the choice $v = \nabla \psi$ (*), $\|\nabla \psi\|_{\text{curl}} = \|\nabla \psi\|_0$ (**), and Friedrichs' inequality for $H^1(\Omega)$ (***) .

- $a(\cdot, \cdot)$ is *ker b -coercive*, i.e. for all $\mathbf{u} \in V$ satisfying $(\mathbf{u}, \nabla \phi) = 0 \, \forall \phi \in H^1(\Omega)$ there holds

$$a(\mathbf{u}, \mathbf{u}) \geq \mu_1^{-1} \|\text{curl } \mathbf{u}\| \stackrel{(*)}{\geq} \mu_1^{-1} (1 + c_{F, \text{curl}}^{-1}) \|\mathbf{u}\|_{\text{curl}}.$$

The main step (*) in this estimation is justified by Friedrichs' inequality for $H(\text{curl})$ stated in Theorem 3.26.

Existence and uniqueness for the variational problem in mixed formulation 3.25 now follows by Brezzi's theorem 3.21:

Corollary 3.27 (Solution theory of mixed and standard magnetostatic problem). *Let the permeability satisfy $0 < \mu_0 \leq \mu(x) \leq \mu_1$, and the source term $\mathbf{j} \in H(\text{curl})^*$ satisfy (3.26). Then*

1. *Brezzi's theorem 3.21 ensures the existence and uniqueness of a solution $(\mathbf{u}, \phi) \in V \times W$ to the magnetostatic problem in mixed form (3.27).*
2. *the solution of the mixed problem is of the form $(\mathbf{u}, \phi) = (\mathbf{u}, 0)$ with \mathbf{u} solving the standard problem (3.25) with $\text{div } \mathbf{u} = 0$ and $\mathbf{u} \cdot \mathbf{n} = 0$.*
3. *the estimate $\|\mathbf{u}\|_{\text{curl}} \preceq \|\mathbf{j}\|_{V^*}$ holds.*

Proof. Let $(\mathbf{u}, \phi) \in V \times W$ denote the unique solution (implied by Brezzi's theorem) of the mixed problem (3.27). Testing (3.27a) with gradient functions $\nabla\psi \in \nabla W \subset V$ yields that $\phi \in W$ solves the Laplace equation. Having in mind that $a(\mathbf{u}, \nabla\psi) + b(\nabla\psi, \phi) = \int_{\Omega} \nabla\psi \cdot \nabla\phi \, d\mathbf{x}$, we obtain

$$\begin{aligned} \int_{\Omega} \nabla\psi \cdot \nabla\phi \, d\mathbf{x} &= \int_{\Omega} \mathbf{j} \cdot \nabla\psi \, d\mathbf{x} \\ &= \int_{\Omega} \text{div } \mathbf{j} \, \psi \, d\mathbf{x} + \int_{\partial\Omega} \mathbf{j} \cdot \mathbf{n} \, \psi \, d\mathbf{x} = 0 \quad \forall \psi \in W. \end{aligned}$$

The source term vanishes since \mathbf{j} was assumed to be consistent, i.e. $\text{div } \mathbf{j} = 0, \mathbf{j} \cdot \mathbf{n} = 0$. Since in case of the Neumann problem $W = H^1(\Omega)/\mathbb{R}$ and in case of the Dirichlet problem $W = H_0^1(\Omega)$, we obtain a unique solution $\phi = 0 \in W$. Hence, the solution of the mixed problem (3.27) is of the form $(\mathbf{u}, \phi = 0)$.

Substituting $(\mathbf{u}, \phi = 0)$ in the mixed problem the first equation (3.27a) yields that \mathbf{u} solves the magnetostatic problem in standard form (3.25). The second equation (3.27b) implies that we achieve $\mathbf{u} \in (\nabla H^1(\Omega))^{\perp}$. \square

While the mixed formulation provides analytic results on existence and uniqueness of solutions in an elegant manner, a numerical realization has certain drawbacks: first the number of unknowns is increased by switching from Problem 3.24 to 3.25. Additionally, the resulting saddle point problems are usually more difficult to solve. In view of a numerical realization we therefore discuss another *regularized* version of the magnetostatic problem.

Regularized magnetostatic problem

We choose a regularization parameter $\varepsilon > 0$ and define the **regularized magnetostatic problem** as

Problem 3.28. *Find $\mathbf{u}^\varepsilon \in V$ s.t.*

$$\int_{\Omega} \text{curl } \mathbf{u}^\varepsilon \text{ curl } \mathbf{v} \, d\mathbf{x} + \varepsilon \int_{\Omega} \mathbf{u}^\varepsilon \mathbf{v} \, d\mathbf{x} = \int_{\Omega} \mathbf{j} \mathbf{v} \, d\mathbf{x} \quad \forall \mathbf{v} \in V. \quad (3.28)$$

As we will see, the regularized Problem 3.28 has the following properties:

- The Lax-Milgram theory is applicable, i.e. the involved bilinear form is coercive.
- The solution \mathbf{u}^ε of the regularized problem converges to a solution \mathbf{u} solving the standard problem with $\varepsilon \rightarrow 0$.

Let us denote the regularized bilinear form by $a_\varepsilon(\mathbf{u}, \mathbf{v}) := \int_\Omega \operatorname{curl} \mathbf{u}^\varepsilon \operatorname{curl} \mathbf{v} \, d\mathbf{x} + \varepsilon \int_\Omega \mathbf{u}^\varepsilon \mathbf{v} \, d\mathbf{x}$.

$$a_\varepsilon(\mathbf{u}, \mathbf{u}) \geq \mu_1^{-1}(\operatorname{curl} \mathbf{u}, \operatorname{curl} \mathbf{u}) + \varepsilon(\mathbf{u}, \mathbf{u}) \geq \min\{\mu_1^{-1}, \varepsilon\} \|\mathbf{u}\|_{\operatorname{curl}}^2 \quad \forall \mathbf{u} \in H(\operatorname{curl}, \Omega). \quad (3.29)$$

Corollary 3.29. *Under the assumptions of Corollary 3.27 and a positive regularization parameter $\varepsilon > 0$ the bilinear form $a_\varepsilon(\mathbf{u}, \mathbf{v})$ is coercive. Hence, the Lemma of Lax-Milgram (Theorem 3.20) provides the unique solvability of the regularized magnetostatic problem (3.28).*

The result follows easily since there holds

$$a_\varepsilon(\mathbf{u}, \mathbf{u}) \geq \mu_1^{-1}(\operatorname{curl} \mathbf{u}, \operatorname{curl} \mathbf{u}) + \varepsilon(\mathbf{u}, \mathbf{u}) \geq \min\{\mu_1^{-1}, \varepsilon\} \|\mathbf{u}\|_{\operatorname{curl}}^2 \quad \forall \mathbf{u} \in H(\operatorname{curl}, \Omega). \quad (3.30)$$

In order to show that \mathbf{u}_ε converges to a uniquely determined solution \mathbf{u} of Problem 3.24 as $\varepsilon \rightarrow 0$, we utilize the mixed formulation. Consider the following mixed formulation of the regularized problem (3.28): Find $(\mathbf{u}^\varepsilon, \phi^\varepsilon)$ in $V \times W := H_0(\operatorname{curl}, \Omega) \times H_0^1(\Omega)$ such that

$$\int_\Omega \mu^{-1} \operatorname{curl} \mathbf{u}^\varepsilon \cdot \operatorname{curl} \mathbf{v} \, d\mathbf{x} + \varepsilon \int_\Omega \mathbf{u}^\varepsilon \mathbf{v} \, d\mathbf{x} + \int_\Omega \mathbf{v} \cdot \nabla \phi^\varepsilon \, d\mathbf{x} = \int_\Omega \mathbf{j} \cdot \mathbf{v} \, d\mathbf{x} \quad \forall \mathbf{v} \in V, \quad (3.31a)$$

$$\int_\Omega \mathbf{u}^\varepsilon \cdot \nabla \psi \, d\mathbf{x} = 0 \quad \forall \psi \in W. \quad (3.31b)$$

Corollary 3.30. *Let the assumptions of Corollary 3.27 hold. Then the following assertions hold:*

1. *The regularized mixed problem (3.31) has a unique solution $(\mathbf{u}^\varepsilon, \phi^\varepsilon = 0) \in V \times W$ satisfying $\|\mathbf{u}^\varepsilon\|_V \preceq \|\mathbf{j}\|_{V^*}$ and $\mathbf{u}^\varepsilon \in (\nabla W)^\perp$.*
2. *If $(\mathbf{u}^\varepsilon, \phi^\varepsilon)$ denotes the unique solution of the regularized mixed problem, then \mathbf{u}^ε solves the regularized standard problem (3.28).*
3. *Suppose that $(\mathbf{u}, \phi = 0)$ denotes the solution of the original mixed problem (3.27). Then*

$$\|\mathbf{u} - \mathbf{u}^\varepsilon\|_V \preceq \varepsilon \|\mathbf{j}\|_{V^*}. \quad (3.32)$$

Proof.

1. Under the assumptions of Corollary 3.27 Brezzi's theorem ensures the existence of a unique solution $(\mathbf{u}_\varepsilon, \phi_\varepsilon)$ of the mixed problem (3.31). Testing the first equation (3.31a) on the subspace $\nabla W \subset V$ and taking into account the consistency (3.26) of the source term we achieve

$$\varepsilon \int_\Omega \mathbf{u}^\varepsilon \nabla \psi \, d\mathbf{x} + \int_\Omega \nabla \psi \cdot \nabla \phi^\varepsilon \, d\mathbf{x} = 0 \quad \forall \psi \in W.$$

Since \mathbf{u}_ε is orthogonal on gradients due to (3.31b), we obtain a homogenous Laplace equation for ϕ^ε , i.e. $\phi^\varepsilon = 0$. Since the constants in the inf-sup-condition and in the ker b -coercivity are independent of ε the stability estimate is implied by one of Brezzi's theorem.

2. Setting $\phi^\varepsilon = 0$ in the mixed formulations implies that \mathbf{u}^ε solves the regularized standard problem with $\mathbf{u}^\varepsilon \in (\nabla H_0^1(\Omega))^\perp$.

3. Let (\mathbf{u}, ϕ) and $(\mathbf{u}^\varepsilon, \phi^\varepsilon)$ denote the solutions of the exact and the perturbed mixed problem. Then $(\mathbf{u} - \mathbf{u}^\varepsilon, \phi - \phi^\varepsilon) \in V \times W$ satisfies

$$\begin{aligned} \int_{\Omega} \mu^{-1} \operatorname{curl}(\mathbf{u} - \mathbf{u}^\varepsilon) \cdot \operatorname{curl} \mathbf{v} \, d\mathbf{x} + \int_{\Omega} \mathbf{v} \cdot \nabla(\phi - \phi^\varepsilon) \, d\mathbf{x} &= \varepsilon \int_{\Omega} \mathbf{u}^\varepsilon \cdot \mathbf{v} \, d\mathbf{x} \quad \forall \mathbf{v} \in V, \\ \int_{\Omega} (\mathbf{u} - \mathbf{u}^\varepsilon) \cdot \nabla \psi \, d\mathbf{x} &= 0 \quad \forall \psi \in W, \end{aligned}$$

i.e. the exact mixed formulation with consistent right hand-side $\varepsilon \mathbf{u}^\varepsilon$. Due to Brezzi's theorem $(\mathbf{u} - \mathbf{u}^\varepsilon)$ is bounded by the source term, i.e. $\|\mathbf{u} - \mathbf{u}^\varepsilon\|_V \leq \varepsilon \|\mathbf{u}^\varepsilon\|_{V^*}$. The estimate of item 1, namely $\|\mathbf{u}^\varepsilon\|_V \preceq \|\mathbf{j}\|_{V^*}$ (where the constant is independent of ε) implies the desired estimate. \square

Remark 3.31. For a numerical realization it will be important to construct solvers for Problem 3.28 that are robust in the parameter ε , in particular as $\varepsilon \rightarrow 0$.

3.4.3 The time-harmonic electromagnetic and magneto-quasi-static problems

Now we turn to a variational formulation of the problem

$$\begin{aligned} \operatorname{curl} \mu^{-1} \operatorname{curl} \mathbf{u} + \kappa \mathbf{u} &= \mathbf{j}, \\ \mu^{-1} \operatorname{curl} \mathbf{u} \times \mathbf{n} &= \mathbf{g}_N \quad \text{on } \Gamma_N, \\ \mathbf{u} \times \mathbf{n} &= \mathbf{g}_D \quad \text{on } \Gamma_D, \end{aligned}$$

which includes the time-harmonic eddy-current problem where $\kappa = i\omega\sigma$ as well as the time-harmonic electromagnetic wave equation in conducting media with $\kappa = i\omega\sigma - \epsilon\omega^2$ for $\sigma > 0$ and $\omega > 0$. In both cases the parameter $\kappa \in \mathbb{C} \setminus \mathbb{R}^-$.

Problem 3.32. Find $\mathbf{u} \in V := H_{\mathbf{g},D}(\operatorname{curl}, \Omega)$ satisfying

$$\int_{\Omega} \mu^{-1} \operatorname{curl} \mathbf{u} \cdot \operatorname{curl} \bar{\mathbf{v}} \, d\mathbf{x} + \int_{\Omega} \kappa \mathbf{u} \cdot \bar{\mathbf{v}} \, d\mathbf{x} = \int_{\Omega} \mathbf{j} \cdot \bar{\mathbf{v}} \, d\mathbf{x} + \int_{\Gamma_N} (\mathbf{n} \times \mathbf{g}_N) \cdot \bar{\mathbf{v}} \, ds \quad \forall \mathbf{v} \in V. \quad (3.33)$$

The sesquilinear form $a(\mathbf{u}, \mathbf{v}) = \int_{\Omega} \mu^{-1} \operatorname{curl} \mathbf{u} \cdot \operatorname{curl} \bar{\mathbf{v}} \, d\mathbf{x} + \int_{\Omega} \kappa \mathbf{u} \cdot \bar{\mathbf{v}} \, d\mathbf{x}$ has the following properties:

- $a(\cdot, \cdot)$ is *bounded* if the parameters σ, κ are bounded, i.e., for all $\mathbf{u}, \mathbf{v} \in H(\operatorname{curl}, \Omega)$ there holds

$$\begin{aligned} |a(\mathbf{u}, \mathbf{v})| &\leq \|\mu^{-1}\|_{\infty} \|\mathbf{u}\|_{\operatorname{curl}} \|\mathbf{v}\|_{\operatorname{curl}} + \|\kappa\|_{\infty} \|\mathbf{u}\|_0 \|\mathbf{v}\|_0 \\ &\preceq \|\mathbf{u}\|_{\operatorname{curl}} \|\mathbf{v}\|_{\operatorname{curl}}. \end{aligned}$$

- $a(\cdot, \cdot)$ is *coercive*: For complex $\kappa = \kappa_R + i\kappa_I$ with $\kappa_I \neq 0$ there exists $\alpha = \alpha_R + i\alpha_i \in \mathbb{C}$ with $|\alpha| > 0$ such that

$$\begin{aligned} |\alpha| |a(\mathbf{u}, \mathbf{u})| &\geq |\operatorname{Re}(\alpha a(\mathbf{u}, \mathbf{u}))| \geq |\alpha_R \mu^{-1}(\operatorname{curl} \mathbf{u}, \operatorname{curl} \bar{\mathbf{u}}) + (\alpha_R \kappa_R - \alpha_i \kappa_i)(\mathbf{u}, \bar{\mathbf{u}})| \\ &\geq \|\mathbf{u}\|_{\operatorname{curl}}^2. \end{aligned}$$

The choice $\alpha = \mu + i \frac{\mu \kappa_R - 1}{\kappa_i}$ implies $\alpha_R \kappa_R - \alpha_i \kappa_i = 1$ and $\alpha_R \mu^{-1} = 1$. Coercivity for the case $\kappa = \kappa_R > 0$ was already discussed in the regularized magnetostatic case.

Corollary 3.33. Let the boundary data satisfy $\mathbf{g}_D \in H^{-\frac{1}{2}}(\Gamma_D)$ and $\mathbf{g}_N \in H^{-\frac{1}{2}}(\Gamma_N)$, and assume $\mathbf{j} \in H(\operatorname{curl}, \Omega)^*$. Then the Lax-Milgram Theorem implies the unique solvability of the variational problem (3.33).

Non-conducting regions $\sigma = 0$

In non-conducting regions, the eddy-current problem 3.32 degenerates to the magnetostatic one and can be treated with similar measures. In particular, we may introduce a regularized version by either setting $0 < \sigma_{nc} \ll \sigma_c$ or by adding the regularization term $\epsilon \int_{\Omega_{nc}} \mathbf{u} \cdot \bar{\mathbf{v}}$.

We conclude this section by recalling the appropriate function spaces for the various variables:

- the electric and magnetic field intensity: $\mathbf{E} \in H(\text{curl}, \Omega)$, $\mathbf{H} \in H(\text{curl}, \Omega)$
- the electric and magnetic fluxes: $\mathbf{D} \in H(\text{div}, \Omega)$, $\mathbf{B} \in H(\text{div}, \Omega)$.
- the scalar potential $\phi \in H^1(\Omega)$ with $\mathbf{E} = \nabla\phi$,
- the vector potential $\mathbf{A} \in H(\text{curl}, \Omega)$ with $\mathbf{B} = \text{curl } \mathbf{A}$.

Chapter 4

The Finite Element Method

In this chapter, we concentrate on standard finite element methods, namely the h-version FEM. We will shortly recall the main ingredients for the FEM and recall the main approximation results. We then introduce the classical low-order FE-spaces for $H^1(\Omega)$, $H(\operatorname{div}, \Omega)$ and $H(\operatorname{curl}, \Omega)$, namely

- the low-order scalar elements for H^1 ,
- the lowest-order Nédélec elements of first kind and second kind for $H(\operatorname{curl})$, and
- the lowest-order Raviart-Thomas elements, which in 3D are also called Raviart-Thomas-Nédélec elements, and Brezzi-Douglas-Marini elements for $H(\operatorname{div})$.

The low order elements will be used also in the construction of the high order elements in the next chapter. We will show that by careful construction, the exact sequence property discussed in Section 3.2.1 carries over to the sequence of finite element spaces, locally (elementwise) as well as globally.

4.1 Basic Concepts

4.1.1 Galerkin Approximation

Galerkin projection provides a general technique for the construction of discrete approximations to the solution of variational problems

$$\text{Find } u \in X : \quad a(u, v) = f(v) \quad \forall v \in X. \quad (4.1)$$

The infinite-dimensional space X is now replaced by a sequence of finite-dimensional spaces X_h , which yields the discrete variational problems,

$$\text{Find } u_h \in X_h : \quad a(u_h, v_h) = F(v_h) \quad \forall v_h \in X_h. \quad (4.2)$$

In this presentation we investigate *conforming methods*, where $X_h \subset X$. The index h typically refers to a discretization parameter. As we will show below, the discrete solution $u_h \in X_h$ converges to the solution $u \in X$ with $h \rightarrow 0$ under reasonable assumptions. We expand the solution u_h in terms of a basis $(\varphi_i)_{1 \leq i \leq N}$ of X_h , i.e.,

$$u_h = \sum_{i=1}^N u_i^h \varphi_i.$$

It suffices to test the variational problem (4.2) only with the basis functions, which yields the Galerkin system

$$\mathbf{A}\mathbf{u} = \mathbf{f}.$$

The system matrix $\mathbf{A} \in \mathbb{R}^{N \times N}$, load vector $\mathbf{f} \in \mathbb{R}^n$, and solution vector $\mathbf{u} \in \mathbb{R}^N$ are defined by

$$\mathbf{A} = (a(\varphi_i, \varphi_j))_{1 \leq i, j \leq N}, \quad \mathbf{f} = (f(\varphi_j))_{1 \leq j \leq N}, \quad \text{and} \quad \mathbf{u} = (u_i^h)_{1 \leq i \leq N}. \quad (4.3)$$

The Finite Element method (FEM) is a special Galerkin method, based on the the following construction of finite-dimensional subspaces X_h :

- The domain $\bar{\Omega}$ is covered by a triangulation \mathcal{T}_h , i.e., a finite union of non-overlapping polyhedral elements K .
- The space X_h consists of piecewise polynomials, i.e., the restriction of a function $v_h \in X_h$ onto an element $K \in \mathcal{T}_h$ is a polynomial.
- X_h has a basis $\{\phi_i\}$ with local supports, i.e., each basis function ϕ_i is non-zero only on a few elements.

The latter implies that system matrix \mathbf{A} is sparse.

4.1.2 The Triangulation

We assume the domain Ω to be a bounded polygonal or polyhedral domain with Lipschitz continuous boundary.

Definition 4.1. A triangulation (mesh) \mathcal{T}_h is a finite non-overlapping subdivision $\mathcal{T}_h = \{K_i\}_{i \in \mathcal{I}}$ of Ω into elements K_i of simple geometry. A triangulation is called regular, if

1. the elements are non-overlapping, i.e. $\text{interior}(K_i) \cap \text{interior}(K_j) = \emptyset$ if $i \neq j$,
2. the triangulation \mathcal{T}_h is a covering of Ω , i.e. $\bigcup_{K_i \in \mathcal{T}_h} K_i = \bar{\Omega}$,
3. the intersection $K_i \cap K_j$ of two different elements ($i \neq j$) is either empty, or a vertex, or an edge or a face of both elements. (Hanging nodes are not allowed.)

We will frequently use the following notations

$$\begin{array}{ll} \text{the set of vertices} & \mathcal{V} = \{V_i\}, & \text{the set of edges} & \mathcal{E} = \{E_i\}, \\ \text{the set of faces} & \mathcal{F} = \{F_i\}, & \text{the set of cells} & \mathcal{T}_h = \{K_i\}. \end{array}$$

The (local) sets of vertices, edges and faces belonging to the element K are denoted by \mathcal{V}_K , \mathcal{E}_K , and \mathcal{F}_K .

4.1.3 The Finite Element

Following BRENNER-SCOTT [31], we require three basic definitions for construction of finite elements. The classical definition is the following, cf., e.g., CIARLET [35]:

Definition 4.2 (Finite Element). *Let*

1. the element domain $K \subset \mathbb{R}^n$ be a bounded closed set with non-empty interior and piecewise smooth boundary,

2. the space of shape functions \mathcal{P}_K be a finite-dimensional space of functions on K ,
3. the set of nodal variables $\Sigma_K = \{N_1^K, N_2^K, \dots, N_k^K\}$, also referred to as degrees of freedom, be a basis for \mathcal{P}'_K , where \mathcal{P}'_K denotes the dual space of \mathcal{P}_K .

Then we call the triple $(K, \mathcal{P}_K, \Sigma_K)$ a finite element.

The main effort in the construction of a finite element is to verify its unisolvence, i.e. the basis property of item 3. This can be done by showing the simpler, but equivalent property:

$$\text{If } v \in \mathcal{P}_K \text{ with } N_i^K v = 0 \text{ for } i = 1, \dots, k \text{ then } v \equiv 0.$$

Definition 4.3 (Nodal basis). *Let $(K, \mathcal{P}_K, \Sigma_K)$ be a finite element. The basis $\{\phi_1, \phi_2, \dots, \phi_k\}$ of \mathcal{P}_K which is dual to the set of nodal variables Σ_K , i.e. $N_i(\phi_j) = \delta_{ij}$, is called the nodal basis of \mathcal{P}_K .*

4.1.4 The reference element and its transformation to physical elements

A key ingredient in the design, analysis and numerical realization of the FEM is the *mapping trick*: The *physical* (global) finite elements $(K, \mathcal{P}_K, \Sigma_K)$ are defined as transformations of a reference (master) element $(\hat{K}, \mathcal{P}_{\hat{K}}, \Sigma_{\hat{K}})$, i.e., a reference geometry \hat{K} of simple shape (e.g. 1D: segment; 2D: triangle, quadrilateral; 3D: tetrahedron, prism, hexahedron). This construction has several advantages, e.g., many computations (e.g., numerical integration, derivation) can be performed a-priori on the reference element.

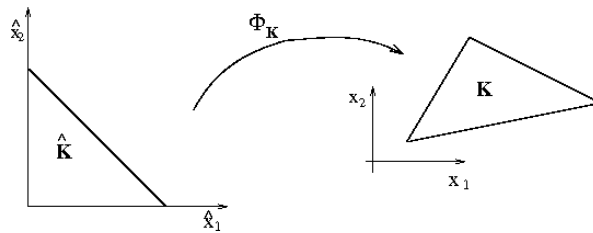


Figure 4.1: Mapping of reference element \hat{K} to physical element K

Suitable transformations

$$\Phi_K : \hat{K} \rightarrow K \quad (4.4)$$

are continuously differentiable, one-to-one and onto maps. If $\hat{\mathbf{x}}$ denotes a coordinate system on the reference element \hat{K} , then $\mathbf{x} = \Phi_K(\hat{\mathbf{x}})$ is the corresponding coordinate system on the physical element K .

The Jacobian matrix of the transformation Φ_K with respect to the reference coordinates and its determinant are denoted by

$$F_K(\hat{\mathbf{x}}) := \left(\frac{\partial \Phi_{K,i}}{\partial \hat{\mathbf{x}}_j}(\hat{\mathbf{x}}_j) \right)_{1 \leq i, j \leq d} \quad \text{and} \quad J_K(\hat{\mathbf{x}}) := \det(F_K(\hat{\mathbf{x}})).$$

Since Φ_K has to be one-to-one and onto, we have $J_K(\hat{\mathbf{x}})$ does not change sign on \hat{K} . A special but important case of element transformation is the affine linear map, i.e.,

$$\Phi_K(\hat{\mathbf{x}}) := B_K \hat{\mathbf{x}} + b_K, \quad B_K \in \mathbb{R}_d^d, b_K \in \mathbb{R}^d$$

where $F_K(\hat{\mathbf{x}}) = B_K$ and $J_K(\hat{\mathbf{x}}) = \det B_K$ are constant over \hat{K} . Using affine mappings ensures that polynomials are mapped to polynomials of the same degree, which simplifies the analysis of the FEM considerably. We will only consider affine transformations in this work.

The *local mesh size* $h(\mathbf{x})$ for $\mathbf{x} = \Phi_K(\hat{\mathbf{x}})$ can be defined by

$$h(\mathbf{x}) := \|F_K(\mathbf{x})\| \quad \text{and} \quad h_K := \sup_{\mathbf{x} \in K} h(\mathbf{x}).$$

Definition 4.4. A triangulation \mathcal{T}_h is called quasi-uniform, if $h_K \simeq h$ for all elements K in \mathcal{T}_h . \mathcal{T}_h is called shape-regular, if the condition number of the Jacobian is bounded for all elements, i.e.,

$$\|F_K(\mathbf{x})\| \|F_K^{-1}(\mathbf{x})\| \leq 1 \quad \forall K \in \mathcal{T}_h, \forall \mathbf{x} \in K. \quad (4.5)$$

For our considerations below we need to know how tangential and normal vectors are mapped between the reference and the physical elements.

Transformation of tangential and normal vectors Let $\hat{\mathbf{n}}(\hat{\mathbf{x}})$ and $\hat{\boldsymbol{\tau}}(\hat{\mathbf{x}})$ denote the outer normal vector and a tangential vector for $\hat{\mathbf{x}} \in \partial\hat{K}$, respectively. Then the corresponding unit normal and tangential vector on the physical element K are given by

$$\mathbf{n}(\mathbf{x}) = \frac{F_K^{-T}(\hat{\mathbf{x}})\hat{\mathbf{n}}(\hat{\mathbf{x}})}{\|F_K^{-T}(\hat{\mathbf{x}})\hat{\mathbf{n}}(\hat{\mathbf{x}})\|} \quad \text{and} \quad \boldsymbol{\tau}(\mathbf{x}) = \frac{F_K(\hat{\mathbf{x}})\hat{\boldsymbol{\tau}}(\hat{\mathbf{x}})}{\|F_K(\hat{\mathbf{x}})\hat{\boldsymbol{\tau}}(\hat{\mathbf{x}})\|}$$

for $\mathbf{x} = \Phi_K(\hat{\mathbf{x}}) \in \partial K$.

4.1.5 Simplicial elements and barycentric coordinates

From now on, we restrict ourselves to a triangulation by simplicial elements, i.e., triangles or tetrahedra. The simplex $K \subset \mathbb{R}^d$ is defined as the convex hull of $(d+1)$ vertices $\mathcal{V}_K \subset \mathcal{V}$. It will turn out to be useful to replace the Euclidian coordinates of the point $\mathbf{x} \in \mathbb{R}^d$ by barycentric coordinates $\lambda_i = \lambda_i(\mathbf{x})$ with respect to the $(d+1)$ vertices $V_i \in \mathcal{V}_K$.

Definition 4.5. Let the simplex $K \in \mathbb{R}^d$ be the convex hull of vertices $(V_i)_{1 \leq i \leq d+1}$. The barycentric coordinate $\lambda_i(\mathbf{x})$ with respect to the vertex V_i is defined as the unique linear polynomial

$$\lambda_i \in P^1(K) \quad \text{such that} \quad \lambda_i(V_j) = \delta_{ij} \quad \forall 1 \leq j \leq d+1. \quad (4.6)$$

As an immediate consequence we obtain that $\sum_{i=1}^{d+1} \lambda_i(\mathbf{x}) = 1$, $\forall \mathbf{x} \in K$. Using the element-wise definition (4.6), the barycentric coordinate $\lambda_i(x)$ associated with the vertex V_i naturally extends to a global function on Ω with the following properties:

$$\lambda_i \in C(\Omega) \quad \text{with} \quad \text{supp}(\lambda_i) = \bigcup_{K: V_i \in K} K \quad \text{and} \quad \lambda_i(V_j) = \delta_{ij} \quad \forall V_j \in \mathcal{V}. \quad (4.7)$$

For $d = 2$, the local reference (master) simplex $\hat{K} \subset \mathbb{R}^d$ is the triangle

$$\hat{K} := \{\hat{\mathbf{x}} \mid 0 \leq \hat{x}_i \leq 1, 0 \leq \hat{x}_1 + \hat{x}_2 \leq 1\}$$

with $\hat{\lambda}_1(\hat{\mathbf{x}}) = 1 - \hat{x}_1 - \hat{x}_2$, $\hat{\lambda}_2(\hat{\mathbf{x}}) = \hat{x}_1$, $\hat{\lambda}_3(\hat{\mathbf{x}}) = \hat{x}_2$ and for $d = 3$. We use the tetrahedron

$$\hat{K} := \{\hat{\mathbf{x}} \mid 0 \leq \hat{x}_i \leq 1, 0 \leq \hat{x}_1 + \hat{x}_2 + \hat{x}_3 \leq 1\}$$

with $\hat{\lambda}_1(\hat{\mathbf{x}}) = 1 - \hat{x}_1 - \hat{x}_2 - \hat{x}_3$, $\hat{\lambda}_2(\hat{\mathbf{x}}) = \hat{x}_1$, $\hat{\lambda}_3(\hat{\mathbf{x}}) = \hat{x}_2$, $\hat{\lambda}_4(\hat{\mathbf{x}}) = \hat{x}_3$.

4.2 Approximation properties of conforming FEM

We assume the variational problem (4.1) to be *coercive*. Then the Lax-Milgram theorem states the existence of a unique solution $u \in X$ to (4.1) as well as the existence of a unique discrete solution $u_h \in X_h$ to the discrete problem (4.2) (due to $X_h \subset X$).

The basis of error estimates for coercive problems is *Céa's Lemma*, which states that the *discretization error* $\|u - u_h\|_X$ is proportional to the approximation error:

Theorem 4.6 (Céa). *Let X_h be a sequence of subspaces of the Hilbert-space X . Suppose that the variational problem (4.1) fulfills the assumptions of Theorem 3.20 (Lax-Milgram). Let $u \in X$ denote the exact solution to (4.1) and $u_h \in X_h$ the solution to the corresponding discrete problem (4.2).*

Then the discretization error can be estimated by the approximation error as follows:

$$\|u - u_h\|_X \leq \frac{\alpha}{\beta} \inf_{v_h \in X_h} \|u - v_h\|_X, \quad (4.8)$$

where α is the continuity constant and β is the coercivity constant of $a(\cdot, \cdot)$ on X .

For the time being, we present the classical approximation result for $H^1(\Omega)$, as used e.g. for the Poisson problem.

Theorem 4.7 (Approximation error in $H^1(\Omega)$).

1. Let \mathcal{T}_h a shape-regular triangulation \mathcal{T}_h of Ω with affine linear element transformations.
2. Let X_h be chosen by the space of continuous, piecewise polynomials order k :

$$X_h := \{ v_h \in C(\Omega) \mid v_h|_K \in P^k(K) \ \forall K \in \mathcal{T}_h \}.$$

3. Assume a regular solution u belonging to $(H^{k+1}(\Omega))^3$.

Then the approximation error in the H^1 -norm can be estimated by

$$\inf_{v_h \in X_h} \|u - v_h\|_{H^m(\Omega)} \preceq h^{k+1-m} |u|_{H^{k+1}(\Omega)},$$

for $m = 0, 1$.

Choosing the discrete space X_h by continuous, piecewise polynomials, we achieve convergence by refining the mesh, i.e. $h \rightarrow 0$. The order of approximation can be improved by increasing the polynomial degree k , but as long as we increase k uniformly on the whole mesh, the benefit is limited by the global regularity of the exact solution $u \in X$.

For the time being, this result suffices as motivation for the choice of piecewise polynomial FE-spaces for approximating the exact solution. Note that in general approximation error estimates are obtained by estimating the interpolation error, which will be presented in Section 4.4.

4.3 An exact sequence of conforming finite element spaces

In the sequel we consider the construction of piecewise polynomial, conforming finite element spaces $X_h \subset X$ of functions over Ω (X usually denotes some Sobolev space), i.e.,

$$X_h = \{ v_h \in X \mid v_h|_K \in P^k(K) \quad \forall K \in \mathcal{T}_h \},$$

and \mathcal{T}_h denotes a regular triangulation of the domain Ω . We want to construct the spaces X_h in such a way, that the exact sequence property discussed in Section 3.2.1 carries over from the continuous spaces to the discrete spaces. In three space dimensions, this means

$$\begin{array}{ccccccccccc} \mathbb{R} & \xrightarrow{id} & H^1(\Omega) & \xrightarrow{\nabla} & H(\text{curl}, \Omega) & \xrightarrow{\text{curl}} & H(\text{div}, \Omega) & \xrightarrow{\text{div}} & L_2(\Omega) & \xrightarrow{0} & \{0\} \\ & & \cup & & \cup & & \cup & & \cup & & \\ \mathbb{R} & \xrightarrow{id} & W_h & \xrightarrow{\nabla} & V_h & \xrightarrow{\text{curl}} & Q_h & \xrightarrow{\text{div}} & S_h & \xrightarrow{0} & \{0\}. \end{array} \quad (4.9)$$

In the two dimensional setting we consider the corresponding shortened sequences, cf. (3.15) and (3.16).

4.3.1 The classical H^1 -conforming Finite Element Method

In this subsection, we introduce the classical lower-order finite elements used for H^1 -conforming methods.

Definition 4.8 (The linear H^1 -conforming finite element). *The classical lowest-order H^1 -conforming finite element for the simplex $K \in \mathbb{R}^d$ (a segment for $d = 1$, a triangle for $d = 2$, and a tetrahedron for $d = 3$), is defined by*

- the local space $\mathcal{P}_K = P^1(K)$ of dimension $\dim(P^1(K)) = d + 1$,
- the $(d + 1)$ vertex-based degrees of freedom, which amount to point-evaluation at the vertices, i.e.

$$N_i^V : v \longrightarrow v(V_i) \quad \forall V_i \in \mathcal{V}_K.$$

Definition 4.9. *The second-order H^1 -conforming finite element on a simplex $K \in \mathbb{R}^d$, $d = 2, 3$ is defined by*

- the local space $\mathcal{P}_K = P^2(K)$ with $\dim(P^2(K)) = \begin{cases} 6 & \text{for } d = 2, \\ 10 & \text{for } d = 3, \end{cases}$
- two types of degrees of freedom (dofs):

- the lowest-order, also denoted as vertex-based dofs:

$$N_i^V : v \rightarrow v(V_i) \quad \text{for } 1 \leq i \leq d + 1$$

- one edge-based degree of freedom over each edge $E_\alpha \in \mathcal{E}_K$ (see [42]):

$$N_\alpha^E : v \rightarrow \int_{E_\alpha} \frac{\partial v}{\partial s} \frac{\partial q_e}{\partial s} ds,$$

with edge-bubble $q_e \in P_0^2(E)$ and $\int_{E_\alpha} q_e^2 ds = 1$.

In classical finite element methods, as described, e.g. in CIARLET [35], so-called *Lagrange-type elements* are commonly used, i.e., the degrees of freedom are associated with evaluation of a function or its derivatives at several nodes located on the element. In view of an implementation of higher-order methods the above formulation will turn out to be more natural.

For practical implementation, we first construct a local basis (shape functions) on the reference element \hat{K} . By (4.6), the barycentric coordinates form a (nodal) basis for the lowest-order H^1 -conforming element, i.e., we choose

$$\hat{\phi}_i^V(\hat{\mathbf{x}}) = \hat{\lambda}_i(\hat{\mathbf{x}}) \quad \text{for } 1 \leq i \leq d+1, \quad (4.10)$$

which obviously span $P^1(\hat{K})$.

As nodal shape functions for the second-order element we use

$$\text{lowest-order functions: } \hat{\phi}_i^V(\hat{\mathbf{x}}) = \hat{\lambda}_i(\hat{\mathbf{x}}) \quad \forall 1 \leq i \leq d+1, \quad \text{and} \quad (4.11a)$$

$$\text{quadratic edge-bubbles: } \hat{\phi}_\alpha^E(\hat{\mathbf{x}}) = \hat{\lambda}_{e_1}(\hat{\mathbf{x}})\hat{\lambda}_{e_2}(\hat{\mathbf{x}}) \quad \forall E_\alpha = [e_1, e_2] \in \hat{\mathcal{E}}. \quad (4.11b)$$

Having defined the shape functions locally only on a reference element \hat{K} , we map the functions by a conforming transformation onto the physical element $K \in \mathcal{T}_h$. The following lemma states that for scalar functions this can be realized by a simple change of variables.

Lemma 4.10 (H^1 -conforming transformation). *Let $\Phi_K : \hat{K} \rightarrow K$ be a continuously differentiable, invertible and surjective map, and $\hat{u} \in H^1(\hat{K})$ be a scalar function. Then the change of variables*

$$u := \hat{u} \circ \Phi_K^{-1} \quad (4.12)$$

implies $u \in H^1(K)$ with

$$\nabla u = F_K^{-T} \hat{\nabla} \hat{u} \circ \Phi_K^{-1}. \quad (4.13)$$

The local shape functions on the physical element K are hence defined by

$$\phi_i^V(\mathbf{x}) = \lambda_i(\mathbf{x}) \quad \text{for } V_i \in \mathcal{V}_K, \quad (4.14a)$$

$$\phi_\alpha^E(\mathbf{x}) = \lambda_{e_1}(\mathbf{x})\lambda_{e_2}(\mathbf{x}) \quad \text{for } E_\alpha = [V_{e_1}, V_{e_2}] \in \mathcal{E}_K. \quad (4.14b)$$

To obtain the global finite element shape functions in W_h we have to piece the element-by-element defined shape-functions together. This is done by identifying the local degrees of freedom with the global ones. The standard element pull-back transformation (4.12) preserves the degrees of freedom of H^1 -conforming finite elements, i.e. $N_i^V(u) = \hat{N}_i^V(\hat{u})$ and $N_i^E(u) = \hat{N}_i^E(\hat{u})$ for $u \circ \Phi_K = \hat{u}$. By identification of the vertex-based and/or edge-based degrees of freedom corresponding to element interfaces we obtain the global finite element spaces as follows:

$$W_{h,1} := \bigoplus_{V_i \in \mathcal{V}} \text{span}\{\phi_i^V\},$$

$$W_{h,2} := \bigoplus_{V_i \in \mathcal{V}} \text{span}\{\phi_i^V\} \bigoplus_{E_i \in \mathcal{E}} \text{span}\{\phi_i^E\}.$$

Due to (4.7) barycentric coordinates are continuous across element interfaces. Hence, the above shape functions (4.14) match continuously at element interfaces. Owing to Corollary 3.5 this implies H^1 -conformity, i.e. for $k = 1, 2$:

$$W_{h,k} = \{w \in H^1(\Omega) \mid w|_K \in P^k(K) \forall K \in \mathcal{T}_h\}.$$

4.3.2 Low-order $H(\text{curl})$ -conforming Finite Element Methods

In curl – curl problems arising from electromagnetics, one is usually not only interested in the primal variable, but in the corresponding differential field. For example, in the vector potential formulations (2.28) the electric field intensity $\mathbf{E} = \frac{\partial}{\partial t} \mathbf{A}$ and the magnetic field intensity $\mathbf{H} = \mu^{-1} \text{curl } \mathbf{A}$ are the quantities of interest. It is therefore desirable to approximate the fluxes with high accuracy. This motivates the use of the following families of $H(\text{curl})$ -conforming finite elements:

- *Nédélec element of second kind* of order k , which involves a local FE-space of full polynomial order:

$$\mathcal{N}_k^{II}(K) := (P^k(K))^d. \quad (4.15)$$

- *Nédélec element of first kind* of order k , which involves a local space containing $P^k(K)$, enriched (in a minimal way) such that the *curl* of the involved functions also spans $P^k(K)$:

$$\mathcal{N}_k^I(K) := P^k(K)^d \oplus \{\mathbf{q} \in (\tilde{P}_{k+1}(K))^d \mid \mathbf{x} \cdot \mathbf{q} = 0\}, \quad (4.16)$$

where $\tilde{P}_{k+1}(K)$ denotes the set of homogenous polynomials of degree $k+1$. This setting implies

$$(P^k(K))^d \subset \mathcal{N}_k^I(K) \subset (P^{k+1}(K))^d \quad \text{and} \quad (P^{k+1}(K))^d = \mathcal{N}_k^I(K) \oplus \nabla \tilde{P}_{k+2}(K).$$

In this section, we consider the low-order finite element spaces where the local spaces are either $\mathcal{N}_0^I(K)$ or $\mathcal{N}_1^{II}(K)$. Both spaces involve finite element functions having piecewise constant curl-fields. As we will see below, these spaces are also natural in the sense that they can be used to build an exact sequence.

Definition 4.11 (Nédélec element of first kind of order 0). *The lowest order edge-element on a triangle, respectively a tetrahedron, K is given by*

- the local space $\mathcal{N}_0^I(K)$ defined as

$$\begin{aligned} \text{for } d = 2: \quad \mathcal{N}_0^I(K) &:= \left\{ \mathbf{a} + b \begin{pmatrix} y \\ -x \end{pmatrix} \mid \mathbf{a} \in \mathbb{R}^2, b \in \mathbb{R} \right\} && \text{with } \dim(\mathcal{N}_0^I(K)) = 3, \\ \text{for } d = 3: \quad \mathcal{N}_0^I(K) &:= \left\{ \mathbf{a} + \mathbf{b} \times \mathbf{x} \mid \mathbf{a}, \mathbf{b} \in \mathbb{R}^3 \right\} && \text{with } \dim(\mathcal{N}_0^I(K)) = 6. \end{aligned}$$

- the edge-based degrees of freedom:

$$N_\alpha^{\mathcal{N}_0} : \mathbf{v} \rightarrow \int_{E_\alpha} \mathbf{v} \cdot \boldsymbol{\tau} \, d\mathbf{x} \quad \text{for } \alpha = 1, \dots, |\mathcal{E}_K|,$$

i.e. the line integrals of the tangential component over each edge $E_\alpha \in \mathcal{E}_K$.

The local space $\mathcal{N}_0^I(K)$ lies between the full polynomial spaces of order 0 and 1, i.e.

$$(P^0(K))^3 \subset \mathcal{N}_0^I(K) \subset (P^1(K))^3 \quad \text{with} \quad \text{curl } \mathcal{N}_0^I(K) = (P^0(K))^3.$$

We choose the lowest-order shape functions corresponding to the *1-form Whitney element*, cf. BOSSAVIT [25].

Lemma 4.12. *The nodal basis of $\mathcal{N}_0^I(K)$ is realized by the edge-based shape functions*

$$\varphi_\alpha^{\mathcal{N}_0} = \nabla \lambda_{\alpha_1} \lambda_{\alpha_2} - \lambda_{\alpha_1} \nabla \lambda_{\alpha_2}$$

for each edge $E_\alpha = [V_{\alpha_1}, V_{\alpha_2}] \in \mathcal{E}_K$. Moreover, the shape functions have constant tangential trace on the edges of K , i.e.,

$$\varphi_\alpha^{\mathcal{N}_0} \cdot \boldsymbol{\tau}|_{E_\beta} = \frac{1}{|E_\beta|} \delta_{\alpha\beta}, \quad \text{for } E_\alpha, E_\beta \in \mathcal{E}_K, \quad (4.17)$$

in particular $N_\beta^{\mathcal{N}_0}(\varphi_\alpha^{\mathcal{N}_0}) = \int_{E_\beta} \varphi_\alpha^{\mathcal{N}_0} \cdot \boldsymbol{\tau} \, d\mathbf{x} = \delta_{\alpha\beta}$.

Proof. We reformulate the local space as $\mathcal{N}_0^I(K) = \{B\mathbf{x} + \mathbf{b} \mid B = -B^T \in \mathbb{R}_d^d\}$. Since the shape functions $\varphi_\alpha^{\mathcal{N}_0}$ are linear, we can express $\varphi_\alpha^{\mathcal{N}_0}(\mathbf{x}) = A\mathbf{x} + \mathbf{a}$ with $A = \nabla(\varphi_\alpha^{\mathcal{N}_0}) = \nabla \lambda_{\alpha_1} : \nabla \lambda_{\alpha_2} - \nabla \lambda_{\alpha_2} : \nabla \lambda_{\alpha_1}$, which is skew-symmetric. Hence, $\varphi_\alpha^{\mathcal{N}_0} \in \mathcal{N}_0^I(K)$. Next we consider a trivial vector field $\mathbf{v} = \sum_{\alpha=1}^{|\mathcal{E}_K|} c_\alpha \varphi_\alpha^{\mathcal{N}_0} = 0$. This implies $\mathbf{v} \cdot \boldsymbol{\tau}|_{E_\alpha} = 0$ on all edges. In combination with (4.17) we obtain $c_\alpha/|E_\alpha| = 0, \forall E_\alpha \in \mathcal{E}_K$ and hence the *linear independence* of the shape functions. Due to the *counting argument* we have $\dim(\mathcal{N}_0^I(K)) = |\mathcal{E}_K|$ and hence

$$\text{span}\{\varphi_\alpha^{\mathcal{N}_0} : E_\alpha \in \mathcal{E}_K\} = \mathcal{N}_0^I(K).$$

To show (4.17), we consider an edge $E_\beta = [V_{\beta_1}, V_{\beta_2}]$ where $\boldsymbol{\tau}$ denotes the associated tangential vector. Then $\nabla \lambda_k \cdot \boldsymbol{\tau}|_{E_\beta} = \frac{1}{|E_\beta|} (-\delta_{k\beta_1} + \delta_{k\beta_2})$ and $\lambda_k = 0$ on E_β if $k \notin E_\alpha$. We obtain

$$\varphi_\beta^{\mathcal{N}_0} \cdot \boldsymbol{\tau}|_{E_\beta} = \frac{1}{|E_\beta|} (\lambda_{\beta_1} + \lambda_{\beta_2})|_{E_\beta} = \frac{1}{|E_\beta|}. \quad (4.18)$$

Concerning the remaining edges, i.e. $E_\alpha \neq E_\beta$ there exists a vertex $V_{\alpha_k} \in E_\alpha$ s.t. $V_k \notin E_\beta$, which implies $\nabla \lambda_{\alpha_k} \cdot \boldsymbol{\tau}|_{E_\beta} = 0$ as well as $\lambda_{\alpha_k}|_{E_\beta} = 0$ and hence $\varphi_\alpha^{\mathcal{N}_0}|_\beta = 0$. Evaluating the line-integral of (4.17) over several edges E_β finally yields the *nodality* of the basis. \square

Definition 4.13 (Lowest-order Nédélec elements of second kind). *The Nédélec element of second kind of order $p = 1$ on a simplex K is defined by*

- the full-order space $\mathcal{N}_1^{II}(K) = (P^1(K))^d$ of dimension 6 for $d = 2$ and 12 for $d = 3$,
- the first and second moment of the tangential components over each edge $E_\alpha \in \mathcal{E}_K$, i.e.

$$N_\alpha^k : \mathbf{v} \rightarrow \int_{E_\alpha} \mathbf{v} \cdot \boldsymbol{\tau} q_k \, d\mathbf{x} \quad \text{for } k = 0, 1,$$

where $\{q_k\}$ is a basis for $P^1(E_\alpha)$ and $q_0 = 1$.

Lemma 4.14. *For an edge $E_\alpha = [V_{\alpha_1}, V_{\alpha_2}] \in \mathcal{E}_K$, $\alpha = 1, \dots, |\mathcal{E}_K|$, define*

$$\varphi_\alpha^{\mathcal{N}_0} = \nabla \lambda_{\alpha_1} \lambda_{\alpha_2} - \lambda_{\alpha_1} \nabla \lambda_{\alpha_2}, \quad \text{and} \quad (4.19a)$$

$$\varphi_\alpha^E = \nabla(\lambda_{\alpha_1} \lambda_{\alpha_2}) \quad (4.19b)$$

Then the set $\{\varphi_\alpha^{\mathcal{N}_0}, \varphi_\alpha^E\}$ of shape functions is a basis for the Nédélec element $\mathcal{N}_1^{II}(K)$ of second kind:

Proof. Following the proof of Lemma 4.12 we obtain the extension of 4.18 as

$$\begin{aligned}\varphi_\alpha^{\mathcal{N}_0} \cdot \boldsymbol{\tau}|_{E_\beta} &= \frac{1}{|E_\alpha|} (\lambda_{\alpha_1} + \lambda_{\alpha_2})|_{E_\beta} = \frac{1}{|E_\alpha|} \delta_{\alpha\beta} \\ \varphi_\alpha^E \cdot \boldsymbol{\tau}|_{E_\beta} &= \frac{1}{|E_\alpha|} (\lambda_{\alpha_1} - \lambda_{\alpha_2})|_{E_\alpha} \delta_{\alpha\beta}\end{aligned}$$

with $(\lambda_{\alpha_1} - \lambda_{\alpha_2})$ being linear on E_α . This implies the linear-independence of the shape functions. Verifying the counting argument $\dim(P^1(K))^d = 2|\mathcal{E}_K|$ concludes the proof. \square

Since the edge-based shape functions, of the element of second type, are gradient functions, there obviously holds

$$\operatorname{curl} \mathcal{N}_0^I(K) = \operatorname{curl} \mathcal{N}_1^{II}(K).$$

$H(\operatorname{curl})$ -conforming element transformation. The conforming transformation of vectorial shape functions on the reference element \hat{K} onto shape functions defined on a physical element K is more involved than in the scalar case. Note that in order to guarantee $H(\operatorname{curl})$ -conformity, we want that the degrees of freedom are preserved by the transformation. Moreover, for establishing a local exact sequence property, we have to ensure that gradient fields on the reference element are mapped onto gradient fields on the physical element. In view of (4.13), we suggest the following transformation:

Lemma 4.15 ($H(\operatorname{curl})$ -conforming transformation). *Let $\Phi_K : \hat{K} \rightarrow K$ be a continuously differentiable, invertible and surjective map, and $\hat{\mathbf{u}} \in H(\operatorname{curl}, \hat{K})$. Then the transformation*

$$\mathbf{u} := F_K^{-T} \hat{\mathbf{u}} \circ \Phi_K^{-1} \quad (4.20)$$

implies $\mathbf{u} \in H(\operatorname{curl}, K)$ with

$$(\operatorname{curl}_{\mathbf{x}} \mathbf{u}) = J_K^{-1} F_K \operatorname{curl}_{\hat{\mathbf{x}}} \hat{\mathbf{u}} \circ \Phi_K^{-1} \quad (4.21)$$

for $K \subset \mathbb{R}^3$. In two dimensions we obtain instead $\operatorname{curl}_{\mathbf{x}} \mathbf{u} = J_K^{-1} \operatorname{curl}_{\hat{\mathbf{x}}} \hat{\mathbf{u}} \circ \Phi_K^{-1}$.

A proof of the lemma can be found in MONK [70] (Lemma 3.57, Corollary 3.58).

In the following we collect some important properties of the transformation above:

1. Tangential traces along edges transform as

$$(\mathbf{u} \cdot \boldsymbol{\tau}) \circ \Phi_K|_{\hat{E}} = \left(F_K^{-T} \hat{\mathbf{u}} \cdot \frac{F_K^T \hat{\boldsymbol{\tau}}}{\|F_K^T \hat{\boldsymbol{\tau}}\|} \right) |_{\hat{E}} = \left(\hat{\mathbf{u}} \cdot \hat{\boldsymbol{\tau}} \frac{1}{\|F_K^T \hat{\boldsymbol{\tau}}\|} \right) |_{\hat{E}}.$$

Taking into account the transformation of line integrals we obtain

$$N_i^k(\mathbf{u}) = \int_{\Phi_K(\hat{E})} \mathbf{u} \cdot \boldsymbol{\tau} q_k ds = \int_{\hat{E}} \hat{\mathbf{u}} \cdot \frac{\hat{\boldsymbol{\tau}}}{\|F_K^T \hat{\boldsymbol{\tau}}\|} \hat{q}_k \|F_K^T \hat{\boldsymbol{\tau}}\| d\hat{s} = \hat{N}_i^k(\hat{\mathbf{u}}),$$

where $q_k \circ \Phi_K := \hat{q}_k$. Hence, the degrees of freedom are preserved by the transformation.

2. Gradient fields $\hat{\mathbf{p}} \in \hat{\nabla} H^1(\hat{K})$ are mapped onto gradient fields $\mathbf{p} \in \nabla H^1(K)$, since for all $\hat{\mathbf{u}} = \hat{\nabla} \hat{w}$:

$$\mathbf{u} \circ \Phi_K = F_K^{-T} \hat{\mathbf{u}} = F_K^{-T} \hat{\nabla} \hat{w} = (\nabla w) \circ \Phi_K$$

with $w \circ \Phi_K := \hat{w}$ and $w \in H^1(K)$.

Applying the conforming transformation (4.20) on the shape functions $\hat{\varphi}_\alpha^{N_0}, \hat{\varphi}_\alpha^E$ defined on the reference element \hat{K} we can deduce the shape functions $\varphi_\alpha^{N_0}, \varphi_\alpha^E$ on the physical element K . This can be verified by performing a change of variables $\mathbf{x} = \Phi_k(\hat{\mathbf{x}})$ in the shape functions (4.19) and taking into account the transformation of gradient fields according to Lemma 4.10 as follows:

$$\begin{aligned}\varphi_\alpha^{N_0}(\mathbf{x}) &= \nabla \lambda_{\alpha_1}(\mathbf{x}) \lambda_{\alpha_2}(\mathbf{x}) - \lambda_{\alpha_1}(\mathbf{x}) \nabla \lambda_{\alpha_2}(\mathbf{x}) \\ &= (F_K^{-T} \hat{\nabla} \hat{\lambda}_{\alpha_1})(\hat{\mathbf{x}}) \hat{\lambda}_{\alpha_2}(\hat{\mathbf{x}}) - \hat{\lambda}_{\alpha_1}(\hat{\mathbf{x}}) (F_K^{-T} \hat{\nabla} \hat{\lambda}_{\alpha_2})(\hat{\mathbf{x}}) \\ &= F_K^{-T}(\hat{\mathbf{x}}) (\hat{\nabla} \hat{\lambda}_{\alpha_1} \hat{\lambda}_{\alpha_2} - \hat{\nabla} \hat{\lambda}_{\alpha_2} \hat{\lambda}_{\alpha_1})(\hat{\mathbf{x}}) \\ &= F_K^{-T}(\hat{\mathbf{x}}) \hat{\varphi}_\alpha^{N_0}(\hat{\mathbf{x}}), \\ \varphi_\alpha^E(\mathbf{x}) &= \nabla(\lambda_1 \lambda_2)(\mathbf{x}) = F_K^{-T}(\hat{\mathbf{x}}) \hat{\nabla}(\hat{\lambda}_{\alpha_1} \hat{\lambda}_{\alpha_2})(\hat{\mathbf{x}}) \\ &= F_K^{-T}(\hat{\mathbf{x}}) \hat{\varphi}_\alpha^E(\hat{\mathbf{x}}).\end{aligned}$$

Global shape functions and $H(\text{curl})$ -conforming FE-space In order to obtain global FE-spaces we identify the degrees of freedom corresponding to the global edges of the mesh, i.e. we glue the shape functions together:

$$\begin{aligned}V_{h,0} &:= \bigoplus_{E_i \in \mathcal{E}} \text{span}\{\varphi_i^{N_0}\}, \\ V_{h,1}^{II} &:= \bigoplus_{E_i \in \mathcal{E}} \text{span}\{\varphi_i^{N_0}, \varphi_i^E\}.\end{aligned}$$

The $H(\text{curl})$ -conformity of the element can be verified by the following argument. Suppose that $\mathbf{v} = \sum c_i \varphi_i \in P^K(K)$. The associated finite element is $H(\text{curl})$ -conforming: whenever the degrees of freedom associated with an interface (an edge E_α or respectively a face F_β) are zero, the tangential trace of \mathbf{v} vanishes on the interface, i.e. $\mathbf{v} \cdot \boldsymbol{\tau}|_{E_\alpha} = 0$, or resp. $(\mathbf{v} \times \mathbf{n})|_{F_\alpha} = 0$. From the proofs of Lemma 4.12 and Lemma 4.14 we know that the edge-based shape functions associated with the interfaces are the only shape functions with non-vanishing tangential trace on the interface. Therefore, the tangential trace on faces (only $d = 3$) and edges is realized by the shape functions associated with this interface. Since the global FE-space is obtained by identification of the corresponding coefficients at the interfaces, we obtain tangential continuity of the global shape functions.

We note that one has to take the global edge-orientation (the orientation of the tangential vector) into account within the setting of global shape functions. If the global edge has the opposite orientation than the transformed global one, the sign of the transformed shape function on the corresponding element has to be changed. This can be done by allowing ± 1 entries in the connectivity matrix during the assembling process.

Summarizing, we obtain tangential continuity over element interfaces and owing to Corollary 3.8 we obtain two $H(\text{curl})$ -conforming FE-spaces:

$$\begin{aligned}V_{h,0} &= \{\mathbf{v} \in H(\text{curl})(\Omega) \mid \mathbf{v}|_K \in \mathcal{N}_0^I(K) \ \forall K \in \mathcal{T}_h\}, \\ V_{h,1}^{II} &= \{\mathbf{v} \in H(\text{curl})(\Omega) \mid \mathbf{v}|_K \in (P^1(K))^d \ \forall K \in \mathcal{T}_h\}.\end{aligned}$$

Since the lowest-order degrees of freedom of $H(\text{curl})$ -conforming elements are associated with the edges of the mesh, it is common to call the Nédélec elements the *edge elements*.

4.3.3 Low-order $H(\text{div})$ -conforming Finite Elements Methods

Due to similar considerations as for the $H(\text{curl})$ -space we introduce the following two types of $H(\text{div})$ -conforming elements, differing in the approximation of divergence fields:

- the *Brezzi-Douglas-Marini* (BDM_k) element of order k with the local FE-space

$$BDM_k(K) := (P^k(K))^d, \quad (4.22)$$

- the *Raviart-Thomas* (\mathcal{RT}_k) element of order k with the enriched local FE-space

$$\mathcal{RT}_k(K) := (P^k(K))^d \oplus \mathbf{x} \tilde{P}_k(K) \quad (4.23)$$

with $\text{div } \mathcal{RT}_k(K) = P^k(K)$. In three dimensions, the Raviart-Thomas element is also called Raviart-Thomas-Nédélec element.

Note that the spaces $\mathcal{RT}_k(K)$ and $BDM_k(K)$ contain the same divergence-free vectors. This time, the triangular and tetrahedral cases have to be treated separately.

$H(\text{div})$ -conforming elements in two dimensions The two-dimensional case can be handled by a simple rotation of 90 degrees of the $H(\text{curl})$ -conforming element.

Definition 4.16. 1. The lowest-order Raviart-Thomas element (of order $k = 0$) on a triangle K is defined by

- the local space $\mathcal{RT}_0(K) = \{\mathbf{a} + b\mathbf{x} \mid \mathbf{a} \in \mathbb{R}^2, b \in \mathbb{R}\}$ with $\dim(\mathcal{RT}_0(K)) = 3$,
- the total flux over each edge $E_\alpha \in \mathcal{E}_K$, i.e.,

$$N_\alpha : \mathbf{v} \rightarrow \int_{E_\alpha} \mathbf{v} \cdot \mathbf{n} \, d\mathbf{x} \quad \alpha = 1, 2, 3.$$

2. The linear BDM -element (of order $k = 1$) on a triangle K is defined by

- the full-polynomial local space $BDM_1(K) = (P^1(K))^2$,
- two degrees of freedom associated with each edge $E_\alpha \in \mathcal{E}_K$, namely

$$N_\alpha : \mathbf{v} \rightarrow \int_{E_\alpha} \mathbf{v} \cdot \mathbf{n} \, q_k \, d\mathbf{x} \quad \text{for } k = 0, 1,$$

with $(q_k)_{k=1,2}$ spanning $P^1(E_\alpha)$.

For a hierarchical definition of BDM -elements of higher order it will be important to choose $q_0 = 1$. We will assume this also for the linear case. As already mentioned above, the fluxes of these elements span the same spaces, i.e.,

$$\text{div } \mathcal{RT}_0(K) = \text{div } BDM_1(K) = P^0(K),$$

and the nodal shape functions can be derived by rotating by 90 degrees the nodal shape functions of the Nédélec element, which yields

$$\begin{aligned} \psi_\alpha^{\mathcal{RT}_0} &= \lambda_{\alpha_1} \text{Curl } \lambda_{\alpha_2} - \text{Curl } \lambda_{\alpha_1} \lambda_{\alpha_2}, \\ \psi_\alpha^E &= \text{Curl} (\lambda_{\alpha_1} \lambda_{\alpha_2}), \end{aligned}$$

for each edge $E_\alpha = [V_{\alpha_1}, V_{\alpha_2}] \in \mathcal{E}_K$.

$H(\text{div})$ -conforming elements in three dimensions

We consider only the lowest-order element $\mathcal{RT}_0(K)$ here, and leave the treatment of BDM_k elements to the next chapter.

Definition 4.17. *The classical, lowest-order, $H(\text{div})$ -conforming element on a tetrahedron K is defined by*

- the local space $\mathcal{RT}_0(K) = \{\mathbf{a} + b\mathbf{x} \mid \mathbf{a} \in \mathbb{R}^3, b \in \mathbb{R}\}$ with $\dim(\mathcal{RT}_0(K)) = 4$,
- the lowest-order degrees of freedom associated with faces, i.e. the total normal fluxes over each $F_\alpha \in \mathcal{F}_K$:

$$N_\alpha : \mathbf{v} \rightarrow \int_{F_\alpha} \mathbf{v} \cdot \mathbf{n} \, d\mathbf{x} \quad \text{for } 1 \leq \alpha \leq 4.$$

For the lowest-order Raviart-Thomas element we obtain

$$(P^0(K))^3 \subset \mathcal{RT}_0(K) \subset (P^1(K))^3 \quad \text{with } \text{div } \mathcal{RT}_0 = P^0(K).$$

Since the degrees of freedom are associated with the faces of the mesh, such elements (of arbitrary order) are often called *face elements*. The *lowest-order face-based shape functions* can be realized by 2-form Whitney-elements as described in BOSSAVIT [25].

Lemma 4.18. *Associating with each face $\hat{F}_\alpha \in \mathcal{F}_{\hat{K}}$ the shape function*

$$\hat{\psi}_\alpha^{\mathcal{RT}_0} = \hat{\lambda}_{f_1} \hat{\nabla} \hat{\lambda}_{f_2} \times \hat{\nabla} \hat{\lambda}_{f_3} + \hat{\lambda}_{f_2} \hat{\nabla} \hat{\lambda}_{f_3} \times \hat{\nabla} \hat{\lambda}_{f_1} + \hat{\lambda}_{f_3} \hat{\nabla} \hat{\lambda}_{f_1} \times \hat{\nabla} \hat{\lambda}_{f_2}, \quad (4.24)$$

where $F_\alpha = [f_1, f_2, f_3]$, yields a nodal basis for $\mathcal{RT}_0(\hat{K})$.

The flux of $\hat{\psi}_\alpha^{\mathcal{RT}_0}$ across the face \hat{F}_α is 1 and vanishes across all other faces, i.e.

$$\int_{\hat{F}_\alpha} \hat{\psi}_\beta^{\mathcal{RT}_0} \cdot \hat{\mathbf{n}} \, d\hat{\mathbf{x}} = \delta_{\alpha\beta}, \quad (4.25)$$

if the counter-clockwise rotation of the vertices $[f_1, f_2, f_3]$ points in the direction of the outer normal vector $\hat{\mathbf{n}}$.

Proof. The outer normal vector $\hat{\mathbf{n}}$ on the face \hat{F}_α , determined by the vertex-triple $[f_1, f_2, f_3]$, can be expressed by $\hat{\mathbf{n}} = -\hat{\nabla} \hat{\lambda}_{f_4} / |\hat{\nabla} \hat{\lambda}_{f_4}|$ where f_4 denotes the vertex on the tetrahedron opposite to the face $[f_1, f_2, f_3]$. Using $\hat{\lambda}_1 + \hat{\lambda}_2 + \hat{\lambda}_3 + \hat{\lambda}_4 = 1$ in \hat{K} and $\hat{\lambda}_4 = 0$ on F_α the relation $|\hat{\nabla} \hat{\lambda}_4| = |F_\alpha|$ implies

$$\hat{\psi}_\alpha^{\mathcal{RT}_0} \cdot \hat{\mathbf{n}}|_{\hat{F}_\alpha} = (\hat{\nabla} \hat{\lambda}_{f_1} \times \hat{\nabla} \hat{\lambda}_{f_2} \cdot \hat{\nabla} \hat{\lambda}_{f_3}) \frac{1}{|\hat{\nabla} \hat{\lambda}_{f_4}|} = (\hat{\nabla} \hat{\lambda}_{f_1} \times \hat{\nabla} \hat{\lambda}_{f_2} \cdot \hat{\nabla} \hat{\lambda}_{f_3}) \frac{1}{|F_\alpha|}.$$

Since $\hat{\nabla} \hat{\lambda}_{f_1} \times \hat{\nabla} \hat{\lambda}_{f_2} \cdot \hat{\nabla} \hat{\lambda}_{f_3} = 1$ if the counter-clockwise rotation of $[f_1, f_2, f_3]$ points out of \hat{K} (otherwise it is -1), integration over F_α yields (4.25) for $\alpha = \beta$.

Now let f_1 denote the vertex opposite to \hat{F}_β with outer unit normal vector $\hat{\mathbf{n}}_\beta = -\hat{\nabla} \hat{\lambda}_{f_1} / |\hat{\nabla} \hat{\lambda}_{f_1}|$. Then there holds

$$\hat{\psi}_\alpha^{\mathcal{RT}_0} \cdot \hat{\mathbf{n}}_\beta = (\hat{\lambda}_{f_1} \hat{\nabla} \hat{\lambda}_{f_2} \times \hat{\nabla} \hat{\lambda}_{f_3}) \cdot \hat{\nabla} \hat{\lambda}_{f_1} = 0 \quad \text{for } \alpha \neq \beta,$$

since $\hat{\lambda}_{f_1} = 0$ on \hat{F}_β . □

$H(\text{div})$ -conforming transformation

We plan to construct global basis functions for $H(\text{div}, T)$ again by a conforming transformation of basis functions on the reference element \hat{K} . The following transformation preserves curl-fields, cf. (4.21):

Lemma 4.19 ($H(\text{div})$ -conforming transformation). *Let $\Phi_K : \hat{K} \rightarrow K$ be a continuously differentiable, invertible and surjective mapping. Given a vector function $\hat{\mathbf{p}} \in H(\text{div}, \hat{K})$ the Piola transformation*

$$\mathbf{p} := J_K^{-1} F_K \hat{\mathbf{p}} \circ \Phi_K^{-1},$$

also called the contravariant transformation, implies $\mathbf{p} \in H(\text{div}, K)$ with

$$\text{div } \mathbf{p} = J_K^{-1} \text{div}_{\hat{\mathbf{x}}} \hat{\mathbf{p}} \circ \Phi_K^{-1}.$$

The proof of this result can be found in MONK [70, Lemma 3.59]. The Piola transformation has the following desired properties:

1. Normal traces transform as

$$(\mathbf{u} \cdot \mathbf{n}) \circ \Phi_K|_{\hat{F}} = \left(J_K^{-1} F_K \hat{\mathbf{u}} \cdot \frac{F_K^{-T} \hat{\mathbf{n}}}{\|F_K^{-T} \hat{\mathbf{n}}\|} \right)|_{\hat{F}} = \left(\hat{\mathbf{u}} \cdot \hat{\mathbf{n}} \frac{1}{J_K \|F_K^T \hat{\mathbf{n}}\|} \right)|_{\hat{F}}$$

Taking into account the transformation of surface integrals, i.e.

$$\int_A dA = \int_{\hat{A}} |J_K| \|F_K^{-T} \hat{\mathbf{n}}\| d\hat{A},$$

we see that the lowest-order degrees of freedom are invariant with respect to the Piola transformation:

$$\int_{F_\alpha} \mathbf{p} \cdot \mathbf{n} d\mathbf{x} = \text{sign}(J_K) \int_{\hat{F}_\alpha} \hat{\mathbf{p}} \cdot \hat{\mathbf{n}} d\hat{\mathbf{x}}.$$

2. Curl fields $\hat{\mathbf{p}} \in \text{curl}_{\hat{\mathbf{x}}} H(\text{curl}, \hat{K})$ are mapped onto curl fields $\mathbf{p} \in \text{curl} H(\text{curl}, K)$:

$$\mathbf{p} \circ \Phi_K = J_K^{-1} F_K \hat{\mathbf{p}} = J_K^{-1} F_K \text{curl}_{\hat{\mathbf{x}}} \hat{\mathbf{v}} = \text{curl } \mathbf{v} \circ \Phi_K.$$

3. The Piola transformation preserves $\hat{\mathbf{p}} = \hat{\nabla} \hat{u} \times \hat{\nabla} \hat{v}$ for scalar functions $\hat{u}, \hat{v} \in H^1(\hat{K})$:

$$\begin{aligned} \mathbf{p} \circ \Phi_K &= J_K^{-1} F_K \hat{\mathbf{p}} = J_K^{-1} F_K (\hat{\nabla} \hat{u} \times \hat{\nabla} \hat{v}) = (F_K^{-T} \hat{\nabla} \hat{u}) \times (F_K^{-T} \hat{\nabla} \hat{v}) \\ &= (\nabla u \times \nabla v) \circ \Phi_K. \end{aligned}$$

4. In the case of an affine linear transformation, the Raviart-Thomas space $\mathcal{RT}_k(K)$ is invariant with respect to the Piola transformation (see BREZZI-FORTIN [32]).

Applying the Piola transformation to the lowest-order Raviart Thomas shape functions on the reference element, we obtain the following shape functions on the physical element K :

$$\begin{aligned} \psi_\alpha^{\mathcal{RT}_0} &= J_K^{-1} F_K^{-T} \psi_\alpha^{\mathcal{RT}_0} \circ \Phi_K^{-1} \\ &= \lambda_{f_1} \nabla \lambda_{f_2} \times \nabla \lambda_{f_3} + \lambda_{f_2} \nabla \lambda_{f_3} \times \nabla \lambda_{f_1} + \lambda_{f_3} \nabla \lambda_{f_1} \times \nabla \lambda_{f_2}. \end{aligned} \quad (4.26)$$

with normal flux $\int_{F_\alpha} \psi_\beta^{\mathcal{RT}_0} \cdot \mathbf{n} d\mathbf{x} = \delta_{\alpha\beta}$ across the face F_α .

Global shape functions and $H(\text{div})$ -conformity Identifying the degrees of freedom associated with the faces of the mesh leads to the global FE-space

$$Q_{h,0} := \bigoplus_{F_i \in \mathcal{F}} \text{span}\{\psi_i^{\mathcal{RT}_0}\}.$$

The $H(\text{div})$ -conformity of the physical elements associated with $\mathcal{RT}_0(K)$ can be verified as follows: Let $\mathbf{q} \in \mathcal{RT}_0(K)$ with $\mathbf{q} \cdot \mathbf{n} = 0$ on the face F_j . In order to verify $H(\text{div})$ conformity we only have to show that all degrees of freedom (dofs) associated with this face vanish, i.e. $N_j^{\mathcal{RT}_0}(\mathbf{q}) = 0$. Now observe that $0 = \mathbf{q} = \sum_{F_i \in \mathcal{F}} N_i^{\mathcal{RT}_0}(\mathbf{q}) \psi_i^{\mathcal{RT}_0}$ and furthermore $0 = \text{tr}_{F_j}(\mathbf{q} \cdot \mathbf{n}) = N_j^{\mathcal{RT}_0}(\mathbf{q}) \text{tr}_{F_j}(\psi_j^{\mathcal{RT}_0}) = N_j^{\mathcal{RT}_0}(\mathbf{q}) \frac{1}{|F_j|}$.

The normal flux through the interface of two adjacent elements is determined by the degree of freedom associated with this face. Since we associated the degrees of freedom explicitly with the fluxes over the faces, the global shape functions have continuous normal components by construction. Hence the global FE-space is a subspace of $H(\text{div})$, i.e.

$$Q_{h,0} = \{\mathbf{q} \in H(\text{div}, \Omega) \mid \mathbf{q}|_K \in \mathcal{RT}_0(K) \forall K \in \mathcal{T}_h\}.$$

4.3.4 The lowest-order L_2 -conforming Finite Element Method

In contrast to the finite element spaces discussed previously, the L_2 -conforming space requires no continuity across the element interfaces. In principle, L^2 -conforming elements can be constructed in an analogy to H^1 -conforming elements, but without regarding continuity across element boundaries. We just sketch the such a construction:

Definition 4.20. *The L_2 -conforming element of order k on a triangle or tetrahedron K is defined by*

- the local space $P^k(K)$,
- the cell-based degrees of freedom:

$$N_l^C : p \rightarrow \int_K p q_l \, d\mathbf{x} \quad 0 \leq l \leq k$$

with $(q_l)_{0 \leq l \leq k}$ a basis of $P^k(K)$

For a hierarchical construction (higher order) it will be important that $\{q_k\}$ is a hierarchical basis of $P^k(K)$, in particular $q_0 = 1$. The nodal lowest-order shape function can be realized as

$$\vartheta_i = \frac{1}{|K_i|} \forall K_i \in \mathcal{T}_h. \quad (4.27)$$

Classically one uses the standard element pull-back transformation (4.12) for scalar functions to define the basis functions on the physical element K . But in view of the global exact sequence property we define the L_2 -conforming transformation by the conforming transformation of divergence fields defined in Lemma 4.19 as follows (cf. DEMKOWICZ ET AL. [44]).

Lemma 4.21 (L_2 -conforming transformation). *Let $\Phi_K : \hat{K} \rightarrow K$ be a continuously differentiable, invertible and surjective mapping. Given a function $\hat{q} \in L_2(\hat{K})$ we define its L_2 -conforming transformation by*

$$q = J_K^{-1} \hat{q} \circ \Phi_K^{-1}. \quad (4.28)$$

Since no continuity across element interfaces is required, the global element space can be locally, i.e.

$$S_{h,0} := \bigoplus_{K_i \in \mathcal{T}_h} \text{span}\{\vartheta_i^C\} = \{g \in L^2(\Omega) \mid g|_K \in P^0(K) \forall K \in \mathcal{T}_h\}. \quad (4.29)$$

4.3.5 Discrete exact sequences

In order to show the exactness of the sequence (4.9) of the global FE-spaces, we first show that the associated local sequence defined on the reference element \hat{K} is exact.

Exact sequences on the reference element level involving spaces of the first family

Lemma 4.22. *Concerning the reference tetrahedron \hat{K} we obtain that the following sequence of local FE-spaces associated with the first kind of low order finite elements is exact:*

$$\mathbb{R} \xrightarrow{id} P^1(\hat{K}) \xrightarrow{\nabla} \mathcal{N}_0^I(\hat{K}) \xrightarrow{\text{curl}} \mathcal{RT}_0(\hat{K}) \xrightarrow{\text{div}} P^0(\hat{K}), \quad (4.30)$$

as illustrated in Figure 4.2.

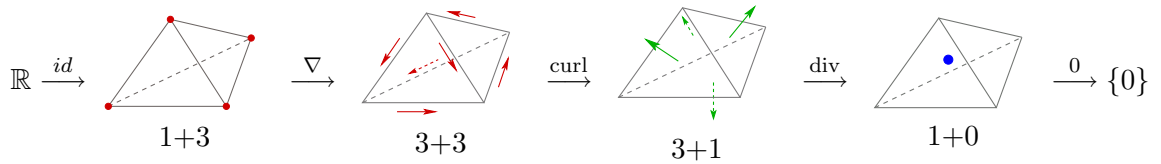


Figure 4.2: This sequence for the elements of the first family with vertex-based(black), edge-based(red), face-based(green) and element-based(blue) dofs is exact. The range of an operator has the same dimension as the kernel of the following operator.

This can be easily verified by two steps:

1. The range of a differential operator is included in the kernel of the following one:

$$\begin{aligned} \nabla P^1(\hat{K}) &= P^0(\hat{K})^3 \subset \mathcal{N}_0^I(\hat{K}), & \text{hence } \nabla P^1(\hat{K}) &\subset \ker(\text{curl } \mathcal{N}_0^I(\hat{K})), \\ \text{curl } \mathcal{N}_0^I(\hat{K}) &= P^0(\hat{K})^3 \subset \mathcal{RT}_0(\hat{K}), & \text{hence } \text{curl } \mathcal{N}_0^I(\hat{K}) &\subset \ker(\text{div } \mathcal{RT}_0(\hat{K})), \\ \text{div } \mathcal{RT}_0(\hat{K}) &= P^0(\hat{K}). \end{aligned}$$

2. We recall the algebraic property of discrete spaces and linear transformations D that

$$\dim(X_h) = \dim(\ker(D)) + \dim(\text{range}(D)). \quad (4.31)$$

A simple counting argument now shows that equality holds instead of only inclusion, i.e., $\text{range}(\text{div}) = \text{span}\{1\}$, $\text{range}(\nabla) = \ker(\text{curl})$, and $\text{range}(\text{curl}) = \ker(\text{div})$; cf. Figure 4.2.

In the two-dimensional case we obtain the following shortened sequences, involving the lowest-order elements of first kind:

Lemma 4.23. *For the triangular reference element \hat{K} the shortened sequences of local lowest order FE-spaces (as illustrated in Figure 4.3 and Figure 4.4)*

$$\mathbb{R} \xrightarrow{id} P^1(\hat{K}) \xrightarrow{\nabla} \mathcal{N}_0^I(\hat{K}) \xrightarrow{\text{curl}} P^0(\hat{K}) \xrightarrow{0} \{0\}, \quad (4.32)$$

and

$$\mathbb{R} \xrightarrow{id} P^1(\hat{K}) \xrightarrow{\text{Curl}} \mathcal{RT}_0(\hat{K}) \xrightarrow{\text{div}} P^0(\hat{K}) \xrightarrow{0} \{0\} \quad (4.33)$$

are exact.

This follows with arguments to those above, by using

$$\begin{aligned} \nabla \mathcal{N}_0(\hat{K}) &= P^0(\hat{K})^2 \subset \mathcal{N}_0(\hat{K}) \quad \text{and} \quad \text{curl} \mathcal{N}_0(\hat{K}) = P^0(\hat{K}), \\ \text{Curl} P^1(\hat{K}) &= P^0(\hat{K})^2 \subset \mathcal{RT}_0(\hat{K}) \quad \text{and} \quad \text{div} \mathcal{RT}_0(\hat{K}) = P^0(\hat{K}), \end{aligned}$$

and comparing the dimensions of the ranges, kernels and spaces; cf. Figure 4.3 and Figure 4.4.

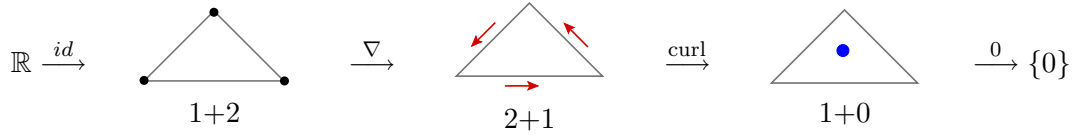


Figure 4.3: 2-dimensional exact sequence involving lowest-order Nédélec element (of first kind) and splitting of space into kernel and range of the consecutive operator

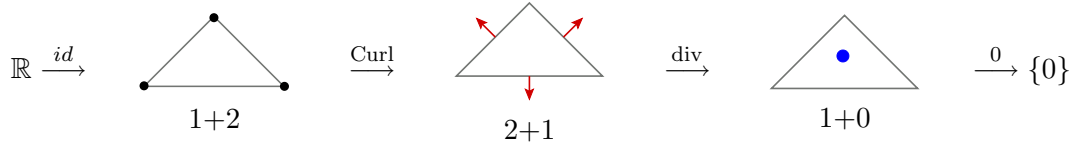


Figure 4.4: 2-dimensional exact sequence involving the lowest-order Raviart-Thomas element

Remark 4.24. *In the proposed sequences of local FE-spaces involving the lowest-order $H(\text{curl})$ - and $H(\text{div})$ -conforming finite elements of the first kind, the polynomial degree is only decreased by 1 throughout the whole de Rham Complex. As we will see in the next chapter, this holds true also for corresponding high-order simplicial finite elements of first kind.*

Exact sequences property for the second family on the reference element level

Analogous considerations imply exact sequences involving $H(\text{curl})$ - and $H(\text{div})$ -conforming elements of the second family. In two dimensions the following shortened exact sequences hold.

Lemma 4.25. *For the triangular reference element \hat{K} the following two sequences of local spaces involving either the Nédélec element of second kind or the Raviart-Thomas element*

(BDM_1) of second kind are exact:

$$\mathbb{R} \xrightarrow{id} P^2(\hat{K}) \xrightarrow{\nabla} \mathcal{N}_1^{II}(\hat{K}) = P^1(\hat{K}) \xrightarrow{\text{curl}} P^0(\hat{K}) \xrightarrow{0} \{0\}, \quad (4.34)$$

$$\mathbb{R} \xrightarrow{id} P^2(\hat{K}) \xrightarrow{\text{Curl}} BDM_1(\hat{K}) = P^1(\hat{K}) \xrightarrow{\text{div}} P^0(\hat{K}) \xrightarrow{id} \{0\}. \quad (4.35)$$

(Compare Figure 4.5 and Figure 4.6.)

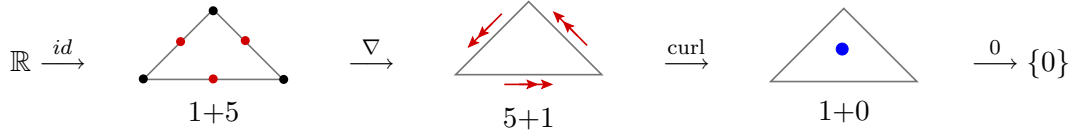


Figure 4.5: 2-dimensional exact sequence involving the linear Nédélec element of second kind and splitting into kernel and range of consecutive differential operator

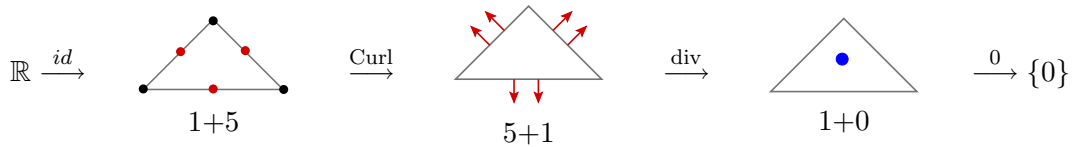


Figure 4.6: 2-dimensional exact sequence involving the linear BDM element and splitting into kernel and range of consecutive differential operator

We observe that in the De Rham sequences, which involve triangular finite elements of the second family, the polynomial degree decreases by order 2 throughout the sequence. In three dimensions, the de Rham Complex involves the application of three consecutive differential operators. Therefore, if one uses spaces of full polynomial degree on tetrahedra, the polynomial degree lowers by 3 throughout the sequence. This leads to the following sequence involving Nédélec and Raviart-Thomas spaces of the second kind.

Lemma 4.26. *Let \hat{K} denote the tetrahedral reference element. The following sequence of local spaces involving only full polynomial spaces*

$$\mathbb{R} \xrightarrow{id} P^3(\hat{K}) \xrightarrow{\nabla} (P^2(\hat{K}))^3 = \mathcal{N}_2^{II}(\hat{K}) \xrightarrow{\text{curl}} (P^1(\hat{K}))^3 = BDM_1(\hat{K}) \xrightarrow{\text{div}} P^0(\hat{K}) \xrightarrow{0} \{0\} \quad (4.36)$$

is exact.

This sequence of spaces is the one involving spaces with lowest degree while still ensuring full polynomial degree and exactness.

The exactness of the three sequences stated in Lemma 4.25 and Lemma 4.26 can be proved with the same arguments as above: By construction the range of each operator is a subspace of the following space. Equality then follows again by a counting argument; cf. Figure 4.5, 4.6, and 4.7).

Remark 4.27. *If we use a conforming transformation onto the physical elements due to Lemma 4.10, Lemma 4.15, or Lemma 4.19 respectively, the exact sequence () on the reference element implies that the exactness still holds on the local spaces of the physical elements.*

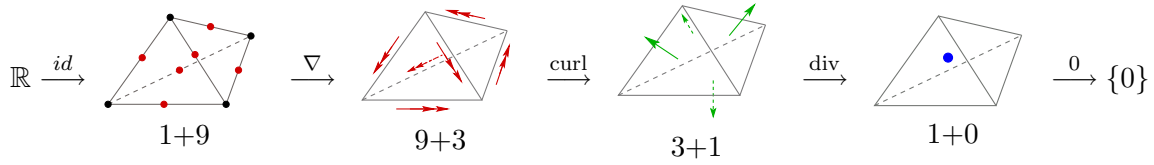


Figure 4.7: Exact sequence involving tetrahedral Nédélec element of the second kind.

Global exact sequence property of discrete FE-spaces

As already outlined above, the use of conforming transformations provides that the exactness is provided for the local spaces defined on the physical elements. Moreover, due to the conforming construction the exactness then also holds for the global finite element spaces.

We summarize results from BOSSAVIT [23], BOSSAVIT [25] (Proposition 5.5), and ARNOLD-FALK-WINTHER [7]:

Theorem 4.28 (Exactness of global discrete sequence). *Let Ω be a simply-connected domain with connected boundary, and let the physical finite elements be constructed by conforming transformations (cf. Lemma 4.10, Lemma 4.15, and Lemma 4.19). Then the sequences of the conforming global FE-spaces corresponding to (4.30)*

$$\mathbb{R} \xrightarrow{id} W_{h,1} \xrightarrow{\nabla} V_{h,0} \xrightarrow{\text{curl}} Q_{h,0} \xrightarrow{\text{div}} S_{h,0} \xrightarrow{0} \{0\}$$

and corresponding to (4.36)

$$\mathbb{R} \xrightarrow{id} W_{h,2} \xrightarrow{\nabla} V_{h,1}^{II} \xrightarrow{\text{curl}} Q_{h,0} \xrightarrow{\text{div}} S_{h,0} \xrightarrow{0} \{0\}$$

are exact.

In two dimensions, the following shortened sequences corresponding to (4.32) or (4.34)

$$\mathbb{R} \xrightarrow{id} W_h \xrightarrow{\nabla} V_h \xrightarrow{\text{curl}} S_h \xrightarrow{0} \{0\}$$

and corresponding to (4.33) or (4.35)

$$\mathbb{R} \xrightarrow{id} W_h \xrightarrow{\text{Curl}} Q_h \xrightarrow{\text{div}} S_h \xrightarrow{0} \{0\}$$

are exact.

Remark 4.29 (Exact sequences involving essential boundary conditions). *Essential boundary conditions can be taken into account in a similar manner as in the continuous case, cf. Remark 3.17. The exactness of the resulting sequences follows then by the same arguments as in the Neumann case.*

4.3.6 Element matrices and assembling of FE-matrices

For an efficient computation, the FE-matrices are assembled from element-matrices $\mathbf{A}_{\alpha,\beta}^K$ for all $K \in \mathcal{T}_h$. The assembling of the global matrix is done via a connectivity matrix C which assigns local to global degrees of freedom.

The global Galerkin system matrix as well as the global load vector, as defined in (4.3), are assembled as follows:

$$\mathbf{A} = \sum_{K \in \mathcal{T}_h} (C^K)^T \mathbf{A}^K C^K, \quad \mathbf{f} = \sum_{K \in \mathcal{T}_h} (C^K)^T \mathbf{f}^K$$

with connectivity matrices

$$C_{i,\alpha}^K = \begin{cases} \pm 1 & \text{if local dof } \alpha \text{ is identified with global dof } i, \\ 0 & \text{otherwise.} \end{cases}$$

The sign factors in the entries of the connectivity matrix ± 1 account for the global edge-orientation (the orientation of the tangential vector) or for the global face-orientation (the direction of the normal vector) and are necessary to enable conformity. The element matrices \mathbf{A}^K , and the element load vector \mathbf{f}^K are stated below. Note that due to the local support of the shape functions, the connectivity matrices as well as the system matrix \mathbf{A} are sparse.

The calculation of the element stiffness matrix and the element load vector is done by integration on the reference element while taking into account the element transformations. We shortly outline the procedure for the electromagnetic model problems we have in mind.

Electrostatic problem

In view of Section 3.4.1, we are looking for solutions $u \in W_h \subset H_D^1(\Omega)$ of the variational problem

$$\int_{\Omega} \nabla u \nabla v \, d\mathbf{x} + \int_{\Omega} \kappa uv \, d\mathbf{x} = \int_{\Omega} f v \, d\mathbf{x} \quad \forall v \in W_h.$$

For discretization we use H^1 -conforming finite elements. The element matrices and vectors can be computed by taking into account the transformation of scalar and gradient functions (cf. Lemma 4.10) in the following way:

$$\begin{aligned} \mathbf{A}_{\alpha\beta}^K &= \int_K \nabla \phi_{\alpha} \nabla \phi_{\beta} \, d\mathbf{x} + \int_K \kappa \phi_{\alpha} \phi_{\beta} \, d\mathbf{x} \\ &= \int_{\hat{K}} (F_K^{-T} \nabla \hat{\phi}_{\alpha}) (F_K^{-T} \nabla \hat{\phi}_{\beta}) J \, d\hat{\mathbf{x}} + \int_{\hat{K}} \kappa \hat{\phi}_{\alpha} \hat{\phi}_{\beta} J \, d\hat{\mathbf{x}}, \\ \mathbf{f}_{\alpha}^K &= \int_K f \phi_{\alpha} \, d\mathbf{x} = \int_{\hat{K}} f \hat{\phi}_{\alpha} J \, d\hat{\mathbf{x}}, \end{aligned}$$

where $\{\hat{\phi}_{\alpha}\}$ denotes the shape functions on the reference element.

Magnetostatic problem

We recall the variational formulations of the magnetostatic problem, cf. Section 3.4.2, and hence consider the following model: Find $\mathbf{u} \in V_h \subset H(\text{curl}, \Omega)$ such that

$$\int_{\Omega} \mu^{-1} \text{curl } \mathbf{u} \text{ curl } \mathbf{v} \, d\mathbf{x} + \int_{\Omega} \kappa \mathbf{u} \mathbf{v} \, d\mathbf{x} = \int_{\Omega} \mathbf{j} \mathbf{v} \, d\mathbf{x} \quad \forall \mathbf{v} \in V_h.$$

Utilizing the $H(\text{curl})$ -conforming transformations (cf. Lemma 4.15) the element matrices and vectors can be computed on the reference element as follows:

$$\begin{aligned} \mathbf{A}_{\alpha\beta}^K &= \int_K \mu^{-1} \text{curl } \boldsymbol{\varphi}_\alpha \text{ curl } \boldsymbol{\varphi}_\beta \, d\mathbf{x} + \int_K \kappa \boldsymbol{\varphi}_\alpha \boldsymbol{\varphi}_\beta \, d\mathbf{x} \\ &= \int_{\hat{K}} \mu^{-1} J^{-1} (F_K \text{ curl } \hat{\boldsymbol{\varphi}}_\alpha) (F_K \text{ curl } \hat{\boldsymbol{\varphi}}_\beta) \, d\hat{\mathbf{x}} + \int_{\hat{K}} \kappa (F_K^{-T} \hat{\boldsymbol{\varphi}}_\alpha) (F_K^{-T} \hat{\boldsymbol{\varphi}}_\beta) J \, d\hat{\mathbf{x}}, \end{aligned}$$

in three spatial dimensions. In two dimensions we obtain instead

$$\mathbf{A}_{\alpha\beta}^K = \int_{\hat{K}} \mu^{-1} J^{-1} \text{curl } \hat{\boldsymbol{\varphi}}_\alpha \text{ curl } \hat{\boldsymbol{\varphi}}_\beta \, d\hat{\mathbf{x}} + \int_{\hat{K}} \kappa (F_K^{-T} \hat{\boldsymbol{\varphi}}_\alpha) (F_K^{-T} \hat{\boldsymbol{\varphi}}_\beta) J \, d\hat{\mathbf{x}}.$$

The element vector allows a unique representation for $K \in \mathbb{R}^3$ and \mathbb{R}^2 :

$$\mathbf{f}_\alpha^K = \int_K \mathbf{j} \boldsymbol{\varphi}_\alpha \, d\mathbf{x} = \int_{\hat{K}} \mathbf{j} (F_K^{-T} \hat{\boldsymbol{\varphi}}_\alpha) J \, d\hat{\mathbf{x}}.$$

Here $\{\hat{\boldsymbol{\varphi}}_\alpha\}$ denote the shape functions on the reference element, spanning a local $H(\text{curl})$ -conforming FE-space on \hat{K} .

4.4 Commuting Diagram and Interpolation Error Estimates

The commuting diagram, which links the global and discrete sequences of spaces, plays an important role in the error analysis of finite element approximations. In view of emphasizing once more the importance of exact sequences, we shortly sketch some ideas and the main results of interpolation operators and the connected error estimates. An extensive analysis on commuting diagrams can be found in BOSSAVIT [25] for nodal interpolation operators, Clément-type interpolation operators in SCHÖBERL [81] and projection-based interpolation in DEMKOWICZ-BUFFA [43].

In the error analysis of finite-element methods as well as for implementing boundary conditions we use interpolation operators which map a (Sobolev) space X into the discrete FE-spaces X_h , i.e. $\Pi_X : X \rightarrow X_h$. In particular we are interested here in the following choice of spaces X : $W \subset H^1(\Omega)$, $V \subset H(\text{curl}, \Omega)$, $Q \subset H(\text{div}, \Omega)$ or $S \subset L_2(\Omega)$. A special case of interpolation operators is realized by the degrees of freedom, namely

$$\Pi_X(v) = \sum_{i=1}^N N_i(v) \varphi_i$$

with $\text{span}\{\varphi_i : i = 1, \dots, N\} = X$.

One essential drawback of nodal interpolation operators is that they are not well-defined on the whole function space $H^1(\Omega)$, $H(\text{curl})$, or $H(\text{div})$, since not all traces, which are involved in the degrees of freedom, are properly defined on the whole space, e.g. point-evaluation in 2D or 3D, is not well-defined in $H^1(\Omega)$.

Interpolation operators which require less smoothness are Clément type operators, which involve non-local averaging over certain patches. For instance, the Clément type operator for H^1 -problems is defined by averaging over the patch of elements associated with one vertex instead of point-evaluation in this vertex.

Let us consider a sequence of conforming finite-element spaces (W, V, Q, S) and interpolation operators Π_i . We summarize all the involved operators and spaces in the following (commuting) diagram:

$$\begin{array}{ccccccc}
H^1(\Omega) & \xrightarrow{\nabla} & H(\text{curl}, \Omega) & \xrightarrow{\text{curl}} & H(\text{div}, \Omega) & \xrightarrow{\text{div}} & L_2(\Omega) \\
\cup & & \cup & & \cup & & \parallel \\
W & & V & & Q & & S \\
\Pi_W \downarrow & & \Pi_V \downarrow & & \Pi_Q \downarrow & & \Pi_S \downarrow \\
W_h & \xrightarrow{\nabla} & V_h & \xrightarrow{\text{curl}} & Q_h & \xrightarrow{\text{div}} & S_h
\end{array}$$

This diagram is said to *commute*, if for sufficiently smooth functions the following hold:

$$\begin{aligned}
\Pi_V \nabla w &= \nabla \Pi_W w & \forall w \in W \subset H^1(\Omega), \\
\Pi_Q \text{curl } \mathbf{v} &= \text{curl } \Pi_V \mathbf{v} & \forall \mathbf{v} \in V \subset H(\text{curl}, \Omega), \\
\Pi_S \text{div } \mathbf{q} &= \text{div } \Pi_Q \mathbf{q} & \forall \mathbf{q} \in Q \subset H(\text{div}, \Omega).
\end{aligned}$$

Such relations can be derived for certain choices of interpolation operators via Stokes and Green's theorems. In the following theorem we collect some results on nodal interpolation error estimates, which are frequently used in approximation error estimates.

Theorem 4.30 (Nodal interpolation error estimates). *The nodal interpolation operators are well defined on the spaces*

$$\begin{aligned}
W &= H^{\frac{3}{2}+\delta}(\Omega), \\
V &= \{ \mathbf{v} \in (H^{\frac{1}{2}+\delta}(\Omega))^3 \mid \text{curl } \mathbf{v} \in (H^{\frac{1}{2}+\delta}(\Omega))^3 \}, \\
Q &= \{ \mathbf{v} \in (H^{\frac{1}{2}+\delta}(\Omega))^3 \mid \text{div } \mathbf{v} \in L_2(\Omega) \} \quad \text{with } \delta > 0.
\end{aligned}$$

Let \mathcal{T}_h denote a regular tetrahedral mesh with meshwidth h .

1. Let W_h be the H^1 -conforming FE-space of order k , and Π_W denote the corresponding nodal interpolation operator. If $w \in (H^s(\Omega))^3$ for $\frac{3}{2} + \delta \leq s \leq k + 1$, then

$$\|w - \Pi_W w\|_1 \leq h^{s-1} \|w\|_s.$$

2. Let Π_V denote the nodal interpolation operator corresponding to the FE-space V_h of Nédélec elements of the first kind and order k . If $\mathbf{v} \in (H^s(\Omega))^3$ and $\text{curl } \mathbf{v} \in (H^s(\Omega))^3$ for $\frac{1}{2} + \delta \leq s \leq k + 1$, then there holds

$$\|\mathbf{v} - \Pi_V \mathbf{v}\|_0 \leq h^s (\|\mathbf{v}\|_s + \|\text{curl } \mathbf{v}\|_s) \quad \text{and} \quad \|\text{curl}(\mathbf{v} - \Pi_V \mathbf{v})\|_0 \leq h^s (\|\text{curl } \mathbf{v}\|_s),$$

see MONK [70] (Theorem 5.41, Remark 5.42) and HIPTMAIR [56] (Theorem 3.14, Corollary 3.17).

3. Let Q_h denote the FE-space of Raviart-Thomas-Nédélec elements of order k , and Π_Q be the corresponding nodal interpolation operator. If $\mathbf{q} \in (H^s(\Omega))^3$ and $\frac{1}{2} + \delta \leq s \leq k + 1$, then

$$\|\mathbf{q} - \Pi_Q \mathbf{q}\|_0 \leq h^s \|\mathbf{q}\|_s \quad \text{and} \quad \|\text{div } \mathbf{q} - \Pi_Q \mathbf{q}\|_0 \leq h^s \|\mathbf{q}\|_s$$

hold, see MONK [70] (Theorem 5.25, Remark 5.26).

Similar results also exist if V_h and Q_h are chosen out of the second exact sequence, cf. (4.36). However, there the approximation order of \mathbf{v} and \mathbf{q} is one order better than that of $\text{curl } \mathbf{v}$ and $\text{div } \mathbf{q}$, respectively, due to the choice of polynomial spaces.

Chapter 5

High Order Finite Elements

In the previous chapter we introduced the classical Finite Element Method, namely h -FEM, where the polynomial degree on all elements is fixed to a uniform order, typically $p = 1$ or $p = 2$. Convergence is achieved by local or global refinement of the underlying mesh \mathcal{T}_h , denoted as h -refinement, and the error in the numerical solution decays algebraically.

The idea of p -version finite element methods is to use a fixed triangulation and obtain convergence by increasing the polynomial order – p -refinement. In case of an analytic solution the p -version FEM yields exponential convergence rates in the energy norm, cf., e.g., BABUSKA-SZABO-KATZ [12]. In case of piecewise analytic solutions with singular behavior near corners, edges or boundary layers, also the p -version yields only algebraic convergence.

The hp -method now combines the two ideas: Exponential convergence can be regained by the combination of (geometric) h -refinement and local increase of the polynomial order. Such a strategy is then called hp -refinement. For a survey on hp -refinements we refer to MELENK [68] and SZABO-DÜSTER-RANK [86].

This chapter is devoted to the construction of conforming hierarchical hp -finite element approximations for the vector-valued spaces $H(\text{curl}, \Omega)$ and $H(\text{div}, \Omega)$. As we will see in our numerical tests, regular geometric h -refinement towards singular corners, singular edges and/or boundary layers naturally leads to various element topologies, involving in particular not only simplices.

Our goal is to provide a general strategy for constructing a sequence of hierarchical finite element spaces allowing for arbitrary and variable polynomial order on a mixture of common element topologies in one single mesh. A main point in such a construction is to ensure the exact sequence property of discrete spaces in a more localized sense. To achieve this, we explicitly use higher-order kernel functions of the natural differential operator (in this space) within the construction of the FE-basis, see also the previous chapter. For instance, in the construction of an $H(\text{curl})$ -conforming basis we include gradient functions. The framework we are going to present, is particularly well suited for a practical implementation, and is extendable to anisotropic polynomial orders.

The construction of finite element spaces presented below is based on the following contributions:

- In WEBB [95] an $H(\text{curl})$ -conforming finite element basis is provided by taking the gradient fields of H^1 -conforming shape functions and then extending the basis to the

full polynomial space. The shape functions are formulated as monomials of the affine coordinates. To avoid very ill-conditioned matrices Gram-Schmidt orthogonalization is used, which is conveniently proposed up to polynomial order 3.

- A first general hierarchical construction strategy of $H(\text{curl})$ -conforming and $H(\text{div})$ -conforming finite elements for arbitrary polynomial order on tetrahedral elements is presented in AINSWORTH-COYLE [2].
- In KARNIADAKIS-SHERWIN [60] H^1 -conforming spaces which yield a general construction for all common element topologies, are suggested. This is obtained by using an underlying tensor-product structure also for simplicial elements, based on the work of DUBINER [46].
- The study of the de Rham diagram of hp -finite element spaces, presented in DEMKOWICZ ET AL. [44] and the implementation of $H(\text{curl})$ -conforming hp -finite elements on hexahedral meshes, as presented in RACHOWICZ-DEMKOWICZ [76].

Our construction provides a more general version of the exact sequence property of the discrete global spaces, which we call the *local exact sequence property*, and formulate in Theorem 5.32. This local exact sequence is a key property in our design of cheap and robust preconditioners for curl-curl problems in Chapter 6.

To avoid confusion, we point out in advance that we distinguish between three levels of the exact sequences of discrete spaces:

1. the *exact sequence* of the local FE-spaces defined *on the reference element* K , which we use for motivating the choice of the appropriate local spaces,
2. the *(discrete) global exact sequence* of the global FE-spaces (cf. Corollary 5.34), which is the classical one,
3. the *local exact sequence of the discrete global spaces* (cf. Theorem 5.32), which is a generalization of the global exact sequence. By this we mean that the exact sequence property even holds for the subspaces of a partially local space splitting.

5.1 High-order FE-spaces of variable order

The classical definition of the degrees of freedom as introduced in NÉDÉLEC [72, 73] is stated for uniform polynomial order p all over the mesh and does not generalize to finite element spaces with varying polynomial order. One of our aims is to be able to vary the polynomial order locally, i.e., in the sense of assigning to each edge, face and cell in the mesh an arbitrary polynomial degree, while still ensuring conformity as well as the exactness of the discrete de Rham complex.

We start with a discussion of using the degrees of freedom for constructing conforming finite element spaces with varying polynomial order distribution over the mesh. The following definition of degrees of freedom, enabling variable order tetrahedral elements and providing commuting interpolation operators, is due to DEMKOWICZ ET AL. [44].

We consider a bounded Lipschitz polyhedral domain Ω , which is covered by a regular tetrahedral mesh \mathcal{T}_h . Let $\mathbf{p} = (p_{E_1}, \dots, p_{E_6}, p_{F_1}, \dots, p_{F_4}, p_C)$ denote the polynomial degrees corresponding to edges, faces and the cell of the tetrahedral element $K \in \mathcal{T}_h$.

H^1 -conforming hp FE-spaces

Let us define the following local finite element space:

$$W_{\mathbf{p}}(K) := P^{\mathbf{p}}(K) := \left\{ w \in P^{p_C} \mid w|_F \in P^{p_F}(F) \forall F \in \mathcal{F}_K, w|_E \in P^{p_E}(E) \forall E \in \mathcal{E}_K \right\}. \quad (5.1)$$

In order to make this definition reasonable we enforce a *minimum order rule*, i.e., for each face $F \in \mathcal{F}_K$ there holds

$$p_C \geq p_F \geq p_E \quad \forall \text{ edges } E \text{ on } F. \quad (5.2)$$

Following DEMKOWICZ ET AL. [44] we define the hp -degrees of freedom as follows:

- Vertex-based degrees of freedom are defined by the point-evaluations

$$N_i^V(\phi) = \phi(V_i) \quad \forall V_i \in \mathcal{V}_K$$

- Edge-based degrees of freedom for each edge $E \in \mathcal{E}_K$:

$$N_i^E(\phi) = \int_E \frac{\partial \phi}{\partial s} \frac{\partial v_i}{\partial s} ds \quad \text{for } \{v_i\}_{2 \leq i \leq p_E} \text{ spanning } P_0^{p_E}(E).$$

- Face-based degrees of freedom for each face F :

$$N_i^F(\phi) = \int_F \nabla_F \phi \cdot \nabla_F v_i d\mathbf{x} \quad \text{for } \{v_i\}_{1 \leq i \leq n_F}, \text{ a basis of } P_0^{p_F}(F),$$

with $n_F = \frac{1}{2}(p_F+1)(p_F+2)$ and the surface gradient is defined as $\nabla_F v := \mathbf{n} \times (\nabla v)|_F \times \mathbf{n}$.

- Cell-based degrees of freedom

$$N_C(\phi) = \int_K \nabla \phi \cdot \nabla v d\mathbf{x} \quad \text{for } \{v_i\}_{1 \leq i \leq n_C}, \text{ a basis of } P_0^{p_C}(T)$$

with $n_C = \frac{1}{6}(p_C+3)(p_C+2)(p_C+1)$.

This choice defines a unisolvent and H^1 -conforming finite element, see MONK [70]. The degrees of freedom can be used to define an interpolation operator $\Pi_W : W \rightarrow W_h$, which is well-defined for $W = H^s(\Omega)$ for $s > \frac{3}{2}$. Under the assumption of uniform order p on all edges, faces and cells, and for $w \in H^s(\Omega)$ with $s \geq 2$ the following interpolation error estimate holds:

$$\|w - \Pi^W w\|_{H^1(\Omega)} \leq h^{\min\{p, s-1\}} p^{1-s} \|w\|_s.$$

 $H(\text{curl})$ -conforming hp -FE space

In order to obtain $H(\text{curl})$ -conformity, we define the local space such that the tangential traces on edges and faces belong to polynomial spaces of some given order

$$V_{\mathbf{p}}(K) := \left\{ \mathbf{v} \in (P^{p_C}(K))^3 \mid tr_{\tau, F}(\mathbf{v}) \in P^{p_F}(F) \forall F \in \mathcal{F}_K, tr_{\tau, E}(\mathbf{v}) \in P^{p_E}(E) \forall E \in \mathcal{E}_K \right\}, \quad (5.3)$$

where we denote the tangential traces onto edges as $tr_{E, \tau}(\mathbf{v}) = tr_E(\mathbf{v} \cdot \boldsymbol{\tau})$ and onto faces as $tr_{F, \tau}(\mathbf{v}) = tr_F(\mathbf{n} \times (\mathbf{v} \times \mathbf{n}))$. In case of a minimum order rule (5.1), the polynomial space $V_{\mathbf{p}}(K)$ is well-defined and there holds $\nabla W_{\mathbf{p}+1}(K) \subset V_{\mathbf{p}}(K)$.

- Edge-based degrees of freedom:

$$N_i^E(\mathbf{u}) = \int_E \mathbf{u} \cdot \boldsymbol{\tau} v_i ds \quad \text{for } \{v_i\}_{0 \leq i \leq p_E}, \text{ a basis of } P^{p_E}(E).$$

- Face-based degrees of freedom:

$$N_i^F(\mathbf{u}) = \int_F \text{curl}_F \mathbf{u} \cdot \text{curl}_F \mathbf{v}_i dA \quad \text{for } \{\mathbf{v}_i\} \text{ s.t. } \{\text{curl}_F \mathbf{v}_i\} \text{ is a basis of } \text{curl}_F(\mathbf{P}_{0,\boldsymbol{\tau}}^{p_F}(F)),$$

$$N_i^F(\mathbf{u}) = \int_F \mathbf{u} \cdot \mathbf{v}_i dA \quad \text{for } \{\mathbf{v}_i\} \text{ a basis of } \nabla_F(P_0^{p_F+1}(F)).$$

with $\text{curl}_F \mathbf{v} = \text{curl } \mathbf{v} \cdot \mathbf{n}$ and $\mathbf{P}_{0,\boldsymbol{\tau}}^{p_F}(F) := (P^{p_F}(F))^2 \cap H_0(\text{curl}, F)$.

- Cell-based degrees of freedom:

$$N_i^C(\mathbf{u}) = \int_K \text{curl } \mathbf{u} \cdot \text{curl } \mathbf{v}_i d\mathbf{x} \quad \text{for } \{\mathbf{v}_i\} \text{ s.t. } \{\text{curl } \mathbf{v}_i\} \text{ is a basis of } \text{curl}(\mathbf{P}_{\boldsymbol{\tau},0}^{p_C}(K)),$$

$$N_i^C(\mathbf{u}) = \int_K \mathbf{u} \cdot \mathbf{v}_i d\mathbf{x} \quad \text{for } \{\mathbf{v}_i\} \text{ a basis of } \nabla(P_0^{p_C+1}(K)).$$

with $\mathbf{P}_{0,\boldsymbol{\tau}}^{p_C}(K) := (P^{p_C}(K))^3 \cap H_0(\text{curl}, K)$.

These degrees of freedom define an $H(\text{curl})$ -conforming unisolvent finite element. Interpolation error estimates for the corresponding commuting projection-based interpolation operators are presented in DEMKOWICZ-BUFFA [43].

Below, we will explicitly construct edge-base, face-based, and cell-based basis functions, which fit into this framework.

$H(\text{div})$ -conforming hp -FE space

The $H(\text{div})$ -conforming local space of order $\mathbf{p} = (p_{F_1}, \dots, p_{F_4}, p_C)$ is defined as a vector-valued polynomial space, where the normal traces on the faces of the element are polynomials of order p_{F_E} :

$$Q_{\mathbf{p}}(K) = \{\mathbf{v} \in P^{p_C}(K) \mid (\mathbf{v} \cdot \mathbf{n})|_F \in P^{p_F} \forall F \in \mathcal{F}_K\}. \quad (5.4)$$

Again, for the spaces to be well-defined, we have to require that

$$p_F \leq p_C \quad \forall F \in \mathcal{F}_K.$$

The degrees of freedom are defined as follows:

- Face-based degrees of freedom:

$$N_i^F(\mathbf{q}) = \int_F \mathbf{q} \cdot \mathbf{n} v_i dA \quad \text{for } \{v_i\} \text{ basis of } P^{p_F}(F).$$

- Cell -based degrees of freedom:

$$N_i^C(\mathbf{q}) = \int_K \text{div } \mathbf{q} \cdot \text{div } \mathbf{v}_i d\mathbf{x} \quad \text{for } \{\mathbf{v}_i\} \text{ s.t. } \{\text{div } \mathbf{v}_i\} \text{ is a basis of } \text{div}(\mathbf{P}_{\mathbf{n},0}^{p_C}(K)),$$

$$N_i^C(\mathbf{q}) = \int_K \mathbf{q} \cdot \mathbf{v}_i d\mathbf{x} \quad \text{for } \{\mathbf{v}_i\} \text{ a basis of } \text{curl}(\mathbf{P}_{\boldsymbol{\tau},0}^{p_C+1}(K)),$$

with $\mathbf{P}_{\mathbf{n},0}^{p_C}(K) := \mathbf{P}^{p_C}(K)^3 \cap H_0(\text{div}, K)$.

The above construction gives rise to an $H(\text{div})$ -conforming unisolvent finite element. Interpolation error estimates for commuting projection-based interpolation operators corresponding to the above defined degrees of freedom are presented in DEMKOWICZ-BUFFA [43].

5.2 Construction of conforming shape functions

In the following we present a general approach for the conforming approximation of the sequence of spaces, namely, $H^1(\Omega)$, $H(\text{curl}, \Omega)$, $H(\text{div})$ and $L_2(\Omega)$. Our main concern lies in

- enabling arbitrary and non-uniform polynomial order possibly varying for each edge, face, cell,
- a strategy which is applicable for all common elements, such as triangles, quadrilaterals, hexahedra, tetrahedra and prisms and, therefore, can be used on hybrid meshes (e.g. coming from geometrically refined meshes)
- fulfilling the local exact sequence property as formulated in Theorem 5.32.

While eluding the application of interpolation operators, we are not concerned with the definition of the degrees of freedom. Instead, we explicitly define the polynomial local finite element spaces and construct H^1 -, $H(\text{curl})$ -, $H(\text{div})$ -conforming polynomial bases spanning the local space.

The construction of the H^1 -conforming shape functions is rather familiar. We start with Vertex-Edge-Face(only in 3d)-Cell based shape functions in tensor-product structure (possibly degenerated in case of simplicial elements) as introduced by DUBINER [46] and KARNIADAKIS-SHERWIN [60]. In our approach we take care of the exact sequence property already during the construction of the basis functions, in particular, we use gradient fields of higher-order H^1 -functions and curl-fields of higher-order $H(\text{curl})$ -functions to construct Nédélec-Edge-Face-Cell (\mathcal{N}_0 - E - F - C) based, respectively Raviart-Thomas-Face-Cell (\mathcal{RT}_0 - F - C) based conforming finite elements. The idea is visualized in Figure 5.1. We point out in advance, that the lowest-order space will always play a special role and therefore has to be treated separately.

5.2.1 Preliminaries

Orthogonal polynomials

We intend to present a general method for constructing linearly independent shape functions based on tensor products of one-dimensional orthogonal polynomials. Although we mainly use Legendre-type polynomials later on, also other orthogonal polynomial bases spanning $P^p([-1, 1])$ respectively $P_0^p([-1, 1])$ could be used in our constructions, e.g. Gegenbauer, Jacobi, Hermitian polynomials. The main aspect of the choice of a special polynomial family is the type of orthogonality, and the possibility of fast and recursive point-evaluation, which are key ingredients for an efficient numerical implementation. Orthogonality influences the sparsity and the condition number of the involved element matrices, whereas the fast evaluation procedures can be exploited in fast assembling techniques, i.e. in sum factorization techniques mentioned in KARNIADAKIS-SHERWIN [60] section 4.1.5. For details on orthogonal polynomials we refer to the classical textbook by SZEGO [88].

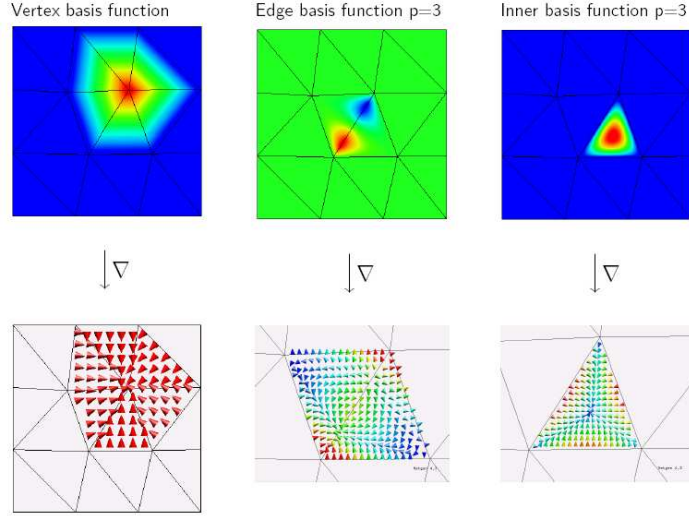


Figure 5.1: Vertex-Edge-Cell-based H^1 -conforming shape functions on triangles and their gradient fields. Edge-based and face-based gradient fields are used as edge-based and as subset of face-based $H(\text{curl})$ -conforming shape functions.

Legendre polynomials, denoted by $(\ell_i)_{0 \leq i \leq p}$ are $L_2(-1, 1)$ -orthogonal polynomials spanning $P^p([-1, 1])$. In particular, they satisfy the orthogonality relation

$$\int_{-1}^1 \ell_i(x) \ell_j(x) dx = \frac{2}{2i+1} \delta_{ij}.$$

Due to the three-term recurrence relation

$$\begin{aligned} \ell_0(x) &= 1, \\ \ell_1(x) &= x, \\ (n+1)\ell_{n+1}(x) &= (2n+1)\ell_n(x)x - n\ell_{n-1}(x), \quad n \geq 1 \end{aligned}$$

efficient and stable point evaluation is possible. The derivatives of Legendre polynomials can be computed by an analogous 3 term recurrence. If both, the Legendre polynomials and their derivatives, are needed at the same time, we recommend to use the recurrence

$$\ell_n(x) = \left(\frac{d}{dx} \ell_{n+1}(x) - \frac{d}{dx} \ell_{n-1}(x) \right)$$

together with the one for the Legendre polynomials. We only mention, that Legendre polynomials are a special case of Jacobi polynomials (see Appendix A.3).

Integrated Legendre polynomials, denoted by $(L_n)_{2 \leq i \leq p}$, are defined as follows:

$$L_n(x) := \int_{-1}^x \ell_{n-1}(\xi) d\xi \quad \text{for } x \in [-1, 1] \text{ and } n \geq 2.$$

They are mutually orthogonal with respect to the H^1 -seminorm, i.e.,

$$\int_{-1}^1 L_i'(x) L_j'(x) dx = 0 \quad \text{for } i \neq j.$$

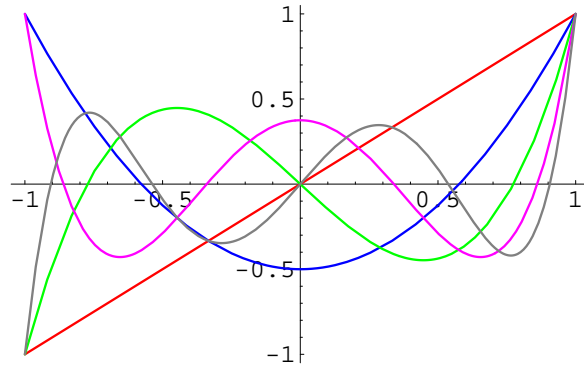


Figure 5.2: Legendre polynomials of order 1 to 5

Moreover, the polynomials L_n , $n \geq 2$ vanish at the interval bounds, i.e. $L_n(-1) = L_n(1) = 0$ and span $P_0^p[-1, 1]$. Once more, there holds a three-term-recurrence allowing fast point-evaluations:

$$\begin{aligned} L_1(x) &= x, \\ L_2(x) &= \frac{1}{2}(x^2 - 1), \\ (n + 1)L_{n+1}(x) &= (2n - 1)x L_n(x) - (n - 2)L_{n-1}(x) \text{ for } n \geq 2. \end{aligned}$$

Here, $L_1(x)$ was added to allow for a general recursion relation. Note that $L_1(x) \neq \int_{-1}^x l_0(y)dy$.

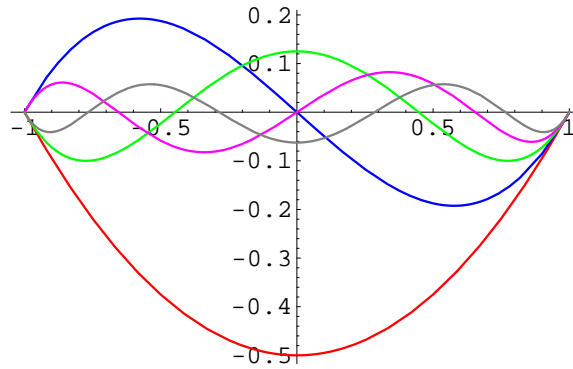


Figure 5.3: Integrated Legendre polynomials of polynomial order 2 to 6

An interesting property of the integrated Legendre polynomials is that they are almost orthogonal also with respect to the L^2 inner product, i.e.,

$$\int_{-1}^1 L_i(x)L_j(x) dx = 0 \quad \text{only for } |i - j| > 2.$$

Scaled Legendre-type polynomials For the construction of tensor-product-based shape functions on triangular faces and tetrahedral cells we will use the *Scaled Legendre Polynomials*

$$\ell_n^S(x, t) := t^n \ell_n\left(\frac{x}{t}\right) \quad \text{for } x \in [-t, t], t \in (0, 1)$$

and the *Scaled Integrated Legendre Polynomials*

$$\begin{aligned} L_n^S(x, t) &:= t^n L_n\left(\frac{x}{t}\right) \\ &= \int_{-t}^x \ell_{n-1}^S(s, t) ds \quad \text{for } n \geq 2. \end{aligned}$$

Note that the limit in zero is well defined and $\lim_{t \rightarrow 0} \ell_n^S(x, t) = 0$ for $n \geq 2$. The scaling parameter $t = 1$ yields the Legendre or respectively the Integrated Legendre polynomials.

Thanks to the multiplication with the monomial t^n , the functions are free of fractions and stay polynomial of order n , i.e. $\ell_n^S \in P^n(T)$ and $L_n^S \in P_0^n(T)$ for $T = [-1, -1] \times [0, 1]$. Moreover, we obtain the following three-term recurrence relations:

$$\begin{aligned} \ell_0^S(x, t) &= 1, \\ \ell_1^S(x, t) &= x, \\ (n+1)\ell_{n+1}^S(x, t) &= (2n+1)x\ell_n^S(x) - nt^2\ell_{n-1}^S(x), \quad \text{for } n \geq 2, \end{aligned}$$

for the scaled Legendre polynomials, and

$$\begin{aligned} L_1^S(x, t) &= x, \\ L_2^S(x, t) &= \frac{1}{2}(x^2 - t^2), \\ (n+1)L_{n+1}^S(x, t) &= (2n-1)xL_n^S(x) - (n-2)t^2L_{n-1}^S(x) \quad \text{for } n \geq 3 \end{aligned}$$

for the scaled integrated Legendre polynomials, respectively.

The orientation problem

One difference of (hierarchical) higher order methods to the well-known Lagrange-type elements is that the degrees of freedom not longer refer exclusively to point-evaluations. In order to enforce continuity over element-interfaces (edges and faces), the orientation of edges and faces becomes important (see Figure 5.4). There are two possibilities to deal with this fact: either one takes the local edge/face orientation into account in the global assembling process, or one introduces a globally unique orientation of edges and faces, which is available on the local-element level.

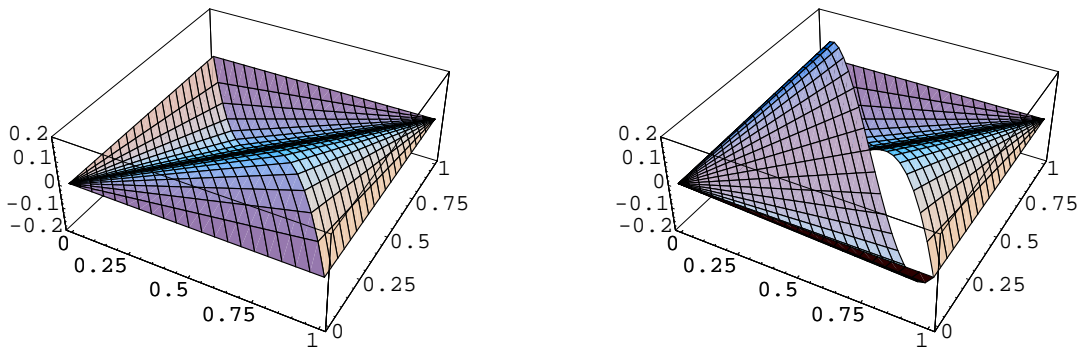


Figure 5.4: Edge-based basis function with correct and converse edge orientation

The first approach is quite simple in 2D, where the problem of locally converse running edges can be easily resolved by a flip of signs of the related edge-based shape functions during the

global assembling process. For tetrahedra, however, such a procedure is rather sophisticated: one has to define two types of reference elements, onto which all global elements can be rotated. See AINSWORTH-COYLE [2] for details.

In this work we address the orientation problem by introducing reference elements which are parameterized by the global vertex indices of the corresponding physical element. By introducing a unique edge and face orientation based on the global vertex indices, the global orientation is also locally available on each edge/face. Let \hat{K} be a reference element of arbitrary shape. On the local element level we assume to have access to the global vertex-indices $V_\alpha^K \in \mathcal{V}_K$ of the local vertices $\alpha \in \{1, \dots, n_V\} = \mathcal{V}_{\hat{K}}$.

We define the *edge orientation* always pointing from the vertex with the higher global vertex number to the one with the lower one. This means, if the element-edge E connects the local vertices α_1^E and α_2^E , we achieve the edge-orientation on the element-level as *from* the local vertex e_1 *to* the local vertex e_2 with

$$\begin{aligned} e_1 &:= \arg \max_{\alpha \in \{\alpha_1^E, \alpha_2^E\}} \{v_\alpha^K\}, \\ e_2 &:= \arg \min_{\alpha \in \{\alpha_1^E, \alpha_2^E\}} \{v_\alpha^K\}, \end{aligned} \quad \text{i.e.} \quad v_{e_1}^K > v_{e_2}^K. \quad (5.6)$$

We refer to an oriented edge by brackets, e.g., $E = [e_1, e_2] \in \mathcal{E}_{\hat{K}}$.

The *triangular face orientation* of the element-face F including the three local vertices $\alpha_1^F, \alpha_2^F, \alpha_3^F$ is defined in the following way: First we set

$$\begin{aligned} f_1 &:= \arg \max_{\alpha \in \{\alpha_1^F, \alpha_2^F, \alpha_3^F\}} \{v_\alpha^K\}, \\ f_3 &:= \arg \min_{\alpha \in \{\alpha_1^F, \alpha_2^F, \alpha_3^F\}} \{v_\alpha^K\}, \\ f_2 &:= 3 - \text{mod}_3(f_1 + f_3), \end{aligned} \quad \text{i.e.} \quad v_{f_1}^K > v_{f_2}^K > v_{f_3}^K. \quad (5.7)$$

Then we refer to an oriented triangular face by $F = [f_1, f_2, f_3] \in \mathcal{F}_{\hat{K}}$.

The unique orientation of a local *quadrilateral face* $F = \{\alpha_1^F, \alpha_2^F, \alpha_3^F, \alpha_4^F\} \in \mathcal{F}_{\hat{K}}$ is defined similarly: we start at the vertex f_1 with maximal global vertex number and then proceed in the direction of the adjacent vertex which has the highest vertex number, i.e., we set

$$F = [f_1, f_2, f_3, f_4] \quad \text{s.t.} \quad \begin{cases} f_1 := \arg \max_{\alpha \in \{\alpha_1^F, \alpha_2^F, \alpha_3^F, \alpha_4^F\}} \{v_\alpha^K\}, \\ f_3 \text{ opposite } f_1 \text{ on } F, \\ v_{f_2} > v_{f_4}. \end{cases} \quad (5.8)$$

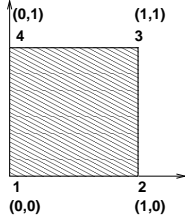
The local vertex f_2 is either a horizontal or vertical neighbor of f_1 , vice versa for vertex f_4 .

Remark 5.1. *Taking into account the orientation, is necessary for enforcing conformity in the construction of global hierarchical high-order finite element spaces. In the following we construct conforming local high-order shape functions on a reference element, which is parameterized by the global vertex numbers. However, the presented construction of local bases is not affected by the choice of orientation.*

If one chooses the strategy proposed by AINSWORTH-COYLE [2], one simply has to exchange the edge orientations, denoted by $[e_1, e_2]$, and face orientations, denoted by $[f_1, f_2, f_3]$ or $[f_1, f_2, f_3, f_4]$ by the local edge and face orientation of the considered reference element.

5.2.2 The quadrilateral element

We define the quadrilateral reference element as $\mathcal{Q} = [0, 1] \times [0, 1]$. Analogous to the construction of shape functions for simplicial shape functions in terms of barycentric coordinates, we state a general construction of shape functions in terms of the bilinear functions λ_i , equal one at the vertex i and zero at all other vertices, and the linear functions σ_i for the quadrilateral \mathcal{Q} as follows:



$$\begin{aligned}
 \lambda_1 &:= (1-x)(1-y) & \sigma_1 &:= (1-x) + (1-y) \\
 \lambda_2 &:= x(1-y) & \sigma_2 &:= x + (1-y) \\
 \lambda_3 &:= xy & \sigma_3 &:= x + y \\
 \lambda_4 &:= (1-x)y & \sigma_4 &:= (1-x) + y
 \end{aligned} \tag{5.9}$$

This notation will simplify the construction of the spaces $H(\text{curl})$ and $H(\text{div})$ later on, and is also helpful in the numerical realization.

The edge $E = [e_1, e_2]$ pointing from vertex e_1 to e_2 can be parameterized over the interval $I = [-1, 1]$ by

$$\xi_E = \sigma_{e_2} - \sigma_{e_1} \in [-1, 1].$$

The unit tangential vector $\boldsymbol{\tau}_E$ and the outer unit normal vector \boldsymbol{n}_E of the edge E can be deduced by

$$\boldsymbol{\tau}_E = \frac{1}{2} \nabla(\sigma_{e_2} - \sigma_{e_1}) \quad \text{and} \quad \boldsymbol{n}_E = \nabla(\lambda_{e_1} + \lambda_{e_2}) \quad \text{for } E = [e_1, e_2]. \tag{5.10}$$

We will later extend functions on the edge E into the domain \mathcal{Q} . For this purpose, we define the *linear edge-extension parameter*

$$\lambda_E = \lambda_{e_1} + \lambda_{e_2} \in [0, 1],$$

which is one on E and zero on the edge opposite of E .

We construct now a sequence of local finite element spaces with uniform polynomial order $k \geq 1$ of the following form:

$$\mathbb{R} \xrightarrow{id} Q_{k+1}(\mathcal{Q}) \xrightarrow{\nabla} Q_{k,k+1}(\mathcal{Q}) \times Q_{k+1,k}(\mathcal{Q}) \xrightarrow{\text{curl}} Q_k(\mathcal{Q}) \xrightarrow{0} \{0\} \tag{5.11}$$

and

$$\mathbb{R} \xrightarrow{id} Q_{k+1}(\mathcal{Q}) \xrightarrow{\text{Curl}} Q_{k+1,k}(\mathcal{Q}) \times Q_{k,k+1}(\mathcal{Q}) \xrightarrow{\text{div}} Q_k(\mathcal{Q}) \xrightarrow{0} \{0\}, \tag{5.12}$$

cf. (3.15), (3.16) for the corresponding sequences on the continuous level.

The H^1 -conforming quadrilateral element

We construct the H^1 -conforming space as a Vertex-Edge-Cell (V - E - C) based hierarchical polynomial space:

For the *vertex-based shape functions* we choose the lowest order bilinear functions

$$\phi_i^V(\boldsymbol{x}) = \lambda_i(\boldsymbol{x}), \quad \text{for } i = 1, \dots, 4.$$

Edge-based shape functions associated with the edge $E = [e_1, e_2]$ are constructed by

1. specification of $p_E - 1$ linearly independent polynomials on the edge such that $\{tr_E(\phi_i^E)\}_i$ span $P_0^{p_E}(E)$. This is achieved by the reparameterization of the edge E by ξ_E on $I = [-1, 1]$ and using a basis $\{L_i\}_{2 \leq i \leq p_E}$ of $P_0^p(I)$, which need not to be necessarily Integrated Legendre polynomials, i.e.,

$$tr_E(\phi_i^E)(\mathbf{x}) = L_{i+2}(\xi_E(\mathbf{x})) \quad \text{for } 0 \leq i \leq p_E - 2,$$

2. polynomial lifting of the edge values into the interior of the element such that $\phi_i^E \in P^{p_E}(\mathcal{Q})$ with vanishing trace on the three remaining edges. For the sake of simplicity, we will use a linear extension by λ_E , i.e.,

$$\phi_i^E(\mathbf{x}) = L_{i+2}(\xi_E(\mathbf{x})) (\lambda_{e_1}(\mathbf{x}) + \lambda_{e_2}(\mathbf{x})) \quad \text{for } 0 \leq i \leq p_E - 2.$$

We define *Cell-based* shape functions which vanish on the whole boundary ∂K and span $Q_k^0(\mathcal{Q})$. This is achieved by the following tensor-product construction:

$$\phi_{ij}^C(\mathbf{x}) := L_{i+2}(2x - 1) L_{j+2}(2y - 1) \quad \text{for } 0 \leq i, j \leq p_C - 2.$$

Summarizing, we have

Hierarchical H^1-conforming quadrilateral element of variable order $\mathbf{p} = (\{p_E\}, p_C)$	
<u>Vertex-based functions</u>	
for $i = 1, \dots, 4$:	$\phi_i^V = \lambda_i$
<u>Edge-based functions</u>	
for $m = 1, 2, 3, 4$: Suppose the edge $E_m = [e_1, e_2]$.	
for $0 \leq i \leq p_{E_m} - 2$:	$\phi_i^{E_m} = L_{i+2}(\sigma_{e_2} - \sigma_{e_1}) (\lambda_{e_1} + \lambda_{e_2})$
<u>Cell-based functions</u>	
for $0 \leq i, j \leq p_C - 2$:	$\phi_{ij}^C = L_{i+2}(2x - 1) L_{j+2}(2y - 1)$

We define the local spaces

$$\begin{aligned} W^V(\mathcal{Q}) &:= \text{span}((\phi_m^V)_{1 \leq m \leq 4}), \\ W_{p_{E_m}}^{E_m}(\mathcal{Q}) &:= \text{span}((\phi_i^{E_m})_{1 \leq i \leq p_{E_m} - 1}), \quad m = 1, \dots, 4, \\ W_{p_C}^C(\mathcal{Q}) &:= \text{span}((\phi_{ij}^C)_{1 \leq i, j \leq p_C}), \end{aligned}$$

and, finally the local FE-space on the quadrilateral for variable polynomial degree $\mathbf{p} = (p_{E_1}, p_{E_2}, p_{E_3}, p_C)$ by

$$W_{\mathbf{p}}(\mathcal{Q}) := W^V(\mathcal{Q}) \oplus \bigoplus_{m=1}^4 W_{p_{E_m}}^{E_m}(\mathcal{Q}) \oplus W_{p_C}^C(\mathcal{Q}). \quad (5.13)$$

Theorem 5.2. *The V-E-C-based shape functions presented above define an H^1 -conforming finite element basis on the quadrilateral \mathcal{Q} . In particular, they are linearly independent and for uniform polynomial order $p = p_{E_m} = p_C$ there holds $W_{\mathbf{p}}(\mathcal{Q}) = Q^p(\mathcal{Q})$.*

Proof. We consider that a trivial element v can be constructed via a linear combination of shape functions, i.e.,

$$v = \sum_{i=1}^4 c_i^V \phi_i^V + \sum_{m=1}^4 \sum_{i=1}^{p_{E_m}-1} c_i^{E_m} \phi_i^{E_m} + \sum_{i,j=1}^{p_C-1} c_{ij}^C \phi_{ij}^C = 0.$$

To prove linear independence of the basis, we have to show that all coefficients are zero: We know that the only shape function not vanishing in the vertex V_i is the one associated with this vertex, i.e. $v(V_i) = 0$ implies $c_i^V = 0$.

Next we restrict v to each edge E_m . Since the cell-based shape functions vanish on all edges as well as all edge-based shape functions associated with $E_k \neq E_m$ vanish on E_m , we obtain $tr_{E_m}(v) = tr_{E_m}(\sum_{i=1}^{p_{E_m}-1} c_i^{E_m} \phi_i^{E_m}) = 0$. Since the edge-based functions are linearly independent and span $P_{p_E}^0(E_m)$ on the edge, the coefficients $c_i^{E_m}$ are zero.

Considering traces of the cell-based shape functions along horizontal or vertical lines:

$$v(x, \bar{y}) = \sum_{i,j} c_{ij} L_i(2x-1) L_j(2\bar{y}-1) = \sum_i \tilde{c}_i L_i(2x-1) = 0$$

implying $\tilde{c}_i := \sum_j c_{ij} L_j(2\bar{y}-1) = 0$ for all $\bar{y} \in [0, 1]$, we can reduce the analysis of the linear-independence to the 1D case.

Hence, we obtain linear independence of all shape functions.

For uniform polynomial order p , every shape function lies in $Q^p(\mathcal{Q})$ by construction. By a simple counting argument we obtain that the stated shape functions are a basis of $Q^p(\mathcal{Q})$:

$$\begin{aligned} |W_p(\mathcal{Q})| &= |W^V(\mathcal{Q})| + \sum_{m=1}^4 |W_p^{E_m}(\mathcal{Q})| + |W_p^C(\mathcal{Q})| \\ &= 4 + 4(p-1) + (p-1)^2 = (p+1)^2, \quad \text{and} \\ |Q^p(\mathcal{Q})| &= (p+1)^2. \end{aligned}$$

□

Remark 5.3. 1. For $p = p_C \geq p_{E_m}$ the shape functions form a basis for

$$W_{\mathbf{p}}(\mathcal{Q}) = \{ w \in P^{\mathbf{p}}(\mathcal{Q}) : tr_E(w) \in P^{p_{E_m}}(E_m) \text{ for } m = 1, \dots, 4 \}.$$

2. The common construction of the shape functions by Integrated-Legendre polynomials $(L_i)_{2 \leq i \leq p}$ is not necessary. In view of conditioning and sparsity of the resulting FE-matrices one can exchange the family of Integrated polynomials by other bases of $P_0^p([-1, 1])$.
3. For $p_C \geq p_{E_m}$, the construction of edge-based shape functions is not limited to the linear extension. One can choose any lifting of the edge onto $P^{p_{E_m}}(\mathcal{Q})$ satisfying vanishing trace on the remaining edges.

$H(\text{curl})$ -conforming shape functions for quadrilaterals

In view of the exact sequence property, we want to construct an $H(\text{curl})$ -conforming finite element basis for a local FE-space $V_{\mathbf{p}}(\mathcal{Q})$ such that

$$\nabla W_{\mathbf{p}+1}(\mathcal{Q}) \subset V_{\mathbf{p}}(\mathcal{Q}).$$

For uniform polynomial order p , this leads to the choice $W_{\mathbf{p}+1}(\mathcal{Q}) = Q^{p+1}(\mathcal{Q})$, and hence

$$V_{\mathbf{p}}(\mathcal{Q}) = Q^{p+1,p}(\mathcal{Q}) \times Q^{p,p+1}(\mathcal{Q}) \quad \text{with } \dim V_{\mathbf{p}}(\mathcal{Q}) = 2(p+2)(p+1).$$

The lowest-order shape functions are chosen to be shape functions for the lowest-order Nédélec element, asking for the tangential component to be one on the associated edge, and zero on all other edges. This can be written in the compact form

$$\varphi_m^{N_0} = \frac{1}{2} \nabla(\sigma_{e_1} - \sigma_{e_2}) \cdot (\lambda_{e_1} + \lambda_{e_2}) \quad \text{for } E_m = [e_1, e_2].$$

The functions lie in $Q^{0,1}(\mathcal{Q}) \times Q^{1,0}(\mathcal{Q})$. Since the tangential vector of the edge $E_m = [e_1, e_2]$ is given by $\boldsymbol{\tau}_{E_m} = \frac{1}{2}\nabla(\sigma_{e_2} - \sigma_{e_1})$, the tangential trace on an edge E_k is

$$tr_{\boldsymbol{\tau}_{E_k}, E_k}(\boldsymbol{\varphi}_m^{N0}) = (\lambda_{e_1} + \lambda_{e_2})\boldsymbol{\tau}_{E_m} \cdot \boldsymbol{\tau}_{E_k} = \begin{cases} 0 & \text{on } E_k \perp E_m, \\ \delta_{m,k} \cdot 1 & \text{on } E_k \parallel E_m. \end{cases}$$

The higher-order *edge-based* $H(\text{curl})$ -conforming shape functions can be chosen as gradient-fields of the corresponding H^1 -conforming edge-based shape functions, i.e. for $0 \leq i \leq p_{E_m} - 1$

$$\boldsymbol{\varphi}_i^{E_m}(\mathbf{x}) = \nabla \phi_i^{E_m}(\mathbf{x}) \quad \text{for } \phi_i^{E_m} \in W_{p_{E_m}+1}^{E_m}(\mathcal{Q}).$$

Since the trace of a scalar edge-based shape function on the edge E_k fulfills

$$tr_{E_k}(\phi_i^{E_m}) = \begin{cases} L_{i+2} & \text{on } E_k = E_m \\ 0 & \text{on } E_k, k \neq m \end{cases} \quad \text{with } \text{span}\{L_{i+2}\}_{i=0, \dots, p_{E_m}-1} = P_0^{p_{E_m}+1}(E_m),$$

the tangential components of the gradients satisfy

$$tr_{\boldsymbol{\tau}, E_k}(\boldsymbol{\varphi}_i^{E_m})(\mathbf{x}) = \frac{\partial}{\partial \boldsymbol{\tau}_{E_k}} \phi_i^{E_m}(\mathbf{x}) = \begin{cases} 2L'_{i+2}(\xi_E(\mathbf{x})) & \text{on } E_m = E_k \\ 0 & \text{on } E_k, k \neq m \end{cases}$$

Note that there holds $\boldsymbol{\varphi}_i^{E_m} \in Q^{i+1, i+2}(\mathcal{Q}) \times Q^{i+2, i+1}(\mathcal{Q})$, and due to the linear independence of the Integrated Legendre polynomials we obtain

$$\text{span}\{tr_{\boldsymbol{\tau}, E_m}(\boldsymbol{\varphi}_i^{E_m}) : 0 \leq i \leq p_{E_m} - 1\} = P^{p_{E_m}}(E_m)/\mathbb{R}.$$

We pursue this strategy also for construction of the *cell-based shape functions*. The gradients of cell-based shape functions $\{\phi_{ij}^C\}_{i,j=0, \dots, p-1}$ spanning $Q_0^{p+1}(\mathcal{Q})$ form p^2 linearly independent functions in $Q^{p,p+1}(\mathcal{Q}) \times Q^{p+1,p}(\mathcal{Q})$ having zero tangential trace on the element boundary $\partial\mathcal{Q}$. Therefore, we start by choosing

$$\boldsymbol{\varphi}_{ij}^{C1} = 2L'_{i+2}(2x-1)L_{j+2}(2y-1)\mathbf{e}_x + 2L_{i+2}(2x-1)L'_{j+2}(2y-1)\mathbf{e}_y.$$

Having a closer look at the contributing terms to the gradient functions, namely $L'_{i+2}(2x-1)L_{j+2}(2y-1)\mathbf{e}_x$ and $L_{i+2}(2x-1)L'_{j+2}(2y-1)\mathbf{e}_y$, we observe that each term on its own fulfills the requirements of cell-based shape functions, i.e., they lie in the required polynomial space $Q^{p,p+1}(\mathcal{Q}) \times Q^{p+1,p}(\mathcal{Q})$ and have zero tangential trace, since either $\mathbf{e}_x \perp \boldsymbol{\tau}_E$ or $L_{j+2}(2y-1) = L_{j+2}(\pm 1) = 0$ on any edge E . Moreover, the functions defined by the two contributions are obviously linearly independent. Therefore, we can add any linearly independent combination of the two terms to the set of cell-based shape functions. We suggest

$$\boldsymbol{\varphi}_{ij}^{C2} = L'_{i+2}(2x-1)L_{j+2}(2y-1)\mathbf{e}_x - L_{i+2}(2x-1)L'_{j+2}(2y-1)\mathbf{e}_y.$$

Finally, also the functions

$$(L_{i+2}(2y+1)\mathbf{e}_x)_{0 \leq i \leq p-1} \quad \text{and} \quad (L_{i+2}(2x-1)\mathbf{e}_y)_{0 \leq i \leq p-1},$$

have zero tangential trace on the boundary, and they are linearly independent of the other cell-based shape functions chosen so far, since they are the only ones which are constant either in x - or in y - direction.

Summarizing we arrive at the following set of shape functions:

Hierarchical quadrilateral $H(\text{curl})$-element of variable order $\mathbf{p} = (\{p_E\}, p_C)$	
Edge-based shape functions	
for $m = 1, 2, 3, 4$: edge $E_m = [e_1, e_2]$	
<u>Lowest-order edge shape function</u>	
$\varphi_m^{\mathcal{N}_0} = \frac{1}{2} \nabla (\sigma_{e_2} - \sigma_{e_1}) (\lambda_{e_1} + \lambda_{e_2})$	
<u>Higher-order edge-based functions</u> (<i>gradient fields</i>)	
for $0 \leq i \leq p_{E_m} - 1$	$\varphi_i^{E_m} = \nabla (L_{i+2}(\sigma_{e_2} - \sigma_{e_1}) (\lambda_{e_1} + \lambda_{e_2}))$
Cell-based functions	
<u>Type 1:</u> (<i>gradient fields</i>):	
for $0 \leq i, j \leq p_C - 1$	$\varphi_{ij}^{C_1} = \nabla (L_{i+2}(2x-1) L_{j+2}(2y-1))$
<u>Type 2:</u>	
for $0 \leq i, j \leq p_C - 1$	$\varphi_{ij}^{C_2} = L'_{i+2}(2x-1) L_{j+2}(2y-1) \mathbf{e}_x - L_{i+2}(2x-1) L'_{j+2}(2y-1) \mathbf{e}_y$
<u>Type 3:</u>	
for $0 \leq i \leq p_C - 1$	$\varphi_i^{C_3} = L_{i+2}(2y-1) \mathbf{e}_x$
	$\varphi_{i+p_C}^{C_3} = L_{i+2}(2x-1) \mathbf{e}_y$

We define $\mathcal{N}_0(\mathcal{Q}) := \text{span}((\varphi_m^{\mathcal{N}_0})_{1 \leq m \leq 4})$, $V_{p_{E_m}}^{E_m}(\mathcal{Q}) := \text{span}((\varphi_i^{E_m})_{0 \leq i \leq p_{E_m} - 1})$,
 $V_{p_C}^{C_1}(\mathcal{Q}) := \text{span}((\varphi_{ij}^{C_1})_{0 \leq i, j \leq p_C - 1})$, $V_{p_C}^{C_2}(\mathcal{Q}) := \text{span}((\varphi_{ij}^{C_2})_{0 \leq i, j \leq p_C - 1})$,
 $V_{p_C}^{C_3}(\mathcal{Q}) := \text{span}((\varphi_i^{C_3})_{0 \leq i \leq 2p_C - 1})$,

and the local FE-space for the quadrilateral of variable polynomial degree $\mathbf{p} = (p_{E_1}, p_{E_2}, p_{E_3}, p_C)$ by

$$V_{\mathbf{p}}(\mathcal{Q}) := \mathcal{N}_0(\mathcal{Q}) \oplus \bigoplus_{m=1}^4 V_{p_{E_m}}^{E_m}(\mathcal{Q}) \oplus V_{p_C}^C(\mathcal{Q}). \quad (5.14)$$

Theorem 5.4. *The \mathcal{N}_0 -E-C based shape functions defined above, form a local $H(\text{curl})$ -conforming finite element basis on the quadrilateral \mathcal{Q} . In case of uniform polynomial degree $p = p_C = p_{E_m}$ for all edges E_m they are a basis for $Q^{p, p+1}(\mathcal{Q}) \times Q^{p+1, p}(\mathcal{Q})$.*

Furthermore, there hold the following relations:

$$\nabla W_{p_{E_m}+1}^{E_m}(\mathcal{Q}) = V_{p_{E_m}}^{E_m}(\mathcal{Q}) \quad \text{for all edges } E_m, m = 1, \dots, 4,$$

and

$$\nabla W_{p_C+1}^C(\mathcal{Q}) = V_{p_C}^{C_1}(\mathcal{Q}) \subset V_{p_C}^C(\mathcal{Q}).$$

Proof. The linear independence of the p_{E_m} edge-based shape functions is implied by their construction as gradient fields of linearly independent polynomials with degree greater than 2. In combination with the lowest-order Nédélec function their tangential traces span $P_{p_{E_m}}(E_m)$ on the edge E_m , and are zero on all other edges. Concerning the cell-based functions, we constructed $2(p_C+1)(p_C+2)$ linearly independent shape functions in $Q^{p_C, p_C+1}(\mathcal{Q}) \times Q^{p_C+1, p_C}(\mathcal{Q})$ with vanishing trace on all edges.

The hierarchical $\mathcal{N}_0 - E_m - C$ construction for the tangential components implies the overall linear independence: assume that $v = 0$ can be built by an arbitrary linear combination of

the shape functions, i.e.

$$\mathbf{v} = \sum_{m=1}^4 [c_m^{\mathcal{N}_0} \varphi_m^{\mathcal{N}_0} + \sum_i c_i^{E_m} \varphi_i^{E_m}] + \sum_{ij} c_{ij}^C \varphi_{ij}^C = 0$$

In the first step we consider the tangential traces over the edges, i.e. $tr_{\boldsymbol{\tau}, E_m}(\mathbf{v}) = 0$, which implies all edge-associated coefficients $c_i^{E_m}$ to be zero due to the linear independence of edge-based functions. The remaining contribution to \mathbf{v} is then spanned only by cell-based functions, which are a set of linearly independent polynomials. Hence, all coefficients in the linear combination have to vanish, and we obtain the linear independence of the shape functions.

By a *counting argument* we have

$$\begin{aligned} |V_p(\mathcal{Q})| &= |V_{\mathcal{Q}}^{\mathcal{N}_0}| + \sum_{m=1}^4 |V_{\mathcal{Q}}^{E_m}| + |V_{\mathcal{Q}}^I| \\ &= 4 + 4p + 2p(p+1) = 2(p+2)(p+1), \quad \text{and} \\ |Q^{p,p+1}(\mathcal{Q}) \times Q^{p+1,p}(\mathcal{Q})| &= 2(p+2)(p+1), \end{aligned}$$

and hence the shape functions span the whole space $Q^{p,p+1}(\mathcal{Q}) \times Q^{p+1,p}(\mathcal{Q})$. \square

In case $p_{E_m} \leq p_C$ for all $m = 1, \dots, 4$ the $H(\text{curl})$ -conforming local FE-space reads

$$V_p(\mathcal{Q}) = \{ \varphi \in Q^{p+1,p}(\mathcal{Q}) \times Q^{p,p+1}(\mathcal{Q}) \mid tr_E(\varphi) \cdot \boldsymbol{\tau}_E = tr_{\boldsymbol{\tau}, E_m}(\varphi) \in P^{p_{E_m}}(E_m), m = 1, \dots, 4 \}.$$

Remark 5.5 ($H(\text{div})$ -conforming shape functions for the quadrilateral element \mathcal{Q}). *In two dimensions the $H(\text{div})$ -conforming shape functions can be generated out of the $H(\text{curl})$ -conforming ones with a rotation by 90 degrees. By this, we achieve:*

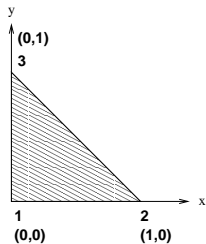
Hierarchical quadrilateral $H(\text{div})$-element of variable order $\mathbf{p} = (\{p_E\}, p_C)$	
<i>Edge-based shape functions: for $m = 1, 2, 3, 4$: edge $E_m = [e_1, e_2]$</i>	
$\psi_m^{\mathcal{RT}_0} = \frac{1}{2} \text{Curl}(\sigma_{e_2} - \sigma_{e_1})(\lambda_{e_1} + \lambda_{e_2})$	
$\psi_i^{E_m} = \text{Curl}(L_{i+2}(\sigma_{e_2} - \sigma_{e_1})(\lambda_{e_1} + \lambda_{e_2}))$	$0 \leq i \leq p_{E_m} - 1$
<i>Cell-based functions:</i>	
$\psi_{ij}^{C_1} = \text{Curl}(L_{i+2}(2x-1)L_{j+2}(2y-1))$	
$\psi_{ij}^{C_2} = L'_{i+2}(2x-1)L_{j+2}(2y-1)\mathbf{e}_y + L_{i+2}(2x-1)L'_{j+2}(2y-1)\mathbf{e}_x$	$0 \leq i, j \leq p_C - 1$
$\psi_i^{C_3} = L_{i+2}(2y-1)\mathbf{e}_y$	$0 \leq i \leq p_C - 1$
$\psi_{i+p_C}^{C_3} = L_{i+2}(2x-1)\mathbf{e}_x$	$0 \leq i \leq p_C - 1$

5.2.3 The triangular element

The triangular reference element is defined by

$$T := \{(x, y) \mid 0 \leq x, y \leq 1, x + y \leq 1\},$$

which involves the vertices $V_1 = (0, 0)$, $V_2 = (1, 0)$, and $V_3 = (0, 1)$. The shape functions will be formulated in terms of barycentric coordinates.



$$\begin{aligned} \lambda_1 &:= 1 - x - y, \\ \lambda_2 &:= x, \\ \lambda_3 &:= y. \end{aligned} \tag{5.15}$$

By viewing the triangle as a collapsed quadrilateral, as suggested in DUBINER [46] and KARNIADAKIS, SHERWIN [60], we can construct a tensorial-type basis also for triangles in a similar manner as for quadrilaterals.

The *Duffy transformation*

$$\mathcal{D} : \begin{array}{l} Q = [-1, 1]^2 \\ (\xi, \eta) \end{array} \rightarrow \begin{array}{l} T \\ (x, y) \end{array} \quad \text{defined as} \quad \begin{array}{l} x = \frac{1}{4}(1 + \xi)(1 - \eta) \\ y = \frac{1}{2}(1 + \eta) \end{array}$$

transforms the quadrilateral Q to the triangle T (see Figure 5.5). Using the inverse of the Duffy transformation, we can parameterize the triangle T by

$$\begin{aligned} \xi &= 2\frac{x}{1-y} - 1 = \frac{\lambda_2 - \lambda_1}{\lambda_1 + \lambda_2} && \in [-1, 1], \\ \eta &= 2y - 1 = 2\lambda_3 - 1 = 1 - 2\lambda_1 - 2\lambda_2 && \in [-1, 1], \end{aligned}$$

where, as above $\lambda_1, \lambda_2, \lambda_3$ denote the barycentric coordinates of the triangle.

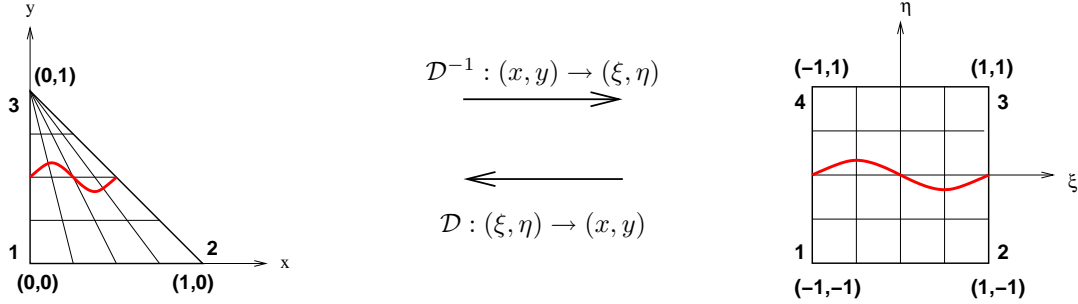


Figure 5.5: Collapsed coordinate system: triangle as degenerated quadrilateral

The horizontal lines $\eta(\lambda_3) = \bar{\eta} = \text{const.}$ in the triangle are then mapped by $\xi(\lambda_1, \lambda_2)$ onto $[-1, 1]$, while $\xi = \bar{\xi} = \text{const.}$ yields a parameterization of the lines radiating out of the top vertex V_3 over $[-1, 1]$, see Figure 5.5. Due to the transformation above, we can reparameterize an edge $E = [e_1, e_2]$ connecting the vertices e_1, e_2 and all lines running parallel to E (bounded by the two other edges) over the reference interval $[-1, 1]$ by

$$\xi_E = \frac{\lambda_{e_2} - \lambda_{e_1}}{\lambda_{e_1} + \lambda_{e_2}}.$$

The outer normal vector \mathbf{n}_E and tangential vector $\boldsymbol{\tau}_E$ of an edge $E = [e_1, e_2]$ with e_3 denoting the opposite vertex can be expressed in barycentric coordinates by

$$\mathbf{n}_E = -\nabla \lambda_{e_3} = \nabla(\lambda_{e_1} + \lambda_{e_2}).$$

We now construct local finite element spaces on the triangle T according to the sequences

$$\mathbb{R} \xrightarrow{id} P_{p+1}(T) \xrightarrow{\nabla} P_p(T) \xrightarrow{\text{curl}} P_{p-1}(T) \xrightarrow{0} \{0\}$$

respectively

$$\mathbb{R} \xrightarrow{id} P_{p+1}(T) \xrightarrow{\text{Curl}} P_p(T) \xrightarrow{\text{div}} P_{p-1}(T) \xrightarrow{0} \{0\},$$

cf. (3.15), (3.16) in the continuous setting.

The H^1 -conforming triangular element

In the following we introduce a V - E - C -based hierarchical local finite element basis based on the collapsed tensor-product representation of the triangle as used in, e.g., DUBINER [46], KARNIADAKIS-SHERWIN [60]. For uniform polynomial order, the basis will span

$$W_p(T) = P^p(T) \text{ with } \dim V_p(T) = \frac{1}{2}(p+1)(p+2).$$

As in the quadrilateral case, the *vertex-based* shape functions are chosen as the lowest-order shape functions spanning $P^1(T)$, i.e.,

$$\phi_i^V(\mathbf{x}) = \lambda_i(\mathbf{x}) \quad \text{for } i = 1, 2, 3.$$

For *edge-based* shape functions we choose the *scaled Integrated Legendre polynomials* of order $2 \leq i+1 \leq p_{E_m}$

$$\phi_i^{E_m} := L_{i+2}^S(\lambda_{e_2} - \lambda_{e_1}, \lambda_{e_1} + \lambda_{e_2}) = L_{i+2}\left(\frac{\lambda_{e_2} - \lambda_{e_1}}{\lambda_{e_1} + \lambda_{e_2}}\right)(\lambda_{e_1} + \lambda_{e_2})^{i+2}. \quad (5.16)$$

We shortly summarize the main properties of these functions:

- The functions $\phi_i^{E_m}$ are zero in all vertices, i.e. $\phi_i^{E_m}(V_k) = 0$, $k = 1, \dots, 3$.
- Since $tr_{E_k}(\phi_i^{E_m}) = \begin{cases} L_{i+2}(\xi_E) & \text{if } E_k = E_m \\ L_{i+2}(\pm 1)(\lambda_{e_1} + \lambda_{e_2})^{i+2} = 0 & \text{if } E_k \neq E_m \end{cases}$ on any edge $E_k \in \mathcal{E}_K$, the traces of the edge-based shape functions span $P_0^p(E_m)$ on the corresponding edge E_m , while vanishing on the other two edges.
- The extension of edge functions $L_{i+2}(\xi)$ onto the triangle by multiplication with factor $(\lambda_{e_1} + \lambda_{e_2})^{i+2}$ corresponds to an extension by $((1-\eta)/2)^{i+2}$ in the quadrilateral coordinates (Duffy transformation). Hence we refer to this extension as *monomial extension*.

Finally we define the *cell-based* shape functions as

$$\phi_{(i,j)}^C = L_{i+2}^S(\lambda_2 - \lambda_1, \lambda_1 + \lambda_2) \lambda_3 \ell_j(2\lambda_3 - 1) \quad (5.17)$$

for $1 \leq i+j \leq p_C - 3$. These functions have following properties:

- They are bubble functions in $P_0^p(T)$. The trace vanishes on ∂T , since $\frac{\lambda_2 - \lambda_1}{\lambda_1 + \lambda_2} = \pm 1$ on the edges opposite vertex 1, 2 and λ_3 vanishes on the edge opposite to vertex 3. The monomial extension, which is performed by using Scaled Integrated Legendere polynomials, implies that $\phi_{(i,j)}^C \in P_0^p(T)$.
- By the inverse Duffy transformation we can interpret the cell-based shape functions in terms of the quadrilateral coordinates (ξ, η) which yields

$$(\varphi_{ij}^C \circ \mathcal{D})(\xi, \eta) = L_{i+2}(\xi) \left(\frac{1-\eta}{2}\right)^{i+2} \frac{\eta+1}{2} \ell_j(\eta). \quad (5.18)$$

- In particular, on the *horizontal lines* of the triangle, i.e. $\lambda_3 = \text{const.}$, the functions can be written as an Integrated Legendre polynomial, since

$$\phi_{ij}^C|_{\eta=\text{const.}} = c_{ij} L_{i+2}\left(\frac{\lambda_1 - \lambda_2}{\lambda_1 + \lambda_2}\right) \in P_0^{i+2}([-1, 1])$$

with $c_{ij} = \lambda_3 \ell_j(2\lambda_3 - 1) (1 - \lambda_3)^{i+2}$ (confer Figure 5.5).

- On "ray" lines of the triangle, i.e. $\frac{\lambda_2 - \lambda_1}{\lambda_1 + \lambda_2} = \text{const.}$, we obtain

$$\phi_{ij}^C|_{\xi=\text{const.}} = c_i \lambda_3 \ell_j (2\lambda_3 - 1) (1 - \lambda_3)^{i+2} \in P^{j+i+3}([-1, 1])$$

with $c_i = L_{i+2}(\frac{\lambda_1 - \lambda_2}{\lambda_1 + \lambda_2})$.

Summarizing, we obtain the following set of shape functions.

Hierarchical H^1 -conforming shape functions on the triangular element T of variable order $\mathbf{p} = (\{p_E\}, p_C)$	
<u>Vertex-based functions</u>	
for $i = 1, 2, 3$:	$\phi_i^V = \lambda_i$
<u>Edge-based functions</u>	
for $m = 1, 2, 3$: edge $E_m = [e_1, e_2]$	
for $0 \leq i \leq p_{E_m} - 2$: $\phi_i^{E_m} = L_{i+2}^S(\lambda_{e_2} - \lambda_{e_1}, \lambda_{e_1} + \lambda_{e_2})$	
<u>Cell-based functions</u>	
for $0 \leq i + j \leq p_C - 3, i, j \geq 1$:	
$\phi_{(i,j)}^C = L_{i+2}^S(\lambda_2 - \lambda_1, \lambda_1 + \lambda_2) \lambda_3 \ell_j (2\lambda_3 - 1)$	

We define the local block spaces via

$$\begin{aligned} W^V(T) &:= \text{span}((\phi_i^V)_{1 \leq i \leq 3}), \\ W_{p_{E_m}}^{E_m}(T) &:= \text{span}((\phi_i^{E_m})_{0 \leq i \leq p_{E_m} - 2}), \\ W_{p_C}^C(T) &:= \text{span}((\phi_{i,j}^C)_{0 \leq i+j \leq p_C - 3}), \end{aligned}$$

and the local FE-space of variable polynomial order $\mathbf{p} = (p_{E_1}, p_{E_2}, p_{E_3}, p_C)$

$$W_{\mathbf{p}}(T) := W^V(T) \oplus \bigoplus_{m=1}^3 W_{p_{E_m}}^{E_m}(T) \oplus W_{p_C}^C(T). \quad (5.19)$$

Theorem 5.6. *The local V - E - C shape functions defined above are H^1 -conforming and linearly independent. For uniform order $\mathbf{p} = p_{E_m} = p_C$ they form a basis for $P^{\mathbf{p}}(T)$.*

Proof. It remains to prove the linear independence of the shape functions. We consider the following arbitrary linear combination:

$$w = \sum_{i=1}^3 c_i^V \phi_i^V + \sum_{m=1}^3 \sum_{i=1}^{p_{E_m}-2} c_i^{E_m} \phi_i^{E_m} + \sum_{\substack{i,j \geq 0 \\ i+j \leq p_C-3}} c_{ij}^C \phi_{ij}^C = 0.$$

Restricting w to the vertices V_i yields $c_i^V = 0$. On edge E_m the only non-zero functions, except for the vertex-based functions, are those associated with this edge. Hence, we obtain $\text{tr}_E(w) = \sum_i c_i^E \text{tr}_E(\phi_i^{E_m}) = 0$, which yields $c_i^{E_m} = 0$ for all i due to the linear-independence of $\{\phi_i^{E_m}\}$ on E_m .

Hence, there are only cell-based contributions in the expansion of w left. Thanks to the tensor-product representation (5.18), the cell-based shape functions are linear-independent. This yields linear-independence of the whole set of shape functions.

The V - E - C -based construction implies H^1 -conformity, e.g. considering an edge $E = [e_1, e_2]$: only the two vertex-based shape functions associated with e_1 and e_2 and the edge-based shape functions corresponding to E , have non-zero trace.

In the case of uniform polynomial order all shape functions are in $P^{\mathbf{p}}(T)$ by construction. The counting argument

$$\begin{aligned}
|W_p(T)| &= |W^V(T)| + \sum_{i=1}^3 |W_{p_{E_m}^{E_m}}(T)| + |W_{p_C}^C(T)| \\
&= 3 + 3(p-1) + \frac{1}{2}(p-2)(p-1) = \frac{1}{2}(p+1)(p+2), \quad \text{and} \\
|P^p(T)| &= \frac{1}{2}(p+2)(p+1)
\end{aligned}$$

verifies that for uniform order p we achieve a local basis of $P^p(T)$. \square

Jacobi-based shape functions We already mentioned that the construction scheme of the FE-basis functions is independent of the special choice of the type of the involved orthogonal polynomials. On the contrary, the conditioning of the involved FE-matrices as well as the fast evaluation of shape functions depends essentially on the chosen polynomial type. We can improve the conditioning and sparsity of the FE-matrices by exploiting the orthogonality within the hierarchical blocks.

As an alternative to the Legendre-type polynomials, let us consider now Jacobi polynomials $P_n^{(\alpha,\beta)}$ as defined in Appendix A.3 for the construction of the cell-based shape functions. A first simple, but motivating suggestion for the basis functions, which is similar to the one given in DUBINER [46], is

$$\phi_{(i,j)}^C = \lambda_1 \lambda_2 P_i^{\mathcal{S},(2,2)}(\lambda_1 - \lambda_2, \lambda_1 + \lambda_2) \lambda_3 P_j^{(2i+5,2)}(2\lambda_3 - 1)$$

for $0 \leq i + j \leq p_C - 3$. Due to the inverse Duffy transformation we obtain

$$(\phi_{(i,j)}^C \circ \mathcal{D})(\xi, \eta) = (1 - \xi)(1 + \xi)(1 - \eta)^2 P_i^{(2,2)}(\xi) \left(\frac{1 - \eta}{2}\right)^i \frac{1 + \eta}{2} P_j^{(2i+5,2)}(\eta).$$

Using this identity in the computation of the L_2 -inner product on the triangle we achieve

$$\begin{aligned}
\int_T \phi_{(i,j)}^C \phi_{(k,l)}^C d\mathbf{x} &= \int_{-1}^1 \int_{-1}^1 (\phi_{(i,j)}^C \circ \mathcal{D})(\xi, \eta) (\phi_{(k,l)}^C \circ \mathcal{D})(\xi, \eta) \frac{1}{8}(1 - \eta) d\xi d\eta \\
&= \frac{1}{2} \int_{-1}^1 (1 - \xi)^2 (1 + \xi)^2 P_i^{(2,2)}(\xi) P_k^{(2,2)}(\xi) d\xi \\
&\quad \times \int_{-1}^1 \left(\frac{1 - \eta}{2}\right)^{i+k+5} (1 + \eta)^2 P_j^{(2i+5,2)}(\eta) P_l^{(2k+5,2)}(\eta) d\eta \\
&= c_{ij} \delta_{ik} \delta_{jl}
\end{aligned}$$

Hence, this set of cell-based functions is L_2 -orthogonal.

In case we are interested in sparsity of the stiffness matrix, it is suggested in BEUHLER-SCHÖBERL [17] to choose

$$\phi_{(i,j)}^C = L_{i+2}^{\mathcal{S}}(\lambda_1 - \lambda_2, \lambda_1 + \lambda_2) \hat{P}_{j+1}^{(2i+1,0)}(2\lambda_3 - 1),$$

where we use integrated Jacobi polynomials $\hat{P}_{j+1}^{(\alpha,\beta)}(x)$ satisfying $\hat{P}_j^{(\alpha,\beta)}(-1) = 0$. This choice yields

$$\int_T (\nabla \phi_{(i,j)}^C)^T \nabla \phi_{(k,l)}^C d\mathbf{x} = 0 \quad \text{for } |i - k| > 2 \text{ or } |i - k + j - l| > 2$$

and therefore, we again obtain sparsity of the stiffness matrix.

Tensor-product representation of cell-based H^1 -conforming shape functions. In the construction of $H(\text{curl})$ - and $H(\text{div})$ -conforming shape functions we will frequently make use of the following product representation of H^1 -conforming cell-based shape functions:

$$\phi_{ij}^C(x, y) = u_i(x, y) v_j(y) \quad \text{for } i, j \geq 0, i + j \leq p_C - 3, \quad (5.20)$$

with $u_i \in P^{i+2}(T)$ vanishing on the edges $E_1 = [1, 3]$ and $E_2 = [2, 3]$ and $v_j \in P^{j+1}(T)$ vanishing on $E_3 = [1, 2]$. Within the family of Legendre-type functions, this can be provided by

$$u_i(x, y) := L_{i+2}^S(\lambda_1 - \lambda_2, \lambda_1 + \lambda_2), \quad v_j(y) := \lambda_3 \ell_j(2\lambda_3 - 1), \quad (5.21)$$

or equivalently in the Duffy-transformed quadrilateral coordinates

$$u_i(\mathcal{D}(\xi, \eta)) = L_{i+2}(\xi) \left(\frac{1-\eta}{2} \right)^{i+2}, \quad v_j(\mathcal{D}(\xi, \eta)) = \frac{1+\eta}{2} \ell_j(\eta). \quad (5.22)$$

$H(\text{curl})$ -conforming triangular element

We define the local FE-space V_p with $\nabla W_{p+1} \subset V_p$ such that, for uniform polynomial order p ,

$$V_p(T) = (P^p(T))^2 \quad \text{with } \dim(P^p(T))^2 = (p+2)(p+1)$$

holds. Note that we have $\nabla P^{p+1}(T) \subset V_p(T)$. In the construction of the basis we first choose gradients of the edge- and cell-based shape functions of W_{p+1} as shape functions in the $H(\text{curl})$ -conforming FE-basis and then extend the shape functions to span the full polynomial spaces on edges and cells, where the latter is defined by

$$P_{0,\tau}^{p_C}(T) := \{ \mathbf{q} \in (P_C^p(T))^2 : \text{tr}_{\tau, \partial T}(\mathbf{q}) = 0 \}.$$

Let us now start with the construction of shape functions for uniform polynomial order p : First we choose the *low-order* shape functions as the lowest-order Nédélec type I functions

$$\varphi_m^{\mathcal{N}_0} = \lambda_{e_1} \nabla \lambda_{e_2} - \nabla \lambda_{e_1} \lambda_{e_2} \quad \text{on each edge } E_m = [e_1, e_2]$$

with $(\boldsymbol{\tau}_{E_k} \cdot \varphi_m^{\mathcal{N}_0})|_{E_k} = \delta_{mk}$.

The *higher order edge-based* Nédélec shape functions can be chosen as the gradients of the H^1 -conforming scalar functions of order p

$$\varphi_i^{E_m} = \nabla \phi_i^{E_m} \quad \text{for } i = 0, \dots, p-1.$$

The verification that $\{ \text{tr}_E(\varphi_i^{E_m}) \cdot \boldsymbol{\tau}_{E_m} : 0 \leq i \leq p_{E_m} - 1 \}$ spans $P^{p_{E_m}}(E_m)/\mathbb{R}$ was already done in the quadrilateral case. Moreover, we obtain zero tangential trace on all edges E_k with $k \neq m$.

It remains to define appropriate *cell-based shape functions*: taking the gradients of cell-based H^1 -conforming shape functions up to order $p+1$ yields $\frac{1}{2}(p-1)p$ linearly independent shape functions in $P_{0,\tau}^p(T)$. In view of the exact sequence property, we therefore choose the first type of $H(\text{curl})$ -conforming cell-based shape functions as:

$$\varphi_{(i,j)}^{C,1}(x, y) = \nabla \phi_{(i,j)}^C(x, y) = \nabla u_i(x, y) v_j + u_i(x, y) \nabla v_j(y) \quad (5.23)$$

for $0 \leq i + j \leq p-2$ and $i, j \geq 0$.

For defining further cell-based shape functions we take the underlying product representation (5.20) of scalar functions into account. Let us first consider the contributions to the gradient fields in more detail.

Lemma 5.7. *Let $u_i := L_{i+2}^S(\lambda_2 - \lambda_1, \lambda_1 + \lambda_2)$ and $v_j := \lambda_3 l_j(2\lambda_3 - 1)$. Then the set $\{\nabla u_i v_j, u_i \nabla v_j, 0 \leq i + j \leq p - 2\}$ forms $p(p + 1)$ linearly independent functions in $\mathbf{P}_{0,\tau}^p(T)$.*

Proof.

1. The trace of u_i vanishes on the two edges opposite to vertex V_1 and V_2 , since $\frac{\lambda_2 - \lambda_1}{\lambda_1 + \lambda_2} = \pm 1$ there. The trace of v_j vanishes on the edge opposite to vertex V_3 , since $\lambda_3 = 0$. Hence, the tangential trace of $u_i \nabla v_j$ and $v_j \nabla u_i$ vanishes on all edges. Since $u_i \in P^{i+2}(T)$ and $v_j \in P^{j+1}(T)$, we obtain $u_i \nabla v_j, \nabla u_i v_j \in \mathbf{P}_{0,\tau}^p(T)$.
2. To show linear independence we first consider the two sets of functions separately. In order to compute gradients on the transformed quadrilateral, we need the Jacobian of the inverse Duffy transformation, i.e. $F_{\mathcal{D}}^{-T} = \begin{pmatrix} \frac{4}{1-\eta} & 0 \\ (\xi + 1)\frac{2}{1-\eta} & 2 \end{pmatrix}$. This yields:

$$\begin{aligned} \nabla_{\mathbf{x}} v_j(\mathbf{x}) u_i(x, y) &= F_{\mathcal{D}}^{-T} \nabla_{(\xi, \eta)} v_j(\mathcal{D}(\xi, \eta)) u_i(x, y) \\ &= 2(l_j(\eta) \frac{1+\eta}{2})' \left(\frac{1-\eta}{2}\right)^{i+2} L_{i+2}(\xi) e_2, \end{aligned}$$

which implies that $\{u_i \nabla v_j\}_{i,j}$ is a set of linearly independent functions.

Concerning $\{\nabla u_i v_j\}_{i,j}$ we consider the derivative in direction of the horizontal lines, denoted by τ_H , more precisely:

$$\begin{aligned} \tau_H \cdot \nabla u_i(x, y) v_j(y) &= \left(\frac{4}{1-\eta}\right) v_j \frac{\partial}{\partial \xi} u_i(\mathcal{D}(\xi, \eta)) \\ &= L'_{i+2}(\xi) \left(\frac{1-\eta}{2}\right)^{i+1} \frac{1+\eta}{2} l_j(\eta) \end{aligned} \tag{5.24}$$

which are linearly independent for all $0 \leq i + j \leq p - 2$.

We can easily verify that the two sets of shape functions are linearly independent by taking into account that v_j is constant on horizontal lines, which implies $\tau_H \cdot \nabla v_j(y) u_i(x, y) = 0$.

□

Due to the linear independence, we can use for the second type of cell-based Nédélec shape functions any combination of $\nabla u_i v_j$ and $u_i \nabla v_j$, which is linearly independent of $\varphi_{(i,j)}^{C,1}$, e.g.,

$$\varphi_{ij}^{C,2} = \nabla u_i v_j - u_i \nabla v_j \quad \text{for } 0 \leq i + j \leq p - 2.$$

Finally, we define a third family of cell-based shape functions which is linearly independent of the first two ones by

$$\varphi_j^{C,3} = (\nabla \lambda_1 \lambda_2 - \lambda_1 \nabla \lambda_2) v_j \quad \text{for } 0 \leq j \leq p - 2.$$

Here also the lowest-order Nédélec function $\nabla \lambda_1 \lambda_2 - \lambda_1 \nabla \lambda_2$ is involved, and the functions $\varphi_j^{C,3}$ are constant along horizontal lines.

The following table collects the suggested $H(\text{curl})$ -conforming shape functions for the triangular master element T of variable order.

**Hierarchical high-order triangular $H(\text{curl})$ -conforming element
of variable polynomial order $\mathbf{p} = (\{p_E\}, p_C)$**

Edge-based shape functions

for $m = 1, 2, 3$: edge $E^m = [e_1, e_2]$

Low-order functions:

$$\varphi_m^{\mathcal{N}_0} = \nabla \lambda_{e_1} \lambda_{e_2} - \lambda_{e_1} \nabla \lambda_{e_2}$$

Higher order edge-based functions (gradient fields):

for $0 \leq i \leq p_{E_m} - 1$

$$\varphi_i^{E_m} = \nabla(L_{i+2}^S(\lambda_{e_1} - \lambda_{e_2}, \lambda_{e_2} + \lambda_{e_1}))$$

Cell-based shape functions:

We define $u_i := L_{i+2}^S(\lambda_2 - \lambda_1, \lambda_1 + \lambda_2)$,

$$v_j := \lambda_3 \ell_j (2\lambda_3 - 1).$$

for $0 \leq i + j \leq p_C - 2$, $i, j \geq 0$:

Type 1 (Gradient fields): $\varphi_{(i,j)}^{C,1} = \nabla(u_i v_j) = \nabla u_i v_j + u_i \nabla v_j$

Type 2: $\varphi_{(i,j)}^{C,2} = \nabla u_i v_j - u_i \nabla v_j$

Type 3: $\varphi_{(0,j)}^{C,3} = (\nabla \lambda_1 \lambda_2 - \lambda_1 \nabla \lambda_2) v_j$

We define the local \mathcal{N}_0 - E - C -based spaces via

$$\begin{aligned} V^{\mathcal{N}_0}(T) &:= \text{span}((\varphi_i^{\mathcal{N}_0})_{1 \leq m \leq 3}), \\ V_{p_{E_m}}^{E_m}(T) &:= \text{span}((\varphi_i^{E_m})_{0 \leq i \leq p_{E_m} - 1}), \\ V_{p_C}^C(T) &:= \text{span}((\varphi_{i,j}^C)_{0 \leq i+j \leq p_C - 2}) \end{aligned}$$

The local FE-space of variable polynomial order $\mathbf{p} = (p_{E_1}, p_{E_2}, p_{E_3}, p_C)$ then is

$$V_{\mathbf{p}}(T) := V^V(T) \oplus \bigoplus_{m=1}^3 V_{p_{E_m}}^{E_m}(T) \oplus V_{p_C}^C(T).$$

Theorem 5.8. *The \mathcal{N}_0 - E - C -based shape functions, summarized in the table above, are $H(\text{curl})$ -conforming and linearly independent. For uniform polynomial order $\mathbf{p} = p_{E_m} = p_C$, we obtain a local $H(\text{curl})$ -conforming FE-basis for $V_{\mathbf{p}}(T) = (P^{\mathbf{p}}(T))^2$.*

Furthermore, there holds $\nabla W_{\mathbf{p}} \subset V_{\mathbf{p}}$, and the construction involving gradient functions provides

$$\nabla W_{p_{E_m}+1}^{E_m}(T) = V_{p_{E_m}}^{E_m}(T) \quad \text{as well as} \quad \nabla W_{p_C+1}^C(T) \subset V_{p_C}^C(T).$$

Proof. The edge-based shape functions are gradients of the corresponding (H^1) edge-based scalar functions (up to order $p_{E_m} + 1$). Hence, we obtain that $\varphi_i^{E_m} \in (P^{p_{E_m}}(T))^2$, their tangential trace $\text{span } P_{E_m}^p(E_m)/\mathbb{R}$ on E_m , and tangential traces vanishes on E_k , $k \neq m$. This implies linear independence within the set of all edge-based functions, including lowest-order Nédélec functions $\varphi_m^{\mathcal{N}_0}$.

Due to Lemma 5.8 the set of cell-based functions of type 1 and type 2 span $\{\nabla u_i v_j, u_i \nabla v_j\}$ and are linearly independent. The functions $\varphi_j^{C,3} = \varphi_3^{\mathcal{N}_0} v_j$ of the third type belong to $(P^{p_C}(T))^2$.

Moreover, there holds $tr_{\tau, \partial T}(\varphi_j^{C_3}) = 0$, since the tangential trace of $\varphi_3^{N_0}$ vanishes on the not-associated edges E_1 and E_2 and because the tangential trace of v_j vanishes on $E_3 = [V_1, V_2]$. Considering equation (5.24), we observe that along the horizontal lines the function $\nabla u_i v_j$ are at least linear, while $\nabla v_j u_i$ vanishes on horizontal lines ($\lambda_3 = \text{const.}$). Since $\varphi_3^{N_0}$ and v_j are constant along the horizontal lines, we obtain linear-independence within the set of cell-based shape functions. Moreover, the set of all cell-based shape functions spans $\mathbf{P}_{0,\tau}^{p_C}(T)$. Since the shape functions associated with an edge E_m are linearly independent, and they are the only functions with non-vanishing trace on the edge E_m , and the cell-based functions are linearly independent, we obtain the linear independence of the whole set of shape functions listed in the table above. The first argument also implies $H(\text{curl})$ -conformity, since the tangential trace on an edge depends only on shape functions corresponding to the edge. For uniform polynomial order p , all shape functions belong to $(P^p(T))^2$ by construction. Due to the linear-independence, a simple counting argument again yields $V_p = P^p(T)$:

$$\begin{aligned} |V_p(T)| &= |V^{N_0}(T)| + \sum_{i=1}^3 |V_p^{E_m}(T)| + |V_p^C(T)| \\ &= 3 + 3p + ((p-1)p + p - 1) = (p+1)(p+2), \quad \text{and} \\ |P^p(T)^2| &= (p+2)(p+1) \end{aligned}$$

□

Remark 5.9. 1. Owing to relation (A.7) the gradient of scaled (Integrated) Legendre polynomials can be expressed as

$$\begin{aligned} \nabla u_i(x, y) &= 2\ell_{i+1}^S(\lambda_2 - \lambda_1, \lambda_1 + \lambda_2) \mathbf{e}_x \\ &\quad + \left(\ell_{i+1}^S(\lambda_2 - \lambda_1, \lambda_1 + \lambda_2) + \ell_i^S(\lambda_2 - \lambda_1, \lambda_1 + \lambda_2) (\lambda_1 + \lambda_2) \right) \mathbf{e}_y, \\ \nabla v_j(x, y) &= \left(2\lambda_3 \ell_j' (2\lambda_3 - 1) + \ell_j (2\lambda_3 - 1) \right) \mathbf{e}_y. \end{aligned}$$

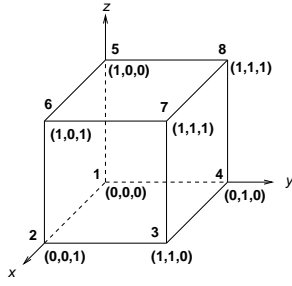
2. The suggested construction principle for $H(\text{curl})$ -conforming shape functions does not depend on the special choice of the type of the chosen orthogonal polynomials. We only need the tensor-product-based construction of the H^1 -functions. For example, using Jacobi-type shape functions yields $\phi_{(i,j)}^C = u_i(\lambda_1 - \lambda_2, \lambda_1 + \lambda_2) v_{(i,j)}(\lambda_3)$. Here, we choose the shape functions of type 3 as $\varphi_{(0,j)}^{C,3} = (\nabla \lambda_1 \lambda_2 - \lambda_1 \nabla \lambda_2) v_{(0,j)}$.

In two dimensions, the $H(\text{div})$ -conforming shape functions are obtained by the rotation by 90 degrees of the $H(\text{curl})$ -conforming ones:

Hierarchical high-order triangular $H(\text{div})$ -conforming element of variable polynomial order $\mathbf{p} = (\{p_E\}, p_C)$	
<u>Edge-based shape functions</u>	
for $m = 1, 2, 3$: edge E^m with vertices $\{e_1, e_2\}$	
$\psi_m^{N_0} = \text{Curl } \lambda_{e_1} \lambda_{e_2} - \lambda_{e_1} \text{Curl } \lambda_{e_2}$	
$\psi_i^{E_m} = \text{Curl}(L_{i+2}^S(\lambda_{e_1} - \lambda_{e_2}, \lambda_{e_2} + \lambda_{e_1}))$,	for $0 \leq i \leq p_{E_m} - 1$
<u>Cell-based shape functions</u>	
$\psi_{i,j}^{C_1} = \text{Curl } u_i v_j + u_i \text{Curl } v_j$,	for $0 \leq i + j \leq p_C - 2$
$\psi_{i,j}^{C_2} = \text{Curl } u_i v_j - u_i \text{Curl } v_j$,	for $0 \leq i + j \leq p_C - 2$
$\psi_j^{C_3} = (\text{Curl } \lambda_1 \lambda_2 - \lambda_1 \text{Curl } \lambda_2) v_j$,	for $0 \leq j \leq p_C - 2$
with $u_i := L_{i+2}^S(\lambda_2 - \lambda_1, \lambda_1 + \lambda_2)$ and $v_j := \lambda_3 \ell_j (2\lambda_3 - 1)$.	

5.2.4 The hexahedral element

We define the reference hexahedron as $\mathcal{H} := [0, 1]^3$. Similarly to the quadrilateral element, we will state the shape functions in terms of the trilinear functions λ_i , equal one at the vertex i and zero at all other vertices. We also introduce additional linear functionals σ_i associated with the vertex V_i :



$$\begin{aligned}
 \lambda_1 &= (1-x)(1-y)(1-z), & \sigma_1 &= (1-x) + (1-y) + (1-z), \\
 \lambda_2 &= x(1-y)(1-z), & \sigma_2 &= x + (1-y) + (1-z), \\
 \lambda_3 &= xy(1-z), & \sigma_3 &= x + y + (1-z), \\
 \lambda_4 &= (1-x)y(1-z), & \sigma_4 &= (1-x) + y + (1-z), \\
 \lambda_5 &= (1-x)(1-y)z, & \sigma_5 &= (1-x) + (1-y) + z, \\
 \lambda_6 &= x(1-y)z, & \sigma_6 &= x + (1-y) + z, \\
 \lambda_7 &= xyz, & \sigma_7 &= x + y + z, \\
 \lambda_8 &= (1-x)yz, & \sigma_8 &= (1-x) + y + z.
 \end{aligned}$$

These vertex-based functions allow us to construct edge-based and face-based shape functions in a unified manner.

- Each edge $E = [e_1, e_2]$ can be parameterized by

$$\xi_E := (\sigma_{e_2} - \sigma_{e_1}) \text{ over } [-1, 1].$$

The tangential vector associated with the edge E is then given by $\boldsymbol{\tau}_E = \frac{1}{2}\nabla(\sigma_{e_2} - \sigma_{e_1})$. The edge extension parameter $\lambda_E := \lambda_{e_1} + \lambda_{e_2}$ is one on the edge E and zero on all other edges parallel to E .

- Each face $F = [f_1, f_2, f_3, f_4]$, where the vertices f_3 and f_1 are not connected by an edge, can be parameterized via

$$(\xi_F, \eta_F) := (\sigma_{f_1} - \sigma_{f_2}, \sigma_{f_1} - \sigma_{f_4}) \text{ over } [-1, 1] \times [-1, 1].$$

The linear *face extension parameter* $\lambda_F = \lambda_{f_1} + \lambda_{f_2} + \lambda_{f_3} + \lambda_{f_4}$ is equal to 1 on the corresponding face F and zero on the opposite face. The outer normal vector of F can be computed via $\mathbf{n}_F = -\nabla\lambda_F$.

Remark 5.10. *The auxiliary functions corresponding to the vertices on an edge or a face, provide all necessary information for constructing the corresponding edge-based or face-based shape functions. We only have to state them for one edge and one face, and then apply the same construction for all edges and faces. This can also be utilized in a numerical implementation. Since the same strategy is used for tetrahedra and prisms, we can easily ensure conformity on hybrid meshes.*

We denote the tensor-product polynomial space on the hexahedron \mathcal{H} by

$$Q^{p_1, p_2, p_3}(\mathcal{H}) := \{q_1(x) \cdot q_2(y) \cdot q_3(z) \mid q_i \in P^{p_i}([0, 1]), i = 1, 2, 3\}, \quad (5.25)$$

$$Q^p(\mathcal{H}) := Q^{p, p, p}(\mathcal{H}). \quad (5.26)$$

For a uniform polynomial order p we try to establish a local exact sequence

$$\mathbb{R} \xrightarrow{id} Q^{p+1, p+1, p+1}(\mathcal{H}) \xrightarrow{\nabla} \begin{pmatrix} Q^{p, p+1, p+1}(\mathcal{H}) \\ Q^{p+1, p, p+1}(\mathcal{H}) \\ Q^{p+1, p+1, p}(\mathcal{H}) \end{pmatrix} \xrightarrow{\text{curl}} \begin{pmatrix} Q^{p+1, p, p}(\mathcal{H}) \\ Q^{p, p+1, p}(\mathcal{H}) \\ Q^{p, p, p+1}(\mathcal{H}) \end{pmatrix} \xrightarrow{\text{div}} Q^{p, p, p}(\mathcal{H}) \xrightarrow{0} \{0\}. \quad (5.27)$$

H^1 -conforming hexahedral element

We aim to construct an H^1 -conforming hierarchical V - E - F - C basis, which in case of uniform polynomial order p spans $W_p = Q^p(\mathcal{H})$. Extending the quadrilateral shape functions by linear extension into the interior of the hexahedron \mathcal{H} and adding tensor-product shape functions spanning $Q_0^{pC}(\mathcal{H})$ yields the following collection:

Hierarchical hexahedral H^1-element of variable order $\mathbf{p} = (p_{E_m}, p_{F_m}, p_C)$	
Vertex-based functions	for $i = 1, \dots, 8$: $\phi_i^V = \lambda_i$
Edge-based functions	
for $m = 1, \dots, 12$: Suppose the edge $E_m = [e_1, e_2]$.	
for $0 \leq i \leq p_{E_m} - 2$ $\phi_i^{E_m} = L_{i+2}(\sigma_{e_1} - \sigma_{e_2})(\lambda_{e_1} + \lambda_{e_2})$	
Face-based functions	
for $m = 1, \dots, 6$: Suppose the face $F_m = [f_1, f_2, f_3, f_4]$.	
for $0 \leq i, j \leq p_{F_m} - 2$ $\phi_{(i,j)}^{F_m} = L_{i+2}(\xi_F) L_{j+2}(\eta_F) \lambda_F$	
with $\lambda_F := \sum_{\alpha=0}^4 \lambda_{f_\alpha}$ and $(\xi_F, \eta_F) := (\sigma_{f_1} - \sigma_{f_2}, \sigma_{f_1} - \sigma_{f_4})$	
Cell-based functions	
for $0 \leq i, j, k \leq p_C - 2$ $\phi_{(i,j,k)}^C = L_{i+2}(2x-1)L_{j+2}(2y-1)L_{k+2}(2z-1)$	

We define the lowest-order space as $W^V(\mathcal{H}) := \text{span}((\phi_i^V)_{1 \leq i \leq 8})$ and denote the span of edge-based (associated with E_m) by $W_{E_m}^{p_{E_m}}(\mathcal{H})$, the span of face-based (associated with F_m) functions by $W_{F_m}^{p_{F_m}}(\mathcal{H})$, and the span of cell-based functions by $W_C^{p_C}(\mathcal{H})$. The local FE-space spanned by the whole set of shape functions on \mathcal{H} up to order $\mathbf{p} = (\{p_{E_m}\}, \{p_{F_m}\}, p_C)$ is given by

$$W_{\mathbf{p}}(\mathcal{H}) = W^V(\mathcal{H}) \oplus \bigoplus_{m=1}^{12} W_{E_m}^{p_{E_m}}(\mathcal{H}) \oplus \bigoplus_{m=1}^6 W_{F_m}^{p_{F_m}}(\mathcal{H}) \oplus W_C^{p_C}(\mathcal{H}).$$

Theorem 5.11. *The shape functions stated in the table above are linearly independent and H^1 -conforming. For uniform polynomial order $p = p_{E_m} = p_{F_m} = p_C$, they form a basis of $Q^p(\mathcal{H})$.*

Proof. The vertex functions are in $Q^1(\mathcal{H})$ and linearly independent, since $\phi_i^V(V_j) = \delta_{i,j}$.

The edge-extension $(\lambda_{e_1} + \lambda_{e_2})$ is independent of $\xi_E = \sigma_{e_2} - \sigma_{e_1}$, and hence the edge-based shape functions $\phi_i^{E_m} \in Q^{p_{E_m}}(\mathcal{H})$, and their traces on the corresponding edge E_m span $P_0^{p_{E_m}}(E_m)$ while being zero on all other edges.

The face-extension λ_F is constant on planes parallel to the face F_m , hence the face based functions are in $Q^{p_{F_m}}(\mathcal{H})$. Obviously, their traces on F_m span $P^{p_{F_m}}(F_m)$, while being zero on all other faces.

Finally, the cell-based functions, defined using the tensor products, span $Q_0^{p_C}(\mathcal{H})$.

To show linear independence and H^1 -conformity, we assume that the trivial function $0 = w \in W_{\mathbf{p}}$ can be assembled with the basis functions, i.e.

$$w = \sum_i c_i^V \phi_i^V + \sum_{E_m \in \mathcal{E}_{\mathcal{H}}} \sum_i c_i^{E_m} \phi_i^{E_m} + \sum_{F_m \in \mathcal{F}_{\mathcal{H}}} \sum_{i,j} c_{ij}^{F_m} \phi_{(i,j)}^{F_m} + \sum_{i,j,k} c_{ijk}^C \phi_{(i,j,k)}^C = 0.$$

Restricting w successively to the vertices, then to the edges, then to faces we obtain $c_i^V = 0$, $c_i^{E_m} = 0$, $c_{ij}^{F_m} = 0$ and finally $c_{ijk}^C = 0$ for all i, j, k . The H^1 -conformity follows with similar

arguments as in the quadrilateral case by the special construction, since, e.g. on a face the only non-zero shape functions are the ones associated with the four involved vertices, the four involved edges and the face itself.

In case of uniform polynomial order p a *counting argument* shows

$$\begin{aligned} |W_{\mathbf{p}}(\mathcal{H})| &= |W^V| + \sum_{m=1}^1 2|W_p^{E_m}| + \sum_{m=1}^6 |W_p^{F_m}| + |W_p^C| \\ &= 8 + 12(p-1) + 6(p-1)^2 + (p-1)^3 = (p+1)^3, \quad \text{and} \\ |Q^p(\mathcal{H})| &= (p+1)^3, \end{aligned}$$

and hence the shape functions span the whole $Q^p(\mathcal{H})$. \square

$H(\text{curl})$ -conforming shape functions for hexahedral elements

Since we want to ensure that $\nabla W_{\mathbf{p}+1} \subset V_{\mathbf{p}}$, we choose for uniform polynomial degree p the finite element space corresponding to the following part of the sequence (5.27)

$$Q^{p+1}(\mathcal{H}) \xrightarrow{\nabla} Q^{p,p+1,p+1}(\mathcal{H}) \times Q^{p+1,p,p+1}(\mathcal{H}) \times Q^{p+1,p+1,p}(\mathcal{H}).$$

We choose lowest-order, higher-order edge-based and face-based shape functions in analogy to the quadrilateral case. The extension onto the hexahedron requires linear extension by multiplication with $\lambda_E := \lambda_{e_1} + \lambda_{e_2}$ and $\lambda_F := \sum_{i=1}^4 \lambda_{f_i}$, and consideration of the edge- and face-orientations similar to the H^1 -conforming case.

The construction of *cell-based* shape functions again involves several types: as first class we choose the gradient functions of the H^1 -conforming shape functions:

$$\begin{aligned} \varphi_{(i,j,k)}^{C,1} &= \nabla \phi_{(i,j,k)}^{C,\nabla} = \nabla (L_{i+2}(2x-1)L_{j+2}(2y-1)L_{k+2}(2z-1)) \\ &= 2\ell_{i+1}(2x-1)L_{j+2}(2y-1)L_{k+2}(2z-1)\mathbf{e}_x \\ &\quad + 2L_{i+2}(2x-1)\ell_{j+1}(2y-1)L_{k+2}(2z-1)\mathbf{e}_y \\ &\quad + 2L_{i+2}(2x-1)L_{j+2}(2y-1)\ell_{k+1}(2z-1)\mathbf{e}_z, \end{aligned}$$

for $0 \leq i, j, k \leq p_C - 2$.

The three terms in the representation above form a set of $3(p-1)$ linearly independent functions with vanishing tangential trace on $\partial\mathcal{H}$, since for any face either e_x, e_y or e_z is normal to the considered face or one of the integrated Legendre polynomials is evaluated at ± 1 .

Hence, we can choose arbitrary linearly independent combinations of the three summands to obtain linearly independent cell-based shape functions. In particular, we set $\varphi_{(i,j,k)}^{C,2} = \text{diag}(\frac{1}{2}, -\frac{1}{2}, \frac{1}{2})\varphi_{(i,j,k)}^{C,1}$ and $\varphi_{\mathbf{p}_C+(i,j,k)}^{C,2} = \text{diag}(\frac{1}{2}, \frac{1}{2}, -\frac{1}{2})\varphi_{(i,j,k)}^{C,1}$ for $0 \leq i, j, k \leq p_C - 2$.

Finally, the following $3(p_C - 1)^2$ functions are linearly independent of any of the functions above:

$$\begin{aligned} \varphi_{(i,j,k)}^{C,3} &= L_{j+2}(2y-1)L_{k+2}(2z-1)\mathbf{e}_x, \\ \varphi_{(i,j,k)}^{C,3} &= L_{i+2}(2x-1)L_{k+2}(2z-1)\mathbf{e}_y, \\ \varphi_{\mathbf{p}_C+(i,j,k)}^{C,3} &= L_{i+2}(2x-1)L_{j+2}(2y-1)\mathbf{e}_z. \end{aligned}$$

The vanishing of the tangential components on all faces of the hexahedron is shown by the same argument as given above for the cell-based functions of the second type. Summarizing, we obtain

**Hierarchical $H(\text{curl})$ -conforming shape functions on the hexahedron \mathcal{H}
with variable polynomial order $\mathbf{p} = (\{p_{E_m}\}, \{p_{F_m}\}, p_C)$**

Edge-based shape functions

for edge E_m , $m = 1, \dots, 12$ with local edge-ordering $E_m = \{e_1, e_2\}$

Lowest-order \mathcal{N}_0 -function

$$\varphi_m^{\mathcal{N}_0} = \frac{1}{2} \nabla(\sigma_{e_1} - \sigma_{e_2})(\lambda_{e_1} + \lambda_{e_2})$$

Higher order edge-based functions (gradient fields)

for $0 \leq i \leq p_{E_m} - 1$

$$\varphi_i^{E_m} = \nabla(L_{i+2}(\sigma_{e_1} - \sigma_{e_2})(\lambda_{e_1} + \lambda_{e_2}))$$

Face-based functions

for faces F_m , $m = 1, \dots, 6$ with local face-vertex ordering $F_m = \{f_1, f_2, f_3, f_4\}$

We define $\lambda_F := \sum_{\alpha=0}^4 \lambda_{f_\alpha}$ and $(\xi_F, \eta_F) := (\sigma_{f_1} - \sigma_{f_2}, \sigma_{f_1} - \sigma_{f_4})$.

for $0 \leq i, j \leq p_{F_m} - 1$

Type 1 (gradient fields):

$$\varphi_{(i,j)}^{F_m,1} = \nabla(L_{i+2}(\xi_F) L_{j+2}(\eta_F) \lambda_F)$$

Type 2: $\varphi_{(i,j)}^{F_m,2} = (L'_{i+2}(\xi_F) L_{j+2}(\eta_F) \nabla \xi_F - L_{i+2}(\xi_F) L'_{j+2}(\eta_F) \nabla \eta_F) \lambda_F$

Type 3: $\varphi_{(0,j)}^{F_m,3} = L_{j+2}(\eta_F) \lambda_F \nabla \xi_F$
 $\varphi_{(i,0)}^{F_m,3} = L_{i+2}(\xi_F) \lambda_F \nabla \eta_F$

Cell-based functions

for $0 \leq i, j, k \leq p_C - 1$

Type 1 (gradient fields)

$$\varphi_{ijk}^{C,1} = \nabla(L_{i+2}(2x-1) L_{j+2}(2y-1) L_{k+2}(2z-1))$$

Type 2: $\varphi_{(i,j,k)}^{C,2} = \text{diag}(1, -1, 1) \varphi_{(i,j,k)}^{C,1}$
 $\varphi_{\mathbf{p}_C+(i,j,k)}^{C,2} = \text{diag}(1, -1, -1) \varphi_{(i,j,k)}^{C,1}$

Type 3: $\varphi_{(0,j,k)}^{C,3} = L_{j+2}(2y-1) L_{k+2}(2z-1) \mathbf{e}_x$
 $\varphi_{(i,0,k)}^{C,3} = L_{i+2}(2x-1) L_{k+2}(2z-1) \mathbf{e}_y$
 $\varphi_{(i,j,0)}^{C,3} = L_{i+2}(2x-1) L_{j+2}(2y-1) \mathbf{e}_z$

We define the lowest-order space as $V^{\mathcal{N}_0}(\mathcal{H}) := \text{span}((\varphi_m^{\mathcal{N}_0})_{1 \leq m \leq 12})$, and denote the span of edge-based associated with E_m by $V_{E_m}^{p_{E_m}}(\mathcal{H})$, the span of face-based functions associated with the face F_m by $V_{F_m}^{p_{F_m}}(\mathcal{H})$, and the span of cell-based functions by $V_C^{p_C}(\mathcal{H})$. The local FE-space spanned by the whole set of shape functions on \mathcal{H} up to order $\mathbf{p} = (\{p_{E_m}\}, \{p_{F_m}\}, p_C)$ is denoted by

$$V_{\mathbf{p}}(\mathcal{H}) := V_{\mathcal{N}_0}(\mathcal{H}) \oplus \bigoplus_{m=1}^{12} V_{E_m}^{p_{E_m}}(\mathcal{H}) \oplus \bigoplus_{m=1}^6 V_{F_m}^{p_{F_m}}(\mathcal{H}) \oplus V_C^{p_C}(\mathcal{H}).$$

Theorem 5.12. *The shape functions listed in the table above are $H(\text{curl})$ -conforming and linearly independent. Moreover, there holds*

$$\nabla W^V(\mathcal{H}) \subset V^{\mathcal{N}_0}(\mathcal{H}), \quad \nabla W_{p_{E_m}+1}^{E_m}(\mathcal{H}) = V_{p_{E_m}}^{E_m}(\mathcal{H}) \quad \forall 1 \leq m \leq 12$$

$$\nabla W_{p_{F_m}+1}^{F_m}(\mathcal{H}) \subset V_{p_{F_m}}^{F_m}(\mathcal{H}) \quad \forall 1 \leq m \leq 6, \quad \text{and} \quad \nabla W_{p_C+1}^C(\mathcal{H}) \subset V_{p_C}^C(\mathcal{H})$$

For uniform polynomial order $p = p_{E_m} = p_{F_m} = p_C$ we obtain an $H(\text{curl})$ -conforming basis spanning

$$V_p(\mathcal{H}) = Q^{p,p+1,p+1}(\mathcal{H}) \times Q^{p+1,p,p+1}(\mathcal{H}) \times Q^{p+1,p+1,p}(\mathcal{H}).$$

Proof. The linear independence of the edge-based and face-based shape functions can be deduced from the linear independence of the quadrilateral case. The linear independence of cell based functions follows from their definition.

Suppose that $0 = \mathbf{v} \in W_{\mathbf{p}}(\mathcal{H})$ has a representation

$$\mathbf{v} = \sum_{E_m \in \mathcal{E}_{\mathcal{H}}} c_m^0 \boldsymbol{\varphi}_m^{\mathcal{N}_0} + \sum_{i=0}^{p_{E_m}-1} c_i^{E_m} \boldsymbol{\varphi}_i^{E_m} + \sum_{F_m \in \mathcal{F}_{\mathcal{H}}} \sum_{i=1}^{n_{F_m}} c_i^{F_m} \boldsymbol{\varphi}_i^{F_m} + \sum_{i=1}^{n_C} c_i^C \boldsymbol{\varphi}_i^C,$$

where $\text{span}\{\boldsymbol{\varphi}_i^{F_m}\} = V_{\mathbf{p}}^{F_m}(\mathcal{H})$ and $\text{span}\{\boldsymbol{\varphi}_i^C\} = V_{\mathbf{p}}^C(\mathcal{H})$.

To prove *linear independence* of the whole set of stated shape functions we set $\mathbf{v} = 0$. Restriction to edges yields $\text{tr}_{\boldsymbol{\tau}, E_m}(\mathbf{v}) = 0$. This implies $c_i^{E_m} = 0, \forall i$, since the edge-based shape functions are the only ones with non-vanishing tangential trace on E_m . By restriction to the faces we obtain $\text{tr}_{\boldsymbol{\tau}, F_m}(\mathbf{v}) = \sum_{i=1}^{n_{F_m}} c_i^{F_m} \boldsymbol{\varphi}_i^{F_m} = 0$, and due to the linear independence of face-based functions $c_i^{F_m} = 0$, since the remaining cell-based part consists of linearly independent functions, we obtain $c_i^C = 0, \forall i$.

H(curl)-conformity: If all dofs associated with a face F_m vanish, i.e. $c_i^{F_m} = c_i^{E_k} = c_k^C = 0$ for E_k on F_m , then due to the \mathcal{N}_0 -E-F-C-based construction $\text{tr}_{\boldsymbol{\tau}, F_m}(\mathbf{v}) = 0$. An analogue statement holds for edges.

Finally, in case of uniform polynomial order p , all shape functions belong to $Q^{p,p+1,p+1}(\mathcal{H}) \times Q^{p+1,p,p+1}(\mathcal{H}) \times Q^{p+1,p+1,p}(\mathcal{H})$. Due to their linear independence the following *counting argument* concludes the proof:

$$\begin{aligned} |V_p(\mathcal{H})| &= |V^{\mathcal{N}_0}| + \sum_{m=1}^1 2|V_p^{E_m}| + \sum_{m=1}^6 |V_p^{F_m}| + |V_p^C| \\ &= 12 + 12p + 12p(p+1) + 3p(p+1)^2 = 3(p+2)^2(p+1), \quad \text{and} \end{aligned}$$

$$|Q^{p,p+1,p+1} \times Q^{p+1,p,p+1} \times Q^{p+1,p+1,p}| = 3(p+2)^2(p+1).$$

□

$H(\text{div})$ -conforming shape functions for hexahedral elements

In view of the sequence (5.27), we intend to construct a basis for local $H(\text{div})$ -conforming FE-space in such a way that, for uniform polynomial order p , it spans

$$Q_p = Q^{p+1,p,p}(\mathcal{H}) \times Q^{p,p+1,p}(\mathcal{H}) \times Q^{p,p,p+1}(\mathcal{H}).$$

The *lowest-order* Raviart-Thomas function corresponding to the quadrilateral face $F_m = [f_1, f_2, f_3, f_4]$ are given by

$$\boldsymbol{\psi}_m^{\mathcal{RT}_0} = \mathbf{n}_{F_m} \lambda_F = -\nabla \lambda_F \lambda_F.$$

Since the linear face extension $\lambda_F := \lambda_{f_1} + \lambda_{f_2} + \lambda_{f_3} + \lambda_{f_4}$ is independent of (ξ_F, η_F) , there holds $\boldsymbol{\psi}_m^{\mathcal{RT}_0} \in Q^{1,0,0} \times Q^{0,1,0} \times Q^{0,0,1}(\mathcal{H})$, and additionally $\text{tr}_{F_k}(\boldsymbol{\psi}_m^{\mathcal{RT}_0} \cdot \mathbf{n}_{F_k}) = \delta_{m,k}$.

The *face-based* shape functions can be chosen as curls of face-based $H(\text{curl})$ -based functions: Since $\text{tr}_{\mathbf{n}, F_m}(\text{curl}(\boldsymbol{\varphi})) = \mathbf{n} \cdot \text{curl}(\text{tr}_{\boldsymbol{\tau}, F_m}(\boldsymbol{\varphi})) = \text{curl}_{F_m}(\text{tr}_{\boldsymbol{\tau}, F_m}(\boldsymbol{\varphi})(\xi_F, \eta_F))$. Hence, if $\mathbf{q}_i(\xi_F, \eta_F) = \text{tr}_{\boldsymbol{\tau}, F_m}(\boldsymbol{\varphi}_i)$ span $Q^{p,p+1}/\mathbb{R} \times Q^{p+1,p}/\mathbb{R}$ then $\text{curl}(\mathbf{q}_i)$ span $Q^{p,p}/\mathbb{R}$. The curl of the gradient functions is zero, i.e. there remains $(p+1)^2 - 1$ linearly independent curl-fields, whose normal traces span $Q^{p,p}(F_m)/\mathbb{R}$ on the corresponding face F_m .

The first choice of *cell-based* shape functions are the curl-fields of cell-based $H(\text{curl})$ -conforming shape functions of order p_C . The curl-fields of type 2 and type 3 H^1 -conforming shape functions, are constructed by linear combination of the following functions:

$$\begin{aligned} &L_{i+2}(2x-1) \ell_{j+1}(2y-1) \ell_{k+1}(2z-1) \mathbf{e}_x, \\ &\ell_{i+1}(2x-1) L_{j+2}(2y-1) \ell_{k+1}(2z-1) \mathbf{e}_y, \\ &\ell_{i+1}(2x-1) \ell_{j+1}(2y-1) L_{k+2}(2z-1) \mathbf{e}_z, \end{aligned}$$

and

$$\begin{aligned} &L_{i+2}(2x-1) \ell_{j+1}(2y-1) \mathbf{e}_x, \quad \ell_{i+1}(2x-1) L_{j+2}(2y-1) \mathbf{e}_y, \quad \ell_{i+1}(2x-1) L_{k+2}(2z-1) \mathbf{e}_z, \\ &L_{i+2}(2x-1) \ell_{k+1}(2z-1) \mathbf{e}_x, \quad L_{j+2}(2y-1) \ell_{k+1}(2z-1) \mathbf{e}_y, \quad \ell_{j+2}(2y-1) L_{k+2}(2z-1) \mathbf{e}_z, \end{aligned}$$

for $0 \leq i, j, k \leq p_C - 1$. All these functions are linearly independent and are in $Q^{(p_C+1, p_C, p_C)} \times Q^{(p_C, p_C+1, p_C)} \times Q^{(p_C, p_C, p_C+1)}(\mathcal{H})$. Moreover, their normal traces vanish on $\partial\mathcal{H}$, since on a face F either $\mathbf{e}_i \perp \mathbf{n}_F$ or the integrated Legendre polynomial is evaluated at ± 1 . Hence, we can choose a set of cell-based functions involving $2p_C^2 + 3p_C$ curl-fields and further $p_C^2 + 3p_C$ linearly independent functions which are linearly independent from the curl-fields. Finally, the set can be further extended by functions

$$L_{i+2}(2x-1) \mathbf{e}_x, \quad L_{j+2}(2y-1) \mathbf{e}_y, \quad L_{k+2}(2z-1) \mathbf{e}_z.$$

Summarizing, we obtain

**Hierarchical $H(\text{div})$ -conforming shape functions on hexahedra
with variable polynomial order $\mathbf{p} = (\{p_{F_m}\}, p_C)$**

Face-based functions

for faces F_m , $m = 1, \dots, 6$ with local face-vertex ordering $F_m = [f_1, f_2, f_3, f_4]$

We define $\lambda_F := \sum_{\alpha=0}^4 \lambda_{f_\alpha}$ and $(\xi_F, \eta_F) := (\sigma_{f_1} - \sigma_{f_2}, \sigma_{f_1} - \sigma_{f_4})$.

Lowest-order Raviart-Thomas \mathcal{RT}_0 function

$$\boldsymbol{\psi}_m^{\mathcal{RT}_0} = -\nabla \lambda_F \lambda_F$$

Higher-order face-based functions (divergence-free)

for $0 \leq i, j \leq p_{F_m} - 1$

$$\begin{aligned} \boldsymbol{\psi}_{(i,j)}^{F_m} &= \text{curl} \boldsymbol{\varphi}_{(i,j)}^{F_m,2} = \text{curl} \left((\nabla L_{i+2}(\xi_F) L_{j+2}(\eta_F) - L_{i+2}(\xi_F) \nabla L_{j+2}(\eta_F)) \lambda_F \right) \\ \boldsymbol{\psi}_{p_{F_m}+(0,j)}^{F_m} &= \text{curl} \boldsymbol{\varphi}_{(0,j)}^{F_m,3} = \text{curl} \left(L_{j+2}(\eta_F) \lambda_F \nabla \xi_F \right) \\ \boldsymbol{\psi}_{p_{F_m}+(i,0)}^{F_m} &= \text{curl} \boldsymbol{\varphi}_{(i,0)}^{F_m,3} = \text{curl} \left(L_{i+2}(\xi_F) \lambda_F \nabla \xi_F \right) \end{aligned}$$

Cell-based functions $(\xi, \eta, \zeta) := (2x - 1, 2y - 1, 2z - 1)$.

for $0 \leq i, j, k \leq p_C - 1$

Type 1: (divergence-free)

$$\begin{aligned} \psi_{(i,j,k)}^{C,1} &= \text{curl } \varphi_{(i,j,k)}^{C,2} &= 4L_{i+2}(\xi) \ell_k(\eta) \ell_k(\zeta) \mathbf{e}_x - 4\ell_i(\xi) \ell_j(\eta) L_{k+2}(\zeta) \mathbf{e}_z \\ \psi_{\mathbf{p}_C+(i,j,k)}^{C,1} &= \text{curl } \varphi_{\mathbf{p}_C+(i,j,k)}^{C,2} &= 4\ell_i(\xi) L_{j+2}(\eta) \ell_k(\zeta) \mathbf{e}_y - 4\ell_i(\xi) \ell_j(\eta) L_{k+2}(\zeta) \mathbf{e}_z \\ \psi_{2\mathbf{p}_C+(0,j,k)}^{C,1} &= \text{curl } \varphi_{(0,j,k)}^{C,3} &= 2L_{j+2}(\eta) \ell_{k+1}(\zeta) \mathbf{e}_y - 2\ell_{j+1}(\eta) L_{k+2}(\zeta) \mathbf{e}_z \\ \psi_{2\mathbf{p}_C^l+(i,0,k)}^{C,1} &= \text{curl } \varphi_{(i,0,k)}^{C,3} &= 2\ell_{i+1}(\xi) L_{k+2}(\zeta) \mathbf{e}_z - 2L_{i+2}(\xi) \ell_{k+1}(\zeta) \mathbf{e}_x \\ \psi_{2\mathbf{p}_C+(i,j,0)}^{C,1} &= \text{curl } \varphi_{(i,j,0)}^{C,3} &= 2L_{i+2}(\xi) \ell_{j+1}(\eta) \mathbf{e}_x - 2\ell_{i+1}(\xi) L_{j+2}(\eta) \mathbf{e}_y \end{aligned}$$

Type 2:

$$\begin{aligned} \psi_{(i,j,k)}^{C,2} &= L_{i+2}(\xi) \ell_j(\eta) \ell_k(\zeta) \mathbf{e}_x + \ell_i(\xi) L_{j+2}(\eta) \ell_k(\zeta) \mathbf{e}_y \\ \psi_{\mathbf{p}_C+(0,j,k)}^{C,2} &= L_{j+2}(\eta) \ell_{k+1}(\zeta) \mathbf{e}_y + \ell_{j+1}(\eta) L_{k+2}(\zeta) \mathbf{e}_z \\ \psi_{\mathbf{p}_C+(i,0,k)}^{C,2} &= \ell_{i+1}(\xi) L_{k+2}(\zeta) \mathbf{e}_z + L_{i+2}(\xi) \ell_{k+1}(\zeta) \mathbf{e}_x \\ \psi_{\mathbf{p}_C+(i,j,0)}^{C,2} &= L_{i+2}(\xi) \ell_{j+1}(\eta) \mathbf{e}_x + \ell_{i+1}(\xi) L_{j+2}(\eta) \mathbf{e}_y \end{aligned}$$

Type 3:

$$\begin{aligned} \psi_{(i,0,0)}^{C,3} &= L_{i+2}(\xi) \mathbf{e}_x \\ \psi_{(0,j,0)}^{C,3} &= L_{j+2}(\eta) \mathbf{e}_y \\ \psi_{(0,0,k)}^{C,3} &= L_{k+2}(\zeta) \mathbf{e}_z \end{aligned}$$

We define $Q_{\mathcal{RT}_0}(\mathcal{H}) := \text{span}\{\psi_m^{\mathcal{RT}_0} : 1 \leq m \leq 6\}$ and denote the span of face-based (associated with F_m) and the span of cell-based shape functions by $Q_{\mathbf{p}_{F_m}}^{F_m}(\mathcal{H})$ and $Q_{\mathbf{p}_C}^C(\mathcal{H})$ respectively, and define

$$Q_{\mathbf{p}}(\mathcal{H}) := Q_{\mathcal{RT}_0}(\mathcal{H}) \oplus \bigoplus_{m=1}^6 Q_{\mathbf{p}_{F_m}}^{F_m}(\mathcal{H}) \oplus Q_{\mathbf{p}_C}^C(\mathcal{H}).$$

Theorem 5.13. *The shape functions collected in the above table are linearly independent and $H(\text{div})$ -conforming. Moreover,*

$$\text{curl } V_{\mathbf{p}_{F_m}}^{F_m}(\mathcal{H}) \subset Q_{\mathbf{p}_{F_m}}^{F_m}(\mathcal{H}), \quad \forall m = 1, \dots, 6, \quad \text{and} \quad \text{curl } V_{\mathbf{p}_C}^C(\mathcal{H}) \subset Q_{\mathbf{p}_C}^C(\mathcal{H}).$$

For uniform polynomial order p we obtain an $H(\text{div})$ -conforming basis spanning

$$Q_{\mathbf{p}}(\mathcal{H}) = Q^{p+1,p,p}(\mathcal{H}) \times Q^{p,p+1,p}(\mathcal{H}) \times Q^{p,p,p+1}(\mathcal{H}).$$

Proof. The linear independence of face-based shape functions is implied by their choice as curl-fields of a set of linearly independent functions. Moreover, we already discussed the linear independence of the set of cell-based shape functions. Since the normal traces of the $p_{F_m}^2$ face-based shape functions (including the lowest-order Raviart-Thomas functions) span $Q_{\mathbf{p}_{F_m}}^{p_{F_m}} \times Q_{\mathbf{p}_{F_m}}^{p_{F_m}}(F_m)$, while the cell-based functions have zero tangential trace, we obtain linear independence of all shape functions.

$H(\text{div})$ -conformity is implied by the \mathcal{RT}_0 - F - C -based construction: all shape functions not associated to the face F_m have zero tangential trace on the face. Hence, the normal trace on F_m is only affected by the degrees of freedom associated with the face.

For uniform order p , all shape functions belong to $Q^{p+1,p,p}(\mathcal{H}) \times Q^{p,p+1,p}(\mathcal{H}) \times Q^{p,p,p+1}(\mathcal{H})$ by construction. A comparison of the dimensions of the spaces under considerations completes the proof:

$$\begin{aligned} |Q_p(\mathcal{H})| &= |Q^{\mathcal{RT}}(\mathcal{H})| + 6|Q_p^{Fm}(\mathcal{H})| + |Q_p^C(\mathcal{H})| \\ &= 6 + 6(p^2 + 2p) + 3p^3 + 6p^2 + 3p \\ &= 3(p+2)(p+1)^2 \\ Q^{p+1,p,p}(\mathcal{H}) \times Q^{p,p+1,p}(\mathcal{H}) \times Q^{p,p,p+1}(\mathcal{H}) &= 3(p+2)(p+1)^2 \end{aligned}$$

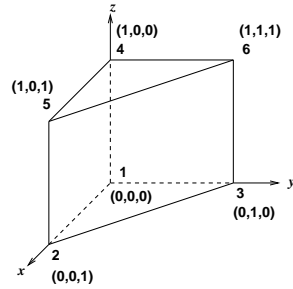
□

5.2.5 The prismatic element

We define the reference prism as the tensor product

$$\mathcal{P} := T \times [0, 1] = \{(x, y, z) : 0 \leq x + y \leq 1, 0 \leq x, y, z \leq 1\}.$$

In this section, we provide a general formulation of shape functions corresponding to this tensor-product representation. We introduce the barycentric coordinates λ_i corresponding to the triangle T and μ_z corresponding to the segment $I_z := [0, 1]$ as follows:



$$\begin{aligned} \lambda_1 &= 1 - x - y, & \mu_1 &= 1 - z, \\ \lambda_2 &= x, & \mu_2 &= 1 - z, \\ \lambda_3 &= y, & \mu_3 &= 1 - z, \\ \lambda_4 &= 1 - x - y, & \mu_4 &= z, \\ \lambda_5 &= x, & \mu_5 &= z, \\ \lambda_6 &= y, & \mu_6 &= z. \end{aligned}$$

The parametrization of horizontal edges and the corresponding tangential vectors are computed as for the tetrahedral element, whereas the parametrization of the vertical edges and the computation of the associated tangential vector follows the construction for the hexahedral element. Thus, the normal component on a quadrilateral face $[f_1, f_2, f_3, f_4]$ can be expressed by

$$\mathbf{n}_F = \frac{1}{2} \nabla \lambda_F \quad (5.28)$$

with $\lambda_F = \lambda_{f_1} + \lambda_{f_2} + \lambda_{f_3} + \lambda_{f_4}$, and on a triangular face $[f_1, f_2, f_3]$ by

$$\mathbf{n}_F = -\nabla \mu_{f_1}. \quad (5.29)$$

Corresponding to the tensor-product domain $\mathcal{P} = T \times [0, 1]$, we introduce the polynomial space,

$$R^{p_1, p_2}(\mathcal{P}) := \{ q_1(x, y) q_2(z) : q_1 \in P^{p_1}(T), q_2 \in Q^{p_2}([0, 1]) \}.$$

The sequence of polynomial spaces – corresponding to the exact sequence (3.14) on the continuous level – we intend to construct, is given by

$$\mathbb{R} \xrightarrow{id} R^{p+1, p+1}(\mathcal{P}) \xrightarrow{\nabla} \begin{pmatrix} R^{p, p+1}(\mathcal{P}) \\ R^{p, p+1}(\mathcal{P}) \\ R^{p+1, p}(\mathcal{P}) \end{pmatrix} \xrightarrow{\text{curl}} \begin{pmatrix} R^{p, p}(\mathcal{P}) \\ R^{p, p}(\mathcal{P}) \\ R^{p-1, p+1}(\mathcal{P}) \end{pmatrix} \xrightarrow{\text{div}} R^{p-1, p}(\mathcal{P}) \xrightarrow{0} \{0\}. \quad (5.30)$$

H^1 -conforming shape functions on the prismatic element \mathcal{P}

As for the previous topologies, we construct the vertex-, edge- and face-based shape functions such that the traces on quadrilateral or triangular faces, respectively, coincide with the cell-based functions of the quadrilateral \mathcal{Q} or the triangle T , respectively. This approach will in particular allow for hybrid meshes and for a locally varying polynomial degree.

On the quadrilateral faces we use linear extension (in terms of μ_i and λ_i) of edge-based shape functions, and on triangular faces we agree on a monomial edge-extension provided by scaled (integrated) Legendre polynomials (in terms of λ_i). The construction of cell-based shape functions is then simple, by considering the tensor-product shape of the prismatic element. Since the cell based shape functions shall span

$$W_{\mathbf{p}_C}^C := \{ q_1(x, y) q_2(z) : q_1(x, y) \in P_0^{p_{C,1}}(T), q_2(z) \in Q_0^{p_{C,2}}([0, 1]) \},$$

with $\mathbf{p}_C := (p_{C,1}, p_{C,2})$, we construct them as products of cell-based triangular shape functions and cell-based shape functions of the segment $I_z = [0, 1]$:

$$\phi_{ijk}^C(x, y, z) = \phi_{ij}^C(x, y) L_{k+2}(z) \quad \text{with } \phi_{ij}^C(x, y) \in W_{\mathbf{p}_C}^C(T), \quad 0 \leq k \leq p_{C,2} - 2.$$

Putting the various sets of shape functions together we get the following representation:

**Hierarchical H^1 -conforming shape functions for prismatic elements
of variable order $\mathbf{p} = (p_{E_m}, p_{F_m}, p_C)$**

Vertex-based functions:

$$\text{for } i = 1, \dots, 6 : \quad \phi_i^V = \lambda_i \mu_i$$

Edge-based functions

for $m = 1, \dots, 6$: *horizontal* edge $E_m = [e_1, e_2]$

$$\text{for } 0 \leq i \leq p_{E_m} - 2 : \quad \phi_i^{E_m} = L_{i+2}^S(\lambda_{e_2} - \lambda_{e_1}, \lambda_{e_1} + \lambda_{e_2}) \mu_{e_1}$$

for $m = 7, 8, 9$: *vertical* edge $E_m = [e_1, e_2]$

$$\text{for } 0 \leq i \leq p_{E_m} - 2 : \quad \phi_i^{E_m} = L_{i+2}^S(2\mu_{e_1} - 1)(\lambda_{e_1} + \lambda_{e_2})$$

Face-based functions

for $m = 1, 2$: *triangular* face $F_m = [f_1, f_2, f_3]$

$$\text{for } 0 \leq i + j \leq p_{F_m} - 3 : \quad \phi_{(i,j)}^{F_m} = L_{i+2}^S(\lambda_{f_1} - \lambda_{f_2}, \lambda_{f_1} + \lambda_{f_2}) \lambda_{f_3} \ell_j (2\lambda_{f_3} - 1) \mu_{f_1}$$

for $m = 3, 4, 5$: *quadrilateral* face $F_m = [f_1, f_2, f_3, f_4]$

$$\text{with horizontal edge } [f_1, f_2^*], \text{ i.e. } f_2^* = \begin{cases} f_2 & \text{if } \mu_{f_1} = \mu_{f_2} \\ f_4 & \text{else} \end{cases}$$

$$\text{for } 0 \leq i, j \leq p_{F_m} - 2 : \quad \phi_{(i,j)}^{F_m} = L_{i+2}^S(\lambda_{f_2^*} - \lambda_{f_1}, \lambda_{f_1} + \lambda_{f_2^*}) L_{j+2}(2\mu_{f_1} - 1)$$

Cell-based functions

for $0 \leq i + j \leq p_C - 3, 0 \leq k \leq p_C - 2$:

$$\phi_{(i,j,k)}^C = L_{i+2}^S(\lambda_1 - \lambda_2, \lambda_1 + \lambda_2) \lambda_3 \ell_j (2\lambda_3 - 1) L_{k+2}(2\mu_1 - 1)$$

We define the lowest-order space as $W^V(\mathcal{P}) := \text{span}((\phi_i^V)_{1 \leq i \leq 6})$ and denote the span of edge-based (associated with E_m) by $W_{E_m}^{pE_m}(\mathcal{P})$, the span of face-based (associated with F_m) functions by $W_{F_m}^{pF_m}(\mathcal{P})$, and the span of cell-based functions by $W_C^{pC}(\mathcal{P})$. The local FE-space spanned by the whole set of shape functions on \mathcal{P} up to order $\mathbf{p} = (\{p_{E_m}\}, \{p_{F_m}\}, p_C)$ is given by

$$W_{\mathbf{p}}(\mathcal{P}) = W^V(\mathcal{P}) \oplus \bigoplus_{m=1}^9 W_{E_m}^{pE_m}(\mathcal{P}) \oplus \bigoplus_{m=1}^5 W_{F_m}^{pF_m}(\mathcal{P}) \oplus W_C^{pC}(\mathcal{P}).$$

Theorem 5.14. *The stated shape functions are H^1 -conforming and linearly independent. For uniform polynomial order p the V - E - F - C -based set of shape functions spans the local FE-space*

$$W_p(\mathcal{P}) = R^{p,p}(\mathcal{P})$$

and in the case of the minimum rule, i.e. $p_{E_m} \leq p_{F_m} \leq p_C$:

$$W_{\mathbf{p}_{\min}}(\mathcal{P}) = \left\{ w \in P^{pC}(\mathcal{P}) \mid \begin{aligned} & \text{tr}_{E_m}(w) \in P_m^{pE_m}(E_m) \forall 1 \leq m \leq 9, \\ & \text{tr}_{F_m}(w) \in P^{pF_m}(F_m) \forall 1 \leq m \leq 2, \\ & \text{tr}_{F_m}(w) \in Q^{p_{F_m}, p_{F_m}}(F_m) \forall 3 \leq m \leq 5 \end{aligned} \right\}.$$

Proof. Vertex-, edge-, face-based shape functions are obtained by linear and monomial extension of H^1 -conforming shape functions on the quadrilateral or the triangular element. The trace of the various functions on the associated face remains unchanged under the extension. Hence, linear independence and the full span of the trace on the associated edges and faces are implied by the considerations for the quadrilateral and triangular elements.

Concerning the *cell-based* shape functions, the construction through tensor-product of cell-based triangular shape functions (having zero tangential trace on all quadrilateral faces) with bubble functions (having zero tangential traces on the remaining triangular faces) in vertical z -direction implies two properties, namely zero tangential trace on $\partial\mathcal{P}$, as well as linear independence within the set of cell-based shape functions.

By the V - E - F - C construction we can easily deduce the linear independence of the whole set of stated shape functions as well as the H^1 -conformity in a similar manner as for the hexahedral element.

Finally, for uniform polynomial order p the counting argument

$$\begin{aligned} |W_p(\mathcal{P})| &= |W^V(\mathcal{P})| + 9|W_p^{E_m}(\mathcal{P})| + \sum_{m=1}^2 |W_p^{F_m}(\mathcal{P})| + \sum_{m=3}^5 |W_p^{F_m}(\mathcal{P})| + |W_p^C(\mathcal{P})| \\ &= 6 + 9(p-1) + (p-2)(p-1) + 3(p-1)^2 + \frac{1}{2}(p-2)(p-1)^2 \\ &= \frac{1}{2}(p+1)^2(p+2), \quad \text{and} \\ |R^{p,p}(\mathcal{P})| &= |P^p(T)| \cdot |Q^p([0,1])| = \frac{1}{2}(p+1)^2(p+2) \end{aligned}$$

completes the proof. □

$H(\text{curl})$ -conforming shape functions on the prismatic element \mathcal{P}

In view of the exact sequence property, we are interested in establishing the following inclusion:

$$W_{p+1}(\mathcal{P}) = R^{p+1,p+1}(\mathcal{P}) \xrightarrow{\nabla} R^{p,p+1}(\mathcal{P}) \times R^{p+1,p}(\mathcal{P}) \times R^{p+1,p} := V_p(\mathcal{P}).$$

Concerning lowest-order shape functions we have to distinguish between horizontal and vertical edges here. The aim is to ensure $\text{tr}_{\tau, E_k}(\varphi_{E_m}^{N_0}) = \delta_{m,k}$, and the extension onto the faces

should coincide with the extension of the lowest-order shape functions on triangular faces of tetrahedra and quadrilateral faces of hexahedra. On horizontal edges $E_m = [e_1, e_2]$ this is provided by

$$\varphi_m^{\mathcal{N}_0} = (\nabla \lambda_{e_1} \lambda_{e_2} - \lambda_{e_1} \nabla \lambda_{e_2}) \mu_{e_1}$$

whereas on vertical edges $E_m = [e_1, e_2]$ we choose

$$\varphi_m^{\mathcal{N}_0} = \lambda_{e_1} \nabla \mu_{e_1}.$$

The *edge-based shape functions* up to order p_{E_m} can be chosen as gradients of H^1 -conforming edge-based shape functions of order $p_{E_m} + 1$.

The *face-based* and *cell-based shape functions* can be defined similarly as in three types of shape functions above.

The following table summarizes $H(\text{curl})$ -conforming shape functions of variable polynomial order:

$H(\text{curl})$-conforming shape functions for prismatic elements of variable polynomial order $p = (\{p_{E_m}\}, p_{F_m}, p_C)$	
<u>Lowest-order Nédélec functions</u>	
for $m=1, \dots, 6$: horizontal edge $E_m = [e_1, e_2]$	$\varphi_m^{\mathcal{N}_0} = (\nabla \lambda_{e_1} \lambda_{e_2} - \lambda_{e_1} \nabla \lambda_{e_2}) \mu_{e_1}$
for $m=7, 8, 9$: vertical edge $E_m = [e_1, e_2]$	$\varphi_m^{\mathcal{N}_0} = \lambda_{e_1} \nabla \mu_{e_1}$
<u>Higher-order edge-based functions</u>	
for $m = 1, \dots, 6$: horizontal edge $E_m = [e_1, e_2]$	
for $0 \leq i \leq p_{E_m} - 1$:	$\varphi_i^{E_m} = \nabla (L_{i+2}^S(\lambda_{e_2} - \lambda_{e_1}, \lambda_{e_1} + \lambda_{e_2}) \mu_{e_1})$
for $m = 7, 8, 9$: vertical edge $E_m = [e_1, e_2]$	
for $0 \leq i \leq p_{E_m} - 1$:	$\varphi_i^{E_m} = \nabla (L_{i+2}(2\mu_E - 1) \lambda_{e_1})$

<u>Face-based functions</u>	
for $m = 1, 2$: triangular face $F_m = [f_1, f_2, f_3]$	
We define	$u_i := L_{i+2}^S(\lambda_{f_2} - \lambda_{f_1}, \lambda_{f_1} + \lambda_{f_2})$ s.t. $\phi_{(i,j)}^{\nabla, F_m} = u_i v_j \mu_{f_1}$.
	$v_j := \lambda_{f_3} \ell_j (2\lambda_{f_3} - 1)$
for $0 \leq i + j \leq p_{F_m} - 2$:	
<u>Type 1:</u> (gradient fields)	$\varphi_{(i,j)}^{F_m, 1} = \nabla (u_i v_j \mu_{f_1})$
<u>Type 2:</u>	$\varphi_{(i,j)}^{F_m, 2} = (\nabla u_i v_j - u_i \nabla v_j) \mu_{f_1}$
<u>Type 3:</u>	$\varphi_{(0,j)}^{F_m, 3} = (\nabla \lambda_{f_1} \lambda_{f_2} - \lambda_{f_1} \nabla \lambda_{f_2}) v_j \mu_{f_1}$
for $m = 3, 4, 5$: quadrilateral face $F_m = [f_1, f_2, f_3, f_4]$ with horizontal edge $[f_1, f_2^*]$,	
i.e. $f_2^* = \begin{cases} f_2 & \text{if } \mu_{f_1} = \mu_{f_2} \\ f_4 & \text{else} \end{cases}$, and $\alpha = \begin{cases} 1 & f_2 = f_2^* \\ -1 & \text{else} \end{cases}$.	
We define	$u_i := L_{i+2}^S(\lambda_{f_2^*} - \lambda_{f_1}, \lambda_{f_1} + \lambda_{f_2^*})$ s.t. $\phi_{(i,j)}^{\nabla, F_m} = u_i w_j$.
	$w_j := L_{j+2}(2\mu_{f_1} - 1)$
for $0 \leq i, j \leq p_{F_m} - 1$:	
<u>Type 1:</u> (gradient fields)	$\varphi_{(i,j)}^{F_m, 1} = \nabla (u_i w_j)$
<u>Type 2:</u>	$\varphi_{(i,j)}^{F_m, 2} = \alpha (\nabla u_i w_j - u_i \nabla w_j)$.
<u>Type 3:</u>	$\varphi_{(0,j)}^{F_m, 3} = (\nabla \lambda_{f_1} \lambda_{f_2^*} - \lambda_{f_1} \nabla \lambda_{f_2^*}) w_j$

Cell-based functions

$$\begin{aligned} \text{We define } u_i &:= L_{i+2}^S(\lambda_2 - \lambda_1, \lambda_1 + \lambda_2) \\ v_j &:= \lambda_3 \ell_j(2\lambda_3 - 1) \\ w_k &:= L_{k+2}(2\mu_1 - 1) \end{aligned}$$

for $0 \leq i + j \leq p_C - 2$, $0 \leq k \leq p_C - 1$:

$$\text{Type 1: (gradient fields)} \quad \varphi_{(i,j,k)}^{C,1} = \nabla(u_i v_j w_k)$$

$$\text{Type 2:} \quad \varphi_{(i,j,k)}^{C,2} = \nabla u_i v_j w_k$$

$$\varphi_{\mathbf{p}_C+(i,j,k)}^{C,2} = u_i \nabla v_j w_k$$

$$\text{Type 3:} \quad \varphi_{(i,j,0)}^{C,3} = u_i v_j \mathbf{e}_z$$

$$\varphi_{(0,j,k)}^{C,3} = (\nabla \lambda_1 \lambda_2 - \lambda_1 \nabla \lambda_2) v_j w_k$$

We define the lowest-order space as $V^{\mathcal{N}_0}(\mathcal{P}) := \text{span}((\varphi_m^{\mathcal{N}_0})_{1 \leq m \leq 9})$, and denote the span of edge-based associated with E_m by $V_{E_m}^{PE_m}(\mathcal{P})$, the span of face-based functions associated with the face F_m by $V_{F_m}^{PF_m}(\mathcal{P})$, and the span of cell-based functions by $V_C^{PC}(\mathcal{P})$. The local FE-space spanned by the whole set of shape functions on \mathcal{P} , up to order $\mathbf{p} = (\{p_{E_m}\}, \{p_{F_m}\}, p_C)$ is denoted by

$$V_{\mathbf{p}}(\mathcal{P}) := V_{\mathcal{N}_0}(\mathcal{P}) \oplus \bigoplus_{m=1}^9 V_{E_m}^{PE_m}(\mathcal{P}) \oplus \bigoplus_{m=1}^5 V_{F_m}^{PF_m}(\mathcal{P}) \oplus V_C^{PC}(\mathcal{P}).$$

Theorem 5.15. *The basis functions defined above are linearly independent and $H(\text{curl})$ -conforming. There holds*

$$\begin{aligned} \nabla W_{\mathbf{p}_{E_m}+1}^{E_m}(\mathcal{P}) \subset V_{\mathbf{p}_{E_m}}^{E_m}(\mathcal{P}) \text{ for } m = 1, \dots, 9, \quad \nabla W_{\mathbf{p}_{F_m}+1}^{F_m}(\mathcal{P}) \subset V_{\mathbf{p}_{F_m}}^{F_m}(\mathcal{P}) \text{ for } m = 1, \dots, 5, \\ \text{and } \nabla W_{\mathbf{p}_C+1}^C(\mathcal{P}) \subset V_{\mathbf{p}_C}^C(\mathcal{P}). \end{aligned}$$

Moreover, for uniform polynomial order p the set of shape functions span

$$V_p(\mathcal{P}) = R^{p,p+1}(\mathcal{P}) \times R^{p,p+1}(\mathcal{P}) \times R^{p+1,p}(\mathcal{P}).$$

Proof. We already verified the linear independence of the set of edge-based shape functions as well as of the set of face-based shape functions. It remains to show linear independence of the cell-based shape functions. Due to the tensor-product-based construction this can be deduced from the linear independence of the H^1 -conforming and $H(\text{curl})$ -conforming shape functions for the triangular element as follows.

First, we consider the functions in $M_1 = \{\nabla u_i v_j w_k, u_i \nabla v_j w_k \nabla w_k + (\nabla \lambda_1 \lambda_2 - \lambda_1 \nabla \lambda_2) w_k\}$, which are built as products of $H(\text{curl})$ -conforming cell-based triangular shape functions $\varphi_{ij}^T(x, y)$ of Theorem 5.6 and linearly independent functions $w_k(z)$. Hence, we obtain linear independence of the functions in M_1 .

Next consider the set $M_2 = \{u_i v_j \nabla w_k = u_i v_j w'_k \mathbf{e}_z, u_i v_j \mathbf{e}_z\}$, which again consists of linearly independent functions due to the tensor-product construction, and the linear independence of $u_i v_j$, cf. Theorem 5.6. Since $\mathbf{e}_z \cdot \varphi = 0$ for $\varphi \in M_1$, we obtain linear independence of the functions

$$\{u_i v_j \nabla w_k, u_i \nabla v_j w_k, \nabla u_i v_j w_k, \phi_{[1,2]}^{\mathcal{N}_0}(x, y) w_k, u_i v_j \mathbf{e}_z, \}$$

which have vanishing tangential trace on ∂P . This implies the linear independence of the complete set of cell-based shape functions.

Thanks to the \mathcal{N}_0 - E - F - C -based construction, linear independence of all shape functions as well as the $H(\text{curl})$ -conformity follows. Moreover, for uniform polynomial order we conclude again with a simple counting argument:

$$\begin{aligned} |V_p(\mathcal{P})| &= 9(p+1) + 2(p+1)(p-1) + 3(2p^2 + 2p) \\ &\quad + \frac{3}{2}(p+1)p(p-1) \\ &= \frac{1}{2}(p+1)(p+2)(3p+7), \quad \text{and} \\ |(R^{p,p+1} \times R^{p,p+1} \times R^{p+1,p})(\mathcal{P})| &= (p+1)(p+2)^2 + \frac{1}{2}(p+1)(p+2)(p+3) \\ &= \frac{1}{2}(p+1)(p+2)(3p+7). \end{aligned}$$

□

Remark 5.16. *In the case of the minimum order rule, i.e., $p_{E_m} \leq p_{F_m} \leq p_C$, the shape functions span the following local FE-space*

$$\begin{aligned} V_{\mathbf{p}_{\min}}(\mathcal{P}) = \{ \mathbf{v} \in X^{p_C}(\mathcal{P}) \mid & \text{tr}_{\tau, E_m}(\mathbf{v}) \in P^{p_{E_m}}(E_m) \quad \forall 1 \leq m \leq 9, \\ & \text{tr}_{\tau, F_m}(\mathbf{v}) \in (P^{p_{F_m}}(F_m))^2 \quad \forall 1 \leq m \leq 2, \\ & \text{tr}_{\tau, F_m}(\mathbf{v}) \in (Q^{p_{F_m}, p_{F_m}+1} \times Q^{p_{F_m}+1, p_{F_m}})(F_m) \quad \forall 3 \leq m \leq 5 \}, \end{aligned}$$

with $X^p(\mathcal{P}) := R^{p,p+1}(\mathcal{P}) \times R^{p,p+1}(\mathcal{P}) \times R^{p+1,p}(\mathcal{P})$.

$H(\text{div})$ -conforming shape functions for the prismatic element \mathcal{P}

Similarly to the previous cases, the lowest order Raviart-Thomas shape functions can be chosen as lowest order shape functions by linear extension of the element normal vector into the interior of the element:

$$\begin{aligned} \psi_m^{\mathcal{RT}_0} &= \mu_{f_1} \mathbf{n} = -\nabla \mu_{f_1} \mu_{f_1} \quad \text{for triangular faces and} \\ \psi_m^{\mathcal{RT}_0} &= \frac{1}{2} \lambda_F \mathbf{n} = -\frac{1}{4} \nabla \lambda_F \lambda_F \quad \text{for quadrilateral faces,} \end{aligned}$$

due to the representation of the normal vector stated in (5.28) and (5.29).

The *higher-order face-based* shape functions can be chosen as the curl-fields of the set of $H(\text{curl})$ -conforming face-based shape functions of $V_{p_{F_m}+1}^{F_m}(\mathcal{P})$ which are linearly independent from gradient functions. Since $c_1 \text{curl}_F(\mathbf{q}_1) + c_2 \text{curl}_F(\mathbf{q}_2) = 0$ implies $\exists \phi$ s.t. $c_1 \mathbf{q}_1 + c_2 \mathbf{q}_2 + \nabla \phi = 0$, the linear independence of the proposed curl-field shape functions follows directly from the linear independence of the $H(\text{curl})$ -conforming shape functions, and their linear independence from the gradient fields. Moreover, the normal trace of the constructed functions span $Q^{p_{F_m}}(F_m)/\mathbb{R}$ on quadrilateral faces, and $P^{p_{F_m}}(F_m)/\mathbb{R}$ on triangular faces, respectively, which can be seen by a comparison of the dimension of the involved spaces.

The first set of *cell-based* functions is provided by the curl-fields of $H(\text{curl})$ -conforming shape functions. Considering the terms involved by these curl-fields in more detail, we can extract the following linearly independent cell-based shape functions, which are already extended to span the full set of cell-based functions.

Lemma 5.17. *Let $u_i = u_i(x, y) := L_{i+2}^S(\lambda_2 - \lambda_1, \lambda_1 + \lambda_2)$, $v_j = v_j(y) := \lambda_3 \ell_j(2\lambda_3 - 1)$, $w_k = w_k(z) := L_{k+2}(2\mu_1 - 1)$ and $\mathcal{N}_0(x, y) := \nabla \lambda_1 \lambda_2 - \nabla \lambda_2 \lambda_1$, and let us define the following*

sets of polynomials:

$$\begin{aligned} M_1 &:= \{ \nabla u_i \times \nabla v_j w_k, \operatorname{curl}(\mathcal{N}_0(\lambda_1, \lambda_2)v_j)w_k, \mathbf{e}_z w_k \}_{0 \leq i+j \leq p, 0 \leq i, j, k \leq p} \\ &= \{ \operatorname{curl}_{(x,y)}(u_i \nabla_{(x,y)} v_j) w_k \mathbf{e}_z, \operatorname{curl}_{(x,y)}(\varphi_{[1,2]}^{\mathcal{N}_0}(x, y) v_j) w_k \mathbf{e}_z, w_k \mathbf{e}_z \} \\ &\quad \text{with } \varphi_{[1,2]}^{\mathcal{N}_0}(x, y) := \nabla_{(x,y)} \lambda_1 \lambda_2 - \nabla_{(x,y)} \lambda_1 \lambda_2, \end{aligned}$$

$$M_2 := \{ \nabla w_k \times \nabla u_i v_j, \mathcal{N}_0(\lambda_1, \lambda_2) \times \nabla w_k v_j, \mathbf{e}_z \times \nabla u_i v_j, \mathcal{N}_0(\lambda_1, \lambda_2) \times \mathbf{e}_z v_j \}_{0 \leq i+j \leq p-2, k \leq p-1},$$

$$\begin{aligned} M_3 &:= \{ \nabla w_k \times \nabla v_j u_i, \nabla v_j \times \mathbf{e}_z u_i \}_{0 \leq i+j \leq p-2, k \leq p-1} \\ &= \{ w'_k(z) v'_j(y) u_i \mathbf{e}_x, v'_j(y) \mathbf{e}_x \}, \end{aligned}$$

The union of $M_1 \cup M_2 \cup M_3$ defines a set of linearly independent vector-fields with vanishing normal trace on $\partial\mathcal{P}$. Moreover, there holds

$$(P^p(\mathcal{P}))^3 \cap H_0(\operatorname{div}, \mathcal{P}) = \operatorname{span} M_1 \oplus \operatorname{span} M_2 \oplus \operatorname{span} M_3.$$

Proof. Due to the inclusion in $(P^p(\mathcal{P}))^3$ as well as the vanishing of tangential traces on $\partial\mathcal{P}$, we only show linear independence of $M_1 \cup M_2 \cup M_3$.

1. First, we show linear independence of functions in M_1 : Since these functions are constructed as the products of curl-fields of $H(\operatorname{curl})$ -conforming triangular-face shape functions, whose linear independence we had proved in the course of the construction of face-based shape functions, and a set of linearly independent functions in the z -component, their linear independence follows directly.
2. The functions of M_3 are linearly independent by construction.
3. Multiplying the vector fields of M_3 with \mathbf{e}_y yields (informally written) $\{\partial_x u_i, (1-y)\} \cdot \{w'_k, 1\} \cdot v_j$ yielding linear independence.
4. We observe that the vector-fields from each set M_i are linearly independent, when restricted to the i -th component. Hence, we obtain the linear independence of $M_1 \cup M_2 \cup M_3$.

Observing that $\dim(M_1) + \dim(M_2) + \dim(M_3) = \frac{1}{2}(3p^2 - 2)(p+1) = \dim(\mathbf{P}_{0,\tau}^p(\mathcal{P}))$ completes the proof. \square

**Hierarchical $H(\operatorname{div})$ -conforming shape functions for prismatic elements
of variable order $p = (p_{F_m}, p_C)$**

Lowest-order Raviart-Thomas functions

for $m = 1, 2$: triangular face $F_m = [f_1, f_2, f_3]$:

$$\psi_m^{\mathcal{RT}_0} = -\nabla \mu_{f_1} \mu_{f_1}$$

for $m = 3, \dots, 5$: quadrilateral face $F_m = [f_1, f_2, f_3]$:

Set $\lambda_F = \sum_{i=1}^4 \lambda_{f_i}$.

$$\psi_m^{\mathcal{RT}_0} = -\frac{1}{4} \nabla \lambda_F \lambda_F$$

Face-based functions (*div-free*)

for $m = 1, 2$: *triangular face* $F_m = [f_1, f_2, f_3]$

$$\begin{aligned} \text{We define } u_i &:= L_{i+2}^S(\lambda_{f_2} - \lambda_{f_1}, \lambda_{f_1} + \lambda_{f_2}) & \text{s.t. } \phi_{(i,j)}^{\nabla, F_m} &= u_i v_j. \\ v_j &:= \lambda_{f_3} \ell_j (2\lambda_{f_3} - 1) \mu_{f_1} \end{aligned}$$

for $0 \leq i + j \leq p_{F_m} - 2$:

$$\begin{aligned} \psi_{(i,j)}^{F_m} &= \text{curl } \varphi_{(i,j)}^{\text{curl}, (F_m, 2)} = 2\nabla v_j \times \nabla u_i \\ \psi_{\mathbf{p}_{F_m} + (0,j)}^{F_m, 1} &= \text{curl } \varphi_{\mathbf{p}_{F_m} + (0,j)}^{\text{curl}, (F_m, 3)} = \nabla v_j \times (\nabla \lambda_{f_1} \lambda_{f_2} - \nabla \lambda_{f_2} \lambda_{f_1}) + 2\nabla \lambda_{f_2} \times \nabla \lambda_{f_1} v_j \end{aligned}$$

for $m = 3, 4, 5$: *quadrilateral face* $F_m = [f_1, f_2, f_3, f_4]$ with horizontal edge $[f_1, f_2^*]$,

$$\text{i.e. } f_2^* = \begin{cases} f_2 & \text{if } \mu_{f_1} = \mu_{f_2} \\ f_4 & \text{else} \end{cases}, \text{ and } \alpha = \begin{cases} 1 & f_2 = f_2^* \\ -1 & \text{else} \end{cases}.$$

$$\begin{aligned} \text{We define } u_i &:= L_{i+2}^S(\lambda_{f_2^*} - \lambda_{f_1}, \lambda_{f_1} + \lambda_{f_2^*}) & \text{s.t. } \phi_{(i,j)}^{\nabla, F_m} &= u_i v_j. \\ w_k &:= L_{k+2}(2\mu_{f_1} - 1) \end{aligned}$$

for $0 \leq i, k \leq p_{F_m} - 1$:

$$\begin{aligned} \psi_{(i,k)}^{F_m} &= \text{curl } \varphi_{(i,k)}^{\text{curl}, (F_m, 2)} = 2\alpha \nabla w_k \times \nabla u_i \\ \psi_{\mathbf{p}_{F_m} + (0,j)}^{F_m} &= \text{curl } \varphi_{(0,j)}^{\text{curl}, (F_m, 3)} = \text{curl}((\nabla \lambda_{f_1} \lambda_{f_2^*} - \lambda_{f_1} \nabla \lambda_{f_2^*}) L_{k+2}(2\mu_{f_1} - 1)) \end{aligned}$$

Cell-based functions

$$\begin{aligned} \text{We define } u_i &:= L_{i+2}^S(\lambda_2 - \lambda_1, \lambda_1 + \lambda_2) & \text{s.t. } \phi_{(i,j,k)}^{\nabla, C} &= u_i v_j w_k. \\ v_j &:= \lambda_3 \ell_j (2\lambda_3 - 1) \\ w_k &:= L_{k+2}(2\mu_1 - 1) \end{aligned}$$

for $0 \leq i + j \leq p_C - 2, 0 \leq k \leq p_C - 1$

$$\begin{aligned} \underline{\text{Type 1: (div-free)}} \quad \psi_{(i,j,k)}^{C,1} &= \text{curl } \varphi_{(i,j,k)}^{\text{curl}, (C,1)} = \nabla w_k \times \nabla u_i v_j - \nabla u_i \times \nabla v_j w_k \\ \psi_{\mathbf{p}_C + (i,j,k)}^{C,1} &= \text{curl } \varphi_{(i,j,k)}^{\text{curl}, (C,2)} = \nabla u_i \times \nabla v_j w_k - \nabla v_j \times \nabla w_k u_i \\ \psi_{2\mathbf{p}_C + (0,j,k)}^{C,1} &= \text{curl } \varphi_{(0,j,k)}^{\text{curl}, (C,3)} = 2v_j w_k \mathbf{e}_z - \mathcal{N}_0(\lambda_1, \lambda_2) \times \nabla(v_j w_k) \\ \psi_{2\mathbf{p}_C + (i,j,0)}^{C,1} &= \text{curl } \varphi_{(i,j,0)}^{\text{curl}, (C,3)} = \nabla(u_i v_j) \times \mathbf{e}_z \end{aligned}$$

$$\begin{aligned} \underline{\text{Type 2:}} \quad \psi_{(i,j,k)}^{C,2} &= \nabla u_i \times \nabla v_j w_k \\ \psi_{\mathbf{p}_C + (0,j,k)}^{C,2} &= \mathcal{N}_0(\lambda_1, \lambda_2) \times \nabla v_j w_k \\ \psi_{\mathbf{p}_C + (i,j,0)}^{C,2} &= \nabla u_i \times \mathbf{e}_z v_j \end{aligned}$$

$$\begin{aligned} \underline{\text{Type 3:}} \quad \psi_{(0,0,k)}^{C,3} &= w_k \mathbf{e}_z \\ \psi_{(0,j,0)}^{C,3} &= \mathcal{N}_0(x, y) \times \mathbf{e}_z v_j \end{aligned}$$

with $\mathcal{N}_0(\lambda_1, \lambda_2) := (\nabla \lambda_1 \lambda_2 - \lambda_1 \nabla \lambda_2)$.

We define the lowest-order space as $Q_{\mathcal{RT}_0}(\mathcal{P}) := \text{span}((\psi_m^{\mathcal{RT}_0})_{1 \leq m \leq 5})$, and denote the span of face-based functions associated with F_m by $Q_{F_m}^{p_{F_m}}(\mathcal{P})$, and the span of cell-based functions by $Q_C^{p_{F_m}}(\mathcal{P})$. The local FE-element space is given by

$$Q_{\mathcal{P}}(\mathcal{P}) := Q_{\mathcal{RT}_0}(\mathcal{P}) \oplus \bigoplus_{m=1}^5 Q_{F_m}^{p_{F_m}}(\mathcal{P}) \oplus Q_C^{p_{F_m}}(\mathcal{P}).$$

Theorem 5.18. *The set of shape functions defined above is linearly independent and $H(\text{div})$ -conforming. For uniform polynomial order p the shape functions are a basis of the local*

FE-space

$$Q_p = R^{p,p}(\mathcal{P}) \times R^{p,p}(\mathcal{P}) \times R^{p-1,p+1}(\mathcal{P}).$$

Proof. The linear independence of lower- and higher-order face based functions, which span either $Q^{p_{F_m}+1,p_{F_m}} \times Q^{p_{F_m},p_{F_m}+1}(F_m)$ if F_m is a quadrilateral or $P^{p_{F_m}}(F_m)$ if F_m is a triangular face, has already been shown.

Since the cell-based shape functions are linearly independent combinations of linearly independent polynomial vector fields, cf. Lemma 5.17, also the set of cell-based functions is linearly independent.

The \mathcal{RT}_0 - F - C -based construction implies the linear independence of all shape functions as well as their $H(\text{div})$ -conformity.

In case of uniform polynomial order p a comparison of the dimension of the involved spaces

$$\begin{aligned} |Q_p(\mathcal{P})| &= 5 + 2\left(\frac{1}{2}(p-1)(p+2)\right) + 3(p^2 + 2p) + \frac{1}{2}(3p^2 - 2)(p+1) \\ |(R^{p,p}(\mathcal{P}))^2 \times R^{p-1,p+1}(\mathcal{P})| &= (p+1)^2(p+2) + \frac{1}{2}p(p+1)(p+2) = \frac{1}{2}(p+1)(p+2)(3p+2) \end{aligned}$$

completes the proof. \square

Remark 5.19. *In the case of the minimum order rule, i.e. $p_{E_m} \leq p_{F_m} \leq p_C$, the shape functions span the following local FE-space*

$$\begin{aligned} V_{\mathbf{p}_{min}}(\mathcal{P}) = \{ \mathbf{v} \in X^{p_C}(\mathcal{P}) \mid & \text{tr}_{\mathbf{n},F_m}(\mathbf{v}) \in (P^{p_{F_m}-1}(F_m))^2 \quad \forall 1 \leq m \leq 2, \\ & \text{tr}_{\mathbf{n},F_m}(\mathbf{v}) \in (Q^{p_{F_m}+1,p_{F_m}} \times Q^{p_{F_m},p_{F_m}+1})(F_m) \quad \forall 3 \leq m \leq 5 \}, \end{aligned}$$

with $X^{p_C}(\mathcal{P}) := R^{p_C,p_C}(\mathcal{P}) \times R^{p_C,p_C}(\mathcal{P}) \times R^{p_C-1,p_C+1}(\mathcal{P})$.

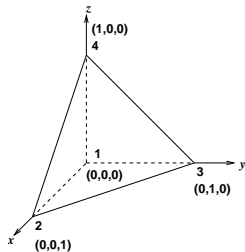
In the end, we now consider the tetrahedron.

5.2.6 The tetrahedral element

We define the reference tetrahedron as

$$\mathcal{T} = \{ (x, y, z) \mid x, y, z \geq 0, 0 \leq x + y + z \leq 1 \},$$

which is the convex hull of the four vertices $V_1 = (0, 0, 0)$, $V_2 = (1, 0, 0)$, $V_3 = (0, 1, 0)$, and $V_4 = (1, 1, 1)$. Similarly as for the triangle, the shape functions can be formulated in terms of the barycentric coordinates λ_i , which are defined as follows:



$$\begin{aligned} \lambda_1 &= 1 - x - y - z, \\ \lambda_2 &= x, \\ \lambda_3 &= y, \\ \lambda_4 &= z. \end{aligned}$$

The outer normal vector on the face $F_m = [f_1, f_2, f_3]$ is given by

$$\mathbf{n}_{F_m} = -\nabla \lambda_o = \nabla \lambda_F \quad \text{with } \lambda_F := \lambda_1 + \lambda_2 + \lambda_3,$$

where λ_o is the coordinate corresponding to the vertex opposite to the face F_m .

To obtain a tensorial basis also for tetrahedral elements, we utilize the 3-dimensional version of the Duffy transformation, i.e.,

$$\mathcal{D} : \begin{array}{ccc} \mathcal{H} & \rightarrow & \mathcal{T} \\ (\xi, \eta, \zeta) & \mapsto & (x, y, z) \end{array} \quad \text{with} \quad \begin{array}{l} x = \frac{1}{8}(1 + \xi)(1 - \eta)(1 - \zeta) \\ y = \frac{1}{4}(1 + \eta)(1 - \zeta) \\ z = \frac{1}{2}(1 + \zeta) \end{array} .$$

The tetrahedron \mathcal{T} is then interpreted as a collapsed hexahedron \mathcal{H} . The inverse map is given by

$$\begin{aligned} \xi &= 2 \frac{x}{1-y-z} - 1 = \frac{\lambda_2 - \lambda_1}{\lambda_2 + \lambda_1} && \in [-1, 1], \\ \eta &= 2 \frac{y}{1-z} - 1 = \frac{2\lambda_3 - (1 - \lambda_4)}{1 - \lambda_4} = \frac{\lambda_3 - (\lambda_1 + \lambda_2)}{\lambda_1 + \lambda_2 + \lambda_3} && \in [-1, 1], \\ \zeta &= 2z - 1 = 2\lambda_4 - 1, && \in [-1, 1]. \end{aligned}$$

We only mention that in KARNIADAKIS-SHERWIN [60] the collapsing procedure is done stepwise from the hexahedra to a prism, then to a pyramid, and finally to the tetrahedron by succesively applying the 2-dimensional Duffy transformation (quadrilaterals to triangles).

For the space of FE-shape functions we choose

$$P^p(\mathcal{T}) := \{x^i y^j z^k : 0 \leq i + j + k \leq p, i, j, k \geq 0\}, \quad (5.31)$$

and we set to define the local finite element spaces in such a way that in the case of uniform polynomial order they correspond to the sequence

$$\mathbb{R} \xrightarrow{id} P^{p+1}(\mathcal{T}) \xrightarrow{\nabla} P^p(\mathcal{T}) \xrightarrow{\text{curl}} P^{p-1}(\mathcal{T}) \xrightarrow{\text{div}} P^{p-2}(\mathcal{T}) \xrightarrow{0} \{0\}. \quad (5.32)$$

The H^1 -conforming tetrahedral element

As for the triangle, the *vertex-based* shape functions can be chosen as the barycentric coordinates, i.e., $\phi_i^V = \lambda_i$ for $i = 1, 2, 3, 4$, satisfying $\phi_i^V(V_j) = \delta_{ij}$. As already seen in the low order construction, the vertex functions span $P^1(\mathcal{T})$.

The *edge-based* shape functions associated with $E_m = [e_1, e_2]$ are also chosen similarly as for triangles, i.e.

$$\phi_i^{E_m} = L_{i+2}^S(\lambda_{e_2} - \lambda_{e_1}, \lambda_{e_2} + \lambda_{e_1}) \quad \text{for } 0 \leq i \leq p_{E_m} - 2.$$

This yields $tr_{E_m}(\phi_i^{E_m}) = L_{i+2}(\lambda_{e_2} - \lambda_{e_1}) = L_{i+2}(\xi_E)$, where $\xi_E = \lambda_{e_2} - \lambda_{e_1}$ is the edge-parameterization over the interval $[-1, 1]$. The scaled Legendre-polynomials provide a monomial extension of the edge values into the interior of the tetrahedron by involving a multiplication with $(\lambda_{e_1} + \lambda_{e_2})^{i+2}$. This ensures $\phi_i^{E_m} \in P^{i+2}(\mathcal{T})$, and also guarantees zero tangential traces on all other edges. Moreover, the set of edge-based shape functions spans $P_0^{p_{E_m}}(E_m)$ on the associated edge.

The *face-based* functions are chosen to coincide with the cell-based shape functions of the triangular element T on the face F_m and use an appropriate extension to the domain. In particular, we set

$$\phi_{(i,j)}^{F_m} = L_{i+2}^S(\lambda_{f_1} - \lambda_{f_2}, \lambda_{f_1} + \lambda_{f_2}) \lambda_{f_3} \ell_j^S(2\lambda_{f_3} - \lambda_F, \lambda_F),$$

where we used the face extension parameter $\lambda_F = \lambda_{f_1} + \lambda_{f_2} + \lambda_{f_3}$. This construction immediately implies linear independence and furthermore,

$$\text{span} \{tr_{F_m}(\phi_{(i,j)}^{F_m}) : i + j \leq p_{F_m} - 3, i, j \geq 0\} = P_0^{p_{F_m}}(F_m).$$

Concerning the extension of face values into the interior of the element, the scaled Legendre polynomial provides a monomial extension by λ_F^j (as illustrated in Figure 5.6) as follows:

$$\phi_{(i,j)}^{F_m} = L_{i+2}^S(\lambda_{f_1} - \lambda_{f_2}, \lambda_{f_1} + \lambda_{f_2}) \lambda_{f_3} \ell_j \left(\frac{2\lambda_{f_3} - \lambda_F}{\lambda_F} \right) \lambda_F^j.$$

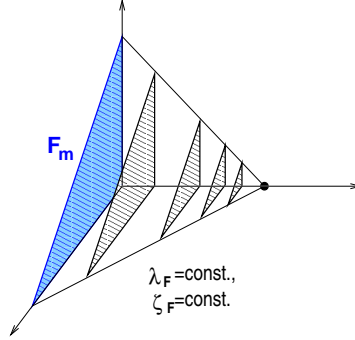


Figure 5.6: Monomial face extension

Finally, we propose *cell-based functions* in collapsed tensor-product-structure of the form

$$\phi_{(i,j,k)}^C(x, y, z) = u_i(x, y, z) v_j(y, z) w_k(z)$$

with factors

$$u_i(x, y, z) := L_{i+2}^S(\lambda_1 - \lambda_2, \lambda_1 + \lambda_2), \quad (5.33a)$$

$$v_j(x, y, z) = v_j(y, z) := \lambda_3 \ell_j^S \left(\frac{2\lambda_3 - (1 - \lambda_4)}{1 - \lambda_4} \right), \quad (5.33b)$$

$$w_k(x, y, z) = w_k(z) := \lambda_4 \ell_k(2\lambda_4 - 1), \quad (5.33c)$$

for $i + j + k \leq p_C - 4$, $0 \leq i, j, k$. In terms of the hexahedral coordinates $(\xi, \eta, \zeta) \in [-1, 1]^3$ (see figure 5.7) this amounts to

$$(u_i \circ \mathcal{D})(\xi, \eta, \zeta) = L_{i+2}(\xi) \left(\frac{1 - \eta}{2} \right)^{i+2} \left(\frac{1 - \zeta}{2} \right)^{i+2}, \quad (5.34a)$$

$$(v_j \circ \mathcal{D})(\xi, \eta, \zeta) = \frac{1 + \eta}{2} \ell_j(\eta) \left(\frac{1 - \zeta}{2} \right)^{j+1}, \quad (5.34b)$$

$$(w_k \circ \mathcal{D})(\xi, \eta, \zeta) = \frac{1 + \zeta}{2} \ell_k(\zeta). \quad (5.34c)$$

The linear independence of the cell-based functions now follows easily, and carries over onto the tetrahedron. Moreover, since there holds $(u_i \circ \mathcal{D})(\pm 1, \eta, \zeta) = 0$, $(v_j \circ \mathcal{D})(\xi, -1, \zeta) = 0$, as well as $(w_k \circ \mathcal{D})(\xi, \eta, -1) = 0$, we obtain vanishing trace on $\partial \mathcal{T}$.

Summarizing, we define the following set of shape functions:

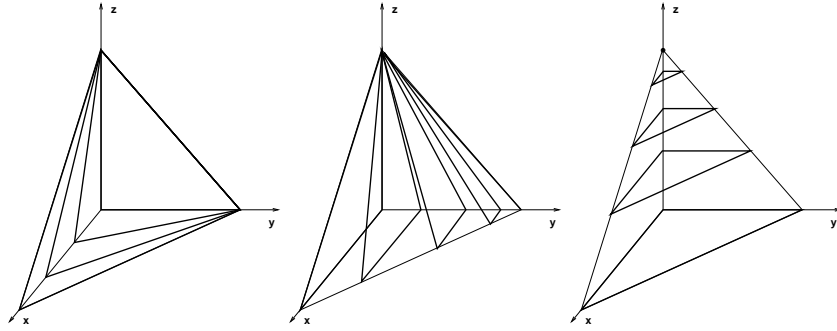


Figure 5.7: Degenerated tensor-product on the tetrahedron: iso-planes where $\xi = \text{const.}$, $\eta = \text{const.}$, or $\zeta = \text{const.}$

H^1 -conforming shape functions for the tetrahedral element \mathcal{T} of variable polynomial order $\mathbf{p} = (\{p_{E_m}\}, \{p_{F_m}\}, p_C)$	
<u>Vertex-based functions:</u>	$\phi_i^V = \lambda_i \quad \text{for } i = 1, 2, 3, 4$
<u>Edge-based functions:</u>	for $m = 1, \dots, 6$: edge $E_m = [e_1, e_2]$ for $0 \leq i \leq p_{E_m} - 2$ $\phi_i^{E_m} = L_{i+2}^S(\lambda_{e_1} - \lambda_{e_2}, \lambda_{e_1} + \lambda_{e_2})$
<u>Face-based functions:</u>	for face $F_m = [f_1, f_2, f_3]$, $m=1, \dots, 4$ We define $\lambda_F := \lambda_{f_1} + \lambda_{f_2} + \lambda_{f_3}$. for $0 \leq i + j \leq p_{F_m} - 3$, $\phi_{(i,j)}^{F_m} = L_{i+1}^S(\lambda_{f_1} - \lambda_{f_2}, \lambda_{f_1} + \lambda_{f_2}) \lambda_{f_3} \ell_j^S(2\lambda_{f_3} - \lambda_F, \lambda_F)$
<u>Cell-based function:</u>	for $0 \leq i + j + k \leq p_C - 4$ $\phi_{(i,j,k)}^C = L_{i+2}^S(\lambda_1 - \lambda_2, \lambda_1 + \lambda_2) \lambda_{f_3} \ell_j^S(2\lambda_3 - (1 - \lambda_4), 1 - \lambda_4) \lambda_{f_4} \ell_k(2\lambda_4 - 1)$

We define the lowest-order space as $W^V(\mathcal{T}) := \text{span}((\phi_i^V)_{1 \leq i \leq 4})$, and denote the span of edge-based functions associated with E_m by $W_{E_m}^{p_{E_m}}(\mathcal{T})$, the span of face-based functions associated with F_m by $W_{F_m}^{p_{F_m}}(\mathcal{T})$, and the span of cell-based functions by $W_C^{p_C}(\mathcal{T})$.

The local FE-space spanned by the whole set of shape functions on \mathcal{T} up to order $\mathbf{p} = (\{p_{E_m}\}, \{p_{F_m}\}, p_C)$ is given by

$$W_{\mathbf{p}}(\mathcal{T}) := W^V(\mathcal{T}) \oplus \bigoplus_{m=1}^6 W_{E_m}^{p_{E_m}}(\mathcal{T}) \oplus \bigoplus_{m=1}^4 W_{F_m}^{p_{F_m}}(\mathcal{T}) \oplus W_C^{p_C}(\mathcal{T}).$$

Theorem 5.20. *The shape functions collected in the table above are linearly independent and*

H^1 -conforming. For uniform polynomial order p , the shape functions span the local FE-space

$$W_p(\mathcal{T}) = P^p(\mathcal{T}).$$

Proof. We have already discussed the linear independence of the set of edge-based, face-based, and of cell-based shape functions. The linear independence of the whole set of shape functions can be verified with similar arguments as in the hexahedral case, i.e., by consecutive consideration of function traces on edges, faces and cells. The same arguments imply the H^1 -conformity. Comparing the dimensions of the involved spaces, namely

$$\begin{aligned} |W_p(\mathcal{T})| &= 4 + 6(p-1) + 2(p-2)(p-1) + \frac{1}{6}(p-3)(p-2)(p-1) \\ &= \frac{1}{6}(p+3)(p+2)(p+1), \quad \text{and} \\ |P^p(\mathcal{T})| &= \frac{1}{6}(p+3)(p+2)(p+1) \end{aligned}$$

implies that $W_p(\mathcal{T}) = P^p(\mathcal{T})$ in case of uniform polynomial order p . \square

Remark 5.21. 1. In the case of the minimum order condition (5.2), the shape functions span the local space

$$W_{p_{\min}}(\mathcal{T}) = \left\{ w \in P^{pc}(\mathcal{T}) \mid \begin{array}{l} \text{tr}_{E_m}(w) \in P_m^{pE_m}(E_m) \quad \forall 1 \leq m \leq 6, \\ \text{tr}_{F_m}(w) \in P^{pF_m}(F_m) \quad \forall 1 \leq m \leq 4 \end{array} \right\}. \quad (5.35)$$

2. The Legendre-type polynomials used in the construction of shape functions can be replaced by other families of orthogonal polynomials, e.g., Jacobi-type polynomials can be used to improve the condition number and sparsity of the resulting FE-matrices. In the case of Jacobi polynomials, the polynomial degrees of the factors are not chosen independently, i.e. one obtains $u_i, v_{(i,j)}, w_{(i,j,k)}$. Still, the construction principle of $H(\text{curl})$ - and $H(\text{div})$ -conforming shape functions, which we present in the following for Legendre-type polynomials carries over also to other classes of polynomials.

The $H(\text{curl})$ -conforming tetrahedral element

Motivated by the previous constructions, we choose for the *lowest-order* edge-based shape functions the lowest-order Nédélec shape functions of the first kind.

The $H(\text{curl})$ -conforming *edge-based* shape functions are chosen as the gradient fields of edge-based H^1 -conforming shape functions up to order $p_{E_m} + 1$. Hence, by Theorem 5.20 we get linear independence and obtain that the tangential traces on the associated edge E_m span $P^{pE_m}(E_m)/\mathbb{R}$, whereas they vanish on all other edges.

The *face-based* shape functions can be derived similarly as for the $H(\text{curl})$ -conforming triangular elements, namely by involving summands of gradient fields of face-based H^1 -conforming functions as follows:

$$\nabla u_i v_j + u_i \nabla v_j, \quad \nabla u_i v_j - u_i \nabla v_j, \quad (\nabla \lambda_{f_1} \lambda_{f_2} - \lambda_{f_1} \nabla \lambda_{f_2}) v_j$$

with $u_i := L_{i+2}^S(\lambda_{f_1} - \lambda_{f_2}, \lambda_{f_1} + \lambda_{f_2})$, $v_j := \lambda_{f_3} \ell_j^S(\lambda_{f_3} - \lambda_F, \lambda_F)$ for $0 \leq i, j, i+j \leq p_{F_m} - 2$. On the associated face $F_m = [f_1, f_2, f_3]$, the tangential traces of these functions coincide with the cell-based $H(\text{curl})$ -conforming shape functions for the triangular element up to order p_{F_m} . Hence, we obtain linear independence of the face-based functions from the corresponding considerations on triangles. Moreover, by construction, the above functions belong to

$(P^{pF_m}(\mathcal{T}))^3$. Their tangential traces span $\mathbf{P}_{\tau,0}^{pF_m}(F_m)$ on the corresponding face, whereas the traces vanish on $F_k \neq F_m$, since there either $u_i = 0$ or $v_j = 0$.

Concerning *cell-based* shape functions, we first consider the gradients of the scalar cell-based shape functions

$$\nabla \phi_{(i,j,k)}^{C,1} = \nabla u_i v_j w_k + u_i \nabla v_j w_k + u_i v_j \nabla w_k \quad 0 \leq i + j + k \leq p_C - 3,$$

where the factors u_i, v_j, w_k are chosen according to (5.33). The set of gradient fields can be enriched in the following way:

Lemma 5.22. *Suppose $u_i := L_{i+2}^S(\lambda_2 - \lambda_1, \lambda_1 + \lambda_2)$, $v_j := \lambda_3 \ell_j^S(2\lambda_3 - (1 - \lambda_{f_4}))$, $w_k := \lambda_4 \ell_k(2\lambda_4 - 1)$, and $\varphi_{[1,2]}^{N_0} = (\nabla \lambda_1 \lambda_2 - \lambda_1 \nabla \lambda_2)$. Then the set*

$$V_p^C(\mathcal{T}) := \text{span}\{\nabla u_i v_j w_k, u_i \nabla v_j w_k, u_i v_j \nabla w_k, \varphi_{[1,2]}^{N_0} v_j w_k : 0 \leq i, j, k, i + j + k \leq p - 3\}$$

contains $\frac{1}{2}(p+1)(p-1)(p-2)$ linearly independent functions in $(P^p(\mathcal{T}))^3$ with vanishing tangential trace on $\partial\mathcal{T}$.

Proof. 1. The trace of u_i as well as the tangential trace $\varphi_{[1,2]}^{N_0}$ vanishes on the faces opposite vertex V_1 and vertex V_2 . Moreover, the trace of v_j vanishes on the face opposite V_3 , and w_k is zero on the face opposite V_4 . Hence, the tangential trace of $\varphi \in V_p^C(\mathcal{T})$ vanishes on the whole of $\partial\mathcal{T}$.

2. We can easily show linear independence by utilizing the tensor-product construction:

(a) The vector fields $\{\varphi_{(i,j,k)} = u_i v_j \nabla w_k\}_{ijk}$ are linearly independent:

Since w_k only depends on z , the linear independence can be deduced analogously to the linear independence of the H^1 -conforming cell-based shape functions.

(b) The vector fields $\{\nabla u_i v_j w_k, u_i \nabla v_j w_k, \varphi_{[1,2]}^{N_0} v_j w_k\}$ are linearly independent: We restrict the vector fields to planes $T_z(\bar{\lambda}_4)$, where $\bar{\lambda}_4$ is constant and hence also w_k is constant. The tangential trace on the triangular faces $T_z(\lambda_4)$ (with $\mathbf{n} = -\nabla \lambda_4$) of the vector fields $\nabla u_i v_j \bar{w}_k$, $\nabla v_j u_i \bar{w}_k$ and $\varphi_{[1,2]}^{N_0} v_j \bar{w}_k$ coincides (up to scaling and a constant) with the cell-based shape functions of the $H(\text{curl})$ -triangular element T . Hence, by Theorem 5.6 and Theorem 5.8, we obtain linear independence of $\nabla u_i v_j \bar{w}_k$, $\nabla v_j u_i \bar{w}_k$ and $\varphi_{[1,2]}^{N_0} v_j \bar{w}_k$ for all i, j .

Considering

$$\tilde{\mathbf{v}} = \sum_{i,j,k} c_{ijk}^1 \nabla u_i v_j w_k + c_{ijk}^2 \nabla v_j u_i w_k + c_{ijk}^4 \varphi_{[1,2]}^{N_0} v_j w_k = 0$$

we obtain by restriction to planes $T_z(\lambda_4)$ that there holds

$$\tilde{c}_{ij}^l = \sum_k c_{ijk}^l w_k = 0 \quad \text{for } l = 1, 2, 4, \forall i, j$$

and for any $\lambda_4 \in (0, 1)$. Due to the linear independence of w_k in the z -component we obtain $c_{ijk}^l = 0$ for $l = 1, 2, 4$.

- (c) Let the trivial function $\mathbf{v} = 0$ be constructed by a combination of basis functions, i.e.,

$$\mathbf{v} = \sum_{i,j,k} c_{ijk}^1 \nabla u_i v_j w_k + c_{ijk}^2 \nabla v_j u_i w_k + c_{ijk}^3 v_j u_i \nabla w_k + c_{jk}^4 \varphi_{[1,2]}^{N_0} v_j w_k = 0.$$

By considering the tangential components of \mathbf{v} on planes $T_z(\lambda_4)$ (where $\nabla_{T_z} w_k = 0$), we obtain $c_{ijk}^l = 0$ for all $l = 1, 2, 4$ due to the linear independence of (b). The remaining part of \mathbf{v} is a linear combination of linearly independent vector fields. Hence, $c_{ijk}^3 = 0$, which implies the overall linear independence. \square

The proposed basis functions are summarized in the following table:

$H(\text{curl})$-conforming shape functions for the tetrahedron \mathcal{T}	
of variable order $\mathbf{p} = (\{p_{E_m}\}, \{p_{F_m}\}, p_C)$	
Edge-based functions	
for $m = 1, \dots, 6$: edge $E_m = [e_1, e_2]$	
<u>Lowest-order Nédélec function:</u>	$\varphi_m^{N_0} = \nabla \lambda_{e_1} \lambda_{e_2} - \lambda_{e_1} \nabla \lambda_{e_2}$
<u>Higher-order edge-based functions (gradient fields):</u>	
for $0 \leq i \leq p_{E_m} - 1$:	$\varphi_i^{E_m} = \nabla (L_{i+2}^S(\lambda_{e_1} - \lambda_{e_2}, \lambda_{e_1} + \lambda_{e_2}))$
Face-based functions	
for $m = 1, \dots, 4$: face $F_m = [f_1, f_2, f_3]$	
We define $u_i := L_{i+2}^S(\lambda_{f_1} - \lambda_{f_2}, \lambda_{f_1} + \lambda_{f_2})$,	s.t. $\phi^{F_m} = u_i v_j$.
$v_j := \lambda_3 \ell_j^S(2\lambda_{f_3} - \lambda_F, \lambda_F)$,	
for $0 \leq i + j \leq p_{F_m} - 2$:	
<u>Type 1 (gradient fields):</u>	$\varphi_{(i,j)}^{F_m,1} = \nabla(u_i v_j)$
<u>Type 2:</u>	$\varphi_{(i,j)}^{F_m,2} = \nabla u_i v_j - u_i \nabla v_j$
<u>Type 3:</u>	$\varphi_{(0,j)}^{F_m,3} = (\nabla \lambda_{f_1} \lambda_{f_2} - \lambda_{f_1} \nabla \lambda_{f_2}) v_j$
Cell-based functions	
We define $u_i := L_{i+2}^S(\lambda_1 - \lambda_2, \lambda_1 + \lambda_2)$,	
$v_j := \lambda_3 \ell_j^S(2\lambda_3 - (1 - \lambda_4), 1 - \lambda_4)$,	s.t. $\phi^{F_m} = u_i v_j w_k$.
$w_k := \lambda_4 \ell_k(2\lambda_4 - 1)$,	
for $0 \leq i + j + k \leq p_C - 3$:	
<u>Type 1 (gradient fields):</u>	$\varphi_{(i,j,k)}^{C,1} = \nabla \phi_{(i,j,k)}^C = \nabla(u_i v_j w_k)$
<u>Type 2:</u>	$\varphi_{(i,j,k)}^{C,2} = \nabla u_i v_j w_k - u_i \nabla v_i w_k + u_i v_j \nabla w_k$
	$\varphi_{\mathbf{p}_C+(i,j,k)}^{C,2} = \nabla u_i v_j w_k + u_i \nabla v_i w_k - u_i v_j \nabla w_k$
<u>Type 3:</u>	$\varphi_{(0,j,k)}^{C,3} = (\nabla \lambda_1 \lambda_2 - \lambda_1 \nabla \lambda_2) v_j w_k$

We define the lowest-order space as $V_{N_0}(\mathcal{T}) := \text{span}((\varphi_m^{N_0})_{1 \leq m \leq 6})$, and denote the span of edge-based functions associated with E_m by $V_{E_m}^{PE_m}(\mathcal{T})$, the span of face-based functions associated with F_m by $V_{F_m}^{PF_m}(\mathcal{T})$, and the span of cell-based functions by $V_C^{PC}(\mathcal{T})$.

The local FE-space spanned by the whole set of shape functions on \mathcal{T} up to order $\mathbf{p} = (\{p_{E_m}\}, \{p_{F_m}\}, p_C)$ is given by

$$V_{\mathbf{p}}(\mathcal{T}) := V_{\mathcal{N}_0}(\mathcal{T}) \oplus \bigoplus_{m=1}^6 V_{E_m}^{p_{E_m}}(\mathcal{T}) \oplus \bigoplus_{m=1}^4 V_{F_m}^{p_{F_m}}(\mathcal{T}) \oplus V_C^{p_C}(\mathcal{T}).$$

Theorem 5.23. *The \mathcal{N}_0 -E-F-C-based shape functions presented in the table above, are linearly independent and $H(\text{curl})$ -conforming. Moreover, they contain gradient fields $\nabla W_{\mathbf{p}+1}(\mathcal{T}) \subset V_{\mathbf{p}}(\mathcal{T})$, i.e.,*

$$\begin{aligned} \nabla W_{p_{E_m}+1}^{E_m}(\mathcal{T}) &= V_{p_{E_m}}^{E_m}(\mathcal{T}) \quad \forall m = 1, \dots, 6, & \nabla W_{p_{F_m}+1}^{F_m}(\mathcal{T}) &\subset V_{p_{F_m}}^{F_m}(\mathcal{T}) \quad \forall m = 1, \dots, 4, \\ \nabla W_{p_C+1}^C(\mathcal{T}) &\subset V_{p_C}^C(\mathcal{T}). \end{aligned}$$

For uniform polynomial order p the shape functions span the local FE-space

$$V_{\mathbf{p}}(\mathcal{T}) = (P^p(\mathcal{T}))^3 \quad \text{with} \quad P^{p+1}(\mathcal{T}) \xrightarrow{\nabla} P^p(\mathcal{T}).$$

Proof. The edge-based shape functions (gradient fields) are linearly independent due to Theorem 5.20. Their tangential traces span $P^{p_{E_m}}(E_m)$ and vanish on all other edges $E_k \neq E_m$. The face-based shape functions are linearly independent and their tangential traces on F_m span $\mathbf{P}_{\tau,0}^{p_{F_m}}(F_m)$ with zero tangential trace on all edges and all faces $F_k \neq F_m$. Due to Lemma 5.22 we obtain linear independence of the cell-based shape functions and the vanishing of their tangential trace on $\partial\mathcal{T}$.

By consecutive consideration of tangential traces on edges and faces we can deduce the linear independence of the whole set of shape functions. The $H(\text{curl})$ -conformity follows with the same arguments.

Finally, for uniform polynomial order p all shape functions belong to $(P^p(\mathcal{T}))^3$ by construction. Comparing the dimensions of the involved spaces, i.e.,

$$\begin{aligned} |V_{\mathbf{p}}(\mathcal{T})| &= 6(p+1) + 4(p-1)(p+1) + \frac{1}{2}(p-2)(p-1)(p+1) = \frac{1}{2}(p+1)(p+2)(p+3) \\ |(P^p(\mathcal{T}))^3| &= \frac{1}{2}(p+1)(p+2)(p+3) \end{aligned}$$

we conclude that the shape functions form a basis for $V_{\mathbf{p}}(\mathcal{T}) = (P^p(\mathcal{T}))^3$. \square

Remark 5.24. *If the minimum order condition (5.2) holds, the stated shape functions span the local space*

$$V_{\mathbf{p}_{\min}}(\mathcal{T}) = \left\{ \mathbf{v} \in (P^{p_C}(\mathcal{T}))^3 \mid \begin{aligned} &tr_{\tau, E_m}(\mathbf{v}) \in P^{p_{E_m}}(E_m) \quad \forall 1 \leq m \leq 6, \\ &tr_{\tau, F_k}(\mathbf{v}) \in (P^{p_{F_k}}(F_k))^2 \quad \forall 1 \leq k \leq 4 \end{aligned} \right\}. \quad (5.36)$$

$H(\text{div})$ -conforming shape functions for tetrahedral elements

We want to construct the local FE-space of order \mathbf{p} in such a way that

$$\text{curl } V_{\mathbf{p}}(\mathcal{T}) \subset Q_{\mathbf{p}}(\mathcal{T}).$$

This requires that the normal trace (on faces) of the local space spans $P^{p_{F_m}-1}(F_m)$, and the cell-based space spans $(P^{p_C-1}(\mathcal{T}))^3 \cap H_0(\text{div}, \mathcal{T})$. In view of the sequence of polynomial spaces (5.32), we choose the FE-space by

$$Q_{\mathbf{p}}(\mathcal{T}) = (P^{p-1}(\mathcal{T}))^3$$

in case of uniform polynomial order p . We remind the reader that the classical definition of the $H(\text{div})$ -conforming local space of order p on the tetrahedral element, coincides with $(P^p(\mathcal{T}))^3$ and corresponds to $Q_{p+1}(\mathcal{T})$ in our notation.

The lowest-order shape functions are provided by the lowest-order Raviart-Thomas functions with constant normal trace on the corresponding face and zero trace normal on all other faces, cf. Lemma 4.18.

The *higher-order face-based* $H(\text{div})$ -conforming shape functions can be chosen as the curl-fields of the face-based $H(\text{curl})$ -conforming shape functions except for gradient fields. This yields $\frac{1}{2}(p_F - 1)(p_F + 2)$ linearly independent shape functions, where the normal traces span $P^{p_{F_m}-1}(F_m)/\mathbb{R}$ on F_m , while vanishing on all other faces.

We choose the curl-fields of $H(\text{curl})$ -conforming cell-based shape functions as subset of the *cell-based* shape functions:

$$\begin{aligned} \text{curl } \varphi_{(i,j,k)}^{C,2} &= 2u_i \nabla v_j \times \nabla w_k - 2\nabla u_i \times \nabla v_j w_k \\ \text{curl } \varphi_{\mathbf{p}_{C^+}(i,j)}^{C,2} &= 2\nabla w_k \times \nabla u_i v_j - 2u_i \nabla v_j \times \nabla w_k \\ \text{curl } \varphi_{(0,j,k)}^{C,3} &= -(\nabla \lambda_1 \lambda_2 - \lambda_1 \nabla \lambda_2) \times \nabla (v_j w_k) - 2\nabla \lambda_1 \times \nabla \lambda_2 v_j w_k \end{aligned}$$

The main properties of these sets of functions are summarized in the following lemma.

Lemma 5.25. *Let $u_i := L_{i+2}^S(\lambda_2 - \lambda_1, \lambda_1 + \lambda_2)$, $v_j := \lambda_3 \ell_j^S(2\lambda_3 - (1 - \lambda_{f_4}))$, $w_k := \lambda_4 \ell_k(2\lambda_4 - 1)$, and $\varphi_{[1,2]}^{N_0} = (\nabla \lambda_1 \lambda_2 - \lambda_1 \nabla \lambda_2)$ and $\psi_{[1,2,3]}^{RT_0} := \lambda_1 \nabla \lambda_2 \times \nabla \lambda_3 + \lambda_2 \nabla \lambda_3 \times \nabla \lambda_1 + \lambda_3 \nabla \lambda_1 \times \nabla \lambda_2$. We use the notation*

$$\begin{aligned} M_1 &:= \{ \nabla u_i \times \nabla v_k w_k, \text{curl}(\psi_{[1,2]}^{N_0} v_j) w_k, \psi_{[1,2,3]}^{RT_0} w_k \mid i, j, k \geq 0, i + j + k \leq p - 3 \} \\ M_2 &:= \{ \nabla w_k \times \nabla u_i v_j, \psi_{[1,2]}^{N_0} \times \nabla w_k v_j \mid i, j, k \geq 0, i + j + k \leq p - 3 \} \\ M_3 &:= \{ \nabla v_j \times \nabla w_k u_i \mid i, j, k \geq 0, i + j + k \leq p - 3 \}. \end{aligned}$$

Then the functions in $M_1 \cup M_2 \cup M_3$ are linearly independent. Moreover, there holds

$$\mathbf{P}_{\mathbf{n},0}^{p-1}(\mathcal{T}) = \text{span}(M_1) \oplus \text{span}(M_2) \oplus \text{span}(M_3).$$

Proof. By construction, all involved functions belong to $\mathbf{P}^p(\mathcal{T})$ and have vanishing normal trace on $\partial\mathcal{T}$. We show linear independence by looking at linear combinations $\mathbf{q} = c_1\psi_1 + c_2\psi_2 + c_3\psi_3 = 0$ with $\psi_i \in M_i$.

1. Restricting \mathbf{q} to the normal trace corresponding to planes T_z where $z = \text{const.}$ yields $tr_{\mathbf{n},T_z}(\mathbf{q}) = c_1 tr_{\mathbf{n},T_z}(\psi_1) = 0$, since $tr_{\mathbf{n},T_z}(\psi_3) = tr_{\mathbf{n},T_z}(\psi_2) = 0$. We observe that up to scaling, the normal traces of the functions in M_1 correspond to the face-based $H(\text{div})$ -conforming shape functions on the triangle/face $[1, 2, 3]$. Since the vector-fields in M_1 are constructed as products of (scaled, but linearly independent) face-based $H(\text{div})$ -conforming shape functions on planes $z = \text{const.}$, and a set of linearly independent polynomials w_k in z , we obtain linear independence of the functions in M_1 . Furthermore, we obtain $c_1 = 0$ in the linear combination of \mathbf{q} .
2. Next, we restrict \mathbf{q} to planes T_η , where $\eta = \text{const.}$ Since there holds $\nabla v_j \times \nabla w_k = 0$ on T_η , we obtain $tr_{\mathbf{n},T_\eta}(\mathbf{q}) = c_2\phi_2 = c_{2,1}\partial_x u_i w'_z + c_{2,2}\varphi_{[1,2]}^{N_0} \cdot \mathbf{e}_x u_i w'_z (1 - z)^j = 0$. Here,

linear independence follows as in the proof of Lemma 5.7 by replacing v_j with w'_k and utilizing the fact that $\partial_x u_i$ is at least linear in x , while $\varphi_{[1,2]}^{\mathcal{N}_0} \cdot \mathbf{e}_x$ is constant in x . Hence, we obtain $c_2 = 0$.

3. We conclude by showing the linear independence of M_3 :

Taking the scalar product with \mathbf{e}_x yields $(\nabla v_j \times \nabla w_k u_i) \cdot \mathbf{e}_x = \partial_y v_j w'_k u_i$. The linear independence can be shown by forming partial derivatives and following the proof of the linear independence of H^1 -conforming cell-based shape functions. Hence, we obtain $c_3=0$.

Since the shape function in $M_1 \cup M_2 \cup M_3$ are linearly independent, counting $\dim(\mathbf{P}_{n,0}^p(\mathcal{T})) = \frac{1}{2}p(p^2 - p - 2)$ concludes the proof. \square

We summarize the shape functions in the following table:

$H(\text{div})$-conforming shape functions for the tetrahedron \mathcal{T} of variable order $\mathbf{p} = (\{p_{F_m}\}, p_C)$	
Face-based functions	
for $m = 1, \dots, 4$ face $F_m = [f_1, f_2, f_3]$	
<u>Raviart-Thomas functions</u>	
$\psi_m^{\mathcal{RT}_0} = \lambda_{f_1} \nabla \lambda_{f_2} \times \nabla \lambda_{f_3} + \lambda_{f_2} \nabla \lambda_{f_3} \times \nabla \lambda_{f_1} + \lambda_{f_3} \nabla \lambda_{f_1} \times \nabla \lambda_{f_2}$	
<u>Higher-order face based functions (divergence-free)</u>	
We define $u_i := L_{i+2}^S(\lambda_{f_1} - \lambda_{f_2}, \lambda_{f_1} + \lambda_{f_2}),$ s.t. $\phi^{\nabla, F_m} = u_i v_j.$	
$v_j := \lambda_3 \ell_j^S(2\lambda_{f_3} - \lambda_F, \lambda_F),$	
for $0 \leq i + j \leq p_{F_m} - 2$	
$\psi_{(i,j)}^{F_m} = \text{curl } \varphi_{(i,j)}^{F_m,2} = -2\nabla u_i \times \nabla v_j$	
$\psi_{\mathbf{p}_{F_m}+(0,j)}^{F_m} = \text{curl } \varphi_{(0,j)}^{F_m,3} = -(\nabla \lambda_{f_1} \lambda_{f_2} - \lambda_{f_1} \nabla \lambda_{f_2}) \times \nabla v_j - 2\nabla \lambda_{f_1} \times \nabla \lambda_{f_2} v_j$	

Cell-based functions	
We define $u_i := L_{i+2}^S(\lambda_1 - \lambda_2, \lambda_1 + \lambda_2),$ s.t. $\phi^{\nabla, F_m} = u_i v_j w_k.$	
$v_j := \lambda_3 \ell_j^S(2\lambda_3 - (1 - \lambda_4), 1 - \lambda_4),$	
$w_k := \lambda_4 \ell_k(2\lambda_4 - 1),$	
for $0 \leq i + j + k \leq p_C - 3$	
<u>Type 1: (div-free)</u>	
$\psi_{(i,j,k)}^{C,1} = \text{curl } \varphi_{(i,j,k)}^{C,2} = 2u_i \nabla v_j \times \nabla w_k - 2\nabla u_i \times \nabla v_j w_k$	
$\psi_{\mathbf{p}_C+(i,j,k)}^{C,1} = \text{curl } \varphi_{\mathbf{p}_C+(i,j)}^{C,2} = 2\nabla w_k \times \nabla u_i v_j - 2u_i \nabla v_j \times \nabla w_k$	
$\psi_{2\mathbf{p}_C+(0,j,k)}^{C,1} = \text{curl } \varphi_{(j,k)}^{C,3}$ <i>rrcl</i>	
$= -(\nabla \lambda_1 \lambda_2 - \lambda_1 \nabla \lambda_2) \times \nabla(v_j w_k) - 2\nabla \lambda_1 \times \nabla \lambda_2 v_j w_k$	

<u>Type 2:</u>	$\psi_{(i,j,k)}^{C,2} = u_i \nabla v_j \times \nabla w_k$
	$\psi_{(0,j,k)}^{C,2} = (\nabla \lambda_1 \lambda_2 - \lambda_1 \nabla \lambda_2) \times \nabla w_k v_j$
<u>Type 3:</u>	$\psi_{(0,0,k)}^{C,3} = \psi_{[1,2,3]}^{\mathcal{RT}_0} w_k$
	with $\psi_{[1,2,3]}^{\mathcal{RT}_0} := \lambda_1 \nabla \lambda_2 \times \nabla \lambda_3 + \lambda_2 \nabla \lambda_3 \times \nabla \lambda_1 + \lambda_3 \nabla \lambda_1 \times \nabla \lambda_2$.

We define the lowest-order space as $Q_{\mathcal{RT}_0}(\mathcal{T}) := \text{span}((\psi_m^{\mathcal{RT}_0})_{1 \leq m \leq 4})$, and denote the span of face-based (associated with F_m) functions by $Q_{F_m}^{p_{F_m}}(\mathcal{T})$, the span of cell-based functions by $Q_C^{p_{F_m}}(\mathcal{T})$ and the local FE-element space by

$$Q_p(\mathcal{T}) := Q_{\mathcal{RT}_0}(\mathcal{T}) \oplus \bigoplus_{m=1}^4 Q_{F_m}^{p_{F_m}}(\mathcal{T}) \oplus Q_C^{p_{F_m}}(\mathcal{T}).$$

Theorem 5.26. *The \mathcal{RT}_0 -F-C-based shape functions listed in the table above, are linearly independent and $H(\text{div})$ -conforming. Moreover, they include gradient fields, i.e.,*

$$\text{curl } V_{p_{F_m}}^{F_m}(\mathcal{T}) \subset Q_{p_{F_m}}^{F_m}(\mathcal{T}) \quad \forall m = 1, \dots, 4 \quad \text{and} \quad \text{curl } V_{p_C}^C(\mathcal{T}) \subset Q_{p_C}^C(\mathcal{T}).$$

For uniform polynomial order p the shape functions span the local FE-space

$$Q_p(\mathcal{T}) = (P^{p-1}(\mathcal{T}))^3 \quad \text{with} \quad P^{p+1}(\mathcal{T}) \xrightarrow{\nabla} P^{p+1}(\mathcal{T}) \xrightarrow{\text{curl}} P^{p-1}(\mathcal{T}).$$

Proof. We already have shown the linear independence of the face-based shape functions, since they are curl-fields of a set of linearly independent functions which are above all linearly independent to gradient fields. In combination with the lowest-order shape functions, their tangential traces span $P^{p_{F_m}-1}(F_m)$ on the associated face F_m , while vanishing on the remaining faces.

The cell-based shape functions are constructed as linearly independent combinations of linearly independent cell-based vector-fields, cf. 5.25. Hence, they are linearly independent and span $P_{0,\mathbf{n}}^{p_C-1}(\mathcal{P})$.

Due to the hierarchical \mathcal{RT}_0 -F-C constructions, we can deduce linear independence of the whole set of shape functions. In the case of uniform polynomial order p , we conclude by counting the dimensions of the involved spaces:

$$|Q_p(\mathcal{T})| = 4 + 2(p-1)(p+2) + \frac{1}{2}p(p^2 - p - 2) = \frac{1}{2}p(p+1)(p+2), \quad \text{and}$$

$$|(P^{p-1}(\mathcal{T}))^3| = \frac{1}{2}p(p+1)(p+2).$$

□

Remark 5.27. *If the minimum order condition (5.2) holds, the shape functions span the local space*

$$Q_{p_{\min}}(\mathcal{T}) = \left\{ \mathbf{q} \in (P^{p_C-1}(\mathcal{T}))^3 \mid \text{tr}_{\mathbf{n}, F_m}(\mathbf{q}) \in P^{p_{F_m}-1}(F_m) \quad \forall 1 \leq m \leq 4 \right\}. \quad (5.37)$$

5.2.7 Nédélec elements of the first kind and other incomplete FE-spaces

In the case of simplicial elements, the presented $H(\text{curl})$ - and $H(\text{div})$ -conforming finite elements are Nédélec elements of second kind or Brezzi-Douglas-Marini elements, respectively. As outlined in Chapter 4, the flux fields of these spaces are approximated with one degree less

than the primal variables. The same approximation order is provided by Nédélec elements of the first kind and Raviart-Thomas-Nédélec elements, respectively.

Due to the explicit usage of differential fields in the construction of basis functions we can easily extend our concepts also to the higher-order Nédélec elements of the first kind and higher-order Raviart-Thomas-Nédélec elements. In the following we shortly summarize some results for the three-dimensional case; the two-dimensional case follows easily then.

We denote the span of $H(\text{curl})$ -conforming face-based shape functions of first, second, and third type associated with the face F_m by $V_{p_{F_m}}^{F_m,1}(K)$, $V_{p_{F_m}}^{F_m,2}(K)$, $V_{p_{F_m}}^{F_m,3}(K)$, and the span of $H(\text{curl})$ -conforming cell-based shape of first, second and third type by $V_{p_C}^{C,1}(K)$, $V_{p_C}^{C,2}(K)$, $V_{p_C}^{C,3}(K)$. The local space of Nédélec element of first kind of order \mathbf{p} is now defined by

$$\begin{aligned} \mathcal{N}_{\mathbf{p}}^I(K) := & V_{\mathcal{N}_0}(K) \oplus \bigoplus_{E_m \in \mathcal{E}_K} V_{p_{E_m}}^{E_m}(K) \oplus \bigoplus_{F_m \in \mathcal{F}_K} V_{p_{F_m}}^{F_m,1}(K) \oplus V_{p_{F_m}+1}^{F_m,2}(K) \oplus V_{p_{F_m}+1}^{F_m,3}(K) \\ & \oplus V_{p_C}^{C,1}(K) \oplus V_{p_C+1}^{C,2}(K) \oplus V_{p_C+1}^{C,3}(K), \end{aligned}$$

and the basis functions are chosen in a similar manner as outlined above.

We note that the reduced spaces do not exactly coincide with the classically defined Nédélec elements of first kind which are rotational invariant. In neither of both cases the resulting FE-basis is orthogonal on the reduced gradient fields. In both variants the spaces of the curl-fields coincide as well as the orders of approximation obtained for the functions and its curl.

Similarly, we denote the span of $H(\text{div})$ -conforming cell-based shape of first, second and third type by $Q_{p_C}^{C,1}(K)$, $Q_{p_C}^{C,2}(K)$, $Q_{p_C}^{C,3}(K)$, and define the local space of the Raviart-Thomas-Nédélec element of order \mathbf{p} as follows:

$$\mathcal{RT}_{\mathbf{p}}(K) := Q_{\mathcal{RT}_0}(K) \oplus \bigoplus_{F_m \in \mathcal{F}_K} Q_{p_{F_m}}^{F_m}(K) \oplus Q_{p_C}^{C,1}(K) \oplus Q_{p_C+1}^{C,2}(K) \oplus Q_{p_C+1}^{C,3}(K).$$

Again the choice of basis functions is very similar to the one outlined in detail above.

In the case of uniform polynomial order p , these definitions are related to the corresponding classical elements, if we take into account that on simplicial elements the classical $H(\text{div})$ -conforming space of order $p \geq 1$ refers to the $H(\text{div})$ -conforming space $p + 1$ in our notation.

Note that since the differential fields are explicitly realized in the FE-basis, we can achieve any order of approximation for the function and for its differential field, separately, by defining incomplete spaces as presented above. For instance, this will be used in gauging strategies in Chapter 6, where we reduce all higher-order gradient shape functions in the $H(\text{curl})$ -conforming FE-basis.

5.2.8 Elements with anisotropic polynomial order distribution

In applications, one may be interesting in highly-anisotropic elements. These arise, e.g., from geometric h -refinement, when handling thin structures within the computational domain or plates and shells. In such cases, there is no need to support full polynomial degree in all directions. Hence, one is interested in allowing variable polynomial order, in particular for tensor-product elements, i.e., on hexahedra and prisms. Since the tensor product structure was explicitly used in the construction the shape functions, such anisotropic polynomial distributions can easily be realized.

First, each quadrilateral face is assigned two polynomial degrees $\mathbf{p}_F = (p_{F,1}, p_{F,2})$, and each hexahedral cell may have three polynomial degrees $\mathbf{p}_C = (p_{C,x}, p_{C,y}, p_{C,z})$. Then the definition of conforming shape functions can easily be extended to anisotropic polynomial order by using different ranges for the indices corresponding to different directions, i.e., $1 \leq i \leq p_{F_1}$, $1 \leq j \leq p_{F_2}$ on quadrilateral faces, and $1 \leq i \leq p_{C_x}$, $1 \leq j \leq p_{C_y}$, $1 \leq k \leq p_{C_z}$ for hexahedral cells. Prismatic elements are treated similarly.

Note that assigning two polynomial degrees $\mathbf{p}_F = (p_{F,1}, p_{F,2})$ to a quadrilateral face, the fixed face orientation establishes automatically the conformity on the global level.

5.3 Global Finite Element Spaces

In this section we show that, based on the local finite element spaces defined on reference elements, the construction of H^1 -, $H(\text{curl})$ -, and $H(\text{div})$ -conforming global finite element spaces on a triangulation \mathcal{T}_h is straightforward. We assume that the triangulation is regular, cf. Section 4.1.2, but may involve a mixture of element topologies, i.e., hexahedra, tetrahedra, and prisms in a three-dimensional setting, respectively quadrilaterals and triangles in the two-dimensional case. We will only treat the three-dimensional case in detail, but the same constructions and results also hold for the simpler two-dimensional case. Moreover, we assume that the element mappings $\Phi_K : \hat{K} \rightarrow K$ satisfy the properties as defined in Section 4.1.4, and utilize the notation introduced there. By restricting ourselves to affine element mappings, the polynomial degree of shape functions is not increased by the mapping to physical coordinates. In the course of this section we mark all quantities concerning the reference element by the hat marker ($\hat{\cdot}$), and use the following notation for local patches:

$$\overline{\omega}_V := \bigcup_{K \in \mathcal{T}_h: V \in \mathcal{V}_K} \overline{K}, \quad \overline{\omega}_E := \bigcup_{K \in \mathcal{T}_h: E \in \mathcal{E}_K} \overline{K}, \quad \overline{\omega}_F := \bigcup_{K \in \mathcal{T}_h: F \in \mathcal{F}_K} \overline{K}, \quad (5.38)$$

which are associated with a vertex $V \in \mathcal{V}$, an edge $E \in \mathcal{E}$, a face $F \in \mathcal{F}$, respectively. Each edge $E \in \mathcal{E}$, face $F \in \mathcal{F}$, and cell $K \in \mathcal{T}_h$ in the mesh is assigned a polynomial degree p_E, p_F , respectively p_C ; the polynomial degrees are collected in a vector \mathbf{p} .

The construction of global basis functions in the physical domains works as follows: first we define the shape functions locally (elementwise) by conforming transformation of functions on the reference domain. The global functions, which have support only on local patches, are then defined by taking the union of the contributing element shape functions. As we will see, global conformity is established easily due to our special constructions.

5.3.1 The H^1 -conforming global finite element space

Shape functions ϕ defined on a physical element $K \in \mathcal{T}_h$ are defined by the H^1 -conforming mapping of shape functions $\hat{\phi} \in W_{h,\mathbf{p}}(\hat{K})$ onto the reference element \hat{K} . Due to Lemma 4.10 we have

$$\phi := \hat{\phi} \circ \Phi_K^{-1}.$$

We associate the vertices, edges, and faces of each physical element with the corresponding entities in the global mesh, and we identify the mapped shape functions (with support on the physical element K) with the restriction of the global basis functions (with support on a patch). Such an identification is meaningful, since the vertices, edges, and faces on interelement boundaries coincide for adjacent physical elements. Here the global orientation of edges

and faces on the reference element level plays an important role. We arrive at a global space

$$W_{h,\mathbf{p}}(\mathcal{T}_h) := W_{h,1}(\mathcal{T}_h) \oplus \bigoplus_{E \in \mathcal{E}} W_{p_E}^E(\mathcal{T}_h) \oplus \bigoplus_{F \in \mathcal{F}} W_p^F(\mathcal{T}_h) \oplus \bigoplus_{K \in \mathcal{T}_h} W_{p_K}^K(\mathcal{T}_h) \quad (5.39)$$

with lowest-order, edge-based, face-based, and cell-based spaces as follows

$$\begin{aligned} W_{h,1}(\mathcal{T}_h) &:= \text{span} \{ \phi^{V_i} : \forall V_i \in \mathcal{V} \}, \\ W_{p_E}^E(\mathcal{T}_h) &:= \text{span} \{ \phi_i^E : 0 \leq i \leq p_E - 2 \} && \text{having support on } \omega_E, \\ W_p^F(\mathcal{T}_h) &:= \text{span} \{ \phi_i^F : 0 \leq i < N_{H^1}(F, p_F) \} && \text{having support on } \omega_F, \\ W_{p_C}^K(\mathcal{T}_h) &:= \text{span} \{ \phi_i^C : 0 \leq i < N_{H^1}(K, p_C) \} && \text{having support on } K, \end{aligned}$$

where $N_{H^1}(F, p_F)$ and $N_{H^1}(K, p_C)$ denote the number of H^1 -conforming degrees of freedom associated with the face F and to the cell K , respectively. These depend on the polynomial degree as well as on the topology of the face or cell. The number of degrees of freedom on the edges is uniquely determined by the polynomial degree p_E .

Theorem 5.28. *The space $W_{h,\mathbf{p}}(\mathcal{T}_h)$ defined in (5.39) is an $H^1(\Omega)$ -conforming finite element space.*

Proof. The shape functions on reference elements are constructed in such a way that they coincide at vertices, on edges and on faces even after transformation to physical coordinates. Since the shape functions associated with an interfaces between elements (a vertex, an edge, or a face) are the only ones with non-vanishing trace on the interface, and the orientation is treated globally (cf. Section 5.2.1), the global basis functions match each other on inter-element boundaries. \square

5.3.2 The $H(\text{curl})$ -conforming global finite element space

We define the restriction of a global basis function φ onto a physical element $K \in \mathcal{T}_h$ through the $H(\text{curl})$ -conforming mapping of the shape function $\hat{\varphi} \in V_{h,\mathbf{p}}(\hat{K})$ defined on the reference element \hat{K} . According to Lemma 4.15 we have

$$\varphi := F_K^{-T} \hat{\varphi} \circ \Phi_K^{-1}.$$

The identification of topological entities on the local and global levels works as in the H^1 case. By numbering the mapped shape functions sequentially on each edge, face, and cell we arrive at the following representation of the global space:

$$V_{h,\mathbf{p}}(\mathcal{T}_h) := V_{h,\mathcal{N}_0}(\mathcal{T}_h) \oplus \bigoplus_{E \in \mathcal{E}} V_{p_E}^E(\mathcal{T}_h) \oplus \bigoplus_{F \in \mathcal{F}} V_p^F(\mathcal{T}_h) \oplus \bigoplus_{K \in \mathcal{T}_h} V_{p_K}^K(\mathcal{T}_h). \quad (5.40)$$

The lowest-order, edge-based, face-based and cell-based spaces are defined as follows

$$\begin{aligned} V_{h,1}(\mathcal{T}_h) &:= \text{span} \{ \varphi_E^{\mathcal{N}_0} : \forall E \in \mathcal{E} \}, \\ V_{p_E}^E(\mathcal{T}_h) &:= \text{span} \{ \varphi_i^E : 0 \leq i \leq p_E - 1 \} && \text{having support on } \omega_E, \\ V_p^F(\mathcal{T}_h) &:= \text{span} \{ \varphi_i^F : 0 \leq i < N_{H(\text{curl})}(F, p_F) \} && \text{having support on } \omega_F, \\ V_{p_C}^K(\mathcal{T}_h) &:= \text{span} \{ \varphi_i^C : 0 \leq i < N_{H(\text{curl})}(K, p_C) \} && \text{having support on } K, \end{aligned}$$

where $N_{H(\text{curl})}(F, p_F)$ and $N_{H(\text{curl})}(K, p_C)$ denote the number of $H(\text{curl})$ -conforming degrees of freedom associated with the face F and with the cell K , respectively, depending on the local polynomial degrees and the topology of the face or cell.

Theorem 5.29. *The space $V_{h,\mathbf{p}}(\mathcal{T}_h)$ is $H(\text{curl})$ -conforming, i.e., a subspace of $H(\text{curl})$. There holds*

$$\nabla W_{h,\mathbf{p}+1}(\mathcal{T}_h) \subset V_{h,\mathbf{p}}(\mathcal{T}_h) \quad (5.41)$$

in particular

$$\nabla W_{h,1}(\mathcal{T}_h) \subset V_{h,\mathcal{N}_0}(\mathcal{T}_h), \quad (5.42a)$$

$$\nabla W_{p_E+1}^E(\mathcal{T}_h) = V_{p_E}^E(\mathcal{T}_h), \quad \nabla W_{p_F+1}^F(\mathcal{T}_h) \subset V_{p_F}^F(\mathcal{T}_h), \quad \nabla W_{p_C+1}^C(\mathcal{T}_h) \subset V_{p_C}^C(\mathcal{T}_h), \quad (5.42b)$$

for all $E \in \mathcal{E}$, for all $F \in \mathcal{F}$ and for all $K \in \mathcal{K}$ even for non-uniform polynomial degrees.

Proof. The shape functions for all reference topologies have been constructed in such a way their tangential traces on edges and faces coincide. Moreover, only shape functions associated with the interface of elements contribute to the tangential trace on common edges and/or the common face. Due to the use of global orientations for edges and faces, the orientation matches also locally on the interfaces which ensures tangential continuity of the mapped basis functions across inter-element boundaries.

The properties (5.42) are easily verified by the construction of the basis functions: The lowest-order space was already considered in Chapter 4. The explicit usage of gradient functions within the construction of the finite-element basis on the reference element implies that the inclusions hold on reference elements. By using $H(\text{curl})$ -conforming transformations for the construction of the shape functions on physical elements, we ensure that the gradient fields on the reference element are mapped onto the gradient fields on the physical element, which yields

$$\begin{aligned} \forall \phi \in W_{p_E+1}^E(\mathcal{T}_h) \exists \varphi \in V_{p_E}^E(\mathcal{T}_h) : \varphi &= \nabla \phi \\ \forall \phi \in W_{p_F+1}^F(\mathcal{T}_h) \exists \varphi \in V_{p_F}^F(\mathcal{T}_h) : \varphi &= \nabla \phi \\ \forall \phi \in W_{p_C+1}^C(\mathcal{T}_h) \exists \varphi \in V_{p_C}^C(\mathcal{T}_h) : \varphi &= \nabla \phi \end{aligned}$$

for all edges $E \in \mathcal{E}$, all faces $F \in \mathcal{F}$, and all cells $K \in \mathcal{T}_h$. Hence, $\nabla W_{h,1}(\mathcal{T}_h) \subset V_{h,\mathcal{N}_0}(\mathcal{T}_h)$, $\nabla W_{p_E+1}^E(\mathcal{T}_h) \subset V_{p_E}^E(\mathcal{T}_h)$ and $\nabla W_{p_E+1}^E(\mathcal{T}_h) \subset V_{p_E}^E(\mathcal{T}_h)$. The counting argument $\dim(\nabla W_{p_E+1}^E(\mathcal{T}_h)) = \dim(V_{p_E}^E(\mathcal{T}_h)) = p_{E_m}$ yields the coincidence of the edge-based spaces. Finally, (5.42) implies (5.41). \square

Remark 5.30. *If one does not use gradient fields explicitly in the construction of $H(\text{curl})$ -conforming shape functions, the following may be observed: The inclusion (5.41) concerning the global spaces only holds in the case when the polynomial degrees on edges, faces and cells satisfy the minimum order rule*

$$\begin{aligned} \forall F \in \mathcal{F} \forall E \in \mathcal{E} \text{ on } F : \quad p_E &\leq p_F, \\ \forall K \in \mathcal{T}_h \forall F \in \mathcal{F}_K : \quad p_F &\leq p_K. \end{aligned} \quad (5.43)$$

The space splitting of higher-order gradients (5.42b) does not hold in general, not even in case of a uniform polynomial degree.

5.3.3 The $H(\text{div})$ -conforming global finite element space

The restriction of global basis functions ψ onto a physical element $K \in \mathcal{T}_h$ is defined via the Piola transformation

$$\psi := J_K^{-1} F_K \hat{\psi} \circ \Phi_K^{-1},$$

of shape functions $\hat{\psi} \in Q_{h,\mathbf{p}}(\hat{K})$ from the reference element \hat{K} . Numbering the global basis functions sequentially on each edge, face and cell yields the global space

$$Q_{h,\mathbf{p}}(\mathcal{T}_h) := Q_{h,\mathcal{RT}_0}(\mathcal{T}_h) \oplus \bigoplus_{F \in \mathcal{F}} Q_{p_F}^F(\mathcal{T}_h) \oplus \bigoplus_{K \in \mathcal{T}_h} Q_{p_C}^K(\mathcal{T}_h) \quad (5.44)$$

with the lowest-order, edge-based, face-based and cell-based spaces defined as follows

$$\begin{aligned} Q_{h,1}(\mathcal{T}_h) &:= \text{span} \{ \psi_F^{\mathcal{RT}_0} : \forall F \in \mathcal{F} \}, \\ Q_{p_{F_m}}^F(\mathcal{T}_h) &:= \text{span} \{ \psi_i^F : 1 \leq i \leq N_{H(\text{div})}(F_m, p_{F_m}) \} && \text{having support on } \omega_F, \\ Q_{p_C}^K(\mathcal{T}_h) &:= \text{span} \{ \psi_i^C : 1 \leq i \leq N_{H(\text{div})}(K, p_C) \} && \text{having support on } K, \end{aligned}$$

where $N_{H(\text{div})}(F_m, p_{F_m})$ and $N_{H(\text{div})}(K, p_C)$ denote the number of $H(\text{div})$ -conforming degrees of freedom associated with the face F_m and to the cell K , respectively.

Theorem 5.31. *The global space $Q_{h,\mathbf{p}}(\mathcal{T}_h)$ is an $H(\text{div})$ -conforming finite element space. Moreover, there holds*

$$\text{curl } V_{h,\mathbf{p}}(\mathcal{T}_h) \subset Q_{h,\mathbf{p}}(\mathcal{T}_h). \quad (5.45)$$

In particular

$$\text{curl } V_{h,\mathcal{N}_0}(\mathcal{T}_h) \subset Q_{h,\mathcal{RT}_0}(\mathcal{T}_h), \quad (5.46a)$$

$$\text{curl } V_{p_F}^F(\mathcal{T}_h) = Q_{p_F}^F(\mathcal{T}_h), \quad \text{curl } V_{p_C}^C(\mathcal{T}_h) \subset Q_{p_C}^C(\mathcal{T}_h) \quad (5.46b)$$

for all $F \in \mathcal{F}$ and for all $K \in \mathcal{K}$.

Proof. We follow the proof of Theorem 5.29: The normal traces of the local shape functions on faces coincide for all types of the reference topologies. Due to the $H(\text{div})$ -conforming transformation and the global orientation of local edges and local faces, we obtain continuity of the normal traces on inter-element boundaries.

Formuly (5.46) was already considered for lowest-order space in Chapter 4. The explicit usage of gradient functions within the construction of the finite element basis on the reference element implies that the inclusions 5.46 hold on the reference element. Similar statements for the physical elements follows again from the construction using the conforming transformation, i.e., we obtain

$$\begin{aligned} \forall \varphi \in V_{p_F}^F(\mathcal{T}_h) \exists \psi \in Q_{p_F}^F(\mathcal{T}_h) : \psi = \text{curl } \varphi \\ \forall \varphi \in V_{p_C}^C(\mathcal{T}_h) \exists \psi \in Q_{p_C}^C(\mathcal{T}_h) : \psi = \text{curl } \varphi \end{aligned}$$

for all faces $F \in \mathcal{F}$ and all cells $K \in \mathcal{T}_h$. This implies the inclusions of the various local curl spaces stated (5.46b). Counting the dimensions yields $\dim |\text{curl } V_{p_F}^F(\mathcal{T}_h)| = \dim |Q_{p_F}^F(\mathcal{T}_h)|$. Finally, (5.46) implies (5.45), which completes the proof. \square

Observations similar to those in Remark 5.30 also hold for the $H(\text{div})$ -conforming spaces.

5.3.4 The L_2 -conforming global finite element space

For the sake of completeness, we also address the L_2 -conforming spaces briefly. The L_2 -conforming global FE-space is defined by divergence-fields of the proposed $H(\text{div})$ -conforming

basis functions. In particular, we use constants on the elements as lowest-order basis functions, and construct the higher-order cell-based functions as divergence-fields

$$\hat{\vartheta}_0 = 1, \quad \hat{\vartheta}_i := \operatorname{div}(\hat{\psi}_i)$$

for $\hat{\psi}_i \in Q_{\mathbf{p}}^C(\hat{K})$ being *linear-independent to curl-fields*. We use the transformation of divergence-fields according to Lemma 4.19 to define the basis function on the physical element K : $\vartheta = J_K^{-1} \hat{\vartheta} \circ \Phi_K^{-1}$.

In the case of L_2 -conforming finite element spaces there are no continuity requirements across inter-element boundaries, hence, there is no need to associate any global degrees of freedom with the boundary of the element. This implies the following global FE-space

$$S_{h,\mathbf{p}}(\mathcal{T}_h) = \operatorname{div}(Q_{h,\mathbf{p}}(\mathcal{T}_h)) = \operatorname{div}(Q_{h,\mathcal{RT}_0}(\mathcal{T}_h)) \oplus \bigoplus_{K \in \mathcal{K}} \operatorname{div}(Q_{\mathbf{p}}^K(\mathcal{T}_h)), \quad (5.47)$$

which coincides with the classical L_2 -conforming global FE-spaces used within the de Rham sequence. By the exact sequence property of the lowest-order global FE-spaces, cf. Theorem 4.28, we obtain $S_{h,0}(\mathcal{T}_h) = \operatorname{div}(Q_{h,\mathcal{RT}_0}(\mathcal{T}_h))$. Moreover, $S_{p_C}^C(\hat{K}) = \operatorname{div}(Q_{p_C}^C(\hat{K}))$ can be easily verified by the definition of $S_{p_C}^C(\hat{K})$ and a counting argument.

5.4 The Local Exact Sequence Property

The global finite element spaces were constructed as direct sums of the lowest-order space and spaces having only local support on edge-patches, on face-patches or single elements. Due to the special construction of the finite element spaces we obtain exact sequences on a finer level. The following theorem summarizes the results of Theorem 5.28 and Theorem 5.29.

Theorem 5.32 (The local exact sequence property). *Let Ω denote a simply-connected domain with connected boundary, \mathcal{T}_h be a regular mesh, and let p_E , p_F , and p_C denote the polynomial orders associated with edges $E \in \mathcal{E}$, faces $F \in \mathcal{F}$, and cells $K \in \mathcal{T}_h$. For ease of notation we collect the polynomial degrees in a vector \mathbf{p} .*

If the sequence of global lowest-order spaces (cf. Theorem 4.28)) is exact, then the sequence of conforming finite element spaces provided by (5.39), (5.40), (5.44), and (5.47) satisfies the following local exact sequence property:

$$\begin{aligned} W_{h,1}^V(\mathcal{T}_h)/\mathbb{R} &\xrightarrow{\nabla} V_h^{\mathcal{N}_0}(\mathcal{T}_h) \xrightarrow{\operatorname{curl}} Q_h^{\mathcal{RT}_0}(\mathcal{T}_h) \xrightarrow{\operatorname{div}} S_{h,0}(\mathcal{T}_h) \xrightarrow{0} \{0\} \\ W_{p_E+1}^E(\mathcal{T}_h) &\xrightarrow{\nabla} V_{p_E}^E(\mathcal{T}_h) \xrightarrow{\operatorname{curl}} \{0\} && \forall E \in \mathcal{E} \\ W_{p_F+1}^F(\mathcal{T}_h) &\xrightarrow{\nabla} V_{p_F}^F(\mathcal{T}_h) \xrightarrow{\operatorname{curl}} Q_{p_F}^F(\mathcal{T}_h) \xrightarrow{\operatorname{div}} \{0\} && \forall F \in \mathcal{F} \\ W_{p_K+1}^K(\mathcal{T}_h) &\xrightarrow{\nabla} V_{p_K}^K(\mathcal{T}_h) \xrightarrow{\operatorname{curl}} Q_{p_K}^K(\mathcal{T}_h) \xrightarrow{\operatorname{div}} S_{p_K}^K(\mathcal{T}_h) \xrightarrow{0} \{0\} && \forall K \in \mathcal{T}_h. \end{aligned}$$

Proof. Due to Theorem 5.28 and Theorem 5.29 we only have to verify that the divergence operator is surjective from $Q_{p_K}^K(\mathcal{T}_h)$ onto $S_{p_K}^K(\mathcal{T}_h)$, which follows by counting the space dimensions. \square

Remark 5.33. *The local exact sequence property is also fulfilled if we use Nédélec elements of the first kind and Raviart-Thomas-Nedelec finite elements, or finite elements with anisotropic polynomial order distribution.*

A general set of $H(\text{curl})$ -conforming and $H(\text{div})$ -conforming shape functions, which does explicitly use differential fields in the construction of the local basis, or at least not provide the analogue of the local exact sequence property on the reference element \hat{K} . Then the sequence (5.48) of global finite element spaces is only exact, if the polynomial order distribution all over the mesh satisfies the minimum order rule (5.43).

Corollary 5.34 (Exactness of the global discrete sequence). *The local exact sequence property implies that the sequence of the constructed conforming global FE-spaces is exact, i.e.*

$$\mathbb{R} \xrightarrow{id} W_{h,\mathbf{p}+1}(\mathcal{T}_h) \xrightarrow{\nabla} V_{h,\mathbf{p}}(\mathcal{T}_h) \xrightarrow{\text{curl}} Q_{h,\mathbf{p}}(\mathcal{T}_h) \xrightarrow{\text{div}} S_{h,\mathbf{p}}(\mathcal{T}_h) \xrightarrow{0} \{0\}. \quad (5.48)$$

Assuming the local exact sequence property is one of main issues of this thesis. Besides the advantage of arbitrary and variable polynomial order distribution over the mesh, we will rely on this property in the course of designing robust preconditioners for curl – curl problems as well as reduced basis approaches in the next chapter.

Chapter 6

Iterative Solvers for Electromagnetic Problems

This chapter is devoted to stable and efficient solution strategies for linear systems arising from $H(\text{curl})$ -conforming discretizations for a general curl-curl-problem $\text{curl } \mu^{-1} \text{curl } \mathbf{u} + \kappa \mathbf{u} = \mathbf{f}$. In general, these linear systems are of huge dimension and ill-conditioned. Hence, direct solving is out of question and even impossible due to memory and time resources. We have to use iterative solvers involving preconditioning.

Unfortunately, standard solution techniques, which yield successive, stable and efficient linear solvers for $H^1(\Omega)$ -problems, usually fail on curl-curl problems. Even classical multigrid techniques (HACKBUSCH [52], BRAMBLE-ZHANG [30]), which provide one of the most efficient solvers for elliptic problems, result in poor convergence rates. Moreover, standard solvers deteriorate for small L_2 -coefficients $0 < \kappa \ll 1$.

The problem can be traced back to the large kernel of the curl-operator. On irrotational fields the curl-curl problem reduces to the identity operator, while acting as second-order differential operator on solenoidal fields. By the choice of appropriate smoothers, respecting the Helmholtz decomposition, multigrid techniques regain their efficiency. We refer to the pioneering works by HIPTMAIR [59], [55], and ARNOLD-FALK-WINTHER [6], [7].

In the following, we focus on the design of parameter(κ)-robust preconditioners, which in addition also provide appropriate smoothers for multigrid schemes. By means of an additive Schwarz framework the parameter-robustness is guaranteed, if the local decomposition of the FE-space also represents a correct splitting of the kernel of the curl-operator. We exploit the local exact sequence property to ensure a correct space splitting even for simple decompositions.

6.1 Basic concepts of iterative solvers

We consider a finite element space V , an associated FE-basis $\{\phi_i : 1 \leq i \leq N\}$ and the corresponding finite dimensional variational problem:

Find $u \in V$ such that

$$a(u, v) = f(v) \quad \forall v \in V. \quad (6.1)$$

Due to the Galerkin isomorphism (cf. Chapter 4) the discrete variational problem is equivalent to the linear system: Find $\underline{u} \in \mathbb{R}^N$ such that

$$\underline{A} \underline{u} = \underline{f}, \quad (6.2)$$

for $\underline{A} \in \mathbb{R}^{N \times N}$ and $\underline{f} \in \mathbb{R}^N$ defined by $\underline{A}_{ij} := a(\phi_i, \phi_j)$, $\underline{f}_i := f(\phi_i)$, and $u = \sum_{i=1}^N u_i \phi_i$.

For a detailed exposition on iterative solvers and preconditioning, we refer to textbooks as BRAESS [27], GROSSMANN-ROOS [51] and HACKBUSCH [53]. In the following, we briefly recall some of the main aspects.

The convergence rate of iterative solvers, such as Richardson's method and the conjugate gradient (CG) method, mainly depends on the condition number $\kappa(\underline{A}) := \|\underline{A}\| \|\underline{A}^{-1}\|$ of the matrix \underline{A} . Hence, these solvers can be tremendously improved by means of a preconditioned system $\underline{C}^{-1}\underline{A}$.

Suppose \underline{A} and \underline{C} to be symmetric, positive definite matrices. A good preconditioner \underline{C} to a matrix \underline{A} must satisfy following two properties:

- the matrix-vector product $\underline{w} = \underline{C}^{-1}\underline{d}$ can be computed fast,
- \underline{C} is spectrally equivalent to \underline{A} , i.e.

$$\gamma_1 \underline{u}^T \underline{C} \underline{u} \leq \underline{u}^T \underline{A} \underline{u} \leq \gamma_2 \underline{u}^T \underline{C} \underline{u} \quad (6.3)$$

with a small condition number $\kappa(\underline{C}^{-1}\underline{A}) \leq \frac{\gamma_2}{\gamma_1}$ of the preconditioned matrix.

A customary and efficient method for solving symmetric positive definite linear systems is the *preconditioned conjugate gradient method* (PCG). The iteration number behaves then as $\mathcal{O}(\sqrt{\kappa(\underline{C}^{-1}\underline{A})})$ in the case of a fixed error bound. The convergence rate is $\frac{\sqrt{\kappa(\underline{C}^{-1}\underline{A})}-1}{\sqrt{\kappa(\underline{C}^{-1}\underline{A})+1}}$.

In case of non-symmetric and indefinite problems one uses Krylov-based subspace methods, such as the generalized minimal residual method (GMRES) or the stabilized bi-orthogonal gradient method (BI-CGSTAB). We refer to standard textbooks on iterative solvers for sparse linear systems as e.g. SAAD [77], VAN DER VORST [91].

6.1.1 Additive Schwarz Methods (ASM)

The additive Schwarz technique provides an abstract framework for the design of preconditioners based on the splitting of the underlying finite element space. For a detailed description we refer to textbooks such as SMITH ET AL. [84] and TOSELLI-WIDLUND [90]. The short overview below follows the latter one.

We consider the finite dimensional variational problem (6.1) with a positive definite bilinear form $a : V \times V \rightarrow \mathbb{R}$. This is equivalent to the linear operator equation

$$Au = F \text{ in } V^*$$

with $A : V \rightarrow V^*$ defined by $\langle Au, v \rangle = a(u, v)$ and $F \in V^*$ defined by $\langle F, v \rangle = f(v)$, where $\langle \cdot, \cdot \rangle$ denotes the duality product in $V^* \times V$.

We consider a family of finite element spaces $\{V_i\} := \{V_i, i = 0, \dots, M\}$ and prolongation operators

$$R_i : V_i \longrightarrow V. \quad (6.4)$$

The corresponding adjoint operators will be denoted by R_i^T . We assume that the whole space can be decomposed in prolonged local spaces:

$$V = \sum_{i=0}^M R_i V_i. \quad (6.5)$$

This splitting need not be unique.

On each space V_i we introduce a symmetric, positive definite local bilinear form

$$c_i(\cdot, \cdot) : V_i \times V_i \rightarrow \mathbb{R}. \quad (6.6)$$

In operator notation, we use $C_i : V_i \rightarrow V_i^*$, which is defined by $\langle C_i u_i, v_i \rangle = c_i(u_i, v_i)$ for $u_i, v_i \in V_i$. The bilinear form $c_i(\cdot, \cdot)$ should provide a local approximation of $a(\cdot, \cdot)$.

Moreover, we define the subspace solution operator $T_i : V \rightarrow V_i$ satisfying

$$c_i(T_i u, v_i) = a(u, R_i v_i). \quad (6.7)$$

The solution operator equals to $T_i = C_i^{-1} R_i^T A$. Due to the symmetry and the positive-definiteness of the original bilinear form and the local ones, the operator $R_i T_i : V \rightarrow V$ is self-adjoint with respect to $a(\cdot, \cdot)$.

We define the global preconditioner $C : V \rightarrow V^*$ by its inverse. In an additive Schwarz framework this is defined by the additive operator

$$C^{-1} = \sum_{i=0}^M R_i C_i^{-1} R_i^T. \quad (6.8)$$

This yields the preconditioned operator of the form

$$T := C^{-1} A = \sum_{i=0}^M R_i T_i. \quad (6.9)$$

A natural choice for the local bilinear form (6.6) is given by the restriction of the original bilinear form to the local spaces:

$$c_i(u_i, v_i) := a(R_i u_i, R_i v_i), \text{ and } C_i = R_i^T A R_i, \text{ respectively.} \quad (6.10)$$

This means that the local problems on V_i are solved exactly, and the operator T_i provides the $a(\cdot, \cdot)$ -orthogonal projection onto the subspace $R_i V_i \subset V$.

The following theorem plays a central role in additive Schwarz theory. A proof can be found in ZHANG [97] (Lemma 4.1).

Theorem 6.1. *The additive Schwarz preconditioner is well defined by its inverse. Moreover, the norm generated by the additive Schwarz preconditioner $\|u\|_C := (Cu, u)_V^{\frac{1}{2}}$ is equal to the splitting norm, i.e the quadratic forms satisfy*

$$(Cu, u)_V = \inf_{\substack{u = \sum_{i \in V_i} R_i u_i}} C_i(u_i, u_i) \quad \forall u \in V. \quad (6.11)$$

In particular, this lemma applies for deducing spectral bounds γ_1, γ_2 of the preconditioned problem, i.e.

$$\gamma_1 \inf_{\substack{u = \sum_{i \in V_i} R_i u_i}} C_i(u_i, u_i) \leq A(u, u) \leq \gamma_2 \inf_{\substack{u = \sum_{i \in V_i} R_i u_i}} C_i(u_i, u_i). \quad (6.12)$$

If only a finite number of subspaces $R_i V_i$ overlap, we obtain $\gamma_2 = \mathcal{O}(1)$.

In practice, one prefers the *multiplicative Schwarz method* (MSM) instead of the additive one, see BRAMBLE-ZHANG [30]. There one defines $T := I - \Pi_{i=0}^M(I - T_i)$ instead of (6.9), but uses the symmetric operator T^*T . Although one can only show that the symmetric multiplicative Schwarz method is not worse than the additive one, in most cases it leads to faster convergence. The additive version corresponds to Block-Jacobi iterations, whereas the multiplicative one to Block-Gauss-Seidel iterations.

A prominent class of Schwarz preconditioners is provided by multigrid/multilevel preconditioners. These techniques have become very popular in the last decades, since they lead to optimal convergence rates with respect to the degrees of freedom. Since in electromagnetics the keypoint is the choice of the correct Schwarz smoother on each level, we permit ourselves to refer to the literature for the issue of multigrid techniques in the sequel.

6.1.2 A two-level concept for linear equations originating from hp -FEM discretization

We proceed with establishing a hierarchical two-level concept for the splitting of finite element spaces. As a start, we introduce the method for $H^1(\Omega)$ problems. An analog concept will be used later for solving $H(\text{curl})$ -problems.

The hierarchical V - E - F - C -based construction of the conforming FE-spaces (cf. Chapter 5) naturally provides a simple space splitting for the FE-space $W \subset H^1(\Omega)$:

$$W = W_{1,h}(\mathcal{T}_h) + \sum_{E \in \mathcal{E}} W_{p_E+1}^E(\mathcal{T}_h) + \sum_{F \in \mathcal{F}} W_{p_F+1}^F(\mathcal{T}_h) + \sum_{K \in \mathcal{T}_h} W_{p_K+1}^K(\mathcal{T}_h) \quad (6.13)$$

By this, we introduce the following two-level concept for solving the discretized equations:

- The lowest-order FE-subspace $W_{1,h}$ plays a special role. We use it as the coarse space, which carries the global information.
On the coarse level we can exploit the full range of well-developed h -version preconditioners, e.g. multigrid techniques. If the coarse system is of modest size, i.e. if the underlying mesh is sufficiently coarse, we can also use an exact solver.
- On the fine level (the high-order FE-space) we use a Block-Jacobi (ASM) or Gauss-Seidel (MSM) smoother according to the hierarchic V - E - F - C -based splitting.

The V - E - F - C -based splitting (6.13) provides a natural, simple decomposition. The quality of the preconditioner can be improved by bigger overlaps of the above local spaces at the cost of higher complexity. For instance, in SCHÖBERL ET AL. [82] we suggest various overlaps combined with some variants of adding monomials of the lowest-order shape functions and achieve h and p robust condition numbers for $H^1(\Omega)$ problems.

Further on, we can improve the condition number by static condensation of the cell-based degrees of freedom.

6.1.3 Static Condensation

Static condensation is a customary tool in solving linear equations arising from the hierarchical hp finite element discretization (cf. the textbooks of SCHWAB [83] and MELENK [68]). The main idea is to exploit the local support of the cell-based shape functions. In the following,

we classify two sets of degrees of freedom, or two sets of shape functions, respectively: the cell-based ones and the remaining ones. The latter we call exterior (ex) degrees of freedom (exterior shape functions). We can rewrite the linear system (6.2) as

$$\begin{pmatrix} A^{\text{ex ex}} & A^{\text{ex } C} \\ A^{C \text{ ex}} & A^{CC} \end{pmatrix} \begin{pmatrix} \mathbf{u}^{\text{ex}} \\ \mathbf{u}^C \end{pmatrix} = \begin{pmatrix} \mathbf{f}^{\text{ex}} \\ \mathbf{f}^C \end{pmatrix}. \quad (6.14)$$

The local support of the cell-based global FE-functions is only the associated element itself. Hence, the cell-based degrees of freedom corresponding to two different elements do not couple. The cell-based submatrix A^{CC} of the stiffness matrix is block-diagonal:

$$A^{CC} = \text{diag}(A_{K_1}^{CC}, \dots, A_{K_n}^{CC}) \quad \text{for } K_i \in \mathcal{T}_h \text{ and } n = |\mathcal{T}_h|.$$

If we perform the Schur-complement with respect to the submatrix A^{CC} within the linear system (6.14), we can extract the *condensed system*

$$\tilde{A} \mathbf{u}^{\text{ex}} = \tilde{\mathbf{f}} \quad (6.15)$$

with $\tilde{A} := A^{\text{ex ex}} - A^{\text{ex } C} (A^{CC})^{-1} A^{C \text{ ex}}$ and $\tilde{\mathbf{f}} := \mathbf{f}^{\text{ex}} - A^{\text{ex } C} (A^{CC})^{-1} \mathbf{f}^C$. The cell-based degrees of freedom can eventually be calculated via

$$\mathbf{u}^C = (A^{CC})^{-1} (\mathbf{f}^C - A^{C \text{ ex}} \mathbf{u}^{\text{ex}}).$$

In a practical implementation, the Schur complement is computed locally on the element level and only the condensed element matrices are assembled into the global matrix.

The application of static condensation provides two main advantages:

- The resulting global condensed linear system is of much smaller dimension: the condensed element matrices are of dimension $\mathcal{O}(p^{d-1})$ compared to $\mathcal{O}(p^d)$ in case of the original element matrices.
- In general, the condensed system matrix is better conditioned. Providing the Schur complement means an orthogonalization of the external shape functions to the cell-based ones (cf. KARNIADAKIS-SHERWIN [60] (Subsection 4.2.3)).

Equipped with the main concepts of preconditioning we turn now to iterative solvers and preconditioners for $H(\text{curl})$ -problems.

6.2 Parameter-Robust Preconditioning for $H(\text{curl})$

We consider a conforming finite element space $V \subset H_{0,D}(\text{curl}, \Omega)$. By this, we define a finite dimensional variational problem:

Find $\mathbf{u} \in V$ such that

$$a^\kappa(\mathbf{u}, \mathbf{v}) = f(\mathbf{v}) \quad \forall \mathbf{v} \in V \quad (6.16)$$

involving the bilinear form

$$a^\kappa(\mathbf{u}, \mathbf{v}) := \int_{\Omega} \text{curl } \mathbf{u} \text{ curl } \mathbf{v} + \kappa \mathbf{u} \mathbf{v} \, dx \quad (6.17)$$

and the linear form

$$f(\mathbf{v}) := \int_{\Omega} \mathbf{j} \cdot \mathbf{v} \, d\mathbf{x}.$$

The impressed current density \mathbf{j} is assumed to be divergence-free, i.e. $\operatorname{div} \mathbf{j} = 0$. Note, that the restriction to homogenous Dirichlet and homogenous Neumann data is done only for the sake of simplicity to avoid the technical treatment of boundary integrals and inhomogeneous Dirichlet data.

Due to the Galerkin isomorphism (cf. Chapter 4) the discrete variational problem (6.16) is equivalent to the linear system in $\mathbb{R}^{N \times N}$ of the form

$$\underline{A} \underline{u} = \underline{f} \quad \text{with } \underline{A} := \underline{K} + \kappa \underline{M} \in \mathbb{R}^{N \times N} \quad (6.18)$$

with $\underline{K}_{ij} := \int_{\Omega} \operatorname{curl} \boldsymbol{\varphi}_i \cdot \operatorname{curl} \boldsymbol{\varphi}_j \, d\mathbf{x}$, $\underline{M}_{ij} := \int_{\Omega} \boldsymbol{\varphi}_i \cdot \boldsymbol{\varphi}_j \, d\mathbf{x}$, and $f_i := \int_{\Omega} \mathbf{j} \cdot \boldsymbol{\varphi}_i \, d\mathbf{x}$ for $\{\boldsymbol{\varphi}_i : 1 \leq i \leq N\}$ denoting the finite element basis of V .

The parameter κ is problem-dependent, see the discussion in Section 2.4. We call a preconditioner C of A robust in κ , if the spectral bounds γ_1, γ_2 in

$$\gamma_1 C(\mathbf{u}, \mathbf{u}) \leq a^\kappa(\mathbf{u}, \mathbf{u}) \leq \gamma_2 C(\mathbf{u}, \mathbf{u})$$

are independent of the parameter κ .

In the following, we are mainly concerned with the design of κ -robust preconditioners for positive and possibly small $\kappa \ll 1$. This corresponds to the following list of problems of interest:

- the magnetostatic problems and non-conducting regions of magneto-quasi-static problems, where the parameter κ originates from a small regularization parameter (cf. Subsection 3.4.2 and Subsection 6.4.1)
- the magneto-quasi-static problem ($\kappa = i\omega\sigma$), where we need good preconditioners for $\underline{A}^\kappa = \underline{K} + |\kappa| \underline{M}$ (cf. Subsection 6.4.2),
- the Maxwell eigenvalue problem, where we need a κ -robust preconditioners for $\underline{A}^\kappa = \underline{K} + \kappa \underline{M}$ with $\kappa > 0$ in each iteration step (cf. Chapter 7).

First, we analyze why classical preconditioners fail on the $H(\operatorname{curl})$ -problems. Next, we introduce the successful smoothers of Arnold-Falk-Winther and Hiptmair, which can be chosen for solving the coarse grid system in a correct and robust way. We use an abstract result of SCHÖBERL [80] on robust preconditioning for parameter dependent problems and reformulate it for $H(\operatorname{curl})$ -problems. We verify that the local exact sequence property implies parameter-robustness even for simple Schwarz preconditioners.

6.2.1 Two Motivating Examples

We consider the magnetostatic problem with small regularization parameter $0 < \kappa \ll 1$ on the lowest-order FE-space $V = V_h^{\mathcal{N}_0}(\mathcal{T}_h)$.

Find $\mathbf{u} \in V_h^{\mathcal{N}_0}(\mathcal{T}_h)$ such that

$$\int_{\Omega} \operatorname{curl} \mathbf{u} \cdot \operatorname{curl} \mathbf{v} \, d\mathbf{x} + \kappa \int_{\Omega} \mathbf{u} \cdot \mathbf{v} \, d\mathbf{x} = \int_{\Omega} \mathbf{j} \cdot \mathbf{v} \, d\mathbf{x} \quad \forall \mathbf{v} \in V_h^{\mathcal{N}_0}(\mathcal{T}_h). \quad (6.19)$$

We refer to the parameter-dependent bilinear form with $a^\kappa(\cdot, \cdot)$. In the following, we state two simple Schwarz preconditioners and their asymptotic behavior as κ gets small:

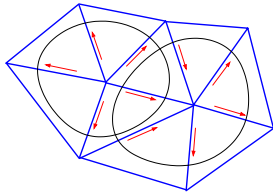
1. The standard diagonal Jacobi-preconditioner is provided by the simple space splitting

$$V_h^{\mathcal{N}_0}(\mathcal{T}_h) = \sum_{E \in \mathcal{E}} \text{span}\{\varphi_E^{\mathcal{N}_0}\}. \quad (6.20)$$

This yields a parameter-dependent condition number even for the preconditioned system, namely

$$\kappa(C_{diag}^{-1} A^\kappa) = \mathcal{O}(h^{-2} \kappa^{-1}). \quad (6.21)$$

2. The Arnold-Falk-Winther block-Jacobi preconditioner is provided by a space decomposition with respect to the vertex patches (as visualized in the figure for the 2D case):



$$V_h^{\mathcal{N}_0}(\mathcal{T}_h) = \sum_{v \in \mathcal{V}} \text{span}\{\varphi_E^{\mathcal{N}_0} : E \in \mathcal{E} \text{ so that } v \text{ on } E\}. \quad (6.22)$$

This choice provides a parameter-independent condition number

$$\kappa(C_{AFW}^{-1} A^\kappa) = \mathcal{O}(h^{-2}). \quad (6.23)$$

A numerical experiment

We consider problem (6.19) on the unit cube $\Omega = [0, 1]^3$, which is covered with a mesh of 12 tetrahedra. In Figure 6.1 we illustrate the condition number of the preconditioned system matrix $C_{diag}^{-1} A$ and $C^{-1} A_{AFW}$ for varying parameters κ from 1 to 10^{-6} and uniform mesh refinements in h .

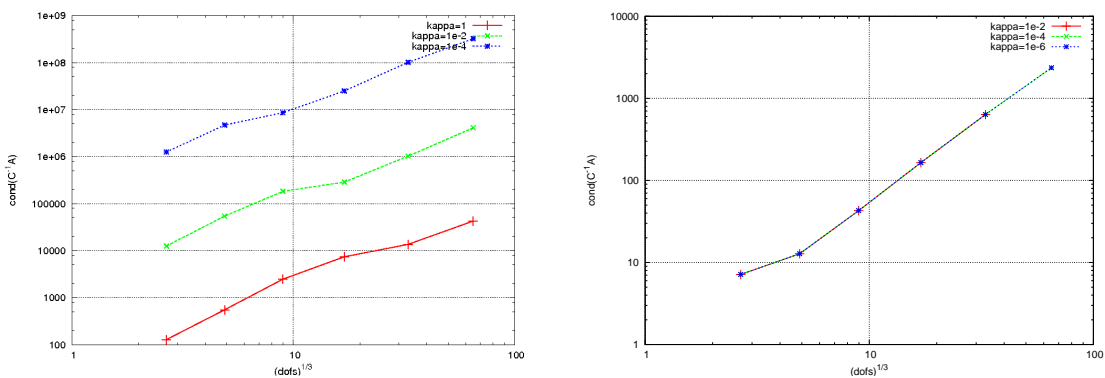


Figure 6.1: Condition numbers of regularized magnetostatic problem, applying a standard Gauss-Seidel preconditioner (left) and an AFW-block Gauss-Seidel preconditioner (right, κ -robust) for varying regularization parameters κ with uniform h -refinement.

We observe that in practice, the condition number of the standard Gauss-Seidel-preconditioner already suffers from modest values of κ . The AFW smoother is apparently robust in κ .

Analysis of the two ASM preconditioners

For analyzing the parameter-dependency of the discussed preconditioners, we have to provide some inverse estimates first:

Remark 6.2 (Some inverse estimates). *We assume a shape-regular triangulation of $\Omega \subset \mathbb{R}^d$ (cf. Chapter 4) so that*

$$\|F_K^T\| \preceq h_K^{-1}, \quad \|F_K^{-T}\| \preceq h_K, \quad \text{and} \quad |J_K| \simeq h_K^d. \quad (6.24)$$

Let $\{\phi_i\}$ and $\{\varphi_E^{\mathcal{N}_0}\}$, respectively, refer to the conforming nodal FE-basis functions of $W_{h,1}(\mathcal{T}_h)$ and $V_h^{\mathcal{N}_0}(\mathcal{T}_h)$, respectively. Assuming conforming transformations we can estimate norms of the finite element basis functions using (6.24) by

$$\begin{aligned} \|\phi_i\|_{L_2(K)}^2 &\preceq h_K^d, & \|\varphi_E^{\mathcal{N}_0}\|_{L_2(K)}^2 &\preceq h_K^{d-2}, \\ \|\nabla\phi_i\|_{L_2(K)}^2 &\preceq h_K^{d-2}, & \|\text{curl}\varphi_E^{\mathcal{N}_0}\|_{L_2(K)}^2 &\preceq h_K^{d-4}. \end{aligned}$$

Concerning the H^1 -conforming and $H(\text{curl})$ -conforming degrees of freedom, we obtain inverse estimates by conforming transformation to the reference element (hat marker), then performing the estimate and afterwards conforming back-transformation onto the physical element. Let K be a physical element sharing either the vertex V_i or the edge E .

$$\begin{aligned} |w(V_i)|^2 &= |\hat{w}(\hat{V}_\alpha)|^2 \preceq \|\hat{w}\|_{L_2(\hat{K})}^2 \preceq h_K^{-d} \|w\|_{L_2(K)}^2, \\ \left| \int_E \mathbf{u}_E \cdot \boldsymbol{\tau} \, ds \right|^2 &= \left| \int_{\hat{E}} \hat{\mathbf{u}}_{\hat{E}} \cdot \hat{\boldsymbol{\tau}} \, d\hat{s} \right|^2 \preceq \|\hat{\mathbf{u}}_{\hat{E}}\|_{L_2(\hat{K})}^2 \preceq h_K^{2-d} \|\mathbf{u}_E\|_{L_2(K)}^2. \end{aligned}$$

Moreover, we will need the discrete analog of the Friedrichs' inequality (cf. Theorem 3.26) as stated in MONK [70] (Lemma 7.20)

Lemma 6.3 (Discrete Friedrichs' inequality for $H(\text{curl})$). *Let Ω be a simply-connected Lipschitz domain. Suppose $\mathbf{v} \in V_{h,p}(\mathcal{T}_h) \subset H(\text{curl}, \Omega)$ is orthogonal to discrete gradient functions, i.e. $(\mathbf{v}, \nabla\psi) = 0$ for all $\psi \in W_{h,p+1}(\mathcal{T}_h) \subset H^1(\Omega)$. Then there exists a constant $c_F > 0$ independent of h such that*

$$\|\mathbf{v}\|_0 \leq c_F \|\text{curl}\mathbf{v}\|_0.$$

Proof of the condition number estimate (6.21) for the Jacobi-preconditioner.

The quadratic form of the splitting norm corresponding to (6.20) evaluates to the unique splitting

$$\mathbf{u} = \sum_{E \in \mathcal{E}} \mathbf{u}_E \quad \text{with} \quad \mathbf{u}_E = \int_E \mathbf{u} \cdot \boldsymbol{\tau} \, ds \cdot \varphi_E^{\mathcal{N}_0}.$$

Let K be an element sharing an edge E . Using the inverse estimates from Remark 6.2, we obtain

$$\begin{aligned} \|\mathbf{u}_E\|_{A^\kappa, K}^2 &= \left(\int_E \mathbf{u} \cdot \boldsymbol{\tau} \, ds \right)^2 \left(\|\text{curl}\varphi_E^{\mathcal{N}_0}\|_{L_2(K)}^2 + \kappa \|\varphi_E^{\mathcal{N}_0}\|_{L_2(K)}^2 \right) \\ &\preceq (h^{-2} + \kappa) \|\mathbf{u}\|_{L_2(K)}^2 \stackrel{(*)}{\preceq} \left(\frac{1}{h^2 \kappa} + 1 \right) \left(\|\text{curl}\mathbf{u}\|_{L_2(K)}^2 + \kappa \|\mathbf{u}\|_{L_2(K)}^2 \right). \end{aligned}$$

The notation for energy norm $\|\cdot\|_{A^\kappa, K}$ indicates that the integrals in the bilinear form $a_\kappa(\cdot, \cdot)$ are evaluated on the physical element K .

In H^1 -problems we can get rid of the κ -dependency within the step (*) by Friedrichs' inequality. But in $H(\text{curl})$ Friedrichs' inequality only holds for the subspace orthogonal to gradients.

Summing up over all edges, and taking into account that only a finite number of edge patches overlap, we obtain

$$C_{diag}(\mathbf{u}, \mathbf{u}) = \sum_{E \in \mathcal{E}} \|\mathbf{u}_E\|_{A^\kappa}^2 \preceq \left(\frac{1}{h^2 \kappa} + 1\right) (\|\text{curl } \mathbf{u}\|_{L_2(K)}^2 + \kappa \|\mathbf{u}\|_{L_2(K)}^2).$$

□

Proof of the condition number estimate (6.23) for the AFW-block Jacobi-preconditioner.

The key of the AFW-subspace splitting is that it provides also a correct splitting of gradient fields in $\nabla W_{h,1}(\mathcal{T}_h)$.

We consider the Helmholtz-decomposition (cf. Theorem 3.14) of $\mathbf{u} \in V_h^{\mathcal{N}_0}(\mathcal{T}_h)$:

$$\mathbf{u} = \mathbf{q} + \nabla w \quad \text{with } w \in W_{h,1}(\mathcal{T}_h) \subset H^1(\Omega), \quad \forall v \in W_{h,1}(\mathcal{T}_h) : (\mathbf{q}, \nabla v)_0 = 0. \quad (6.25)$$

and analyze the solenoidal and the irrotational field, separately.

Concerning the decomposition of gradient field ∇w , we consider first the decomposition of w with respect to the H^1 -conforming shape functions $\{\phi_i\}$, namely $w = \sum_{v_i \in \mathcal{V}} w(v_i) \phi_i$. Since $\nabla \phi_i \in V_i$, we obtain a decomposition of the gradient field ∇w in V_i :

$$\nabla w = \sum_{v_i \in \mathcal{V}} \nabla w_i \quad \text{with } \nabla w_i = w(v_i) \nabla \phi_i \in V_i.$$

We consider now a physical element K , sharing vertex v_i , and use the inverse inequality from Remark 6.2, to obtain

$$\|\nabla w_i\|_{A^\kappa, K}^2 = \kappa \|\nabla w_i\|_{L_2(K)}^2 \preceq h^{-2} \kappa \|w\|_{L_2(K)}^2.$$

Summing up we obtain

$$\sum_{v_i \in \mathcal{V}} \|\nabla w_i\|_{A^\kappa}^2 \preceq h^{-2} \kappa \|w\|_{L_2(\Omega)}^2 \stackrel{(**)}{\preceq} h^{-2} \kappa \|\mathbf{u}\|_{L_2(\Omega)}^2 \preceq h^{-2} \|\mathbf{u}\|_{A^\kappa}^2. \quad (6.26)$$

Note that we have used Friedrichs' inequality for $H^1(\Omega)$ in (**) and have exploited the L_2 -orthogonality of the decomposition in the sense of $\|\mathbf{u}\|_0^2 = \|\mathbf{q}\|_0^2 + \|\nabla w\|_0^2$.

Now, we consider the solenoidal part $\mathbf{q} \in (\nabla W_{h,1})^\perp$ with $\text{curl } \mathbf{q} = \text{curl } \mathbf{u}$. Since the decomposition into Nédélec basis functions $\varphi_i^{\mathcal{N}_0}$ provides a finer decomposition of the AFW-splitting, we can use the estimate from the proof of the Jacobi-preconditioner. But here, we can use Friedrichs' inequality

$$\|\mathbf{q}\|_0 \preceq \|\text{curl } \mathbf{q}\| = \|\text{curl } \mathbf{u}\|. \quad (6.27)$$

in the estimate (*), which yields

$$\begin{aligned} \sum_{v_i \in \mathcal{V}} \|\mathbf{q}_i\|_{A^\kappa}^2 &\preceq (h^{-2} + \kappa) \|\mathbf{q}\|_{L_2(\Omega)}^2 \preceq h^{-2} \|\text{curl } \mathbf{u}\|_0^2 + \kappa \|\mathbf{u}\|_0^2 \\ &\preceq (h^{-2} + 1) (\|\text{curl } \mathbf{u}\|_0^2 + \kappa \|\mathbf{u}\|_0^2) \preceq (h^{-2} + 1) \|\mathbf{u}\|_{A^\kappa}^2. \end{aligned} \quad (6.28)$$

Concluding, we consider the decomposition $\mathbf{u}_i = \mathbf{q}_i + \nabla w_i$ and combine the two estimates (6.26) and (6.28). This yields

$$\inf_{\mathbf{u}=\sum \mathbf{u}_i} \|\mathbf{u}_i\|_{A^\kappa}^2 \preceq (h^{-2} + 1) \|\mathbf{u}\|_{A^\kappa}^2.$$

□

The AFW-decomposition provides a correct space splitting of gradient fields in the following sense

$$\sum_{v_i \in \mathcal{V}} \nabla W_{h,1} \cap V_i = \nabla W_{h,1}.$$

The h^{-2} -dependency of condition number can be tackled by multigrid methods.

6.2.2 The smoothers of Arnold-Falk-Winther and Hiptmair

The two preceding examples demonstrate the importance and necessity of applying an appropriate smoother for $H(\text{curl})$ -problems. The operator scales differently on the solenoidal and the irrotational fields. Appropriate smoothers can be designed by means of a Schwarz splitting of the underlying Nédélec FE-space, which respects the Helmholtz-decomposition. Only then can associated multigrid/multilevel methods work efficiently.

We assume an $H(\text{curl})$ -conforming Nédélec space $V_{h,p}(\mathcal{T}_h)$ of uniform order p , and an appropriate H^1 -conforming FE-space $W_{h,p+1}(\mathcal{T}_h)$, which satisfy the *global exact sequence property*, i.e. $\nabla W_{h,p+1}(\mathcal{T}_h) \subset V_{h,p}(\mathcal{T}_h)$.

Up to the author's knowledge, there are two established and commonly used techniques for designing appropriate smoothers which can be defined using the discussed space splittings within the Schwarz framework:

- The *Arnold-Falk-Winther* (AFW) smoother is based on an overlapping space splitting according to the vertex patches:

$$V_{h,p} = \sum_{v \in \mathcal{V}} V_{\omega_v} \quad \text{with} \quad V_{\omega_v} := \{\mathbf{u} \in V : \text{supp}(\mathbf{u}) \subset \omega_v\}, \quad (6.29)$$

where ω_v denotes the vertex patch as defined in (5.38) (cf. ARNOLD-FALK-WINTHER [7]).

- The space splitting suggested by *Hiptmair* explicitly respects the Helmholtz decomposition:

$$V_{h,p} = \sum_{E \in \mathcal{E}} V^E + \sum_{v \in \mathcal{V}} \nabla W^v \quad (6.30)$$

with the subspaces $W^v := \{w \in W_{h,p+1} : \text{supp}\{w\} \subset \omega_v\}$ corresponding to the vertex-patch ω_v as defined in (5.38) and $V^E := \{\mathbf{v} \in V_{h,p} : \text{supp}\{\mathbf{v}\} \subset \omega_E\}$ corresponding to the edge-patch ω_E .

The smoothing iteration corresponding to the explicit splitting of gradient fields can be performed by a solver on the scalar potential problem. For a detailed description see HIPTMAIR-TOSELLI [58].

Unfortunately, we observe that as the polynomial degree \mathbf{p} increases, these local spaces can grow quite large. For instance, the suggested vertex-patch space involved in the AFW-splitting is spanned by the following shape functions

$$V^v = \bigoplus_{E_m \in \mathcal{E} : v \text{ on } E_m} \left\{ V_{\mathbf{p}E_m}^{E_m} \oplus \text{span} \{ \varphi_{E_m}^{\mathcal{N}_0} \} \right\} \oplus \bigoplus_{F_m \in \mathcal{F} : v \text{ on } F_m} V_{\mathbf{p}F_m}^{F_m} \oplus \bigoplus_{K \in \mathcal{T}_h : v \text{ on } K} V_{\mathbf{p}C}^C.$$

At this point, we can exploit the *local exact sequence property* of the shape functions discussed in Chapter 5, which ensures parameter-robust preconditioning even for simple space splittings. Toward this goal, we will need a more general result on Schwarz preconditioners for parameter-dependent problems.

6.2.3 Schwarz methods for parameter-dependent problems

In the following, we present a key result stated and proved in SCHÖBERL [80] (Theorem 4.2), which provides a general framework for defining robust Schwarz preconditioners driven by parameter dependent problems in structural mechanics. In advance, we remark that we present a simplified version of this theorem with $Q = L_2(\Omega)$ and $\| \cdot \|_{Q,0} = \| \cdot \|_c = \| \cdot \|_0$ on $\text{curl} V$, coresponding to the problem setting in $H(\text{curl})$.

Theorem 6.4 (Robust one-level ASM preconditioners for parameter-dependent problems). *We consider a finite-dimensional Hilbert space V . Let $A^\kappa : V \times V \rightarrow \mathbb{R}$ be a parameter-dependent coercive bilinear form*

$$A^\kappa(u, v) = a(u, v) + \kappa^{-1}(\Lambda u, \Lambda v)_{L_2} \quad (6.31)$$

with

- an energy norm, which for $\kappa = 1$ is equivalent to the norm of the underlying space, i.e.

$$\| \cdot \|_{A^1} \simeq \| \cdot \|_V, \quad (6.32)$$

- a continuous linear operator

$$\Lambda : V \rightarrow L_2(\Omega)$$

with a non-trivial nullspace $V_0 := \ker \Lambda$ and that satisfies the inverse estimate

$$\forall \mathbf{q} \in \Lambda V \exists \mathbf{v} \in V : \quad \| \mathbf{v} \|_V \leq c_3(h) \| \mathbf{q} \|_0. \quad (6.33)$$

Let $\{V_i\}$ be a local space splitting with finite overlap such that the kernel V_0 can be split locally into kernel functions, i.e.

$$V = \sum_{i=0}^M V_i \quad \text{and} \quad V_0 = \sum_{i=0}^M (V_i \cap V_0). \quad (6.34)$$

Furthermore, we assume that the local splittings of the functions $u \in V$ and $u_0 \in V_0$ can be estimated in $\| \cdot \|_V$ as follows

$$\inf_{\substack{u = \sum_{i=0}^M u_i \\ u_i \in V_i}} \sum_{i=0}^M \| u_i \|_V^2 \leq c_1(h) \| u \|_V^2, \quad (6.35)$$

$$\inf_{\substack{u_0 = \sum_{i=0}^M u_{0,i} \\ u_{0,i} \in V_i \cap V_0}} \sum_{i=0}^M \| u_{0,i} \|_a^2 \leq c_2(h) \| u_0 \|_V^2. \quad (6.36)$$

Then the additive Schwarz preconditioner C built on the space splitting $\{V_i\}$ fulfills

$$(c_1(h) + c_2(h)c_3(h)^2)^{-1}C(\mathbf{u}, \mathbf{u}) \preceq A^\kappa(\mathbf{u}, \mathbf{u}) \leq N_o C(\mathbf{u}, \mathbf{u}) \quad \forall \mathbf{u} \in V_{h,\mathbf{p}}(\mathcal{T}_h) \quad (6.37)$$

with bounds $c_1(h)$ and $c_2(h)$ independent of the parameter $0 < \kappa \leq 1$. The constant N_o denotes the maximal number of overlapping subspaces.

The main achievement of this theorem is that for a subspace splitting which provides (6.34) we obtain parameter-robustness and that the spectral bounds of the preconditioned problem hold with the estimates of the splitting norms, separately for u and the kernel functions u_0 for $\kappa = 1$.

We set $\Lambda := \text{curl}$. Then (6.33) holds by choosing \mathbf{v} such that $\mathbf{q} = \text{curl } \mathbf{v}$ with $(\mathbf{v}, \mathbf{w}) = 0, \forall \mathbf{w}$ and using the discrete Friedrichs' inequality for $H(\text{curl})$

$$\|\mathbf{v}\|_0^2 \leq c_F(p) \|\text{curl } \mathbf{v}\|_0^2 \quad \forall \mathbf{v} \in (V \cap \ker(\text{curl}))^\perp. \quad (6.38)$$

Hence, we can directly deduce a result on parameter-robust preconditioners for the variational problem (6.20) in $H(\text{curl})$.

Corollary 6.5 (Parameter-robust ASM preconditioner for $H(\text{curl})$).

Let $V_{h,\mathbf{p}}(\mathcal{T}_h) \subset H(\text{curl}, \Omega)$ denote a Nédélec FE-space of order \mathbf{p} and $W_{h,\mathbf{p}+1}(\mathcal{T}_h) \subset H^1(\Omega)$ an appropriate scalar FE-space of order $\mathbf{p} + 1$ with $\ker(\text{curl}, V_{h,\mathbf{p}}(\mathcal{T}_h)) = \nabla W_{h,\mathbf{p}+1}(\mathcal{T}_h)$ and $\nabla W_{h,\mathbf{p}+1}(\mathcal{T}_h) \subset V_{h,\mathbf{p}}(\mathcal{T}_h)$.

We consider following subspace splitting of the FE-spaces, assuming finite overlap:

$$W_{h,\mathbf{p}}(\mathcal{T}_h) = \sum_{j=0}^{M_W} W_j \quad \text{and} \quad V_{h,\mathbf{p}}(\mathcal{T}_h) = \sum_{i=0}^M V_i.$$

If

$$\forall W_j \exists V_i : \nabla W_j \subset V_i \quad (6.39)$$

and if the local splitting of the functions in $V_{h,\mathbf{p}}$ and the involved gradient fields provide the estimates

$$\inf_{\mathbf{u} = \sum_{\mathbf{u}_i \in V_i} \mathbf{u}_i} \sum_{i=0}^M \|\mathbf{u}_i\|_{H(\text{curl})}^2 \leq c_1(h, \mathbf{p}) \|\mathbf{u}\|_{H(\text{curl})}^2, \quad (6.40)$$

$$\inf_{w = \sum_{w_j \in W_j} w_j} \sum_{j=0}^{M_W} M_W \|\nabla w_j\|_0^2 \leq c_2(h, \mathbf{p}) \|\nabla w\|_0^2, \quad (6.41)$$

then the additive Schwarz preconditioner C built on the space splitting $\{V_i\}$, applied to the parameter-dependent curl-curl-problem (6.16), is robust in κ :

$$(c_1(h, \mathbf{p}) + c_2(h, \mathbf{p})(1 + c_F)^2)^{-1}C(v, v) \preceq A^\kappa(v, v) \leq N_o C(v, v) \quad \forall v \in V. \quad (6.42)$$

with c_F the constant from the discrete Friedrichs' inequality (6.38) is independent of h and p (see DEMKOWICZ-BUFFA [43] and GOPALAKRISHNAN-DEMKOWICZ [50]).

6.2.4 Parameter-robust ASM methods and the local exact sequence property

In the following, we apply Corollary 6.5 first for general H^1 -conforming and $H(\text{curl})$ -conforming FE-spaces satisfying the local exact sequence property and next for FE-spaces based on the finite element shape functions presented in Chapter 5.

Corollary 6.6.

1. Let the FE-spaces $W_{h,\mathbf{p}+1}(\mathcal{T}_h) \subset H^1(\Omega)$ and $V_{h,\mathbf{p}}(\mathcal{T}_h) \subset H(\text{curl}, \Omega)$ satisfy the local exact sequence property (Theorem 5.32). Then any space splitting $\{V_i\}$ of the Nédélec space $V_{h,\mathbf{p}}(\mathcal{T}_h)$ built on the (possibly finer) \mathcal{N}_0 -E-F-C-based splitting

$$V_{h,\mathbf{p}} = V_h^{\mathcal{N}_0}(\mathcal{T}_h) + \sum_{E \in \mathcal{E}} V_{\mathbf{p}_{E+1}}^E(\mathcal{T}_h) + \sum_{F \in \mathcal{F}} V_{\mathbf{p}_{F+1}}^F(\mathcal{T}_h) + \sum_{K \in \mathcal{T}_h} V_{\mathbf{p}_{K+1}}^K(\mathcal{T}_h) \quad (6.43)$$

fulfills (6.39) and specifies a parameter-robust ASM preconditioner.

2. Let $W_{h,\mathbf{p}+1}(\mathcal{T}_h) \subset H^1(\Omega)$ be defined by (5.39) and $V_{h,\mathbf{p}}(\mathcal{T}_h) \subset H(\text{curl}, \Omega)$ defined by (5.39), i.e. the Nédélec FE-basis explicitly contains the gradients of the higher-order basis functions of the scalar FE-basis. Then any Nédélec space splitting $\sum_i V_i = V_{h,\mathbf{p}}(\mathcal{T}_h)$ which is built on a two-level concept, where the lowest-order space $V_h^{\mathcal{N}_0}(\mathcal{T}_h)$ is either solved exactly or is split corresponding to the Arnold-Falk-Winther splitting (6.29) or to the one of Hitpmair (6.30) fulfills (6.39) of Corollary 6.5 and implies a parameter-robust ASM preconditioner.

Of course, the choice of the local subspaces influences the condition number through h and p dependency. But, a splitting based on the FE-basis, suggested in Chapter 5, automatically respects the Helmholtz-decomposition for higher-order FE-subspaces. To achieve parameter-robustness we only have to care about the correct splitting of lowest-order space within the design of appropriate smoothers.

The following numerical experiment verifies the κ -robustness using the $H(\text{curl})$ -conforming FE-basis of Chapter 5.

Numerical experiments

We consider $A^\kappa(\mathbf{u}, \mathbf{v}) = \int_\Omega \text{curl } \mathbf{u} \text{ curl } \mathbf{v} \, dx + \int_\Omega \kappa \mathbf{u} \mathbf{v} \, dx$ on the unit cube $\Omega = [0, 1]^3$, which is covered by a triangulation of 12 tetrahedra. We use a Schwarz preconditioner with the \mathcal{N}_0 -E-F-C-based space splitting (6.43). On the lowest-order space $V_h^{\mathcal{N}_0}(\mathcal{T}_h)$ we use a direct solver.

We run the experiment for two parameters $\kappa = 1$ and $\kappa = 10^{-6}$. Alternatively, we apply static condensation of the cell-based degrees of freedom.

Due to the local exact sequence property the space splitting recovers the gradient fields in the sense of (6.39). As stated by Corollary 6.5, we can observe in Figure 6.2 that the condition number is not affected by the choice of the parameter κ .

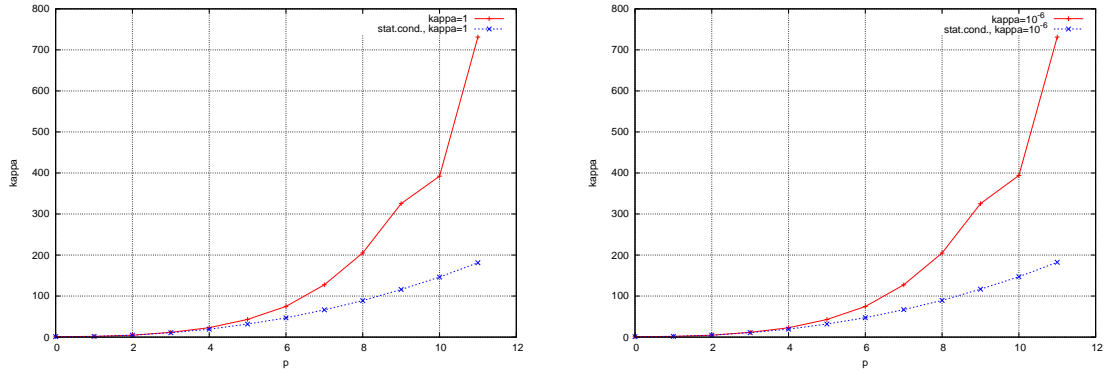


Figure 6.2: Robustness of condition numbers of parameter-dependent curl – curl problem on the unit cube for $\kappa = 1$ (left) and $\kappa = 10^{-6}$ (right)

6.3 Reduced Nédélec Basis and Special Gauging Strategies

In this section, we review the gauging strategy of magnetostatic problems, which also apply in non-conducting regions of magneto-quasi-static problems. We start with the initial variational formulation: Find $\mathbf{u} \in V \subset H(\text{curl})$ such that

$$\int_{\Omega} \text{curl } \mathbf{u} \text{ curl } \mathbf{v} \, d\mathbf{x} = \int_{\Omega} \mathbf{j} \mathbf{v} \, d\mathbf{x}, \quad \forall \mathbf{v} \in V.$$

The solution of the curl – curl problem is determined up to gradients. In the following, we suggest a practical method for gauging high-order gradient functions.

The idea is simple and practical convenient, if we assume the $H(\text{curl})$ -conforming finite element basis, suggested in Chapter 5, which explicitly involves (higher-order) gradient functions:

- The higher-order gradients can be gauged by locally skipping the corresponding degrees of freedom and basis functions in the higher-order edge-based, face-based and cell-based finite element subspaces.
- On the lowest-order subspace, we follow the former strategy of adding a regularization term.

The reduced Nédélec basis Following Subsection 5.2.7 we introduce the *reduced local FE-space* on the element K as

$$V_{\mathbf{p}}^{\text{red}}(K) := V^{\mathcal{N}_0}(K) \oplus \bigoplus_{F_m \in \mathcal{F}_K} V_{p_{F_m}}^{F_m,2}(K) \oplus V_{p_{F_m}}^{F_m,3}(K) \oplus V_{p_C}^{C,2}(K) \oplus V_{p_C}^{C,3}(K). \quad (6.44)$$

and the corresponding *reduced global finite space* $V_{h\mathbf{p}}^{\text{red}}(\mathcal{T}_h)$.

Here, we have skipped the higher-order gradient functions spanning the local subspaces $V_{p_{F_m}}^{E_m}(K)$, $V_{p_{F_m}}^{F_m,1}(K)$, and $V^{C,1}(K)$. We remark that, in general, the reduced finite element space is not orthogonal to higher-order gradient fields. Moreover, the skipping of gradient functions can be done separately on each edge, face and cell, hence we can perform reduced basis gauging only on single subdomains as required for magneto-quasi-static problems involving subdomains corresponding to non-conducting materials.

Gauging on the lowest-order space Gauging with respect to lowest-order shape functions is performed by adding a zero-order term with small regularization parameter. Hence, in practice, it is sufficient to apply only a low-order integration formula within the integration of the element mass matrix denoted by $(\cdot, \cdot)_{L_2(\Omega), \text{red}}$.

Note, that for gauging in lowest-order spaces, the spanning tree technique, which is based on a graph theoretic treatment (cf. BOSSAVIT [25], Section 5.3), provides an alternative. But, since we are equipped with κ -robust preconditioners gauging by regularization is more suitable, in particular from the implementational point of view.

The discrete variational problem on the reduced FE-space Hence, for magnetostatic problem or for non-conducting regions of magneto-quasi-static problems we state the discrete problem in the reduced FE-basis with a regularization parameter $0 < \kappa \ll 1$ as follows.

Find $\mathbf{u} \in V_{h,\mathbf{p}}^{\text{red}}(\mathcal{T}_h)$ such that

$$\int_{\Omega} \text{curl } \mathbf{u} \text{ curl } \mathbf{v} \, d\mathbf{x} + \kappa(\mathbf{u}, \mathbf{v})_{L_2(\Omega), \text{red}} = \int_{\Omega} \mathbf{j} \mathbf{v} \, d\mathbf{x}, \quad \forall \mathbf{v} \in V_{h,\mathbf{p}}^{\text{red}}(\mathcal{T}_h). \quad (6.45)$$

We remark that the resulting magnetic induction field $\mathbf{B} = \text{curl } \mathbf{u}$, in which we are mainly interested, is unchanged by the choice of the full FE-basis or the reduced FE-basis.

We observe two main advantages in using the reduced FE-basis:

- More than one third of degrees of freedom can be saved (for $p \geq 1$), which results in a decrease of the non-zero entries in the system matrix to 55 %.
- As to be observed in the following numerical experiments, the condition numbers highly improves within the reduced FE-basis setting.

Numerical experiment Again, we consider the unit cube covered with a mesh of 6 tetrahedra. In Figure 6.3 we present the condition numbers of the preconditioned system $C_{\text{red}}^{-1} A_{\text{red}}$ computed in the reduced bases to the ones computed in the full FE-basis. In both cases, we use \mathcal{N}_0 - E - F - C -based multiplicative Schwarz preconditioners using a direct solver on the coarse level. We run our tests for uniform p -refinement and choose the regularization term by $\kappa = 10^{-6}$. Optionally, we use static condensation of the cell-based degrees of freedom. We observe a considerable improvement of the condition numbers in case of the reduced basis gauging.

6.4 Numerical Results

In the following, we are concerned with the numerical evidence of κ -robust preconditioning and reduced basis gauging within more involved problems.

We choose a two-level Schwarz solver analogous to the one stated in (6.1.2), which is based on the local \mathcal{N}_0 - E - F - C -based splitting and uses either exact solvers on the coarse level, i.e. on the space of lowest-order Nédélec functions, or h -version multigrid methods with Arnold-Falk-Winther smoothers, if the problem size of the coarse system increases.

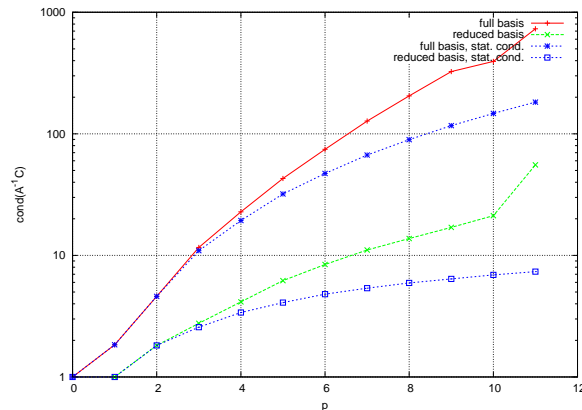


Figure 6.3: Condition numbers using full basis vs. reduced basis on unit cube with/without static condensation

6.4.1 The magnetostatic problem

We consider the magnetostatic boundary value problem

$$\operatorname{curl} \mu^{-1} \operatorname{curl} \mathbf{A} = \mathbf{j},$$

where \mathbf{j} denotes the given current density with $\operatorname{div} \mathbf{j} = 0$, and \mathbf{A} is the vector potential of the magnetic flux $\mathbf{B} = \operatorname{curl} \mathbf{A}$. For gauging, we add a small zero-order term (with $\kappa = 10^{-6} \mu^{-1}$) to the operator. In order to show the performance of the constructed shape functions we compute the magnetic field induced by a cylindrical coil.

The mesh generated by NETGEN (cf. SCHÖBERL [79]) contains 2029 curved tetrahedral elements. Figures 6.4 and 6.5, show the magnetic field lines and the absolute value of the magnetic flux simulated with $H(\operatorname{curl})$ -elements of uniform degree $p = 6$.

We have chosen various uniform polynomial degrees p , and compared the number of unknowns (dofs), the condition numbers of the preconditioned system, the required iteration numbers of the PCG for an error reduction by 10^{-9} , and the required computation time on a Dual Processor Intel Xeon 64Bit 2,8 GHz machine. We run the experiments once keeping the gradient shape functions, and a second time skipping them. The computed \mathbf{B} -field is the same for both versions. One can observe a considerable improvement of the required solver time in the Table 6.1.

We run the experiments a third and a fourth time, but extend the solution algorithm by static condensation of the cell-based degrees of freedom. Again, one observes a considerable improvement, when using the reduced basis (cf. Table 6.2).

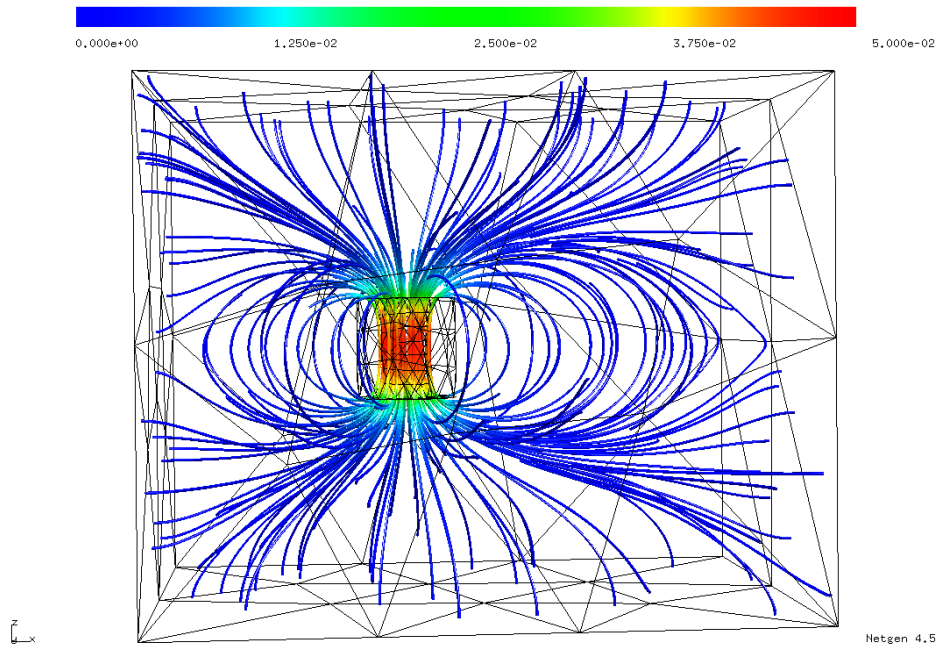


Figure 6.4: Magnetic field induced by the coil, order $p=6$.

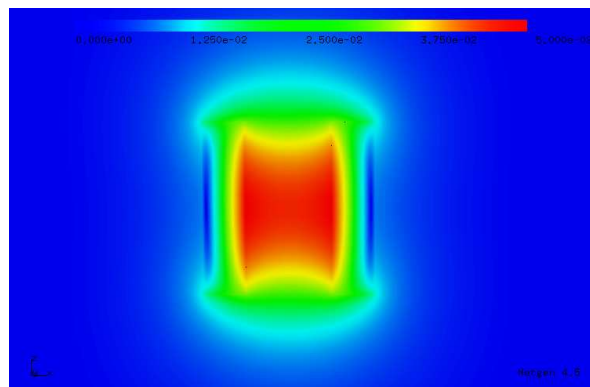


Figure 6.5: Absolute value of the magnetic flux $B = \text{curl } \mathbf{A}$ (zoom to coil), order $p=6$.

p	dofs	grads	$\kappa(C^{-1}A)$	iter	solvetime
2	19707	yes	16.99	31	1.5 s
2	10676	no	6.64	23	0.4 s
3	50820	yes	46.17	49	6.6 s
3	29084	no	15.48	34	1.6 s
4	104350	yes	102.07	69	27.8 s
4	61744	no	26.27	44	5.5 s
5	186384	yes	210.34	96	94.8 s
5	112714	no	43.52	54	16.7 s
6	303009	yes	406.11	127	314.0 s
6	186052	no	67.48	63	43.5 s
7	460312	yes	751.06	171	923.3 s
7	285816	no	95.08	72	106.6 s
8	664380	yes	1033.05	201	2080.8 s
8	416064	no	128.61	82	272.4 s

Table 6.1: Performance of solver: full vs. reduced basis (no static condensation)

p	dofs	grads	$\kappa(C^{-1}A)$	iter	solvetime
2	19707	yes	16.99	31	1.2 s
2	10676	no	6.64	23	0.4 s
3	50820	yes	42.81	46	5.2 s
3	29084	no	13.79	32	1.3 s
4	104350	yes	79.86	62	20.2 s
4	61744	no	21.01	39	3.2 s
5	186384	yes	135.70	78	51.5 s
5	112714	no	27.45	44	6.9 s
6	303009	yes	207.02	91	120.3 s
6	186052	no	33.33	48	13.5 s
7	460312	yes	295.79	103	244.5 s
7	285816	no	38.63	51	24.2 s
8	664380	yes	398.03	114	430.1 s
8	416064	no	43.38	54	41.7 s

Table 6.2: Performance of solver: full vs. reduced basis with static condensation

6.4.2 The magneto quasi-static problem: A practical application

The intention of this section is to verify the applicability of the constructed FE-basis, the parameter-robust preconditioners and the reduced basis gauging (in non-conducting regions) in a practical industrial application. We consider the industrial problem setting of computing the eddy currents within a bus bar, a common device in transformers.

We consider the magneto-quasi-static problems, i.e., Problem 3.32 Find $\mathbf{u} \in V := H_{0,D}(\text{curl}, \Omega)$ satisfying

$$\int_{\Omega} \mu^{-1} \text{curl } \mathbf{u} \cdot \text{curl } \bar{\mathbf{v}} \, d\mathbf{x} + \int_{\Omega} \kappa \mathbf{u} \cdot \bar{\mathbf{v}} \, d\mathbf{x} = \int_{\Omega} \mathbf{j} \cdot \bar{\mathbf{v}} \, d\mathbf{x} \quad \forall \mathbf{v} \in V. \quad (6.46)$$

with $\kappa = i\omega\sigma$ with given frequency ω and given conductivity coefficient $\sigma \geq 0$.

In non-conducting domains we perform gauging by a small regularization parameter $\sigma = \varepsilon \ll \mu^{-1}$.

A solver strategy for the magneto-quasi-static problem

We briefly outline the chosen strategy for solving the magneto-quasi-static system:

- In non-conducting domains, e.g. air, where $\sigma = \varepsilon$ due to regularization or $\sigma \ll \mu^{-1}$ we can apply the reduced basis gauging strategy. We simply skip the higher-order gradients in the FE-basis on edges, faces and cells belonging to non-conducting domains.
- For solving $A^\kappa u = f$ with $K + \kappa M$ we use a complex PCG method, i.e. PCG with complex-valued matrices and a complex-valued search parameter.
- The preconditioner for $A^\kappa = K + \kappa M$ is chosen to be a κ -robust preconditioner of the system $\tilde{A}^\kappa = K + |\kappa|M$.

A detailed description and justification of the solution algorithm provided by the second and the third item can be found in BACHINGER ET AL. [14], [13]. Concerning the solution of symmetric complex-valued systems we further refer to CLEMENS-VAN RIENEN-WEILAND [36] and CLEMENS-WEILAND [37].

Numerical Simulation of Eddy-currents in a bus bar

We want to simulate the eddy currents which are originated in a bus bar of a power transformer.

Since we are only interested in simulating the eddy currents in the bus bar we separate it from the transformer by cutting the bars. Hence, we have to construct artificially a current distribution in the non-resolved domain, which models the current distribution of the original problem. This can be done by solving a scalar Neumann problem where the Neumann data is specified by the prescribed normal currents on the cutting planes of the bars and vanishing on the remaining boundary. This results in a current density \mathbf{j} in the outer domain, which we use in the right hand side of the magneto-quasi-static problem (6.46). Note that the obtained current density is not divergence-free.

Figure 6.6 shows the eddy-currents in the bus bar of a transformer for polynomial order $p = 3$. In the air domain we use the reduced basis with polynomial order $p = 3$. The mesh consists

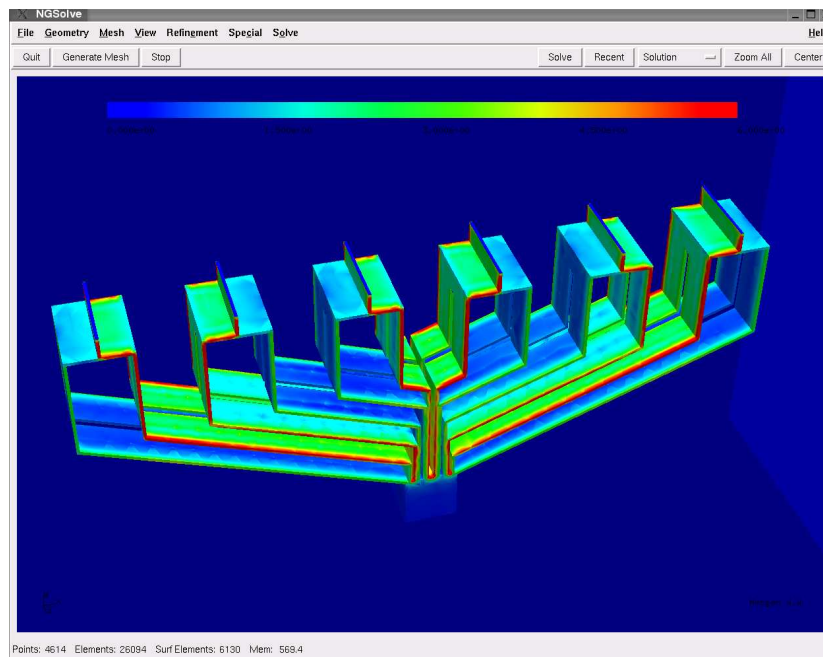


Figure 6.6: Eddy currents in a bus bar

p	partially reduced basis	dofs	solver time
2	no	249297	968 s
2	yes	193502	768 s
3	no	645932	4824 s
3	yes	503601	3682 s

Table 6.3: Comparison of degrees of freedom and solver times by using a partially reduced basis for the bus bar eddy-current problem

of 26094 tetrahedral elements.

In Table 6.3 we compare the numbers of degrees of freedom and the solution time of the magneto-quasi-static problem running the experiment once using the full FE-basis and a second time using the partially reduced basis gauging in the non-conducting outer domain.

Chapter 7

The Maxwell Eigenvalue Problem

The numerical solution of eigenvalue problems is in general more challenging than the one of boundary value problems. Eigenvalue problems for Maxwell's equations involve even further difficulties, in particular due to large kernels of the involved operators, e.g., the curl-operator. The discretization with $H(\text{curl})$ -conforming finite elements is highly important in order to avoid spurious (non-physical) eigenvalues within the computed spectrum. Moreover, the involved H^1 -conforming and $H(\text{curl})$ -conforming FE-spaces have to satisfy the exact sequence property.

The numerical analysis of Maxwell eigenvalue problems (cf. e.g. BOFFI ET AL [20], MONK ET AL. [71], CAORSI ET AL. [34], BOFFI ET AL. [21],[19], and KIKUCHI [61]) and preconditioned eigensolvers (cf. e.g. KNYAZEV-NEYMEYR [64], KNYAZEV [62], and NEYMEYR [74]) is very challenging and subject of ongoing research. A rigorous analysis is available only for subproblems, and many approaches are justified mainly by numerical evidence.

The aim of this section is to present a reasonable approach for attacking Maxwell eigenvalue problems. We will see that the local exact sequence property, which holds for our construction of conforming FE-spaces, has certain advantages in the solution of the eigenvalue problems, in particular in efficient preconditioning. We will finally demonstrate the performance of the proposed algorithm by solving a benchmark problem involving highly-singular eigensolutions. For the numerical solution we will also use anisotropic hp -discretizations and geometric mesh refinement.

7.1 Formulation of the Maxwell Eigenvalue Problem

An important problem in electromagnetics is the simulation of bounded cavities, which are characterized by

- a bounded domain filled with non-conducting dielectric materials ($\sigma = 0$, $\rho = 0$) with strictly positive, piecewise constants μ and ϵ ,
- surrounding perfectly conducting materials, e.g. metallic surfaces.

By reflection at the perfectly conducting walls, standing waves can be excited within the cavity. Therefore, even with homogenous boundary conditions and no sources in form of charges or currents, non-trivial solutions arise at special, so-called *resonant frequencies*. The problem

of determining resonant frequencies $\omega \neq 0$ and the corresponding eigenmodes satisfying the time-harmonic Maxwell equations is the following:

Find the electric field \mathbf{E} , the magnetic field \mathbf{H} and resonant frequencies $\omega > 0$ satisfying

$$\operatorname{curl} \mathbf{E} + i\omega\mu\mathbf{H} = 0, \quad (7.1a)$$

$$\operatorname{curl} \mathbf{H} - i\omega\epsilon\mathbf{E} = 0, \quad (7.1b)$$

$$\operatorname{div}(\mu\mathbf{H}) = 0, \quad (7.1c)$$

$$\operatorname{div}(\epsilon\mathbf{E}) = 0. \quad (7.1d)$$

For simplicity, we assume the material parameters μ and ϵ to be strictly positive scalars. The surrounding perfect electric conductor yields homogenous Dirichlet boundary condition for the tangential components of the electric field, which in turn corresponds to homogenous Neumann condition for the magnetic field. By eliminating either the magnetic or the electric field, we can reduce the system (7.1) to one of the following problems:

The electric eigenvalue problem: Find resonant frequencies $\omega \neq 0$ and the related electric fields \mathbf{E} such that

$$\operatorname{curl} \mu^{-1} \operatorname{curl} \mathbf{E} = \omega^2 \epsilon \mathbf{E} \quad \text{in } \Omega, \quad (7.2a)$$

$$\operatorname{div} \epsilon \mathbf{E} = 0 \quad \text{in } \Omega, \quad (7.2b)$$

$$\mathbf{E} \times \mathbf{n} = 0 \quad \text{on } \partial\Omega. \quad (7.2c)$$

The magnetic eigenvalue problem: Find $\omega \neq 0$ and the related magnetic fields \mathbf{H} such that

$$\operatorname{curl} \epsilon^{-1} \operatorname{curl} \mathbf{H} = \omega^2 \mu \mathbf{H} \quad \text{in } \Omega, \quad (7.3a)$$

$$\operatorname{div} \mu \mathbf{H} = 0 \quad \text{in } \Omega, \quad (7.3b)$$

$$(\epsilon^{-1} \operatorname{curl} \mathbf{H} \times \mathbf{n}) \times \mathbf{n} = 0 \quad \text{on } \partial\Omega. \quad (7.3c)$$

In the following, we focus only on the electric formulation, but similar considerations also apply to the magnetic case.

Variational formulation of the eigenvalue problem:

Problem 7.1. Find $\lambda \neq 0$ and $\mathbf{u} \in H_0(\operatorname{curl}, \Omega)$ such that

$$\int_{\Omega} \mu^{-1} \operatorname{curl} \mathbf{u} \operatorname{curl} \mathbf{v} \, d\mathbf{x} = \lambda \int_{\Omega} \epsilon \mathbf{u} \mathbf{v} \, d\mathbf{x} \quad \forall \mathbf{v} \in H_0(\operatorname{curl}, \Omega). \quad (7.4)$$

Note that this formulation does not explicitly involve the divergence conditions (7.2b) and (7.3b). But testing (7.4) with gradient fields $\mathbf{v} = \nabla\phi \in \nabla H^1(\Omega)$ yields $\lambda(u, \nabla\phi)_0$. Hence, eigenvectors corresponding to non-zero eigenvalues are L_2 -orthogonal to gradient fields.

We summarize the main properties of the electric eigenvalue problem (cf. MONK [70] Theorem 4.18):

1. The eigenvalue $\lambda = 0$ (which is excluded in our definition of the problem) corresponds to the infinite space of gradient functions $\nabla H^1(\Omega)$.

2. The discrete set of eigenvalues $\lambda_i \neq 0$ correspond to eigenfunctions \mathbf{u}_i with $\operatorname{div} \mathbf{u}_i = 0$ solving the eigenvalue problem (7.4). The eigenvalues form an increasing sequence

$$0 < \lambda_1 \leq \lambda_2 \leq \cdots \nearrow \infty,$$

where every $\lambda_i > 0$ has finite multiplicity.

We want to mention that $H(\operatorname{curl}, \Omega)$ is not compactly embedded in $(L_2(\Omega))^3$, which makes the statement on the behavior of the spectrum difficult. On the other hand, the embedding of $H_0(\operatorname{curl}, \Omega) \cap \ker(\operatorname{div})$ in $(L_2(\Omega))^3$ is compact, and standard results apply. This already indicates that kernel functions will play an important role in the consideration of Maxwell eigenvalue problems.

Galerkin approximation of the eigenvalue problem: We choose an $H(\operatorname{curl})$ -conforming FE-space $V_{h,\mathbf{p}}(\mathcal{T}_h) \subset H_0(\operatorname{curl}, \Omega)$, and formulate the discrete Maxwell eigenvalue problem as follows:

Find $\lambda_h > 0$ and $\mathbf{u}_h \in V_{h,\mathbf{p}}(\mathcal{T}_h)$ such that

$$\int_{\Omega} \mu^{-1} \operatorname{curl} \mathbf{u}_h \operatorname{curl} \mathbf{v}_h \, d\mathbf{x} = \lambda_h \int_{\Omega} \epsilon \mathbf{u}_h \mathbf{v}_h \, d\mathbf{x} \quad \forall \mathbf{v} \in V_{h,\mathbf{p}}(\mathcal{T}_h). \quad (7.5)$$

There is an ongoing debate on how to involve the divergence condition in the solution of the eigenvalue problem. Here, we address this point by excluding the zero eigenvalues within the definition of the eigenvalue problem, and projection onto the complement of gradient fields. Alternatively, one of the following approaches could be used: utilizing a mixed-formulation as introduced in BOFFI [21]; introduction of Lagrange-Multiplier, cf. KIKUCHI [61]; adding a term which penalizes the divergence as suggested in WANG ET AL. [93].

Before we discuss numerical schemes in more detail, we make some brief remarks concerning the convergence analysis of FE-discretizations of Maxwell eigenvalue problems, which is still fairly incomplete:

A Galerkin approximation is called *spectrally correct* (cf. CAORSI ET AL. [34]), if all discrete eigenvalues of (7.5) converge to exact eigenvalues of (7.5), and vice versa, all exact eigenvalues are approximated by discrete ones respecting their multiplicity.

By the *discrete compactness* of Galerkin approximations, a convergence proof for h -version FEM, including edge-elements of general order, is given in MONK ET AL. [71]. Concerning general hp -discretizations in three dimensions, the required discrete compactness of FE-approximations is not fully proved yet, up to our knowledge.

The algebraic Maxwell eigenvalue problem: By means of the Galerkin isomorphism we deduce the generalized algebraic eigenvalue problem equivalent to (7.5):

$$\text{Find } \lambda > 0 \text{ and } u \in \mathbb{R}^N \text{ s.t.} \quad Au = \lambda Mu. \quad (7.6)$$

The matrices are defined by $A_{ij} = (\operatorname{curl} \varphi_i, \operatorname{curl} \varphi_j)_0$ and $M_{ij} = (\varphi_i, \varphi_j)_0$, and the solution vector u is given by $\mathbf{u} = \sum u_i \varphi_i$, where $\{\varphi_i : 1 \leq i \leq N\}$ is a FE-basis of $V_{h,\mathbf{p}}(\mathcal{T}_h)$. We obtain that $A \in \mathbb{R}^{N \times N}$ is *symmetric positive semi-definite* but has a large nullspace associated with the gradient fields, and $M \in \mathbb{R}^{N \times N}$ is *symmetric positive definite*.

7.2 Preconditioned Eigensolvers

System matrices originating from Finite Element discretization of second-order partial differential equations are typically of huge size and ill-conditioned. Due to the large dimension, classical eigensolvers which rely on factorizations of the system matrices can therefore not be applied. On the other hand, also classical matrix-free iterative schemes cannot be used for an efficient solution, due to the ill-conditioned matrices. We refer to BAI ET AL. [15] for an overview of the full range of classical and iterative eigensolvers.

In recent years, preconditioned eigensolvers have attracted significant interest, particularly for the solution of elliptic eigenvalue problems; we refer to D'YAKONOV [47], KNYAZEV [62] and NEYMEYR [74] in this context. Note however, that even for symmetric positive definite generalized eigenvalue problems, sharp non-asymptotic convergence estimates are only available for the simplest iterative scheme, i.e., for the preconditioned inverse iteration, which will be defined below.

In the following, we focus on gradient type preconditioned eigensolvers, which offer some advantages:

- The implementation can be matrix-free, since they only use matrix-vector products of the system matrices or the preconditioner.
- They involve and can exploit the same preconditioners as used for solving the corresponding linear systems.
- The iterative schemes are simple and easy to implement.

We start with considering symmetric positive-definite eigenvalue problems originating, e.g., from self-adjoint elliptic partial differential equations, and then turn back to the Maxwell problems we have in mind.

The symmetric positive definite generalized eigenvalue problem: Let A and M be real, symmetric, positive definite N -by- N matrices. We consider the following (algebraic) eigenvalue problem:

Find an eigenvalue $\lambda \in \mathbb{R}$ and a non-zero eigenvector $u \in \mathbb{R}^N$ such that

$$Au = \lambda Mu. \quad (7.7)$$

We briefly recall some basic results:

1. The generalized eigenvalue problem (7.7) admits N positive eigenvalues λ_i with arbitrary multiplicity such that

$$0 < \lambda_1 \leq \lambda_2 \leq \dots \leq \lambda_N. \quad (7.8)$$

The corresponding eigenvectors u_i can be chosen to be mutually M -orthogonal, i.e. $u_i^T M u_j = \delta_{ij}$, with $u_i^T A u_j = \lambda_i \delta_{ij}$.

2. All stationary points u_i of the Rayleigh quotient

$$\lambda(u) := \frac{u^T A u}{u^T M u} \quad \text{for } u \neq 0, \quad (7.9)$$

are eigenvectors, and $\lambda_i = \lambda(u_i)$ the corresponding eigenvalues.

7.2.1 Preconditioned gradient type methods

Gradient type methods for eigenvalue problems are based on the idea of minimizing the Rayleigh-quotient. Since $\nabla\lambda(u) = \frac{2}{u^T M u}(Au - \lambda(u)Mu)$, the resulting iterative scheme is given by

$$u^{n+1} = u^n - \tau(Au^n - \lambda(u_n)Mu^n). \quad (7.10)$$

The optimal a-priori choice for τ is such that the Rayleigh quotient is minimized, i.e. $\tau_{\text{opt}} := \arg \min_{\tau>0} \lambda(u^n - \tau(Au^n - \lambda(u_n)Mu^n))$.

We assume that our matrices arise from FE-discretization of second order differential operators, and hence we have to deal with the case that A is ill-conditioned by implementing an appropriate preconditioner. Let $C \in \mathbb{R}^{N \times N}$ be a *symmetric positive definite preconditioner* for the matrix A satisfying

$$\gamma_1 u^T C u \leq u^T A u \leq \gamma_2 u^T C u,$$

with spectral bounds $\gamma_1, \gamma_2 \in (0, 1]$. A *preconditioned gradient type method* then has the form

$$u^{i+1} = u^i - \tau C^{-1}(Au^i - \lambda(u_i)Mu^i). \quad (7.11)$$

We shortly comment on the choice of the scaling parameter τ :

- The *preconditioned inverse iteration* is defined by the choice $\tau := 1$.
- The *preconditioned steepest descent* method is defined by choosing the optimal scaling parameter τ_{opt} in the following way. We define the new iterate u^{n+1} as the minimizer of the Rayleigh-quotient on the two-dimensional subspace

$$\text{span} \left\{ u^i, C^{-1}(A - \lambda(u^i)M)u^i \right\}. \quad (7.12)$$

This can be done via the Rayleigh-Ritz subspace method, which requires the solution of the following 2-by-2 projected eigenvalue problem:

Find the smallest Ritz-value $\lambda_{\min} > 0$ and the corresponding Ritz-vector $y_{\min} \in \mathbb{R}^2$ solving

$$X^T A X y = \lambda X^T M X y \quad \text{with } X = [u^i, C^{-1}(A - \lambda(u^i)M)u^i] \in \mathbb{R}^{N \times 2}. \quad (7.13)$$

By setting $u^{i+1} = X y_{\min}$ we obtain an optimal subspace iteration in the sense that we implicitly chose the optimal parameter $\tau = \tau_{\text{opt}}$ in (7.11).

The following estimate for the preconditioned steepest descent method has been obtained in KNYAZEV-NEYMEYR [65] via the ones for preconditioned inverse iteration.

Theorem 7.2. *Let $\lambda_1 \leq \dots \leq \lambda_N$ denote the discrete spectrum of the generalized EVP (7.7) and assume that $\lambda(u^i) \in [\lambda_k, \lambda_{k+1})$. Then $\lambda(u^{i+1})$ computed by iterate (7.11) of the steepest descent method satisfies either $\lambda(u^{i+1}) < \lambda_k$, or $\lambda(u^{i+1}) \in [\lambda_k, \lambda(u^i))$. In the latter case, there holds*

$$\frac{\lambda(u^{i+1}) - \lambda_k}{\lambda_{k+1} - \lambda(u^{i+1})} \leq q^2 \frac{\lambda(u^i) - \lambda_k}{\lambda_{k+1} - \lambda(u^i)}$$

with convergence factor

$$q := 1 - \frac{2}{\kappa(C^{-1}A) + 1} \left(1 - \frac{\lambda_k}{\lambda_{k+1}} \right).$$

In the following, we expand the local space (7.12) in order to improve the iterative scheme. The locally optimal preconditioned conjugate gradient method was introduced in KNYAZEV [63]. Motivated by the preconditioned conjugate gradient method for solving linear systems, Knyazev suggested to enlarge the local space (7.12) with the approximate eigenvector from the previous iteration. The new eigenvector approximation u^{i+1} is chosen to minimize the Rayleigh-quotient within the three-dimensional subspace

$$\text{span} \left\{ u^{i-1}, u^i, C^{-1}(A - \lambda(u^i)M)u^i \right\}.$$

Since the previous iterate u^{i-1} and the current iterate u^i get closer and closer as the iteration proceeds, the Gram-matrices of the Rayleigh-Ritz eigenvalue problem can get more and more ill-conditioned. We address this fact by utilizing an auxiliary vector p^i instead of the previous iterate u^{i-1} : Let $(\lambda_{\min}, y_{\min} = (y_1, y_2, y_3)^T) \in \mathbb{R}^+ \times \mathbb{R}^3$ denote the minimal Ritz-pair of

$$X^T A X y = \lambda X^T M X y \quad \text{with } X = [u^i, w^i, p^i]. \quad (7.14)$$

Then, we choose

$$p^{i+1} = \text{diag}(0, 1, 1)X y_{\min} = u^{i+1} - y_1 u^i.$$

This approach yields the same local space, i.e.,

$$u^{i+1} \in \text{span} \left\{ u^{i-1}, u^i, C^{-1}(A - \lambda(u^i)M)u^i \right\} = \text{span} \left\{ p^i, u^i, C^{-1}(A - \lambda(u^i)M)u^i \right\}. \quad (7.15)$$

Numerical evidence, cf. KNYAZEV [63], suggests that the ill-conditioning of the Gram-matrices is partially resolved in this way. Otherwise, we apply an A -orthogonalization step first. Concerning initial values for the iteration, we start with some vector u^0 and perform the steepest descent method to obtain an initial vector for p^1 .

We want to note that the only convergence result for the LOPCG method is that the method converges at least as fast as the preconditioned gradient methods (7.11), i.e., the bounds of Theorem 7.2 apply. However, besides the Jacobi-Davidson method, the block version of the LOPCG algorithm is accepted to be one of the most efficient preconditioned eigenvalue solvers for symmetric-positive definite generalized EVPs arising from FEM-discretization. We refer to KNYAZEV [63] and ARBENZ-GEUS [5] for detailed numerical results.

7.2.2 Block version of the locally optimal preconditioned gradient method

Block methods (also called subspace iterations) enable us to compute groups of eigenvalues within a special part of the spectrum simultaneously, e.g., the smallest eigenvalues and corresponding eigenvectors. The Rayleigh-Ritz method can easily be extended to a multiple-vector iterative scheme. The main advantages of iterating sets of vectors simultaneously are the following. First, multiple eigenvalues can be calculated in a correct and stable way. Secondly, we can expect much faster convergence, since the error estimates of subspace methods involve the ratio λ_i/λ_{m+1} (m is the subspace dimension and $i \leq m$) instead of λ_1/λ_2 , see e.g. BRAMBLE ET AL. [28].

The basic algorithm for the LOBPCG method

Starting values:

A set of $m \geq 1$ initial vectors $U^0 = [u_1^0, \dots, u_m^0] \in \mathbb{R}^{N \times m}$.

Perform one step of (7.13) to obtain $U^1 = Xy_{\min}$ and $P^1 = \text{diag}(0, 1)Xy_{\min} \in \mathbb{R}^{N \times n}$.

LOBPCG-iteration: for $i = 1, \dots, m$

1. Compute the preconditioned residuals $W^i = C^{-1}(AU^i - MU^i\Lambda_i)$ with $\Lambda_i = \text{diag}(\lambda(u_1^i), \dots, \lambda(u_N^i))$.
2. Solve the $3m$ -by- $3m$ Rayleigh-Ritz-problem with $y \in \mathbb{R}^{3m}$

$$X^T AXy = \lambda X^T M Xy \quad \text{with } X = [U^i, W^i, P^i].$$

3. Take the m smallest Ritz-Pairs $(\lambda_1, Xy_1), \dots, (\lambda_m, Xy_m)$ and set

$$U^{i+1} = [Xy_1, \dots, Xy_m] \quad \text{and} \quad P^{i+1} = [\text{diag}(0, 1, 1)Xy_1, \dots, \text{diag}(0, 1, 1)Xy_m].$$

7.3 Preconditioned Eigensolvers for the Maxwell Problem

We intend to apply the LOBPCG method to the solution of the Maxwell eigenvalue problem (7.6). Note that, similar to iterative linear system solvers, the large kernel of the curl-operator makes the problem more difficult:

1. The curl-curl system matrix A is only positive-semidefinite. Apparently, we cannot apply the algorithms presented above directly.
Solution: We shift the spectrum of the problem by some positive value σ and arrive at the following positive-definite eigenvalue problem:

$$(A + \sigma M)u = (\lambda + \sigma)Mu. \quad (7.16)$$

The corresponding gradient type iteration reads

$$\begin{aligned} u^{i+1} &= u^i - \tau C_{A+\sigma M}^{-1} (A + \sigma M - (\lambda(u^i) + \sigma)M)u^i \\ &= u^i - \tau C_{A+\sigma M}^{-1} (A - \lambda(u^i)M)u^i. \end{aligned} \quad (7.17)$$

with $\lambda(u) = \frac{u^T Au^T}{u^T M u^T}$ denoting the Rayleigh-quotient of the original problem.

Due to the results of Chapter 6, we already have σ -robust preconditioners for $A + \sigma M$ at hand.

2. Iterative scheme, like the gradient type methods, tend to recover the eigenvectors corresponding to the small eigenvalues first. This affects the positive-semidefinite EVP (7.6) as well as the shifted problem (7.16).
Solution: By projecting the iterates u^{i+1} into the complement of the kernel functions, this problem can be resolved, cf. HIPTMAIR-NEYMEYR [57] for the preconditioned inverse iteration.

For the remainder of this section we investigate a combination of the LOBPCG method with (in)exact projection onto the complement of the kernel functions.

7.3.1 Exact and inexact projection onto the complement of the kernel function

We leave the algebraic context for a moment, and first consider the projection operators for the discrete FE-spaces in the operator framework. We want to construct the projection operator of $V_{h,\mathbf{p}}(\mathcal{T}_h)$ onto the complement of the discrete gradient functions $(\nabla W_{h,\mathbf{p}+1}(\mathcal{T}_h))^\perp$.

Lemma 7.3 (Exact Projection). *We consider the finite element spaces $V := V_{h,\mathbf{p}}(\mathcal{T}_h)$ and $W := W_{h,\mathbf{p}+1}(\mathcal{T}_h)$ with $\nabla W \subset V$ as introduced in Chapter 5. Let $B_\nabla : W \rightarrow \nabla W$ denote the gradient operator, $M_V : V \rightarrow V^*$ denote natural embedding operator and $K_\Delta : W \rightarrow W^*$ denote the Laplace-operator.*

Then the L_2 -orthogonal projection operator

$$P_{\ker(A)}^\perp : V \rightarrow (\nabla W)^\perp$$

onto the complement of the gradient functions is given by

$$P_{\ker(A)}^\perp \mathbf{u} = (I - B_\nabla K_\Delta^{-1} B_\nabla^* M_V) \mathbf{u} \quad \forall \mathbf{u} \in V_{h,\mathbf{p}}.$$

Proof. We consider the L_2 -orthogonal projection onto the kernel of the curl-operator

$$P_{\ker(A)} : V \rightarrow \nabla W$$

The action of the projection operator on an element $\mathbf{u} \in V$ can be written in variational form:

For $\mathbf{u} \in V$ find a function $w \in W$ such that $P_{\ker(A)} \mathbf{u} = \nabla w$, i.e.,

$$(\nabla w, \nabla \phi)_0 = (\mathbf{u}, \nabla \phi)_0 \quad \forall \phi \in W. \quad (7.18)$$

This is equivalent to

$$\langle K_\Delta w, \phi \rangle_{W^* \times W} = \langle M_V \mathbf{u}, B_\nabla \phi \rangle_{V^* \times V} = \langle B_\nabla^* M_V \mathbf{u}, \phi \rangle_{W^* \times W}.$$

Setting $P_{\ker(A)}^\perp \mathbf{u} = \mathbf{u} - B_\nabla w$ yields the stated result. \square

For the preconditioned eigensolver with projection, we have to apply this projection for each iterate in order to avoid that the approximated eigenvector converges to a kernel vector. As can be seen from above, the exact L_2 -orthogonal projection requires the solution of a Poisson problem in each iteration step, which usually is much too expensive. We propose to use an inexact projection instead, requiring only an approximative inverse of the Laplace-operator; for details on this approach we refer to HIPTMAIR-NEYMEYR [57].

Definition 7.4 (Inexact Projection). *Let C_Δ denote a scaled preconditioner for the Laplace-operator K_Δ such that $\|K_\Delta\| \leq \|C_\Delta\|$. We define the inexact projection operator $\tilde{P}_{\ker(A)}^\perp : V \rightarrow V$ (corresponding to the exact projection operator $P_{\ker(A)}^\perp$) by*

$$\tilde{P}_{\ker(A)}^\perp \mathbf{u} := (I - B_\nabla C_\Delta^{-1} B_\nabla^* M_V) \mathbf{u} \quad \forall \mathbf{u} \in V.$$

Here we used the notation of the previous lemma.

7.3.2 A preconditioned eigensolver for the Maxwell problem with inexact projection

We return now to the matrix notation, i.e., the algebraic version of the Maxwell eigenvalue problem (7.6), and use the notation introduced for the discrete operators in the previous section now also for the matrix notation. Hence, the (in)exact projection operator can be defined like above.

The inexact projection is realized by repeated application ($k \geq 1$) of the inexact projector $\tilde{P}_{\ker(A)}^\perp$. The basic iteration step of the *inexact inverse iteration method with inexact projection* is then given by

$$\begin{aligned} u^{i+1} &= (\tilde{P}_{\ker(A)}^\perp)^k (I - C_{A+\sigma M}^{-1}(A + \lambda(u^i)M)) u_i \\ &= (I - B_\nabla C_\Delta^{-1} B_\nabla^* M_V)^k (I - C_{A+\sigma M}^{-1}(A + \lambda(u^i)M)) u_i, \end{aligned} \quad (7.19)$$

where M_V denotes the mass matrix with respect to the $H(\text{curl})$ -conforming FE-space V and B_∇ denotes the matrix corresponding to the *discrete gradient operator*, i.e., the representation of gradient fields within the basis of V . Note that in general, the generation of this matrix is non-trivial. However, as we will see below, due to the special choice of basis functions, assembly is rather simple.

We observe that preconditioned gradient methods with inexact projections involve both a curl-curl-preconditioner $C_{A+\sigma M}$ as well as a Laplace preconditioner C_Δ .

The basic algorithm: LOBPCG with inexact projection

Initial setting:

Choose initial vectors $U^0 = (\tilde{P}_{\ker(A)}^\perp)^k U^0 \in \mathbb{R}^{N \times m}$.

Perform one step of (7.13) to obtain $U^1 = (\tilde{P}_{\ker(A)}^\perp)^k X y_{\min}$

and $P^1 = (\tilde{P}_{\ker(A)}^\perp)^k \text{diag}(0, 1) X y_{\min} \in \mathbb{R}^{N \times m}$.

The $(i + 1)$ -iteration:

1. Compute the preconditioned residuals $W^i = C_{A+\sigma M}^{-1}(AU^i - MU^i \Lambda_i)$ with $\Lambda_i = \text{diag}(\lambda(u_1^i), \dots, \lambda(u_N^i))$
2. Solve the $3m$ -by- $3m$ Rayleigh-Ritz-problem with $y \in \mathbb{R}^{3m}$

$$X^T A X y = \lambda X^T M X y \quad \text{with } X = [U^i, W^i, P^i].$$

3. Take the m smallest Ritz-Pairs $(\lambda_1, X y_1), \dots, (\lambda_m, X y_m)$ and set

$$\begin{aligned} U^{i+1} &= (\tilde{P}_{\ker(A)}^\perp)^k [X y_1, \dots, X y_m], \\ P^{i+1} &= (\tilde{P}_{\ker(A)}^\perp)^k [\text{diag}(0, 1, 1) X y_1, \dots, \text{diag}(0, 1, 1) X y_m]. \end{aligned}$$

Concerning the practical implementation, the repeated application of the inexact projection after each iteration is performed by the application of k steps of a preconditioned iterative solver in the potential space. The scaling of the Poisson-preconditioner required in 7.4 is provided by using a multiplicative Schwarz preconditioner C_Δ .

7.3.3 Exploiting the local exact sequence property

The discrete gradient matrix

By means of the local exact sequence property, the discrete gradient matrix is block-diagonal with respect to the low-order, single edge-based, face-based and cell-based blocks. Assuming a reordering of the degrees of freedom corresponding to edges, faces and cells we obtain

$$B_{\nabla} = \text{diag} (B_{\nabla,0}, B_{\nabla,EE}, B_{\nabla,FF}, B_{\nabla,CC}), \quad (7.20)$$

where $B_{\nabla,EE}$, $B_{\nabla,FF}$, $B_{\nabla,CC}$ are again block-diagonal corresponding to each single edge, each single face and each single cell of the triangulation. Since higher-order gradient fields are explicitly used in the construction of the new $H(\text{curl})$ -conforming FE-basis, stated in Chapter 5, several blocks further simplify to the identity matrix I:

$$B_{\nabla,EE} = \mathbf{I}, \quad (7.21)$$

$$B_{\nabla,FF} = \text{diag} (\text{diag}(\mathbf{I}, 0, 0), \dots, \text{diag}(\mathbf{I}, 0, 0)), \quad (7.22)$$

$$B_{\nabla,CC} = \text{diag} (\text{diag}(\mathbf{I}, 0, 0), \dots, \text{diag}(\mathbf{I}, 0, 0)). \quad (7.23)$$

The lowest-order discrete gradient operator $B_{\nabla,0}$ is given by

$$(B_{\nabla,0})_{i,j} = \begin{cases} 1 & \text{if } E_i = [e_1, e_2] \text{ and } j = e_2 \\ -1 & \text{if } E_i = [e_1, e_2] \text{ and } j = e_1 \\ 0 & \text{else} \end{cases}$$

which can be seen by considering the lowest-order degrees of freedom of the Nédélec basis: For a $w \in W_{h,0}(\mathcal{T}_h) \subset H^1(\Omega)$ there holds $\nabla w = \sum_{V_j \in \mathcal{V}} w_j \nabla \phi_j = \sum_E \tilde{w}_i \varphi_i$ with $w_j = w(V_j)$ and $\tilde{w}_i = \int_{e_1}^{e_2} \nabla w \cdot \boldsymbol{\tau} \, d\mathbf{x} = w(V_{e_2}) - w(V_{e_1}) = w_{e_2} - w_{e_1}$.

Remark 7.5. *In case of a general H^1 -conforming and $H(\text{curl})$ -conforming finite element basis, the calculation of the discrete gradient operator requires the inversion of the element mass matrix on each element.*

Review of the applied $H(\text{curl})$ preconditioner

The best choice for preconditioning the residual $Au^i - \lambda(u^i)Mu^i$, would be to apply the pseudo-inverse A^\dagger , which would naturally include also the projection to the complement of the kernel. Note that application of the approximative inverse $C_{A+\sigma M}^{-1}$ may introduce artificial kernel components. This can be suppressed by applying the reduced basis preconditioner $C_{A+\sigma M}^{\text{red}}$ instead. Due to our special construction of the FE-basis (cf. Section (6.3)), the reduced space preconditioner can be realized easily. Although we cannot give a rigorous mathematical justification that the reduced basis preconditioner is a better approximation for the pseudo-inverse, this choice is at least as good the original one. The reduced basis preconditioner is however typically much less ill-conditioned and its application requires much less numerical effort.

7.4 Numerical Results

In the following we verify the performance of our chosen finite element basis in combination with the Locally Optimal Block PCG method with (in)exact projection by means of various

benchmark problems. We consider the electric eigenvalue problem, Problem 7.1, with homogeneous Dirichlet conditions and constant material parameters $\epsilon = 1$ and $\mu = 1$:

Find $\lambda \neq 0$ and $\mathbf{u} \in H_0(\text{curl}, \Omega)$ such that

$$\int_{\Omega} \mu^{-1} \text{curl} \mathbf{u} \text{curl} \mathbf{v} \, d\mathbf{x} = \lambda \int_{\Omega} \epsilon \mathbf{u} \mathbf{v} \, d\mathbf{x} \quad \forall \mathbf{v} \in H_0(\text{curl}, \Omega). \quad (7.24)$$

On the webpage of Monique DAUGE [39] a convenient range of benchmark problems for above Maxwell eigenvalue problem is provided. The focus lies on considering geometries with re-entrant corners and edges, where a part of the spectrum is conjectured to correspond to highly-singular eigenfunctions.

We consider the following two domains:

- The *thick L-shape* $\Omega = \Psi_2 \times (0, 1)$ with $\Psi_2 := (-1, 1)^2 \setminus (-1, 0)$, we obtain singularities due to the re-entrant corner. For this setting benchmark results are available on DAUGE [39].
- The *Fichera corner* $\Omega = (-1, 1)^3 \setminus (-1, 0)^3$, where all three re-entrant edges as well as the re-entrant corner produce singularities. There are no benchmark results yet available, but we will compare our results with the ones of Costabel-Dauge, stated on the webpage DAUGE [39], and BRAMBLE ET AL. [29].

In the context of computing Maxwell eigenvalue problems on polyhedral domains we also refer to FRAUENFELDER [48] and AINSWORTH ET AL. [3] contributing numerical results on the Maxwell eigenvalue computation on polyhedral domains.

7.4.1 An h - p -refinement strategy

In order to resolve singularities due to re-entrant corners and edges we use the following hp -refinement strategy, which is based on marking re-entrant corners and edges a priori in the geometry as singular.

Our h - p -strategy is the following:

- k steps of *geometric h -refinement* with a progression factor $0 < q \leq 0.5$ are performed towards a priori marked faces, edges and corners. The strategy should become clear considering the example of the thick L-shape domain, illustrated in Figure 7.1. The optimal progression factor q depends on the solution, but a commonly used choice is $q = 0.17$ (see e.g. MELENK [68]).
- *Anisotropic distribution of polynomial degrees (p)*: On each element the level of actual refinement $r_{\hat{x}_i}$ in each direction \hat{x}_i is known, i.e. $0 \leq r_{\hat{x}_i} \leq k$. Let p_{\min} denote the initial polynomial order. Then we choose the degree $p_{\hat{x}_i} = p_{\min} + (k - r_{\hat{x}_i})$ in the direction \hat{x}_i of the element.

7.4.2 The Maxwell EVP on the thick L-Shape

The eigenvalues on the thick L-shape can be deduced by addressing to its tensor-product structure, i.e. the $\Psi_2 \times (0, 1)$, where Ψ_2 denotes the two-dimensional L-shaped domain.

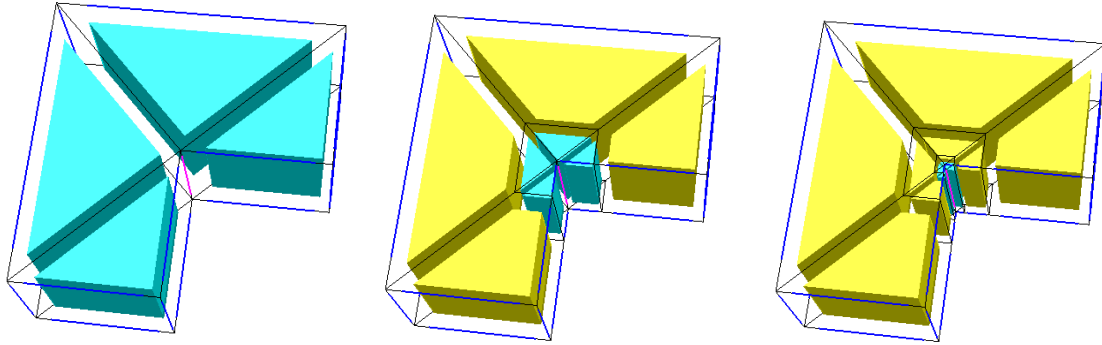


Figure 7.1: Geometric h -refinement towards the re-entrant edge: original prismatic mesh (left), level 1 (center) and level 2 (right); involving prisms (blue) and hexahedra (yellow).

The eigenvalues on the tensorized L-shape are realized by the sum of a non-zero Neumann eigenvalue of the 2D L-shape and a Dirichlet eigenvalue on the L-shape domain or the sum of a Dirichlet eigenvalue on Ψ_2 and a non-zero Neumann eigenvalue on $(0, 1)$. Accurate numerical solutions for the two-dimensional L-shape are available. The following benchmark results for the 8 smallest eigenvalues on the thick L-shape are due to DAUGE [39]:

$$\begin{aligned}
 \lambda_1 &= 9.63972384472 & \lambda_2 &= 11.3452262252 & \lambda_3 &= 13.4036357679 \\
 \lambda_4 &= 15.1972519265 & \lambda_5 &= 19.5093282458 & \lambda_6 &= 19.7392088022 \\
 \lambda_7 &= 19.7392088022 & \lambda_8 &= 19.7392088022
 \end{aligned} \tag{7.25}$$

The first, the second and the fifth eigenvalue correspond to the first Dirichlet or Neumann eigensolutions on the two-dimensional L-shape Ψ_2 , which has a strong unbounded singularity in the corner. The third and the fourth eigenvalue refer to an eigenvector, which is in $H^1(\Psi_2)$. The eigenvalues number 6, 7, and 8 are related to an analytic eigenvector on the 2 dimensional domain.

We first run the eigenvalue computation for uniform p -refinement on a fixed mesh, namely the first level of h -refinement depicted in Figure 7.1 with progression factor $q = 0.17$. The log-log-plot in Figure 7.2 illustrates the convergence history of the relative errors $\frac{|\lambda_i - \tilde{\lambda}_i|}{|\lambda_i|}$ of the computed 8 smallest eigenvalues $\tilde{\lambda}_i$ with respect to the degrees of freedom (dofs). As expected when using a p -method, we observe only algebraic convergence rates for the eigenvalues of rank 1, 2, and 5.

In the second test series we repeat the eigenvalue calculations with uniform p -refinement on fixed meshes generated by various levels of geometric h -refinements ($k = 1, \dots, 5, q = 0.17$). The convergence history of the mean of the relative errors of the 8 smallest eigenvalues is presented in Figure 7.3. Finally, we combine the geometric mesh refinement with anisotropic p -refinement as described above. The envelope of the convergence curve in Figure 7.4 corresponds to the hp -refined eigenvalue computation with refinement factor $q = 0.25$. We obtain the conjectured exponential convergence in the number of unknowns even in the presence of eigenvalues corresponding to highly-singular eigenfunctions.

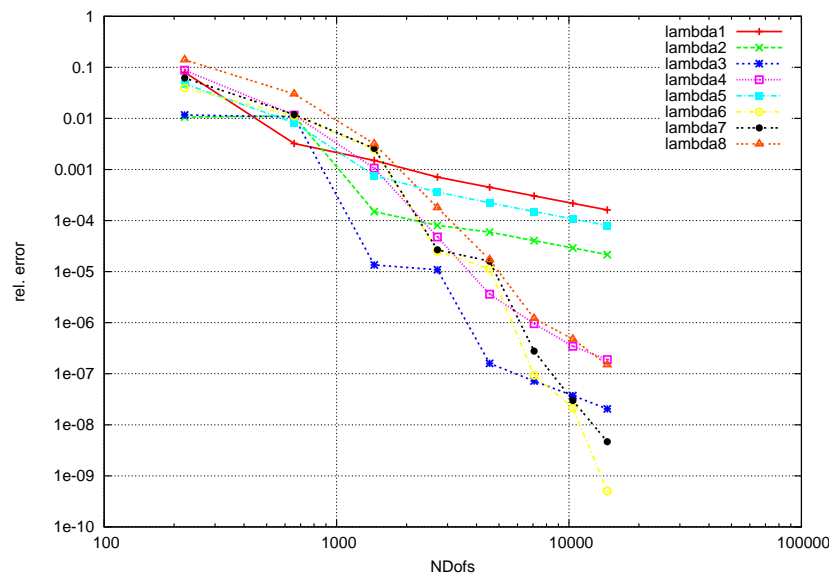


Figure 7.2: L-Shape: Average relative errors of the 8 smallest eigenvalues. 1 level of geometric refinement. Uniform p refinement.

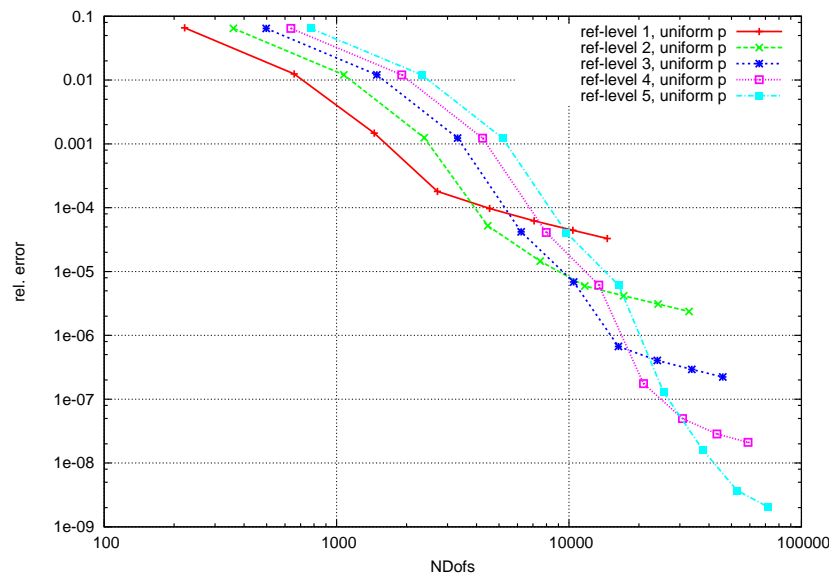


Figure 7.3: L-Shape: Average relative errors of the 8 smallest eigenvalues. Uniform p refinement on fixed geometric refined meshes.

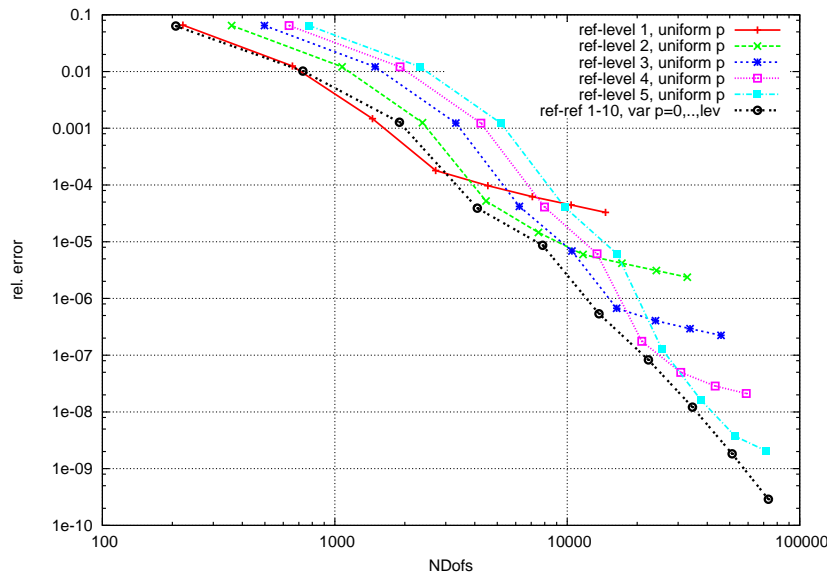


Figure 7.4: L-Shape: Average relative error of 8 the smallest eigenvalues. Exponential convergence: Combination of geometric h -refinement and p -anisotropic order distribution

7.4.3 The Maxwell EVP on the Fichera corner

As already mentioned no benchmark results are available for the Fichera corner. In the following we contribute with our results. First, we cite the results available on the website DAUGE [39] and in BRAMBLE ET AL. [29] in Table 7.1.

j	$\tilde{\lambda}_j$ (DAUGE [39])	reliable digits(?)	conject. ev	j	$\tilde{\lambda}_j$ (BRAMBLE [29])
1	3.31380523357	1	3.2??	1	3.23432
2	5.88634994607	3	5.88?	2	5.88267
3	5.88634994619	3	5.88?	3	5.88371
4	10.6945143272	4	10.694	4	10.6789
5	10.6945143276	4	10.694	5	10.6832
6	10.7005804029	2	10.7??	6	10.6945
7	12.3345495948	3	12.32?	7	12.23653
8	12.3345495949	3	12.32?	8	12.23723

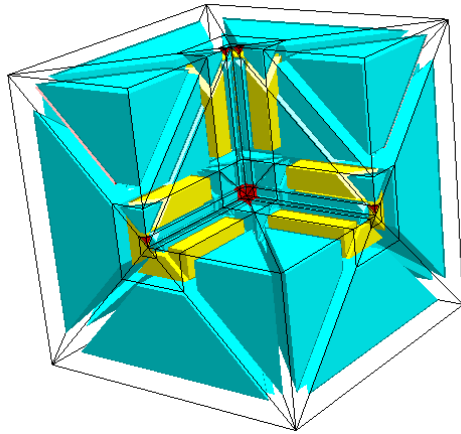
Table 7.1: Results by Dauge and Costabel from DAUGE [39] with conjectured eigenvalue and hopefully reliable digits (left table) and results corresponding to BRAMBLE-KOLEV-PASCIAK [29] (right table)

Table 7.2 presents the results of our computation of the 8 smallest eigenvalues using the LOBPCG method with inexact projection in following problem setting:

We started with an initial mesh consisting of 12 tetrahedra and performed 3 levels of geometric h -refinement. The refined mesh contains hexahedra, tetrahedra and prisms and is depicted in Table 7.2.

We use the anisotropic polynomial order distribution as described at the beginning of this section. The degrees on each element vary from $p = 3$ to $p = 6$ for the $H(\text{curl})$ -conforming space, which yields 53982 degrees of freedom, and from $p = 4$ to $p = 7$ for the corresponding potential space $H^1(\Omega)$, which involves 19318 degrees of freedom. The total solution time on a Dual Processor Intel Xeon 64Bit 2,8 GHz is 6460 seconds. The number of LOBPCG iterations is 14. Note that one has to provide an H^1 -preconditioner with sufficiently smooth blocks to avoid zero eigenvectors in the solution. The iteration numbers and results are independent from the choice of the shift parameter σ in the $H(\text{curl})$ -preconditioner. We used the reduced basis preconditioner, since as already verified in the last chapter it is better conditioned and faster in its application compared to the one in the full basis.

For visualization we rerun the numerical test for our problem setting with homogenous Neumann boundary conditions and present the computed eigenfunctions corresponding to the first and the seventh eigenvalue in in Figure 7.5.



j	$\tilde{\lambda}_j$
1	3.21999388904
2	5.88044248619
3	5.88045528405
4	10.6856632462
5	10.6936955486
6	10.6937289163
7	12.3168796291
8	12.3176900965

Table 7.2: The 8 smallest eigenvalues on Fichera corner, computed on left mesh with anisotropic order of $p = 3, \dots, 6$ (NgSolve). On the left hybrid mesh by 3 levels of hp -refinement with hexahedra (yellow), prisms (blue), tetrahedra (red).

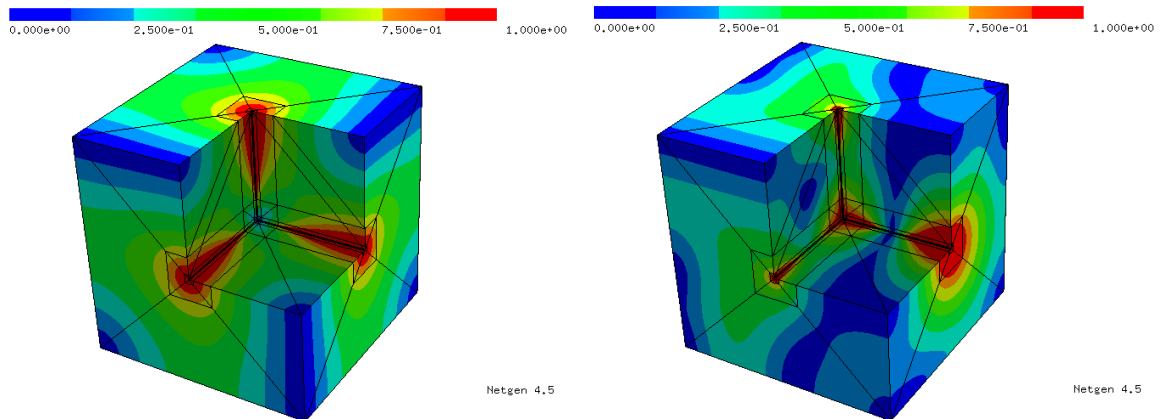


Figure 7.5: Absolute value of first (left) and seventh (right) eigenfunction (only for visualization computed with homogenous Neumann data)

Appendix A

APPENDIX

A.1 Notations

We use the symbol \preceq for referring to \leq up to a constant.

Polynomial spaces

Let $K \subset \mathbb{R}^3$.

- $P_p(K)$... space of polynomials of maximal total degree p , i.e.
 $P_p(K) = \{\sum_{i+j+k \leq p} c_{ijk} x^i y^j z^k \mid c_{ijk} \in \mathbb{R}\}$.
- $\tilde{P}_p(K)$... set of homogenous polynomials of exact degree p , i.e.
 $\tilde{P}_p(K) = \{\sum_{i+j+k=p} c_{ijk} x^i y^j z^k \mid c_{ijk} \in \mathbb{R}\}$.
- $Q_p(K)$... space of polynomials of maximal degree p , i.e.
 $Q_p(K) = \{\sum_{0 \leq i,j,k \leq p} c_{ijk} x^i y^j z^k \mid c_{ijk} \in \mathbb{R}\}$.

A.2 Basic Vector Calculus

Let α denote a scalar function in x , while \mathbf{v} is a vector-valued function.

$$\operatorname{div}(\alpha \mathbf{v}) = \mathbf{v} \cdot \nabla \alpha + \alpha \operatorname{div} \mathbf{v} \tag{A.1}$$

$$\operatorname{curl}(\alpha \mathbf{v}) = \alpha \operatorname{curl} \mathbf{v} + \nabla \alpha \times \mathbf{v} \tag{A.2}$$

$$\operatorname{div}(\operatorname{curl} \mathbf{v}) = 0 \tag{A.3}$$

$$\operatorname{curl}(\nabla \alpha) = 0 \tag{A.4}$$

$$\begin{aligned} \operatorname{tr}_{\mathbf{n}, F_m}(\operatorname{curl}(\boldsymbol{\varphi})) &= \mathbf{n} \cdot \operatorname{curl}(\boldsymbol{\varphi}) = \mathbf{n} \cdot \operatorname{curl}(\boldsymbol{\varphi}_\tau \boldsymbol{\tau} + \boldsymbol{\varphi}_n \mathbf{n}) \\ &= \mathbf{n} \cdot (\nabla \boldsymbol{\varphi}_\tau \times \boldsymbol{\tau} + \nabla \boldsymbol{\varphi}_n \times \mathbf{n}) = \mathbf{n} \cdot (\nabla \boldsymbol{\varphi}_\tau \times \boldsymbol{\tau}) \\ &= \operatorname{curl}_{F_m}(\boldsymbol{\varphi}_\tau) \end{aligned}$$

A.3 Some more orthogonal polynomials

Jacobi-polynomials , denoted by $P_n^{(\alpha, \beta)}$, are orthogonal polynomials associated with the weight function $(1-x)^\alpha (1+x)^\beta$ (for $\alpha > -1, \beta > -1$) in the interval $[-1, 1]$. This means

they fulfill

$$\int_{-1}^1 (1-x)^\alpha (1+x)^\beta P_m^{(\alpha,\beta)} P_n^{(\alpha,\beta)} dx = 0 \text{ for } m \neq n.$$

They can be defined by the Rodrigues formula

$$P_n^{(\alpha,\beta)}(x) = \frac{(-1)^n}{2^n n!} (1-x)^{-\alpha} (1+x)^{-\beta} \frac{d^n}{dx^n} \left((1-x)^{\alpha+n} (1+x)^{\beta+n} \right).$$

Fast point-evaluation up to order p is established by the three-term recurrence formula

$$\begin{aligned} P_0^{(\alpha,\beta)} &= 1, \\ P_1^{(\alpha,\beta)} &= \frac{1}{2} (\alpha - \beta) + \frac{1}{2} (\alpha + \beta + 2)x, \\ P_{n+1}^{(\alpha,\beta)}(x) &= (a_n + b_n x) P_n^{(\alpha,\beta)}(x) + c_n P_{n-1}^{(\alpha,\beta)}(x), \end{aligned} \tag{A.5}$$

where the coefficients are given as

$$\begin{aligned} a_n &= \frac{(2n + \alpha + \beta + 1)(\alpha^2 - \beta^2)}{2(n+1)(n + \alpha + \beta + 1)(2n + \alpha + \beta)}, \\ b_n &= \frac{(2n + \alpha + \beta + 1)(2n + \alpha + \beta + 2)}{2(n+1)(n + \alpha + \beta + 1)}, \\ c_n &= -\frac{(n + \alpha)(n + \beta)(2n + \alpha + \beta + 2)}{(n+1)(n + \alpha + \beta + 1)(2n + \alpha + \beta)}. \end{aligned}$$

The Legendre polynomials are a special case of the Jacobi ones. Choosing $\alpha = \beta = 0$ yields

$$\ell_n(x) = P_n^{(0,0)}(x) \text{ for } x \in [-1, 1].$$

Integrated Legendre polynomials are related to Jacobi polynomials by the relation

$$L_n(x) = -\frac{1}{2(n-1)} (1-x^2) P_{n-2}^{(1,1)}(x) \quad \text{for } x \in [-1, 1], n \geq 2.$$

Scaled Jacobi polynomials are defined as

$$P_n^{\mathcal{S},(\alpha,\beta)}(x, t) := P_n^{(\alpha,\beta)}\left(\frac{x}{t}\right) t^n.$$

We can compute them by the recurrence formula

$$P_{n+1}^{\mathcal{S},(\alpha,\beta)}(x, t) = (a_n t + b_n x) P_n^{\mathcal{S},(\alpha,\beta)}(x, t) + c_n t^2 P_{n-1}^{\mathcal{S},(\alpha,\beta)}(x, t) \tag{A.6}$$

with a_n, b_n, c_n as defined in (A.5). We remark that the recurrence formula is free of divisions by t .

Choosing $\alpha = \beta = 0$ yields the scaled Legendre polynomials

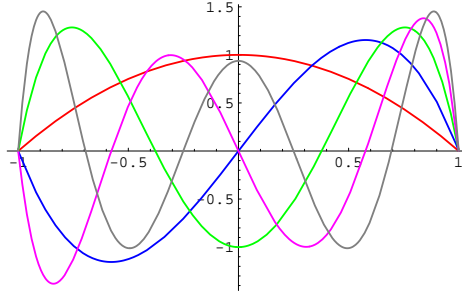
$$\ell_n^{\mathcal{S}}(x) = P_n^{\mathcal{S},(0,0)}(x).$$

Jacobi-based bubble functions We can define Jacobi-based polynomials spanning $P_p^0([-1, 1])$ by the set of bubble functions

$$\phi_j = (1-x)(1+x) P_{j-2}^{(2,2)}(x)$$

is L_2 -orthogonal in the interval $[-1, 1]$ in the sense of

$$\int_{-1}^1 \phi_i \phi_j dx = 0 \text{ for } i \neq j.$$

Figure A.1: Jacobi-based bubble functions ϕ_j of order 2 to 7

A.3.1 Some Calculus for Scaled Legendre Polynomials

By the relation

$$\begin{aligned} x L'_n(x) - n L_n(x) &= L'_{n-1}(x) \\ x \ell'_n(x) - n \ell_n(x) &= \ell'_{n-1}(x) \end{aligned}$$

we can show that

$$\begin{aligned} \nabla (L_n^{\mathcal{S}}(s, t)) &= -L'_{n-1}\left(\frac{s}{t}\right) t^{n-1} \nabla t + L'_n\left(\frac{s}{t}\right) t^{n-1} \nabla s \\ &= -\ell_{n-2}^{\mathcal{S}}(s, t) t \nabla t + \ell_{n-1}^{\mathcal{S}}(s, t) \nabla s \end{aligned} \quad (\text{A.7})$$

holds. The same holds for Legendre polynomials

$$\begin{aligned} \nabla (\ell_n^{\mathcal{S}}(s, t)) &= -\ell'_{n-1}\left(\frac{s}{t}\right) t^{n-1} \nabla t + \ell'_n\left(\frac{s}{t}\right) t^{n-1} \nabla s \\ &= -(\ell'_{n-1})^{\mathcal{S}}(s, t) t \nabla t + (\ell'_n)^{\mathcal{S}}(s, t) \nabla s. \end{aligned} \quad (\text{A.8})$$

A.3.2 Some technical things

$$\nabla_{\mathbf{x}}(\xi, \eta, \zeta) = \begin{pmatrix} 2\frac{2}{1-\eta} \frac{2}{1-\zeta} & 0 & 0 \\ (1+\xi) \frac{2}{1-\eta} \frac{2}{1-\zeta} & \frac{2}{1-\zeta} & 0 \\ (1+\xi) \frac{2}{1-\eta} \frac{2}{1-\zeta} & (1+\eta) \frac{2}{1-\zeta} & 2 \end{pmatrix}$$

$$\begin{aligned} \nabla u_i(x, y, z) &= \nabla (L_{i+2}^{\mathcal{S}}(2x-1+y+z, 1-y-z)) \\ &= \ell_i^{\mathcal{S}}(\lambda_2 - \lambda_1, \lambda_1 + \lambda_2) (\lambda_1 + \lambda_2) \begin{pmatrix} 0 \\ 1 \\ 1 \end{pmatrix} + \ell_{i+1}^{\mathcal{S}}(\lambda_2 - \lambda_1, \lambda_1 + \lambda_2) \begin{pmatrix} 2 \\ 1 \\ 1 \end{pmatrix} \\ \nabla v_j(y, z) &= \nabla (\lambda_3 \ell_j^{\mathcal{S}}(\lambda_3 - \lambda_1 - \lambda_2, 1 - \lambda_4)) \\ &= \lambda_3 (\ell'_{j-1})^{\mathcal{S}}(\lambda_3 - \lambda_1 - \lambda_2, 1 - \lambda_4) (1 - \lambda_4) \begin{pmatrix} 0 \\ 0 \\ 1 \end{pmatrix} \\ &\quad + \lambda_3 (\ell'_j)^{\mathcal{S}}(\lambda_3 - \lambda_1 - \lambda_2, 1 - \lambda_4) \begin{pmatrix} 0 \\ 2 \\ 1 \end{pmatrix} + \ell_j^{\mathcal{S}}(\lambda_3 - \lambda_1 - \lambda_2, 1 - \lambda_4) \begin{pmatrix} 0 \\ 1 \\ 0 \end{pmatrix} \\ \nabla w_k(z) &= \nabla (\lambda_4 \ell_k(2\lambda_4 - 1)) \\ &= (\ell_k(2z - 1) + 2\ell'_k(2z - 1)) \mathbf{e}_z \end{aligned}$$

$$\begin{aligned}
(\nabla u_i)(\mathcal{D}(\xi, \eta, \zeta)) &= \left(\ell_i(\xi) \begin{pmatrix} 0 \\ 1 \\ 1 \end{pmatrix} + \ell_{i+1}(\xi) \begin{pmatrix} 2 \\ 1 \\ 1 \end{pmatrix} \right) \left(\frac{1-\eta}{2} \right)^{i+1} \left(\frac{1-\zeta}{2} \right)^{i+1} \\
(\nabla v_j)(\mathcal{D}(\xi, \eta, \zeta)) &= \left(\ell'_{j-1}(\eta) \begin{pmatrix} 0 \\ 0 \\ 1 \end{pmatrix} + \ell'_j(\eta) \begin{pmatrix} 0 \\ 2 \\ 1 \end{pmatrix} \right) \frac{1+\eta}{2} \left(\frac{1-\zeta}{2} \right)^{j-1} + \ell_j(\eta) \left(\frac{1-\zeta}{2} \right)^j \begin{pmatrix} 0 \\ 1 \\ 0 \end{pmatrix} \\
(\nabla w_k)(\mathcal{D}(\xi, \eta, \zeta)) &= (\ell_k(\zeta) + 2\ell'_k(\zeta)) \mathbf{e}_z
\end{aligned}$$

Bibliography

- [1] M. Ainsworth. A hierarchical domain decomposition preconditioner for h - p finite element approximation on locally refined meshes. *SIAM Journal on Scientific Computing*, 17(6):1395–1413, 1996.
- [2] M. Ainsworth and J. Coyle. Hierarchic finite element bases on unstructured tetrahedral meshes. *International Journal of Numerical Methods in Engineering*, 58(14):2103–2130, 2003.
- [3] M. Ainsworth, J. Coyle, P. Ledger, and K. Morgan. Computation of Maxwell eigenvalues using higher order edge elements in three dimensions. *IEEE Transactions on Magnetics*, pages 2149–2153, 2003.
- [4] C. Amrouche, C. Bernardi, M. Dauge, and V. Girault. Vector potentials in three-dimensional non-smooth domains. *Mathematical Methods in the Applied Sciences*, 21:823–864, 1998.
- [5] P. Arbenz and R. Geus. A comparison of solvers for large eigenvalue problems occurring in the design of resonant cavities. *Numerical Linear Algebra with Applications*, 6(1):3–16, 1999.
- [6] D.N. Arnold, R.S. Falk, and R. Winther. Preconditioning in $H(\text{div})$ and applications. *Mathematics of Computation*, 66(219):957–984, July 1997.
- [7] D.N. Arnold, R.S. Falk, and R. Winther. Multigrid in $H(\text{div})$ and $H(\text{curl})$. *Numerische Mathematik*, 85:197–218, 2000.
- [8] D.N. Arnold, R.S. Falk, and R. Winther. Finite element exterior calculus, homological techniques, and applications. *Acta Numerica*, 15:1–155, 2006.
- [9] D.N. Arnold, R.S. Falk, and R. Winther. Differential complexes and stability of finite element methods. I. the de Rham complex. In *Proceedings of the IMA workshop on Compatible Spatial Discretizations for PDE*, to appear.
- [10] I. Babuska and B.Q. Guo. Approximation properties of the h - p version of the finite element method. *Computational Methods of Applied Mechanical Engineering*, 133:319–346, 1996.
- [11] I. Babuska and M. Suri. The p and h - p versions of the finite element method, basic principles and properties. *SIAM Review*, 36(4):578–632, 1994.
- [12] I. Babuska, B.A. Szabo, and I.N.Katz. The p -version of the finite element method. *SIAM Journal on Numerical Analysis*, 18(3):515–545., 1981.

- [13] F. Bachinger, U. Langer, and J. Schöberl. Efficient solvers for nonlinear time-periodic eddy current problems. SFB-Report 2004-16, Johannes Kepler University Linz, 2004. submitted to Computing and Visualization in Science.
- [14] F. Bachinger, J. Schöberl, and U. Langer. Numerical analysis of nonlinear multiharmonic eddy current problems. *Numerische Mathematik*, 100(4):593–616, 2005.
- [15] Z. Bai, J. Demmel, J. Dongarra, A. Ruhe, and H. van der Vorst, editors. *Templates for the Solution of Algebraic Eigenvalue Problems: A Practical Guide*. SIAM, Philadelphia, 2000. online available: <http://www.cs.utk.edu/~dongarra/etemplates/index.html>.
- [16] R. Beck, P. Deuffhard, R. Hiptmair, R.H.W. Hoppe, and B. Wohlmuth. Adaptive multilevel methods for edge element discretizations of Maxwell’s equations. *Surveys Math. Industry*, 8(3–4):271–312, 1999.
- [17] S. Beuchler and J. Schöberl. New shape functions for triangular p-fem using integrated jacobi polynomials. *Numerische Mathematik*, 103:339–366, 2006.
- [18] O. Bíró. Numerische Aspekte von Potentialformulierungen in der Elektrodynamik. Habilitationsschrift, TU Graz, 1992.
- [19] D. Boffi. Discrete compactness and Fortin operator for edge elements. *Numerische Mathematik*, 87:229–246, 2000.
- [20] D. Boffi, M. Costabel, D. Monique, and L. Demkowicz. Discrete compactness for the *hp* version of rectangular edge finite elements. *SIAM Journal on Numerical Analysis*, 44(3):979–1004, 2006.
- [21] D. Boffi, P. Fernandes, L. Gastaldi, and I. Perugia. Computational models of electromagnetic resonators: Analysis of edge element approximation. *SIAM Journal on Numerical Analysis*, 36:264–1290, 1999.
- [22] A. Bossavit. Mixed finite elements and the complex of Whitney forms. In J. Whiteman, editor, *The Mathematics of Finite Elements and Applications VI*, pages 137–144. Academic Press, 1988.
- [23] A. Bossavit. A rationale for edge elements in 3d field computations. *IEEE Transactions on Magnetism*, 24(1):74–79, 1988.
- [24] A. Bossavit. Whitney forms: a class of finite elements for three-dimensional computations in electromagnetism. *IEE Proceedings*, 135(8):493–500, 1988.
- [25] A. Bossavit. *Computational Electromagnetism: Variational formulation, complementary, edge elements*. Academic Press Inc., San Diego, CA, 1989.
- [26] A. Bossavit. Solving Maxwell equations in a closed cavity, and the question of ‘spurious modes’. *IEEE Transactions on Magnetism*, 26(2):702 – 705, 1990.
- [27] D. Braess. *Finite Elemente: Theorie, schnelle Löser und Anwendungen in der Elastizitätstheorie*. Springer Verlag Berlin Heidelberg, 3rd edition edition, 2003.
- [28] J.H. Bramble, A.V. Knyazev, and J.E. Pasciak. A subspace preconditioning algorithm for eigenvector/eigenvalue computation. *Advances in Computational Mathematics*, 6:159–189, 1996.

- [29] J.H. Bramble, T.V. Kolev, and Pasciak J.E. The approximation of the Maxwell eigenvalue problem using a least-squares method. *Mathematics of Computation*, 74(252):1575–1598, 2005.
- [30] J.H. Bramble and X. Zhang. The analysis of multigrid methods. In P.G. Ciarlet and J.L. Lions, editors, *Handbook of Numerical Analysis*, volume 7, pages 173–415. North-Holland, 2000.
- [31] S.C. Brenner and L.R. Scott. *The Mathematical Theory of Finite Element Methods*, volume 15 of *Texts in Applied Mathematics*. Springer-Verlag New York, 2nd edition, 2002.
- [32] F. Brezzi and M. Fortin. *Mixed and Hybrid Finite Element Methods*. Springer Verlag, Berlin, 1991.
- [33] A. Buffa and P. Jr. Ciarlet. On traces for functional spaces related to Maxwell’s equation. Part I: An integration by parts formula in Lipschitz polyhedra. *Mathematical Methods in the Applied Sciences*, 24(1):9–30, 2001.
- [34] S. Caorsi, P. Fernandes, and M. Raffetto. On the convergence of galerkin finite element approximations of electromagnetic eigenproblems. *SIAM Journal on Numerical Analysis*, 38(2):580–607, 2000.
- [35] P.G. Ciarlet. *The Finite Element Method for Elliptic Problems*. North Holland, Amsterdam, 1978.
- [36] M. Clemens, U. van Rienen, and T. Weiland. Comparison of krylov-type methods for complex linear systems applied to high-voltage problems. *IEEE Transactions on Magnetics*, 34(5):3335–3338, 1998.
- [37] M. Clemens and T. Weiland. Iterative methods for the solution of very large complex-symmetric linear systems of equations in electrodynamics. In *Copper Mountain Conference on Iterative Methods*, volume 2, 1996. available via MGNET.
- [38] M. Costabel and M. Dauge. Singularities of electromagnetic fields in polyhedral domains. *Archive for Rational Mechanics and Analysis*, 151(3):221 – 276, 2000.
- [39] Monique Dauge. Benchmark computations for Maxwell equations for the approximation of highly singular solutions. <http://perso.univ-rennes1.fr/monique.dauge/benchmax.html>.
- [40] R. Dautray and J.-L. Lions. *Spectral Theory and Applications*, volume 3 of *Mathematical Analysis and Numerical Methods for Science and Technology*. Springer-Verlag, 1990.
- [41] L. Demkowicz. Edge finite elements of variable order for Maxwell’s equations - a discussion. Technical report, TICAM, 2000. TICAM Report 00-32.
- [42] L. Demkowicz. *Computing with hp Finite Elements. I. One- and Two-Dimensional Elliptic and Maxwell Problems*. CRC Press, Taylor and Francis, 2006. in press.
- [43] L. Demkowicz and A. Buffa. H^1 , $H(\text{curl})$ - and $H(\text{div})$ -conforming projection-based interpolation in three dimensions. quasi-optimal p -interpolation estimates. *Comput. Meth. Appl. Mech. Engrg.*, 194(2-5):267–296, 2005.

- [44] L. Demkowicz, P. Monk, L. Vardapetyan, and W. Rachowicz. De Rham diagram for hp finite element spaces. *Computers and Mathematics with Applications*, 39(7-8):29–38, 2000.
- [45] L. Demkowicz and L. Vardapetyan. hp-adaptive finite elements in electromagnetics. *Computers Methods in Applied Mechanics and Engineering*, 169:331–344, 1999.
- [46] M. Dubiner. Spectral methods on triangles and other domains. *Journal of Scientific Computing*, 6(4):345–390, 1991.
- [47] E. D’yakonov. *Optimization in Solving Elliptic Problems*. CRC Press, 1996.
- [48] Philipp Frauenfelder. *hp-Finite element methods on anisotropically, locally refined meshes in three dimensions with stochastic data*. Mathematische wissenschaften, Eidgenössische Technische Hochschule ETH Zürich, 2004.
- [49] V. Girault and P.A. Raviart. *Finite Element Methods for Navier-Stokes Equations: Theory and Algorithms*. Springer Series in Computational Mathematics. Springer-Verlag, Berlin-Heidelberg, 1986.
- [50] J. Gopalakrishnan and L. Demkowicz. Quasioptimality of some spectral mixed methods. *Journal on Computational and Applied Mathematics*, 167:163–182, 2004.
- [51] C. Grossmann and H.G. Roos. *Numerik partieller Differentialgleichungen*. Teubner, 1994.
- [52] W. Hackbusch. *Multi-Grid Methods and Applications*. Springer, Berlin, Heidelberg, New York, 1985.
- [53] W. Hackbusch. *Iterative Solution of Large Sparse System of Equations*. Springer-Verlag, 1994.
- [54] R. Hiptmair. Canonical construction of finite elements. *Mathematics of Computation*, 68:1325–1346, 1990.
- [55] R. Hiptmair. Multigrid method for Maxwell’s equations. *SIAM Journal of Numerical Analysis*, 36(1):204–255, 1999.
- [56] R. Hiptmair. Finite elements in computational electromagnetism. *Acta Numerica*, pages 237–339, 2002.
- [57] R. Hiptmair and K. Neymeyr. Multilevel method for mixed eigenproblems. *SIAM Journal of Scientific Computing*, 23(6):2141–2164, 2002.
- [58] R. Hiptmair and A. Toselli. Overlapping Schwarz methods for vector valued elliptic problems in three dimensions. In *Parallel solution of PDEs*, IMA Volume in Mathematics and its Applications. Springer, Berlin-Heidelberg-New York, 1997.
- [59] R. Hitpmair. Multigrid method for $H(\text{div})$ in three dimensions. *Electronic Transactions on Numerical Analysis*, 6:7–77, 1997.
- [60] G.E. Karniadakis and S.J. Sherwin. *Spectral/hp Element Methods for CFD*. Numerical Mathematics and Scientific Computation. Oxford University Press, New York, Oxford, 1999.

- [61] F. Kikuchi. Mixed and penalty formulations for finite element analysis of an eigenvalue problem in electromagnetism. *Computer Methods in Applied Mechanics and Engineering*, pages 509–521, 1987.
- [62] A.V. Knyazev. Preconditioned eigensolvers - an oxymoron? *Electronic Transactions on Numerical Analysis*, 7:104–123, 1998.
- [63] A.V. Knyazev. Toward the optimal preconditioned eigensolver: Locally optimal block preconditioned conjugate gradient method. *SIAM Journal on Scientific Computing*, 23(2):517541, 2001.
- [64] A.V. Knyazev and K. Neymeyr. Efficient solution of symmetric eigenvalue problems using multigrid preconditioners in the locally optimal block preconditioned gradient method. *Electronical Transaction of Numerical Analysis*, 15:38–55, 2003.
- [65] A.V. Knyazev and K. Neymeyr. A geometric theory for preconditioned inverse iteration. iii: A short and sharp convergence estimate for generalized eigenvalue problems. *Linear Algebra and its Application*, 358:95–114, 2003.
- [66] J.F. Lee, D.K. Sun, and Z.J. Cendes. Tangential vector finite elements for electromagnetic field computation. *IEEE Transactions on Magnetics*, 27(5):4032 – 4035, 1991.
- [67] W. McLean. *Strongly Elliptic Systems and Boundary Integral Equations*. Cambridge University Press, 2000.
- [68] J.M. Melenk. *hp-Finite Element Methods for Singular Perturbations*, volume 1796 of *Lecture notes in in mathematics*. Springer Berlin Heidelberg, 2002.
- [69] P. Monk. On the p - and hp -extension of Nedelec’s curl-conforming elements. *Journal of Computational and Applied Mathematics*, 53(1):117–137, 1994.
- [70] P. Monk. *Finite Element Methods for Maxwell’s Equations*. Numerical Mathematics and Scientific Computation. The Clarendon Press Oxford University Press, New York, 2003.
- [71] P. Monk, L. Demkowicz, and Vardapetyan L. Discrete compactness and the approximation of Maxwell’s equations in \mathbb{R}^3 . *Mathematics of Computation*, 70:507–523, 2001.
- [72] J.C. Nédélec. Mixed finite elements in \mathbb{R}^3 . *Numerische Mathematik*, 35:315–341, 1980.
- [73] J.C. Nédélec. A new family of mixed finite elements in \mathbb{R}^3 . *Numerische Mathematik*, 50:57–81, 1986.
- [74] K. Neymeyr. A hierarchy of preconditioned eigensolvers for elliptic differential operators, 2001. Habilitation.
- [75] J. Pasciak and J. Zhao. Overlapping Schwarz methods in $H(\text{curl})$ on nonconvex domains. *East West Journal on Numerical Analysis*, 10:221–234, 2002.
- [76] W. Rachowicz and L. Demkowicz. An hp -adaptive finite element method for electromagnetics. part 2: A 3d implementation. *International Journal for Numerical Methods in Engineering*, 53:147–180, 2002.
- [77] Y. Saad. *Iterative Methods for Sparse Linear Systems*. PWS, Boston, 1996.

- [78] J. Schöberl. A multilevel decomposition result in $H(\text{curl})$. In TUDelft, editor, *Proceedings of the 8th European Multigrid Conference EMG 2005*, Netherlands. to appear.
- [79] J. Schöberl. NETGEN - An advancing front 2D/3D-mesh generator based on abstract rules. *Computing and Visualization in Science*, 1:41–52, 1997.
- [80] J. Schöberl. *Robust Multigrid Methods for Parameter Dependent Problems*. PhD thesis, Institute for Computational Mathematics, J.K. University Linz, 1999.
- [81] J. Schöberl. A posteriori error estimates for Maxwell equations. *Mathematics of Computation*, submitted.
- [82] J. Schöberl, J. Melenk, Pechstein C., and Zaglmayr S. Additive Schwarz preconditioning for p -version triangular and tetrahedral finite elements. *IMA Journal of Numerical Analysis*, 2005. submitted.
- [83] Ch. Schwab. *p - and hp - Finite Element Methods: Theory and Applications in Solid and Fluid Mechanics*. Numerical Mathematics and Scientific Computation. Oxford University Press, Oxford, 1998.
- [84] B.F. Smith, P.E. Bjørstad, and W.D. Gropp. *Domain decomposition: Parallel multilevel algorithms for elliptic partial differential equations*. Cambridge University Press, 1996.
- [85] D.-K. Sun, J.-F. Lee, and C. Zoltan. Construction of nearly orthogonal nedelec bases for rapid convergence with multilevel preconditioned solvers. *SIAM Journal on Scientific Computing*, 23(4):1053–1076, 2001.
- [86] B. Szabo, A. Düster, and E. Rank. The p -version of the finite element method. In E. Stein, R. de Borst, and J.R.T. Hughes, editors, *Encyclopedia Of Computational Mechanics*, volume 1 Fundamentals, chapter 5, pages 119–139. John Wiley and Sons, Chichester, 2004.
- [87] B. Szabo and Babuska I. *Finite Element Analysis*. J. Wiley and Sons, New York, 1991.
- [88] G. Szegö. *Orthogonal Polynomials*, volume 23 of *Colloquium Publications*. American Mathematical Society, Providence, Rhode Island, 3 edition, 1974.
- [89] A. Toselli. Overlapping Schwarz methods for Maxwell's equations in three dimensions. *Numerische Mathematik*, 86(4):733–752, 2000.
- [90] A. Toselli and O. Widlund. *Domain Decomposition Methods - Algorithms and Theory*, volume 34 of *Series in Computational Mathematics*. Springer, 2005.
- [91] H. van der Vorst. *Iterative Krylov Methods for Large Linear Systems*. Cambridge University Press, 2003.
- [92] U. van Rienen. *Numerical Methods in Computational Electrodynamics: Linear Systems in Practical Applications*, volume 12 of *Lecture notes in computational science and engineering*. Springer-Verlag Berlin Heidelberg, 2001.
- [93] Y. Wang, P. Monk, and Szabo B. Computing cavity modes using the p version of the finite element method. *IEEE Transaction on Magnetics*, (32):1934–1940, 1996.

- [94] T.C. Warburton, S.J. Sherwin, and G.E. Karniadakis. Basis functions for triangular and quadrilateral high-order elements. *SIAM Journal on Scientific Computing*, 20(5):1671–1695, 1999.
- [95] J.P. Webb. Hierarchical vector basis functions of arbitrary order for triangular and tetrahedral finite elements. *IEEE Transactions on Antennas and Propagation*, 47(8):1495–1498, August 1999.
- [96] J.P. Webb and Forghani B. Hierarchical scalar and vector tetrahedra. *IEEE Transactions on Magnetism*, 29(2):1495–1498, March 1993.
- [97] X. Zhang. Multilevel Schwarz methods. *Numerische Mathematik*, 63:521–539, 1992.

Eidesstattliche Erklärung

Ich, Sabine Zaglmayr, erkläre an Eides statt, dass ich die vorliegende Dissertation selbständig und ohne fremde Hilfe verfasst, andere als die angegebenen Quellen und Hilfsmittel nicht benutzt bzw. die wörtlich oder sinngemäß entnommenen Stellen als solche kenntlich gemacht habe.

Linz, Juli 2006

Sabine Zaglmayr

Curriculum Vitae

Personal Data

Name: Sabine Zaglmayr
Nationality: Austria
Date of Birth: 11. 5. 1978
Place of Birth: Schärding, Austria

Education

1984 - 1988 Elementary School St.Marienkirchen
1988 - 1996 Comprehensive Secondary School Schärding
1996 - 2002 Studies in Technical Mathematics,
Branch of study: Industrial Mathematics,
Johannes Kepler University Linz
since 2002 PhD studies at Johannes Kepler University Linz

Professional Career

since 2002 Research assistant at FWF-START Project Y-192
"3D hp-Finite Elements: Fast Solvers and Adaptivity"
since 2004 hosted at J. Radon Institute for Computational and Applied Mathematics,
Austrian Academy of Sciences

Awards

2004 Master's thesis awarded with the Hansjörg Wacker Memorial Prize,
European Consortium for Mathematics in Industry (ECMI)